The design and synthesis of inhibitors of the mitotic human kinesin, Eg5

A thesis submitted to the University of Strathclyde for the Degree of Doctor of Philosophy by

Murad Najib Abualhasan

2011

Strathclyde Institute of Pharmacy and Biomedical Science

University of Strathclyde

Glasgow

Table of contents

List of Figures

VII

List of Tables

X

Abbreviations

Å	Angstrom(s)
ADP	Adenosine diphosphate
Ala	Alanine
Arg	Arginine
Asp	Aspartic acid
atm	Atmosphere(s)
ATP	Adenosine triphosphate
ATR	Attenuated Total Reflection Mode
$(BOC)_2O$	Di-*tert*-butyl dicarbonate (BOC-anhydride)
BF_3.etherate	Boron trifluoride etherate
°C	Degree(s) celsius
CADD	Computer-aided drug design
CD_3OD	Deuterated methanol
^{13}C NMR	Carbon NMR
$CDCl_3$	Deuterated chloroform
C-terminus	Carboxylic acid-terminus
D	Doublet
Da	Dalton(s)
dd	Doublet of doublet
DIAD	Diisopropyl azodicarboxylate
DMSO-d_6	Deuterated dimethyl sulfoxide
DNA	Deoxyribonucleic acid

EC50	Effective dose
Eq	Equivalent(s)
eV	Electron volt(s)
FT-IR	Fourier Transform Infrared spectroscopy
G	Gramme(s)
Glu	Glutamic acid
Gln	Glutamine
Gly	Glycine
GOLD	Genetic Optimization for Ligand Docking
H	Hour(s)
^{1}H NMR	Proton NMR
H_2SO_4	Sulphuric acid
H-bond	Hydrogen bond
hERG	human *Ether-à-go-go* Related Gene
HMQC	Heteronuclear Multiple Quantum Coherence
HPLC	High pressure liquid chromatography
HRMS-ESI	High resolution mass spectrometry-electrospray ionization
HTS	High throughput study
Hz	Hertz
IC_{50}	Half maximal inhibitory concentration
Ile	Isoleucine
J	Coupling constant
k	Kilogram
K_2CO_3	Potassium carbonate
KBr	Potassium bromide
KHC	Kinesin heavy chain
KRP	Kinesin related proteins
KSP	Kinesin Spindle Protein
LAH	Lithium aluminium hydride

Leu	Leucine
μg	Microgram
μM	Micromolar
μL	Microlitre(s)
M	Molar
m	Multiplet
MD	Molcular dynamics
MDR	Multidrug resistance
Met	Methionine
mg	Milligramme(s)
MgSO$_4$	Magnesium sulphate
MHz	Megahertz
mL	Millilitre(s)
mM	Millimole(s)
mpt	Melting point
nM	Nanomolar
n.i.	No inhibition
NaBH$_4$	Sodium borohydride
NCI	National Cancer Institute
NMR	Nuclear magnetic resonance
NSCLC	Non-small-cell lung cancer
Pgp	P-glycoprotein
pKa	Acid dissociation constant
PPh$_3$	Triphenylphosphine
ppm	Parts per million
Pro	Proline
q	Quartet
rt	Room temperature
RMSD	Root mean square deviation

s	Singlet
SAR	Structure activity relationship
SiO$_2$	Silicon dioxide
S$_N$1	Unimolecular nucleophilic substitution
STDC	*S*-Trityl-D-cysteine
STLC	*S*-Trityl-L-cysteine
t	Triplet
TEA	Triethylamine
TFA	Trifluoroacetic acid
THF	Tetrahydrofuran
TLC	Thin-layer chromatography
TMSCN	Trimethyl silyl cyanide
Trp	Tryptophan
Tyr	Tyrosine
Val	Valine

Acknowledgement

First and foremost I want to thank my supervisor Prof. Simon Mackay. I appreciate all his contributions of time, ideas, and for giving me the opportunity and funding to make my Ph.D. I am also very thankful to my second supervisor Dr. Oliver Sutcliffe for his support, guidance and advice.

I would like to thank Prof. Frank Kozielski (Beatson Institute for Cancer Research-Glasgow) for conducting the *in vitro* assays and teaching me the art of performing Eg5 enzyme inhibition assays. I am also grateful to all members of his team, especially Dr. Oliver Rath who helped in conducting the cell assays of my compounds.

A special thanks to the Solid-State Research Group at the University of Strathclyde led by Prof. Alastair Florence and his team members Scott McKellar and Ryan Taylor for their help in the lab with the crystallisation studies.

Thanks are also due Dr. Dave Watson and Dr. Tong Zhang for their advice and allowing me to use the HPLC instruments in their lab for the method development work. Many thanks also to Prof. Sandy Gray and Dr. Ruangelie Edrada-Ebeland for their help in the NMR interpretation.

I am also indebted to Dr. Rachel Clark for her help in the molecular modeling and docking experiments and for her invaluable advice regarding my thesis writing. I am also very grateful to all the medicinal chemistry post doctorate members; Dr. Nahoum Anthony, Dr. Murray Robertson, Dr. Judith Huggan and Dr. Fang Wang for their continuous help and advice throughout my PhD.

I would like to thank all my post graduate colleagues in SIPBS-312 (Bilal, Nizar, Hasan, Giacomo, Sabin, James, Jessica, Salha and Azra for their friendship and support.

Very special thanks to the management and all staff of Tesco St. Rollox-Glasgow for being very kind and supportive to me during my part-time job with them. Working with this company helped me with some financial support and was a rich experience for me.

Lastly, I would like to thank my family in Palestine for all their love and encouragement, to my parents, brothers and sisters for their endless spiritual support, and most of all for my loving, supportive, encouraging, and patient wife Hadeel for her faithful support during all stages of my Ph.D. To my beloved daughter Mayar, my sons Abdullah and Mohammed; I am very sorry for giving you so little time throughout my busy PhD.

Thank you all and may Allah bless you.

Abstract

Vinca alkaloids and taxanes are natural products used to treat cancer, which interfere with microtubule function to induce mitotic arrest. Unfortunately, like all antitumour drugs, they have several undesired side effects, which are specifically related, in this case, to tubulin function. There is a need to develop more effective and less toxic drugs that target those mitotic proteins that have specialized and specific functions in cell mitosis. Eg5 motors plays a specific role in spindle pole separation and are responsible for the maintenance of the bipolar spindle, and targeting these motors will cause mitotic arrest in tumour cells undergoing uncoordinated proliferation.

After the discovery of monastrol, the first Eg5 inhibitor, compounds with greater specificity and potency have been discovered, such as S-trityl-L-cysteine (STLC). In this study, we have attempted to optimize the STLC hit and produced compounds that have a range of activities, some of which were more active than STLC. The most active compounds were tested on four cancer cell lines and were evaluated against Pgp over-expressed cells for multi-drug resistance.[1]

Chapter 1: Introduction

1.1 Mitosis and cancer therapy

Antimitotic agents have generated considerable interest as cytotoxic agents due to the tremendous success and widespread application of these agents in clinical oncology. Mitosis is a fundamental process during cell division, which can be divided into four substages [2-5] (**Figure 1.1**).
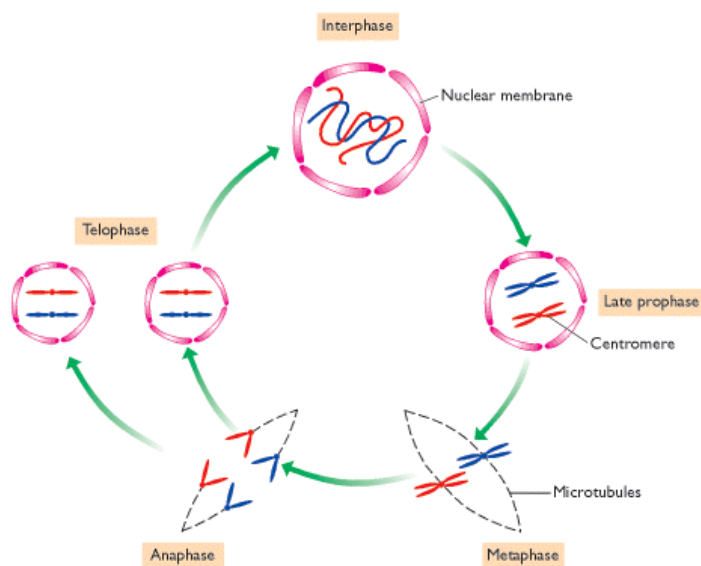
Figure 1.1: Stages of cell division.[2]

Prophase: in this stage of mitosis, the chromatin condenses into an ordered structure called a chromosome. When chromosomes are paired up and attached, each individual part of the chromosome pair is called a chromatid. They are held together in a region called the centromere. In mitosis, only one copy of each sister chromatid goes to each daughter cell after cell division. The centrosome is an organelle located in the cytoplasm that controls the polymerization and polar orientation of the cell's microtubules throughout the cell cycle. During prophase, the microtubule-nucleating activity of the centrosomes is increased by γ-tubulin and forced apart to opposite ends of the cell by the action of protein motors acting on the microtubules. This marks the end of prophase (**Figure 1.2a**).
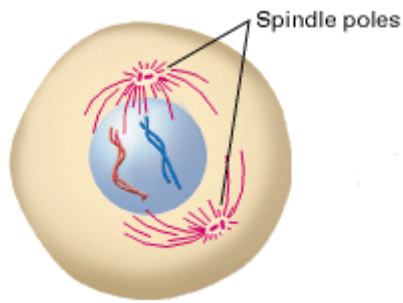
Prophase: the chromosomes have begun to condense and the centrosomes have separated towards the poles on opposite sides of the cell.

Figure 1.2(a): Prophase stage[5]

Metaphase: the chromosomes align in the middle of the cell before being separated into two daughter cells (**Figure 1.2b**). The centromeres of the chromosomes are arranged at an equal distance from the two centrosome poles. This equal alignment is a result of counterbalanced pulling powers generated by the opposing kinetochore microtubules.

Metaphase: the microtubules have entered the nuclear region and the chromosomes have aligned along the metaphase plate

Figure 1.2(b): Metaphase stage[5]

Anaphase: this is the stage when chromosomes separate (**Figure 1.2c**) and can be divided with two phases:
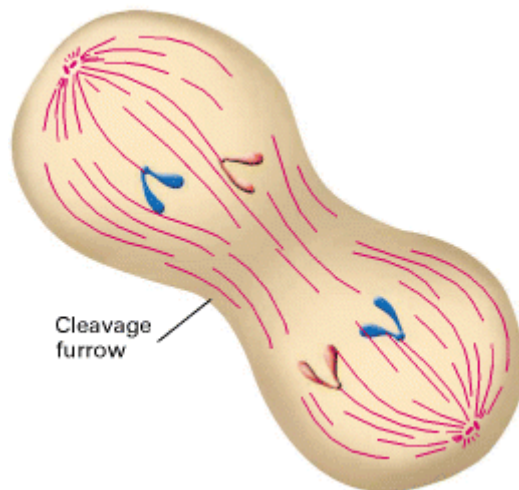
Anaphase: the sister chromatids have been separated to opposite spindle poles.

Figure 1.2(c): Anaphase stage[5]

Anaphase A: the chromatids separate and move towards the spindle poles, which is achieved by the shortening of the spindle microtubules via the kinetochore microtubules.

Anaphase B: when the chromatids are fully separated, the polar microtubules will slide relative to each other to push the spindle poles apart, which is achieved by specific kinesins called Eg5 motors attached to polar microtubules pushing the microtubules away from each other.

Mitosis ends when the cell enters the telophase stage; the cytoplasm of the original cell is divided into two daughter cells by a process called cytokinesis. The chromosomes at this stage begin to decondense, a new nuclear membranes starts to form and the new daughter cells enter G1 (first gap) of the interphase stage. Following G1 is the S phase, when the cell replicates its DNA. At the completion of this stage, all of the chromosomes have replicated but they are still decondensed and not distinctly visible. The cell then enters G2 (second gap) of the interphase stage and the cytoplasmic organelles replicate preparing for a new cell cycle.

1.1.1 Anti-mitotic drugs targeting tubulin or microtubules

Microtubules play a very important role in mitosis as kinetochore microtubules pull the condensed chromatids to the pole of the mitotic spindle. To date, compounds

which target microtubules are the only approved anti-mitotic drugs used in cancer therapy.[6]

The vinca alkaloids were the first identified agents to have an anti-mitotic effect.[7] Colchicine,[8] vincristine and vinblastine are currently used in combination with other therapies in the treatment of testicular cancer, Hodgkin's disease and acute lymphocytic leukemia.[9]

Taxanes also have an anti-mitotic effect by targeting β-tubulin. Paclitaxel and docetaxel were introduced in the late 1980s and both drugs have since proved to be effective in the treatment of a variety of solid tumors including: breast, ovarian, lung and bladder.

Although the vinca alkaloids and taxanes both have an anti-microtubule effect, their modes of action are different; taxanes stabilise and block microtubule depolymerization, whereas vinca alkaloids destabilise microtubules and promote depolymerisation.[10-13]

1.1.2 Problems associated with anti-microtubule agents

In addition to mitosis, microtubules have many other physiological functions, such as regulating motility and organelle transport, and it is postulated that some of the therapeutic benefits of the anti-microtubule drugs may be due to these activities, in addition to their anti-mitotic effects. Microtubules are also required for the transport of proteins and vesicles along axon fibres, which may explain the peripheral neurological side effects observed in the treatment with these agents. These include tingling of the fingers or toes, abdominal pain, constipation, and muscle weakness.

The major factor in the failure of many forms of chemotherapy is drug resistance. Tumour cells become resistant to anti-microtubule agents through various mechanisms, such as drug efflux pumps where the tumour cell expels the drug to avoid toxic effects within the nucleus or the cytoplasm of the cell.

The main protein pump that is responsible for drug resistance is P-glycoprotein (Pgp). This protein is a product of the MDR1 gene which is overexpressed in resistant cells, and acts as a drug efflux pump, for drugs with broad substrate structure specificity. It can also reduce the bioavailability of certain drugs, lowering their therapeutic concentrations and rendering them ineffective.

Pgp is an ATP- binding cassette transporter (ABC-transporter) that is a 170 kDa, 1280 amino acid transmembrane protein that has two homologous regions of approximately equal length, each containing a hydrophobic region with six segments, followed by a highly conserved intracellular ATP- binding site.[14]

The mechanism of drug transport has been studied by a variety of techniques. ATP hydrolysis appears to be the energy source for the drug specific transport process across the membrane, and most Pgp substrates are hydrophobic and partition into the lipid bilayer. The drug substrate and ATP bind to the protein simultaneously, whereupon ATP hydrolysis shifts the substrate to a position to be excreted out of the cell.[15] **Figure 1.3** is a model which explains the process of substrate transport.[16]

(A) Substrate (red) partitions into the bilayer and the drug binding site (blue).

(B) ATP (yellow) binds to nucleotide binding domain (NBD) making conformational change to the binding site and expelling the substrate into the extracellular space.
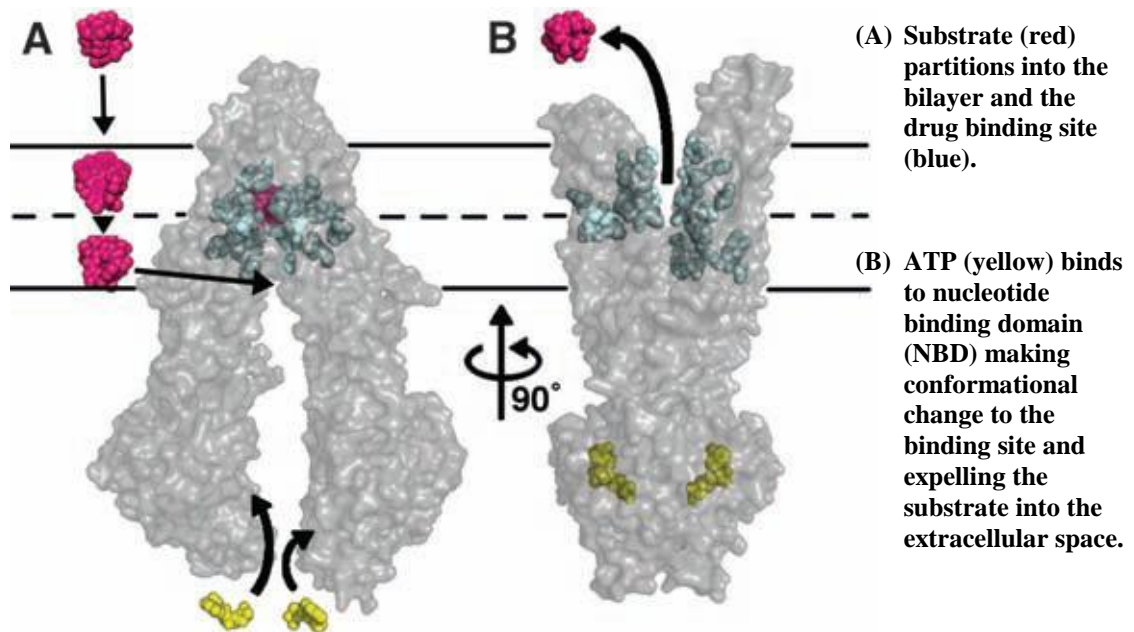
Figure 1.3: Mechanism of substrate transport.

The poor efficacy of the antimicrotubule vinca alkaloids and taxanes in certain cancers is due to multidrug resistance; Pgp is overexpressed in resistant colon and kidney cancers treated with these agents.[17] Successful modulation of multiple drug resistance has been achieved using agents such as calcium channel blockers (verapamil), cyclosporin A, tamoxifen and quinidine. These drugs appear to compete with vinca alkaloids and taxanes for the same transport binding site in Pgp, and reverse drug resistance.[18]

1.1.3 Anti-mitotic drugs targeting kinesins

Recently, mitotic kinesins have gained significant attention as new targets for cancer therapy - agents that inhibit the function of kinesins specifically could have reduced side effects and lower drug resistance compared with microtubule targeting drugs.

The first kinesin discovered in the mid 1980's was named conventional kinesin or kinesin heavy chain (KHC).[19,20] Kinesins are mechano-chemical proteins that use the energy generated by ATP hydrolysis to exert a movement force on microtubules. These proteins are classified as microtubule motor proteins,[21] and their *in vivo* microtubule motility mediates diverse functions within the cell, including the transport of vesicles, organelles and chromosome movement during meiosis and mitosis.[22]

All the kinesin related proteins (KRP) in the 14 member kinesin superfamily have a highly conserved motor domain of about 350 amino acids that typically show >35% sequence with conventional kinesin. The main sequence difference is usually outside the motor domain, and accounts for the differences in velocity and direction of movement between the related proteins.[23-25] Individual kinesin family members have very specific functions. Certain members function exclusively during cell division and are required for various aspects of mitosis, including bipolar spindle assembly. Eg5 is a member of the Kinesin 5 (Kin N_2) subfamily, which is sometimes called Kinesin Spindle Protein (KSP). Eg5 homologues have been found in *Aspergillus* (BimC), *Schizosaccharomyces pombe* (cut7), *Saccharomyces cerevisiae* (cin8p), Drosophila (Klp61F) and in Xenopus (Eg5). [26]

Inactivation of Eg5 in Drosphila and Xenopus by mutation or antibodies blocks centrosome separation, which leads to mitotic arrest with a monoastral spindle.[27, 28] In proliferating cells, Eg5 expression is prominent and overexpression of Eg5 is associated with the development of different tumour types.[29] The requirement of Eg5 in early mitosis makes this kinesin a very attractive target for pharmacological intervention.[30] The predicted clinical use of inhibitors of Eg5 has not been limited to a specific kind of cancer, as Eg5 has been expressed in all cell-proliferating tumours. The use of these compounds in cancer therapy could overcome some of the toxicities and resistance experienced with microtubule-targeting drugs.

1.2 Eg5 motors

1.2.1 Eg5 function on microtubules

Eg5 has a globular *N*-terminal head which possesses microtubule-activated ATPase activity. The *C*-terminal end of the heavy chain is essential for motility, which is linked to a coiled coil region called the neck and causes the molecule to dimerize.[27, 31] Unlike the conventional kinesin which has two motor domains that form a dimer, Eg5 has two dimers which interact anti-parallel to each other to form a bipolar tetrameric structure with two motor domains at each end (**Figure 1.4**).[32-35]
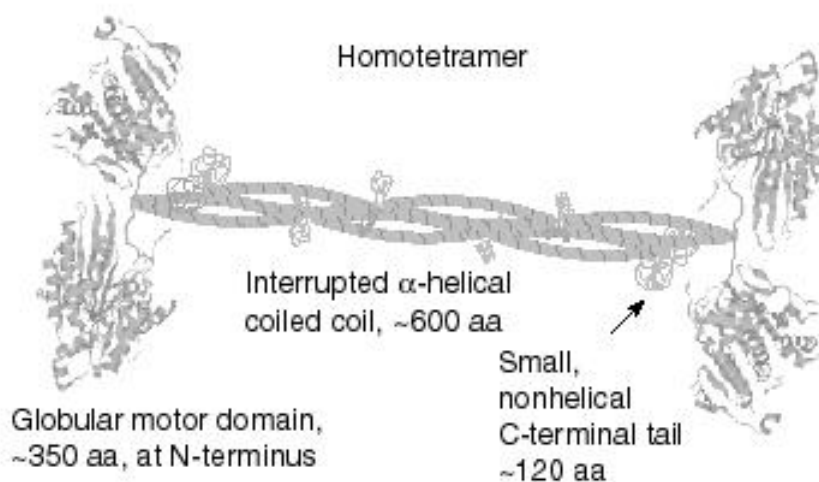
Figure 1.4: Tetrameric structure of Eg5.[16]

Microtubules in the mitotic spindle have their minus ends oriented towards the centrosome and their plus end outwards. Many microtubules overlap with a parallel

shape near the poles and are antiparallel in the middle zone. The bipolar tetrameric structure of the Eg5 enables it to bind to the microtubules. Eg5 moves toward the plus ends of the two cross linked microtubules arranging parallel microtubules into bundles within the half spindles and sliding antiparallel microtubules apart in the middle zone. The sliding effect of Eg5 on the microtubules is illustrated in **Figure 1.5**.[36-39]
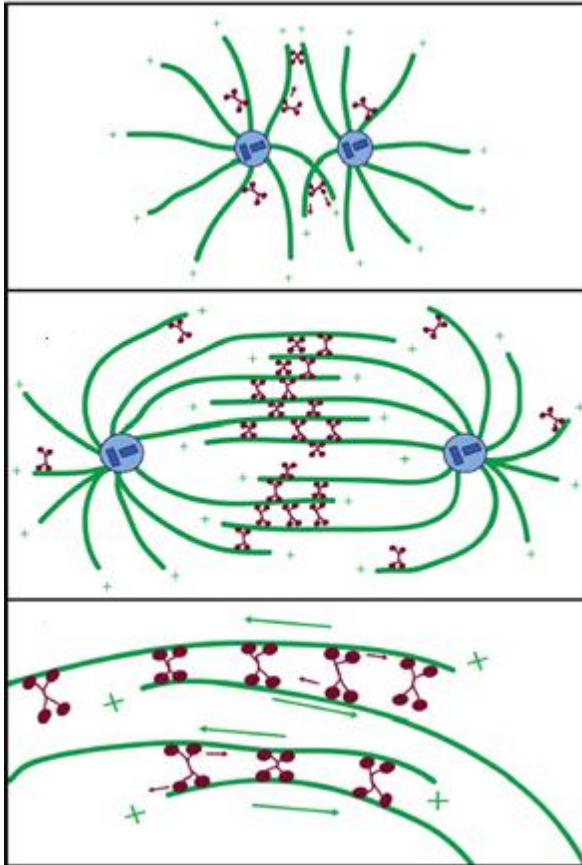
The tetrameric Eg5 motors cross-linking microtubules;

moving to their plus ends;

sliding them toward the spindle centrosomes; generating a poleward flux.

Figure 1.5: Eg5 movement on the microtubules[38].

An *in vitro* fluorescence study[38] showed that Eg5 proteins walk in a processive manner with a step size of 8.1nm, which is the same step size as conventional kinesin and the space between α and β tubulin heterodimers of microtubules.[40] The velocity of Eg5 is slower than conventional kinesin, with a stepping speed rate of 100nm/s compared to 650nm/s.[41]

1.2.2 Eg5 mechano-chemical movement

Kinesin motors translate chemical changes to mechanical motion, which they achieve through a conformational change in the motor as ATP is hydrolysed to ADP.

The long helix α4 (switch-II) undergoes conformational changes that resemble the motions of a piston. The up-stroke motion of the helix is an inward motion of switch-II in the ATP binding state, whereas the down-stroke is initiated by phosphate release to the ADP binding state (**Figure 1.6**). The long and incompressible shape of the helix makes it a perfect device for transmitting movement from the nucleotide site to the neck linker. In the ATP state, the neck linker C-terminus becomes docked in the catalytic core which drives a forward motion of the neck linker and any object attached to its C-terminus. The detached head with a free mobile neck linker in its ADP bound state is thrown forward to the next tubulin binding site.[41-43]
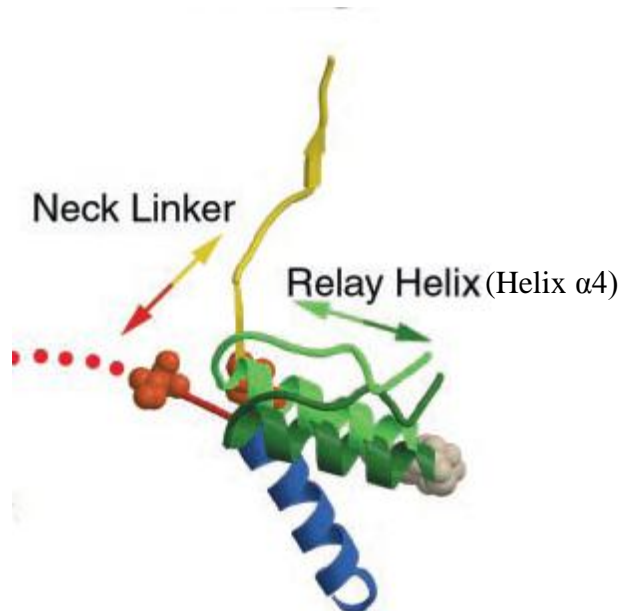
The conformational changes occur to the helix α4 (Switch II) during the transitional changes from the ATP binding state (dark green; upstroke) to the ADP binding state (light green; downstroke). The neck linker shifts its position in response to motion of the Switch II helix; ATP (yellow) and ADP (red) binding state.

Figure 1.6: Conformational changes to the helix α4 (Switch II).[43]

1.2.3 Eg5 motor domain structure in comparison to the conventional kinesin

To gain a better understanding of Eg5 function, its detailed motor domain structure has been studied and compared with the structure of conventional kinesin. The phosphate binding site (P-loop) is present in all kinesins and was used to overlay different kinesins to check for structural differences. Generally, the β sheet arrangements are almost identical in the two structures. The Eg5 protein has an end

tip which is slightly tilted and lengthened compared with conventional kinesin, which may play an important role in its interaction with the microtubules (**Figure 1.7**).

Figure 1.7: Eg5 motor domain.

The helix α2 is interrupted by a loop called the insertion loop L5, which is the largest in the kinesin 5 family, and plays an important role in regulating the motor activity (**Figure 1.8**).
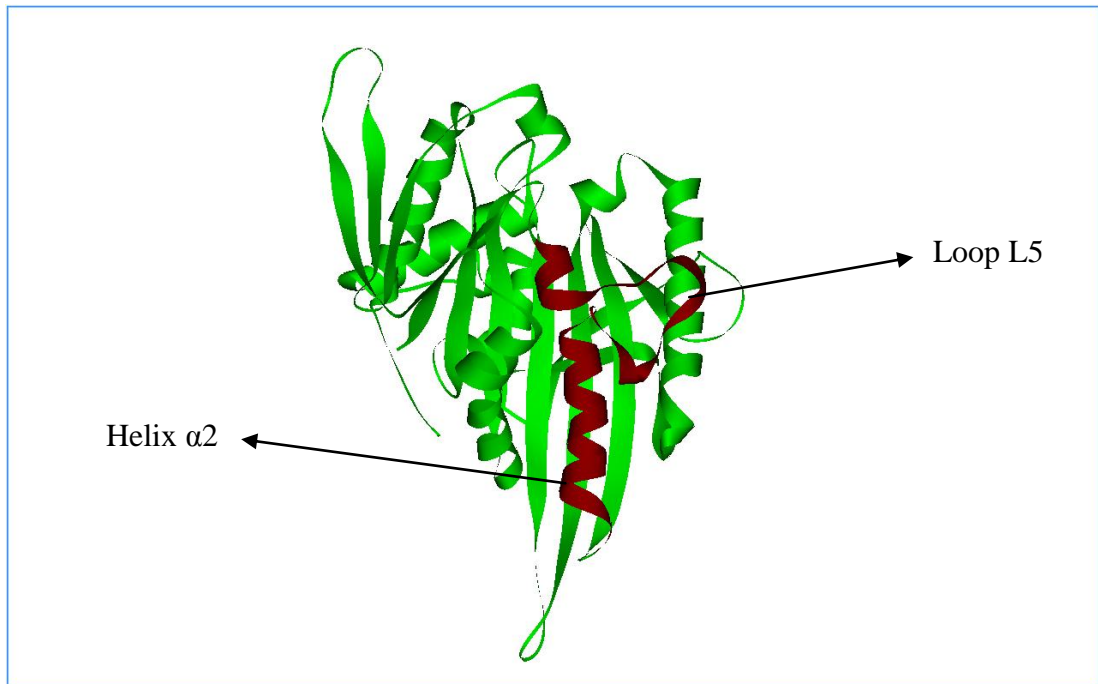
Figure 1.8: Helix α2 interrupted by insertion loop L5

The switch-I region is found in the helix α3, which, while being a short helix in the KHC, is a flexible loop in Eg5 (**Figure 1.9**). It is assumed that switch-I with ATP-bound has the same shape in all kinesins, while, in the ADP-bound state, this region is flexible.[44-46]
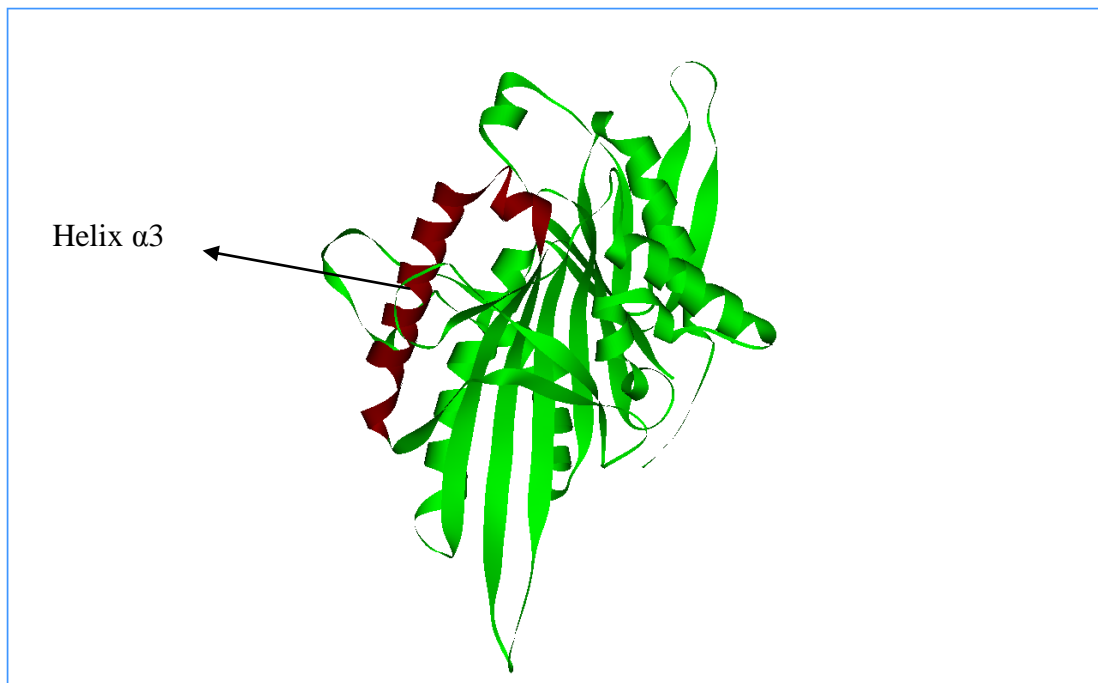
Figure 1.9: Helix α3 of Eg5 motors

The helix α4 (switch-II) of Eg5 is one and a half turns more than switch-II of the KHC (**Figure 1.10**). All known kinesins can be classified as switch-II helix-up in the ATP binding state or switch-II helix-down in the ADP binding state.

Helix α4
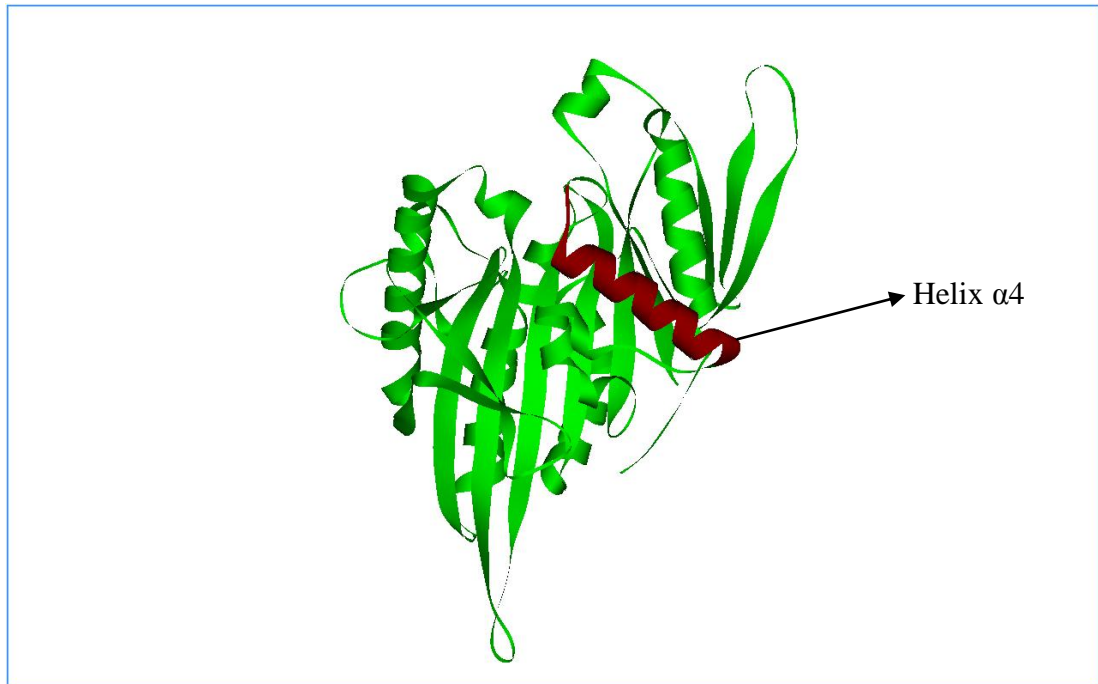
Figure 1.10: Helix α4 of Eg5 motors

The end region of the helix α6 of Eg5 is very different from the KHC. This region is termed as the neck linker (**Figure 1.11**), and attaches to the coiled coil region where the Eg5 dimerises. It adopts a different position in the ADP and ATP bound states, and is where chemico-mechanical movement is transmitted through the tetrameric motor structures. [44-48]

Figure 1.11: The neck linker of Eg5.

1.3 Inhibitors of Eg5

A large number of KSP inhibitors have been reported in the scientific and patent literature, all of which share a common allosteric site in the Eg5 structure that is distinct from the nucleotide binding site. Detailed studies of how these inhibitors bind have been instrumental in understanding how Eg5 works, and in the development of new and potent Eg5 inhibitors.

1.3.1 Monastrol

Monastrol

The first specific Eg5 inhibitor discovered by Mayer *et al* was monastrol, a 1,4 dihydropyrimidine,[49] which has provided many insights into the specific function of Eg5, its role in cell division, and how it can be inhibited. Mayer *et al* showed that inhibition of Eg5 with antibodies induced monoasters similar to those observed after treatment with monastrol, and that the effect of monastrol was reversible and did not affect the activity of organelles, such as lysosomes or golgi apparatus in the cell.[49] Further studies demonstrated that monastrol was not ATP competitive, did not bind to the nucleotide binding site and was not a microtubule competitive inhibitor.[50-52] Monastrol was shown to bind to a complex of Eg5 and ADP, slowing down ADP release through induction of a stable conformational change to the motor domain that favours ATP re-synthesis, which then alters the ability of Eg5 to generate force, thereby yielding non-productive motors (IC_{50}=30 µM). [53, 54]

A co-crystal structure of the *S*-enantiomer of monsatrol with Eg5 was solved by Youwei Yan *et al*.[55] and clearly showed that monastrol bound to an allosteric binding site of an induced-fit pocket consisting of 20 amino acids 12 Å from the nucleotide binding site and situated between helix α3 and loop5 of helix α2. The crystal structure revealed full occupancy of the inhibitor in the *S*-configuration and there was no evidence of binding by the *R*-enantiomer (**Figure 1.12**). The 3-hydroxy group on the phenyl ring makes H-bonds with the main chain carbonyl group of Glu118, the main chain amino group of Ala133, and the side chain nitrogen of Arg119. The carbonyl oxygen of the ester group acts as a hydrogen bond acceptor and forms a H-bond with the main chain amino group of Arg119 and with a structural water molecule.
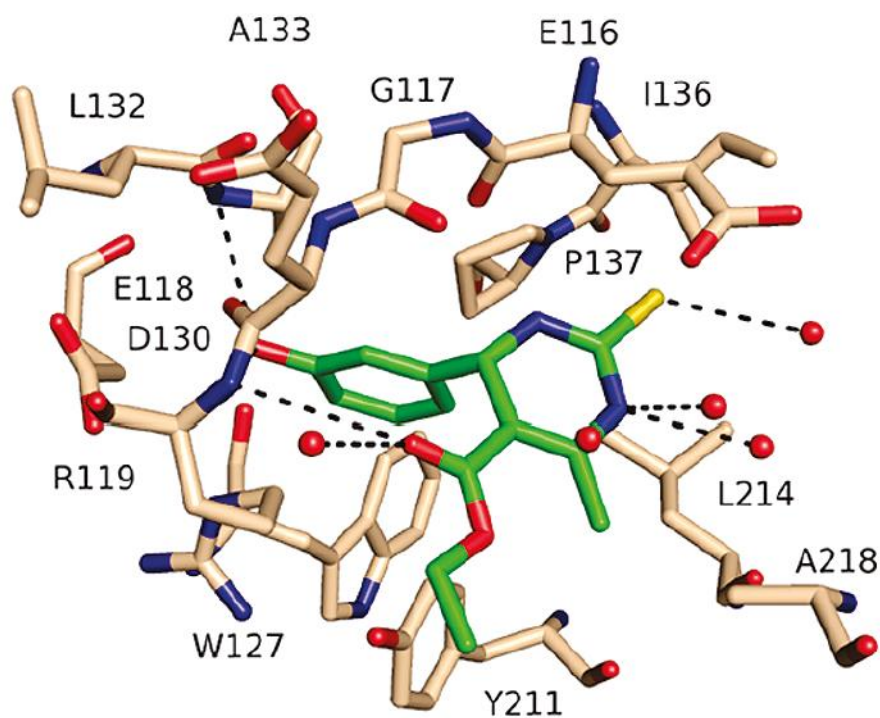
Figure 1.12: S-Monastrol interaction with Eg5 residues[56]

The pocket is created by the downward movement of loop 5 by 7 Å. The side chain of Trp127 moved inward while the two side chains of Arg119 on helix α2 and Tyr211 on helix α3 moved outward. A comparison of the region before (red) and after (green) monastrol binding is shown in **Figure 1.13**
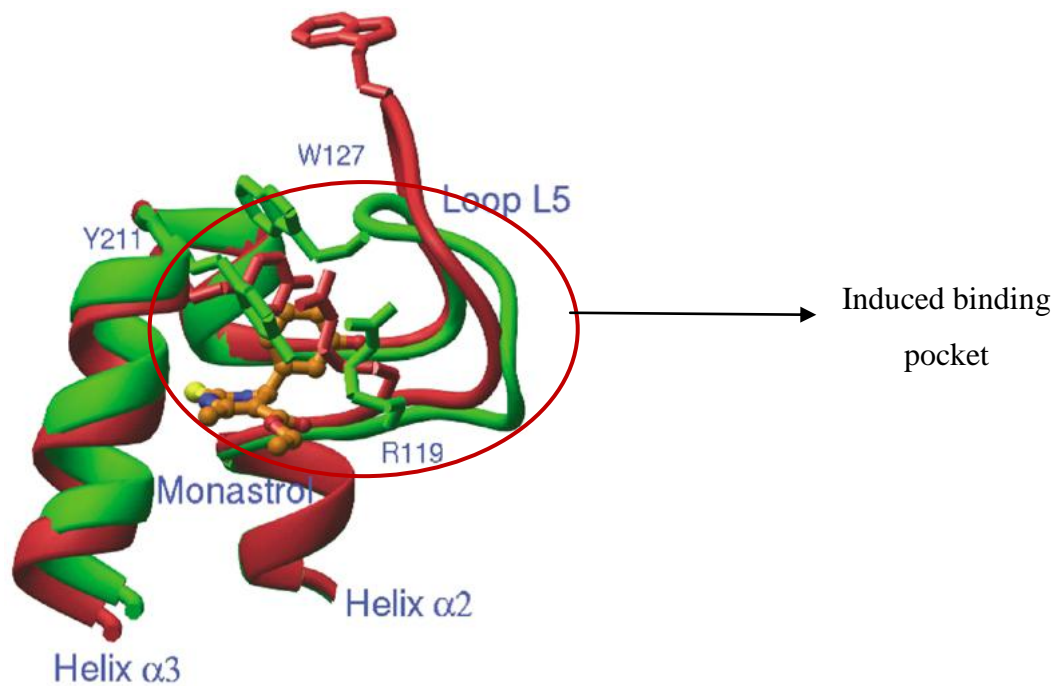
Figure 1.13: Induced binding pocket before (red) and after (green) monastrol binding.[55]

Other changes observed upon monastrol binding away from the binding pocket are in the switch-I, switch-II and neck linker regions. Switch-I changed from a featureless loop to a short helix and the main chain was shifted by 6 Å. The V-shape of switch-II, which is located on the backside of the motor away from monastrol by about 30 Å, expanded by 20° to yield a wider opening. This widening generated a space for the neck linker. The residues Asn358 and Lys362 of the neck linker rotated by 120° and locked into the new opening of switch-II. These changes in the neck linker are the most significant because of its very important role in the mechanical movement of the motor.[57] The changes in the shape of the three regions are illustrated in **Figure 1.14**.
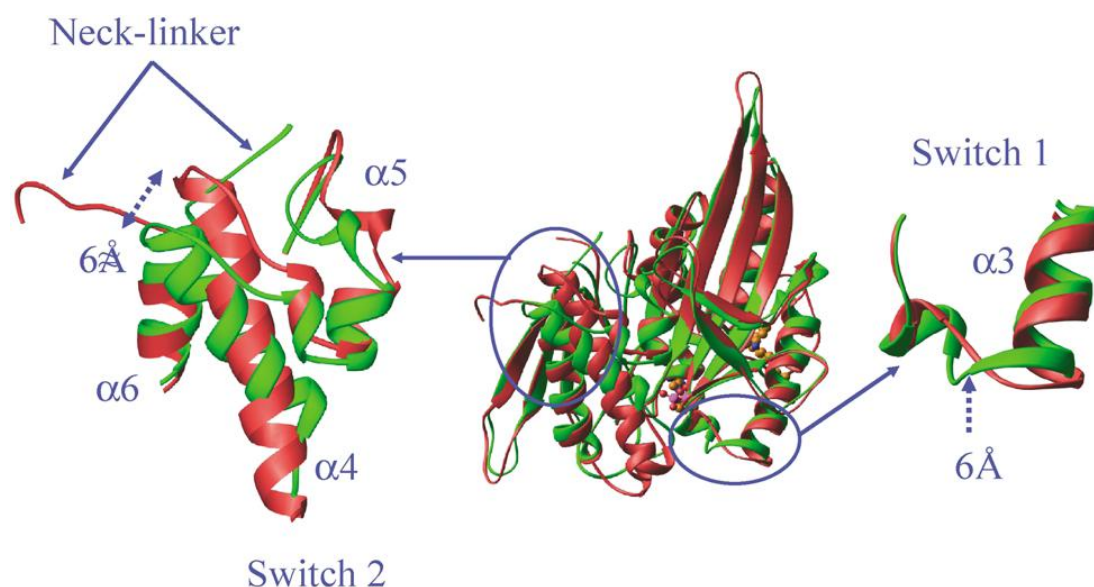
Figure 1.14: Changes in switch-I, switch-II and the necklinker before (red) and after (green) monastrol binding to Eg5.[55]

1.3.1.1 Monastrol analogues (dihydropyrimidine derivatives)

The development of more potent monastrol analogues has focused on introducing structural rigidity into the molecule by modifying the sidechain ester into a cyclic ketone.[58, 59] These derivatives showed significantly better inhibition of Eg5 compared to monastrol; enastron (**1**) and dimethylenastron (**2**) were 10 and 100 fold more active respectively. Reduction of the carbonyl to the corresponding alcohol (compound **3**) also resulted in moderate inhibitory activity (IC_{50}= 2µM).

Further modifications to monsatrol were carried out by Klein *et al*,[60] who showed that substitution on the sulphur atom completely abolished activity and a furyl moiety at C5 of the dihydropyrimidine (compound **4**) resulted in improved activity (IC_{50}= 9.2µM).

The monastrol-related fused heterocyclic analogue (compound **5**) was inactive,[61-63] whereas compound **6**, a keto dihydropyrimidine related to the furyl analogue (**4**) known as monastrol-97, has better ATPase basal inhibitory activity (0.12µM). The crystal complex of this compound with Eg5 has been solved, and in contrast to monastrol, the more effective form is the *R*-enantiomer.[64] The chemical structures

and the inhibition activities of these monastrol analogues are summarised in **Figure 1.15**.

1   R=H enastron (MIC$_{50}$= 2μM)
2   R=CH$_3$ dimethylenastron (IC$_{50}$= 0.2μM)

3   IC$_{50}$= 0.2μM

4   (IC$_{50}$= 1.5μM)

5   No inhibition

Mon 97

6   (IC$_{50}$= 0.12μM)
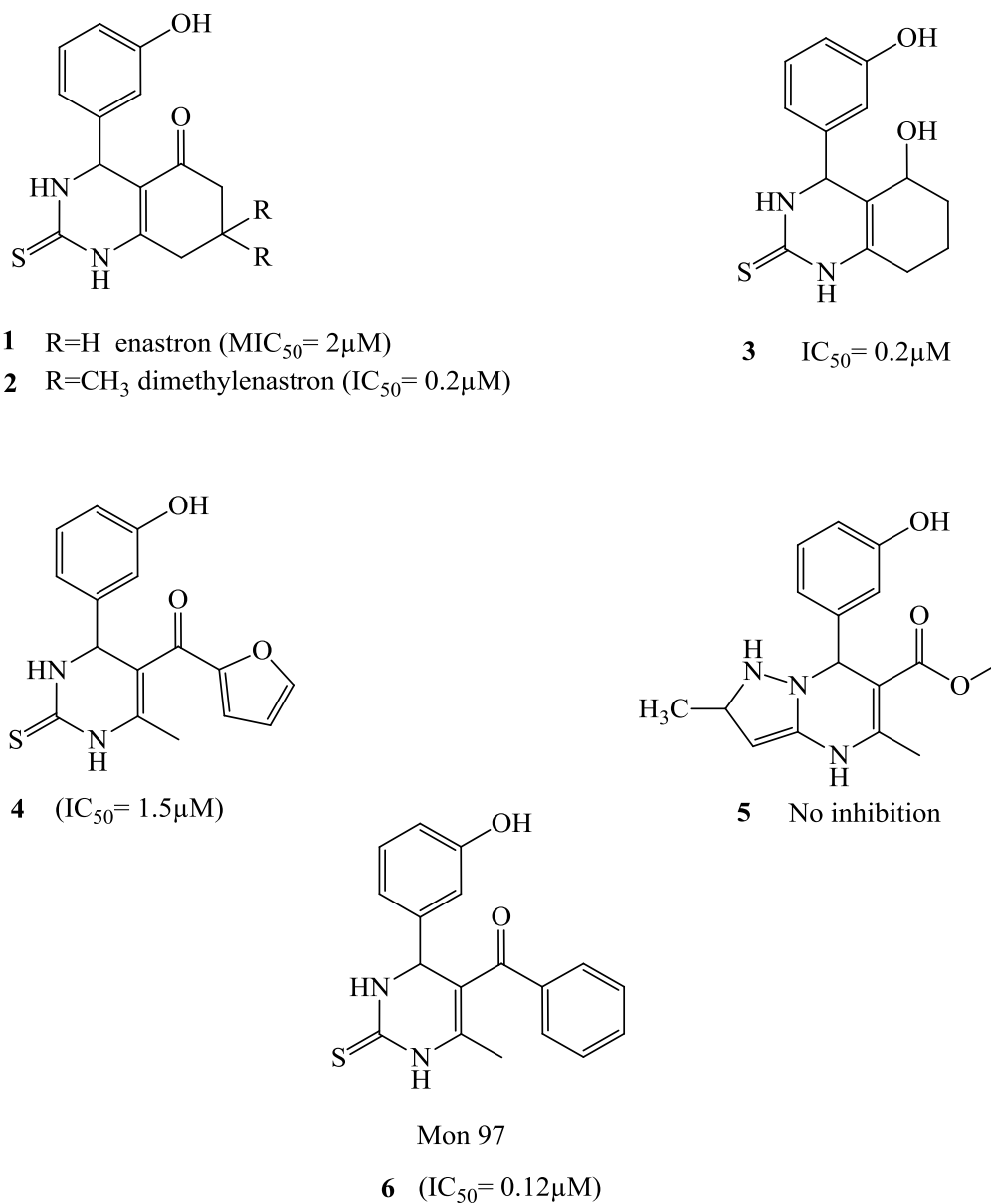
Figure 1.15: Dihydropyrimidine derivatives.

1.3.2 *S*-Trityl-L-cysteine (STLC)

A screening study by Debonis *et al*[65] using a small-molecule library of 2869 molecules from the National Cancer Institute (NCI) to search for Eg5 inhibitors identified 154 molecules that inhibited microtubule activated Eg5 activity, of which only 15 were found to inhibit Eg5 basal ATPase activity. STLC was the most

effective inhibitor of Eg5 ATPase basal activity (IC_{50} 1.0 µM) and induced a phenotype mitotic arrest in dividing cells (IC_{50}, 700 nM) with no visible effect on the microtubules. Additionally, STLC showed no toxicity in interphase cells at high concentrations (100 µM), with no obvious visual defects on the cells. Most interestingly, STLC inhibited tumour growth in the NCI 60 tumour cell line screen. While STLC has one chiral centre and can exist as the enantiomer STDC, both have comparable activity against the ATPase activity of Eg5 motors. The cell based assay against HeLa cell also showed that their anti-mitotic arrest was almost equally potent.

STDC   STLC
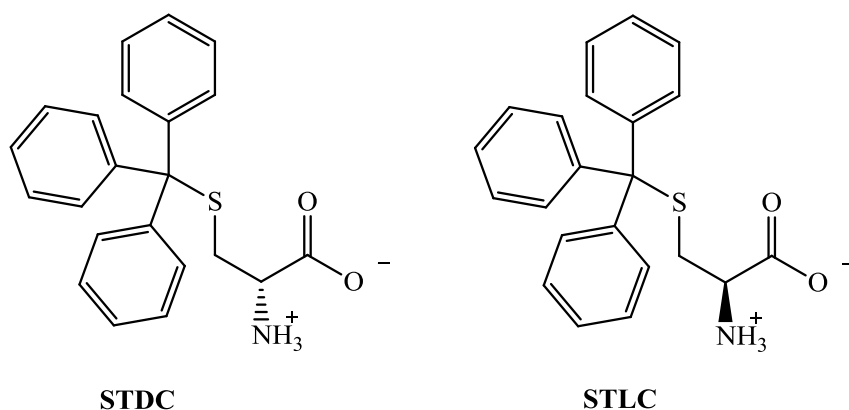
STLC does not inhibit cell cycle progression in the S or G2 phases and exerts a specific anti-mitotic arrest through the inhibition of centrosome separation leading to unseparated centrosomes with condensed arrays of microtubules coming from the centre of the cells. STLC does not interfere with centrosome duplication, with microtubule distribution and nucleation, or the microtubules network (**Figure 1.16**). STLC is a reversible inhibitor of mitosis; when washed out of HeLa cells, more than 50% of the cells completed mitosis after 2 hours. It appears to be non-toxic at high concentrations and, when tested against different kinesins in the superfamily, it was specific for Eg5 motors.[66]
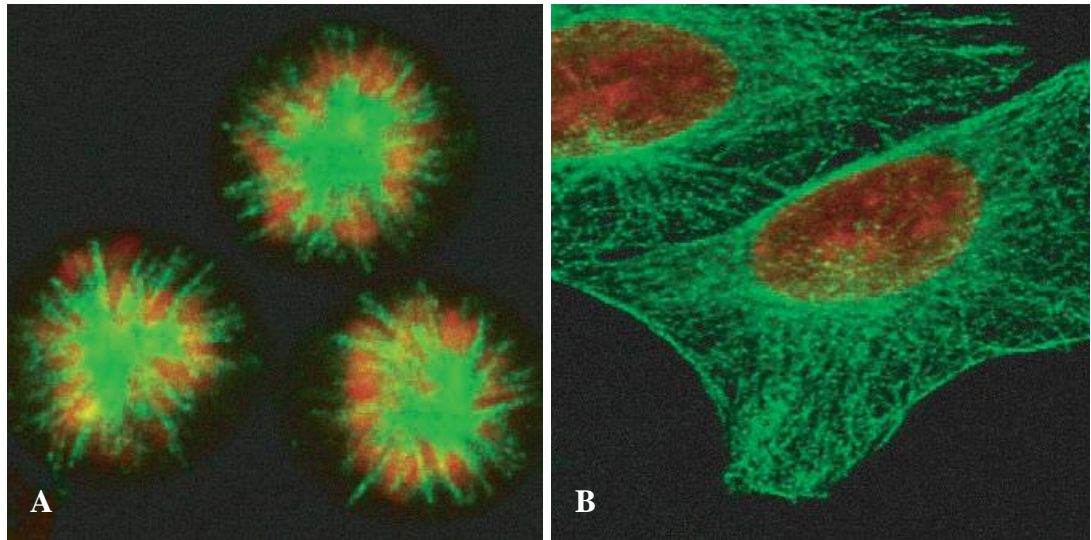
Figure 1.16: Observed phenotype of (A) monoastral cells treated with STLC (B) normal interphase microtubule network treated with 100 μM STLC.[65]

The IC_{50} of STLC varies according to Eg5 concentration because it is a slow, tight binding inhibitor. A dose response curve of fractional velocities (**Figure 1.17**) is required to calculate the IC_{50} using the Morrison Equation, which is the best fit for tight binding inhibitors:[67]

where v_0 is the velocity in the absence of inhibitor; v_i is the measured velocity; [E] is the total enzyme concentration; [I] is the added inhibitor concentration, and K_{iapp} is the apparent equilibrium inhibition constant depending on the inhibition type.
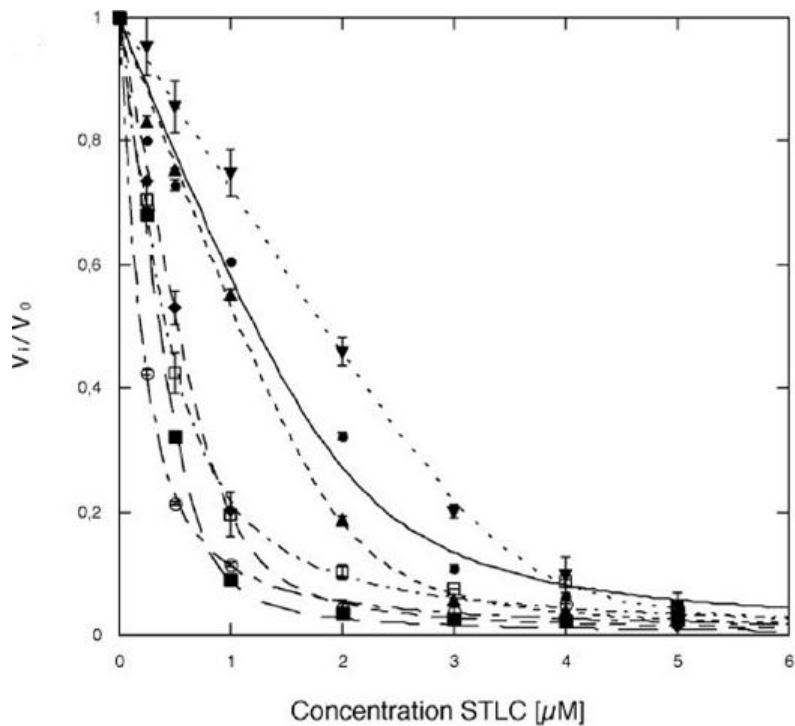
Figure 1.17: Dose-response plot of fractional velocities as a function of increasing STLC concentrations.[66]

The calculated IC_{50} at variable Eg5 concentrations was then plotted against different concentrations of STLC, with the intercept at the Y axis representing the estimated K_{iapp} (**Figure 1.18**). The calculated K_{iapp} of STLC inhibition of basal Eg5 using this approach was found to be 140 nM.[66] This procedure is recommended in order to get a consistent and a representative IC_{50} for known tight binding inhibitors.
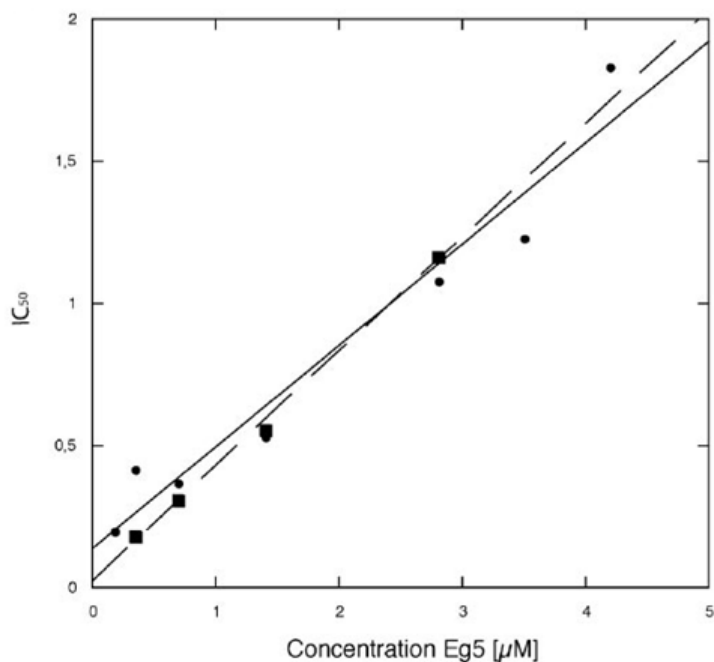
Figure 1.18: Plot of IC$_{50}$ values for STLC and STDC.[66]

1.3.2.1 Crystal structure of Eg5–STLC complex

The co-crystal structure of Eg5-STLC was solved at a resolution of 2.0Å.[68, 69] STLC was found to occupy the same allosteric pocket as monastrol bordered by helix α2, loop L5 and helix α3 (**Figure 1.19a**). The three phenyl rings in STLC were situated inside the hydrophobic pocket with several hydrophobic interactions; one of the phenyl groups formed a hydrophobic interaction with alkyl side chains of Glu215 and Arg119, and a C–H–π interaction was observed between one phenyl group of STLC and the pyrrolidine ring of Pro137. The phenyl ring of Trp127 formed an edge–face (T shape) interaction with one of the STLC phenyl groups. The cysteine amino acid moiety was solvent-exposed outside the pocket. The primary amine formed a hydrogen bond with the backbone carbonyl oxygen of Gly117 and the side chain carboxylate oxygen of Glu116. The oxygen of the carboxylic acid also formed a hydrogen bond with the side chain NH$_2$ of Arg221. Both these moieties were able to form hydrogen bonds with structural water molecules (**Figure 1.19b**).

23
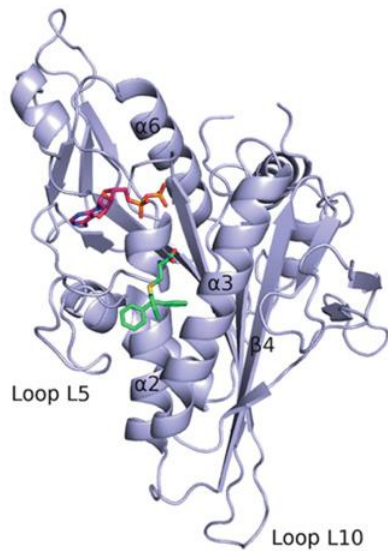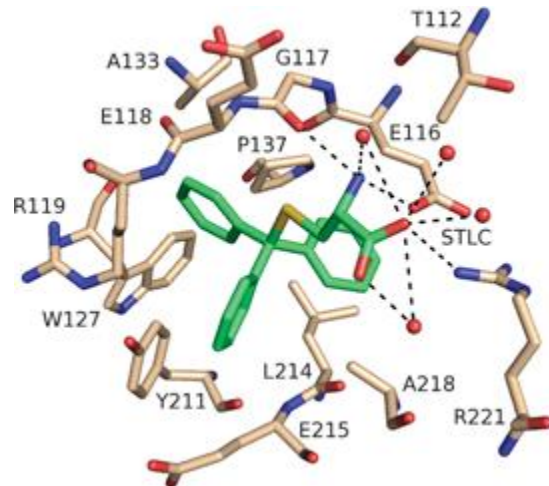
Figure 1.19: (a) STLC bound to an allosteric pocket distinct from the nucleotide binding site (b) STLC interactions with pocket residues.[69]

The conformational changes induced by STLC in Eg5 were almost identical to those induced by monastrol. Loop 5 moved downward by approximately 7Å after binding STLC (**Figure 1.20a**); the switch-I of helix α3 was shifted towards the solvent by approximately 6Å with an additional one turn of the helix; the switch-II cluster rotated approximately 15° from the native Eg5 structure (**Figure 1.20b**), which made space allowing the neck linker to move by 32° and dock in a position parallel to helix α6 (**Figure 1.20c**).
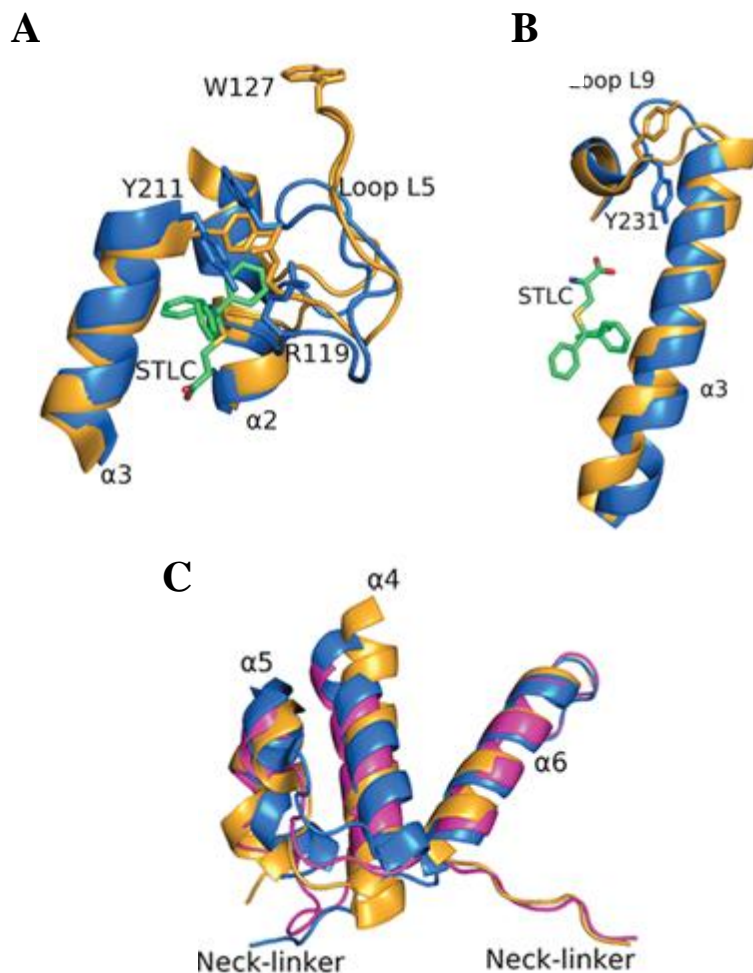
Figure 1.20: Conformational changes of (a) Loop 5 (b) Switch-I (c) Switch-II before (yellow) and after (blue) STLC binding to Eg5 motor.[69]

1.3.2.3 STLC analogues
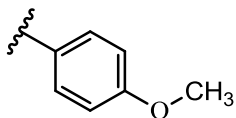
Structure activity relationship (SAR) studies[70, 71] for related STLC analogues (**Table 1.1**) showed that different substituents on the sulphur resulted in a loss of activity (compounds **7-14)**, suggesting that a triaryl-substituted methyl group was essential for activity. Furthermore, STLC analogues with only two phenyl rings had much lower activity, and bridging two phenyl rings in a fluorene motif to restrict the free rotation of the phenyl rings also decreased activity (compounds **19 and 20**).Conversion of the carboxylic acid to the primary amide or ester slightly increased the activity, especially in the cell based assay (compounds **15 and 16**).
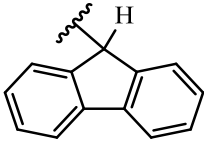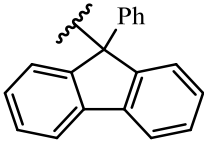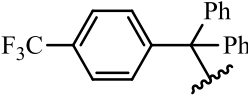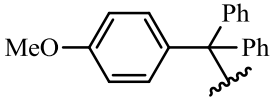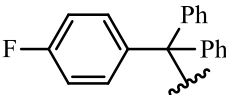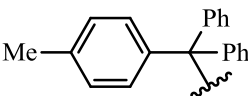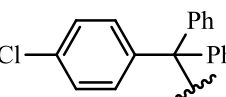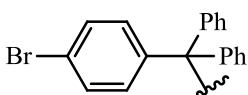
High increases in activity were observed through incorporation of different substitutions on the phenyl ring (compounds **21-26**). Substitution at the *para* position

with methoxy, fluoro, chloro, bromo, methyl and trifluoromethyl yielded compounds with 7-10 fold increases in their ATPase inhibition activity against Eg5 compared to STLC.

The primary amino group was found to be essential for activity: protection of this group, conversion to the secondary or tertiary amines (compounds **17,18, 27-29,**), or its removal altogether, resulted in total loss of activity.
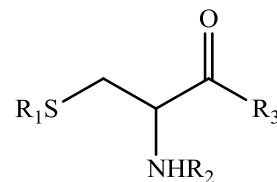
Compound	R$_1$	R$_2$	R$_3$	ATPase IC$_{50}$ (μM)	Cell based assay EC$_{50}$ (μM)
STLC	CPh3	H	OH	1.8	3.29
7	H	H	OH	>63	>50
8	CH$_3$	H	OH	>63	>50
9	t-But	H	OH	>63	>50
10	CH$_2$Ph	H	OH	>63	>50
11		H	OH	>63	>50
12	CH$_2$COOH	H	OH	>63	>50
13	CH$_2$CH$_2$NH$_2$	H	OH	>63	>50
14	CHPh$_2$	H	OH	>63	>50
15	CPh$_3$	H	OMe	5.8	1.72
16	CPh$_3$	H	NH$_2$	3.1	1.78
17	CPh$_3$	Fmoc	OH	55	11.9
18	CPh$_3$	Boc	OH	>63	>50

#	Structure				
19		H	OH	>63	>50
20		H	OH	1.5	>5
21		H	OH	0.22	0.53
22		H	OH	0.15	0.21
23		H	OH	0.15	1.55
24		H	OH	0.1	0.21
25		H	OH	0.2	0.51
26		H	OH	0.25	0.31
27	CPh_3	-NH-Tr	OH	No inhibition	No inhibition

28
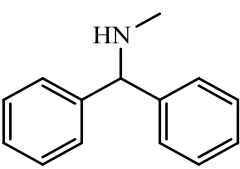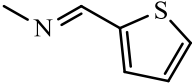
28	CPh$_3$		OH	No inhibition	No inhibition
29	CPh$_3$		OH	No inhibition	No inhibition

Table 1.1: SAR studies of STLC analogues.

The minimum structure required for activity is represented by compound **30**.
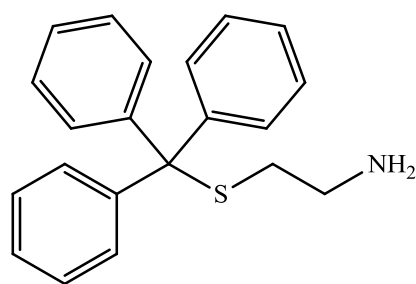
Compound 30

1.3.3 Dihydropyrazole derivatives

A breakthrough in the discovery of potent and selective Eg5 inhibitors was the 3,5-diaryl-4,5-dihydropyrazole derivatives by Cox *et al* (**Figure 1.21**).[72] These compounds inhibited activity against ovarian carcinoma at low nanomolar concentrations. Substitution on one of the aryl rings with a difluoro substituent (compound **31**) improved inhibitory activity against Eg5 to an IC_{50} of 94 nM. Adding a *m*-hydroxyl group to the second ring further improved the inhibitory activity against the Eg5 proteins to 51 nM (compound **32**). The pure *S*-enantiomer of compound **31** was separated using HPLC chiral column chromatography (compound **33**) and was 5 times more active than the racemic mixture (IC_{50}= 26nM).

31 (IC_{50}=94 nM) **32** (IC_{50}=51nM) **33** (IC_{50}=26 nM)
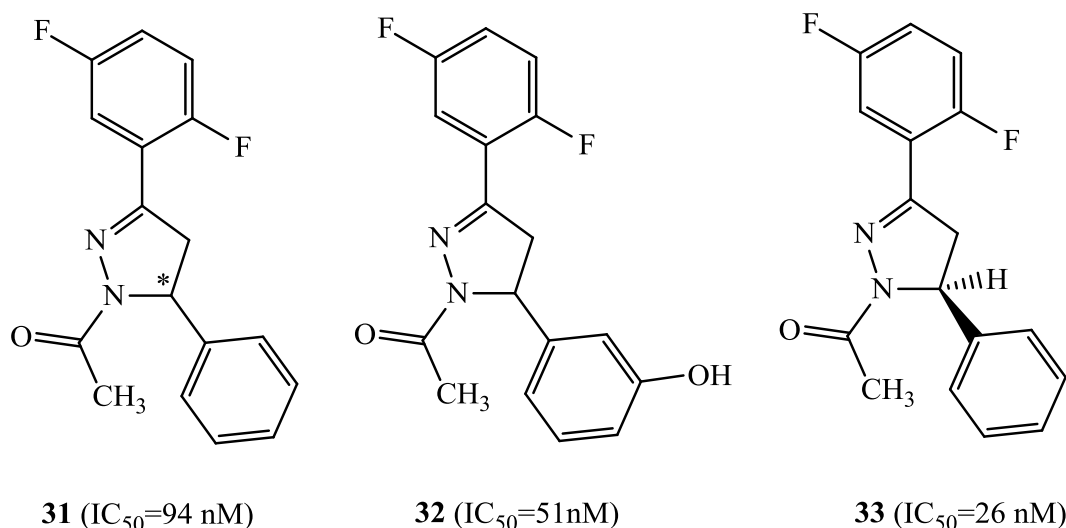
Figure 1.21: Dihydropyrazole derivatives

The main problem with the development of compound **33** was its poor aqueous solubility that prohibited its formulation for intravenous administration. The introduction of an alkylamino group at the C5 position of the 4,5-dihydropyrazole core produced an Eg5 inhibitor that displayed improved potency, pharmacokinetics and water solubility (compound **34**).[73] In a continued attempt to lower the intrinsic susceptibility for Pgp efflux because of the alkyloamine motif, a single β-fluorine substitution was introduced to lower its pKa (compound **35**), which preserved cellular potency in Pgp over-expressed cells without affecting the *in vivo* activity.[74]
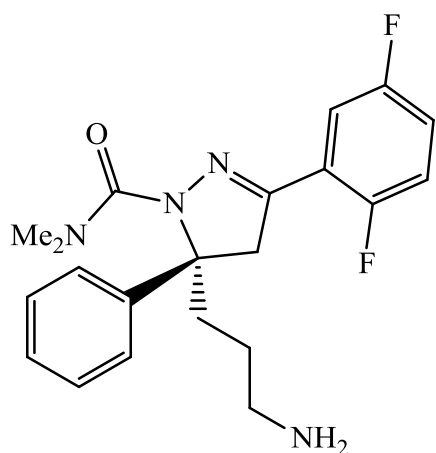
34 (IC$_{50}$=1.9 nM)
MDR 491
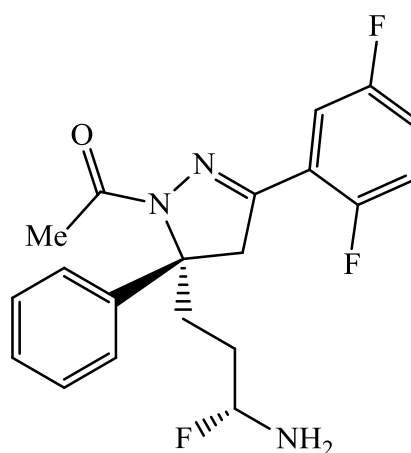
35 (IC$_{50}$=0.82 nM)
MDR 5.2

1.3.4 Dihydropyrrole derivatives

The aim of this work was to modify the core structure of the 4,5-dihydropyrrazole to a dihydropyrrole in order to improve the reactivity of the amide forming unit whilst maintaining the orientation of the two aryl groups to increase the potency.[75] In racemic mixtures, a branched acyl group was found to be necessary for activity, which was further modified to improve aqueous solubility for intravenous injection (**Table 1.2**). Resolution of the enantiomers produced compounds with very potent Eg5 inhibitory activity (**39**, **41** and **42**).
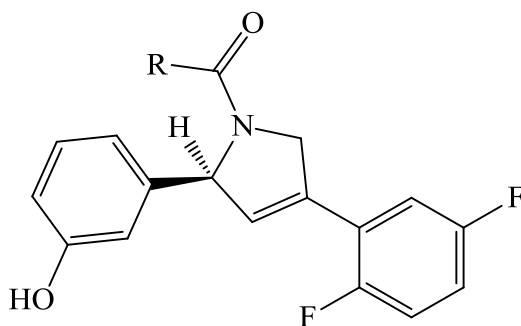
Compound	R	Eg5 IC$_{50}$ (nM)
36*	Me	94
37*	t-But	113
38*	NMe$_2$	84
39		2.6
40		50
41		5.2
42		2.0

Table 1.2: Structure activity relationship studies of dihydropyrrole derivatives.

* Racemic mixtures tested

In a parallel study by the same research group,[76] an aminopropyl substituent (**Figure 1.22**) was incorporated at the 2-position of the dihydropyrrole moiety to successfully increase potency to 2.2 nM (compound **43**), although this compound suffered significantly from Pgp efflux (MDR ratio = 1200). As before, modulation of the basicity of the amine by fluorination yielded compounds with an improved MDR ratio (**44** and **45**),[77, 78] but with poor *in vivo* activity (**45**) in a mouse xenograft assay. Compound **46** was developed with an optimized *in vitro* and *in vivo* profile; mouse xenograft assays showed it induced dose dependent mitotic arrest in tumours with inhibitory profiles comparable to paclitaxel. Compound **46** is currently in phase I clinical trials in patients with taxane refractory solid tumours.[79]

43 (IC$_{50}$ 2.2 nM)
MDR=1200

44 (IC$_{50}$ 110 nM)
MDR=1

45 (IC$_{50}$ 5.2 nM)
MDR= 5

46 (MK-0730)
(IC$_{50}$ 7.6 nM)
MDR=4.5
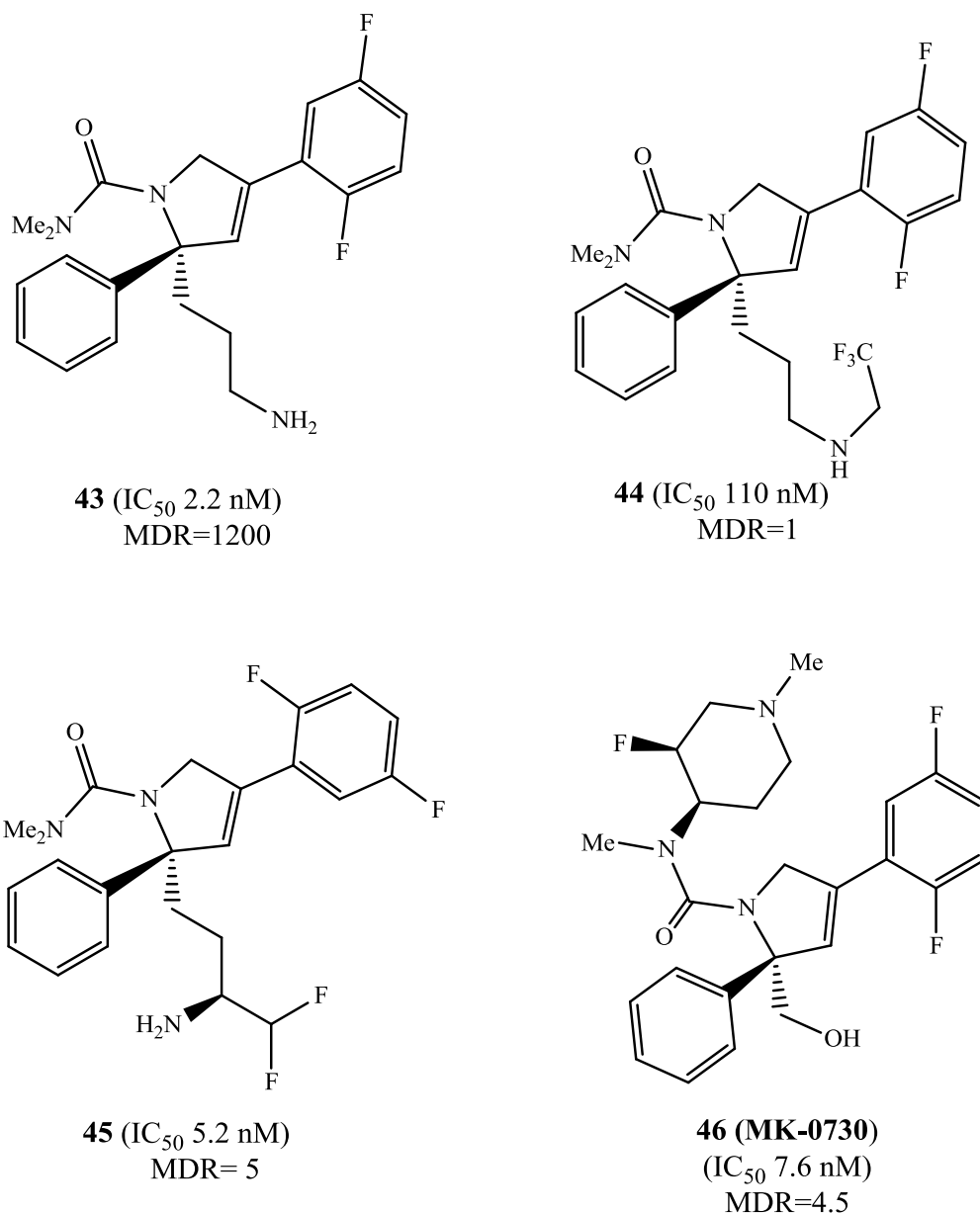
Figure 1.22: Dihydropyrrol derivatives.

1.3.5 Dihydropyrazolobenzoxazines

An SAR study[80] (**Table 1.3**) on dihydropyrazolobenzoxazines showed substitution at R$_1$ with F, Cl and methyl resulted in a similar potency ratio, whereas the nature of the R$_2$ substituent had a significant impact on hERG binding and the MDR ratio. Generally, amines with reduced basicity showed weaker hERG binding (compounds (**50, 52, 53, 54, 56**), while stronger basic compounds had stronger hERG binding (compounds **47-49, 55, 57**). MDR appeared to be less of an issue with this class of

compounds, and independent of pKa. Only compound **57** showed a tendency to undergo Pgp-induced efflux compared with all of the other amines.
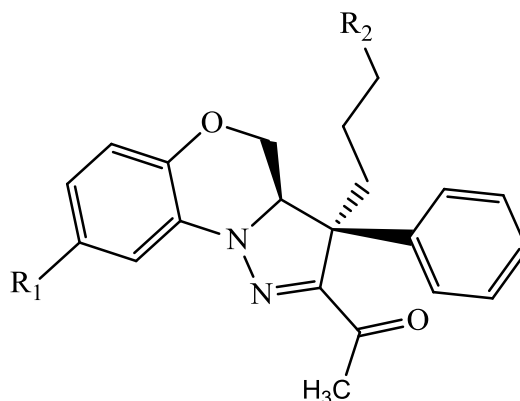
Compound	R_1	R_2	KSP IC$_{50}$ (nM)	MDR ratio	hERG IC$_{50}$(nM)
47	F	Me$_2$N—	1.6	2.3	5940
48	Cl	Me$_2$N—	1.0	2.5	2000
49	Me	Me$_2$N—	1.8	2.3	2400
50	F	morpholine	0.4	0.8	6100
51	Cl	morpholine	1.8	1.5	300
52	Me	morpholine	1.0	1.4	6300
53	F	AcN-piperazine	1.6	1.0	10000
54	Cl	AcN-piperazine	1.0	1.6	5600
55	F	NH$_2$	0.5	1.7	940
56	F	OH	5.2	0.6	18000
57	F	HN-piperazine	4.3	40	4600

Table 1.3: Structure activity relationship studies of dihydropyrazolobenzoxazine derivatives.

1.3.6 Tetrahydro-β-carboline derivatives

Tetrahydro-β-carbolines were discovered by Hotha *et al*[63] to be specific Eg5 inhibitors. HR22C16 showed an inhibitory activity of 800 nM, which was improved 9-fold by terminating the aliphatic side chain of the imidazolidine ring with an

ethylamino group (compound **58**). *Trans* isomers at position C11 were generally more active that the corresponding *cis* isomers, for example the *trans* isomer of HR22C16 has an IC_{50} of 21µM, compound **59** with a phenyl substitution had an inhibitory activity of IC_{50} 0.68µM.[78, 81]
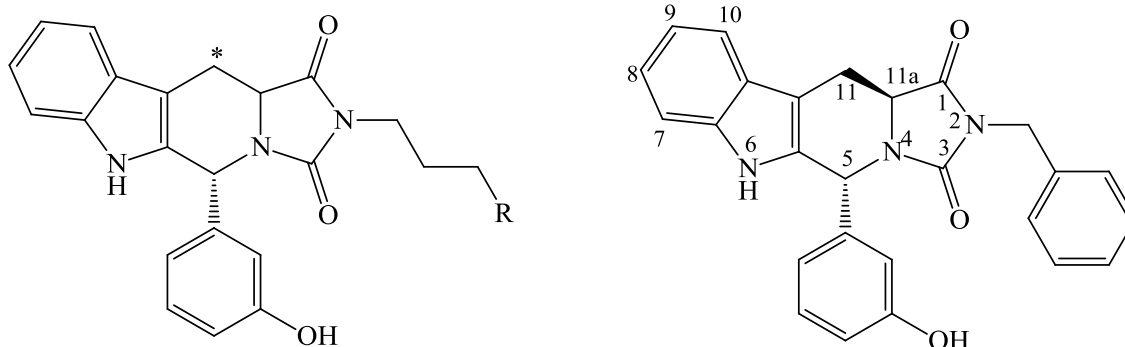
HR22C16	R=H (***Trans***)*	(IC_{50} 0.8 µM)
	R=H (***Cis***)*	(IC_{50} 21 µM)
58	R=$CH_2CH_2NH_2$ (***Trans***)*	(IC_{50} 0.094 µM)

59 (IC_{50} 0.68 µM)

A recent HTS campaign[82] against Eg5 (**Table 1.4**) identified the tetrahydro-β-carboline derivative (compound **60**) as an inhibitor with an IC_{50} of 2.5µM. The addition of a single methyl group in the aryl ring yielded a compound (**61**) with a 10 fold increase in activity. When co-crystallized with Eg5 motors as a racemic mixture, only the *R*-enantiomer was bound to the characteristic allosteric binding site. The crystal structure showed that the phenolic hydroxyl group formed a hydrogen bond with the backbone carbonyl of Glu118 in a similar way to the phenolic group in monastrol, and was essential for activity - when replaced by H; the activity decreased 10 fold, and by 100 fold when replaced by methyl (compounds **61-63**).

The introduction of an amino functionality of differing chain lengths (compounds **65** and **66**), to pick up additional hydrogen bonds increased potency further. Small hydrophobic groups in the aromatic ring of the tetrahydro-β-carboline nucleus were required and followed the trend of Et > Me = Br > Cl in terms of inhibitory activity (compounds **66-69**).
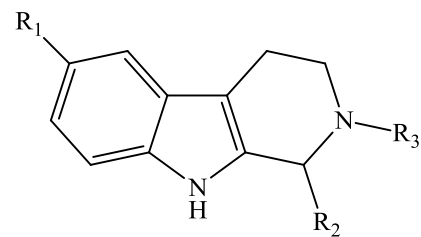
Compound	R_1	R_2	R_3	Eg5 IC$_{50}$ (µM)
60	H			2.5
61	CH$_3$			0.2
62	CH$_3$			25
63	CH$_3$			250

37
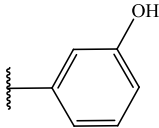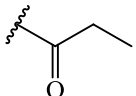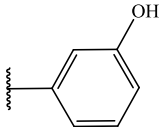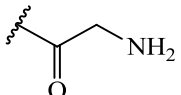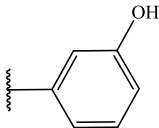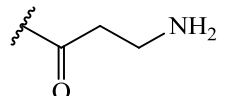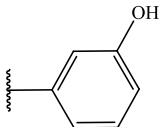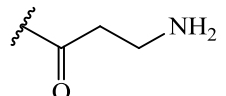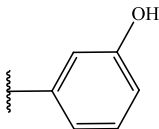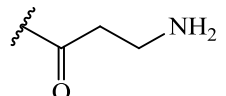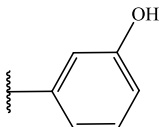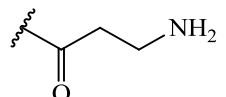
| 64 | CH₃ | | | 0.46 |

64	CH₃			0.46

64	CH$_3$			0.46
65	CH$_3$			0.049
66	CH$_3$			0.020
67	CH$_2$CH$_3$			0.011
68	Br			0.027
69	Cl			0.039

Table 1.4: Structure activity relationship studies of the tetrahydro-β-carbolines.

1.3.7 Ispinesib related compounds

Ispinesib was first discovered by Roman Sakowicz *et al*[83] when screening a small synthetic organic library; he identified a series of quinazolinones which had Eg5 inhibitory activity. The synthetic optimization of these compounds led to ispinesib, with an Eg5 inhibitory activity of 12nM.

Ispinesib showed a mitotic arrest in varieties of human cancer cell lines with an average growth inhibitory activity of 364 nM (**Table 1.5**) and an average MDR ratio of approximately 5.

Cell line	IC$_{50}$ (nM)	Tumour type
SKOV3	126 ± 26	Ovarian carcinoma
A2780	191 ± 47	Ovarian carcinoma
A549	238 ± 77	Non-small cell lung carcinoma
NCI H460	307 ± 31	Non-small cell lung carcinoma
SF-268	297 ± 51	CNS
HT29	533 ± 135	Colon carcinoma
U2OS	426 ± 69	Osteosarcoma
DU145	466 ± 71	Prostate
HCT-15	295 ± 68	Multidrug-resistant colon carcinoma
B16	399 ± 72	Murine melanoma

Table 1.5: Cell inhibitory activities of ispinesib.

Ispinesib contains a single chiral centre and is a racemic mixture of *R* and *S* enantiomers. When resolved, the *R*-enantiomer (**R-Ispinesib**) was 1000 fold more potent than the *S*-enantiomer (**S-Ispinesib**). Stereospecificity was also apparent in the cellular activity; the *S*-enantiomer was 100-fold less effective in inhibiting cell growth than the *R*-enantiomer. Ispinesib showed *in vivo* 71% tumour growth inhibition in doses of 25mg/kg when administered daily for 5 days to mice with human carcinoma xenografts.

Since the discovery of ispinesib, research has been directed towards further optimization (**Figure 1.23**), such as the replacement of the quinazolinone core. Cytokinetics (jointly with GSK) have disclosed a large number of patent applications regarding such modifications: an isoquinolin-1-one[84] (compound **70**), a 4*H* -pyrano[2,3-*b*]pyridine-4-one[85] (compound **71**), an oxazolin-2-one[86] (compound **72**), an imidazolin-2-one[87] (compound **73**) and an 1,2,4-oxadiazol-5-one[88] (compound **74**), although there is no inhibitory data given for these compounds.

Cytokinetics also disclosed chromen-4-one derivatives such as **SB-743921**[89] which is currently undergoing Phase II clinical trials. This compound is superior to ispinesib with regard to its ATPase inhibitory activity (IC_{50} = 0.1 nM compared with 0.6 nM)

Researchers at Chiron have also identified fused pyrimidin-4-one derivatives as Eg5 inhibitors: the thieno[3,2-*d*]pyrimidin-4-one[90] (compound **75**) and the pyrido[1,2-*a*]pyrimidin-4-one[91] (compound **76**) had ATPase IC_{50} inhibitory activity of < 1 μM and < 0.1 μM, respectively.

AstraZeneca have also disclosed patent applications for compounds with the quinazoline moiety replaced by isothiazolo[4,5-*d*]pyrimidines[92] (compound **77**) and pyrimido[2,1-*b*]-1,3-thiazines[93] (compound **78**). The ATPase IC_{50} inhibitory activity for the racemic mixture was 90 nM and 331 nM, respectively.

Overall, a large number of reports have demonstrated a successful improvement in activity by replacement of the quinazoline moiety with different heterocycles and

modifications of the *N*-aminoalkyl chain both improved activity and reduce susceptibility to Pgp efflux.[94]
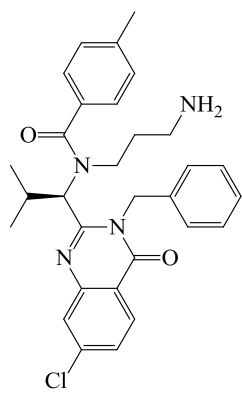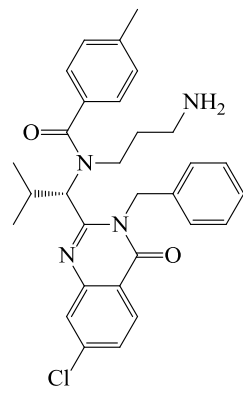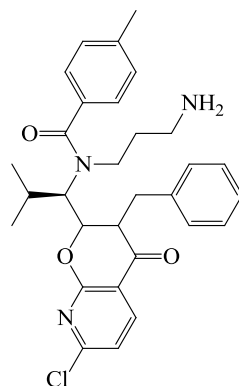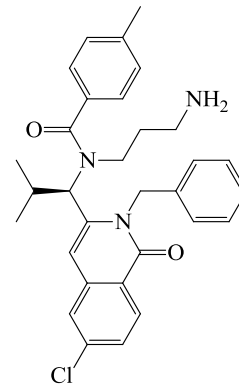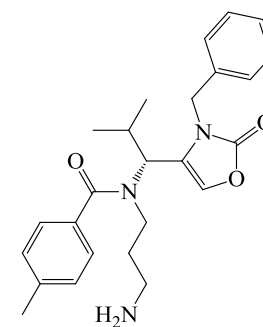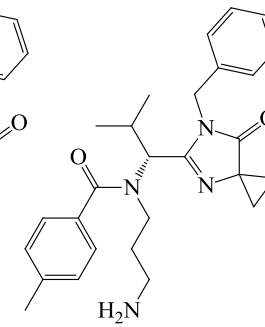
R-Ispiniseb   **S- Ispiniseb**   **70**   **71**   **72**   **73**
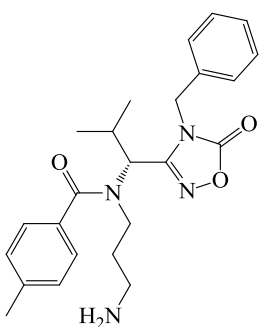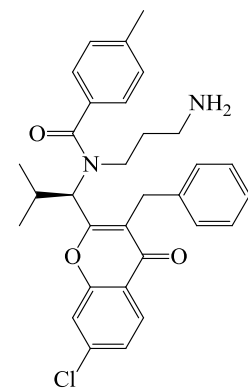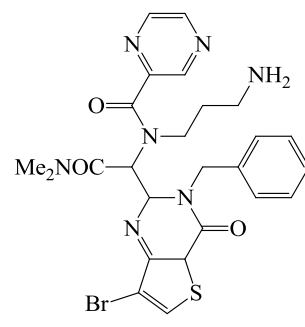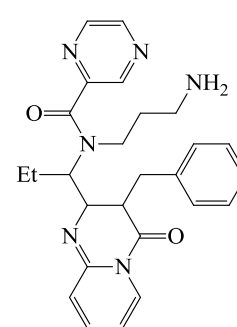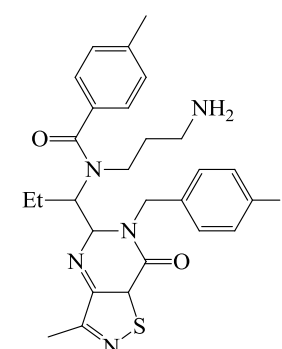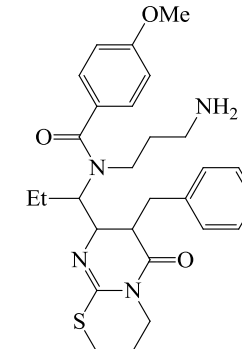
74   **SB-743921**   **75**   **76**   **77**   **78**

Figure 1.23: Ispinesib and related compounds

1.4 Clinical experience with Eg5 inhibitors

The anticipated clinical use of Eg5 inhibitors has not been limited to specific tumours because Eg5 is essential for cell replication and expressed in different tumour cells. Furthermore, because Eg5 does not target microtubules, the neuropathic side effects experienced with the vinca alkaloids and taxanes are expected to be less of a problem. Several Eg5 inhibitors have already entered clinical trials (**Table 1.6**) and more are under development.

The first Eg5 inhibitor in clinical trials was ispinesib,[95] which was developed by Cytokinetics and GlaxoSmithKline.[96] Ispinesib is currently in Phase II clinical trials in patients with locally advanced or metastatic breast cancer, ovarian cancer, non-small-cell lung cancer (NSCLC) and head and neck cancer.[97] The most promising results were observed in patients with locally advanced or metastatic breast cancer.[98] However, clinical efficacy was limited in some of the clinical trials which failed to meet continuation criteria, including trials conducted on metastatic colorectal cancer and head and neck cancer.

Clinical trials have so far shown that ispinesib was well-tolerated with an acceptable safety profile with no indications of neurotoxicity. Some side effects were neutropenia, fatigue, anaemia, leukopenia, thrombocytopenia, diarrhoea, nausea, and vomiting.[99, 100] Ongoing clinical trials using ispinesib in conjunction with other cytotoxic drugs are showing an acceptable tolerability profile and promising results.[101]

Cytokinetics/GSK are now conducting Phase II clinical trials on SB-743921 for patients with solid tumours.[102] Despite neutropenia being dose-limiting, as with ispinesib, the toxicity was manageable.[103]

AZD4877 is in a clinical trial for the treatment of solid tumours. EMD534085 has entered phase II for the treatment of solid tumours and haematological tumours. ARRY-520 is currently being investigated as a single agent; results from Phase I clinical trials indicate that it is well tolerated and has shown encouraging preliminary

results in the treatment of multiple myeloma.[104] Additionally, Merck have recently announced a Phase I trial for EMD534085 for solid tumours and hematological

malignancies. [94] The phase I study of MK-0731 was stopped because it did not meet the objective response criteria. [79, 105]
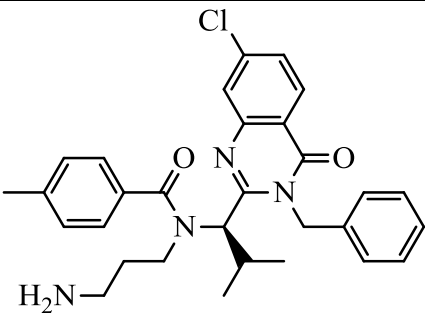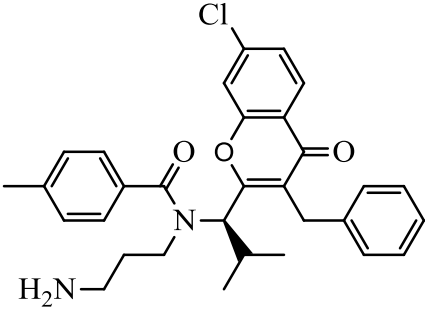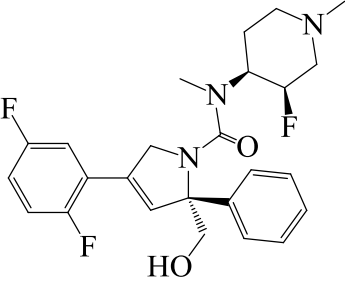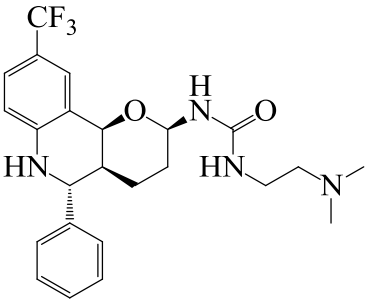
Compound	Chemical structure	company	Clinical phase
Ispinesib		Cytokinetics	II
SB-743921		Cytokinetics	II
MK-0731		Merck	Stopped
EMD534085		Merck	II
ARRY-520	Not known	Array BioPharma	I
AZD4877	Not known	AstraZeneca	I
LY2523355	Not known	Eli Lily	I

Table 1.6: Eg5 inhibitors undergoing clinical trials.

1.5 Cell resistance to Eg5 inhibitors

Many Eg5 inhibitors sustain their activity in cells overexpressing Pgp, suggesting that they are not substrates for the transporter. Growth inhibition assays in cell lines with and without overexpressed Pgp which are used to assess antiproliferative effects in comparison to paclitaxel, have shown promising results for Eg5 inhibitors.[17,106]

Tumour resistance to anticancer drugs can also result from an alteration in the drug target (enzymes and proteins).[107-109] For Eg5, the tumour cell may develop resistance through mutations in which the enzymatic activity is retained, but inhibition by specific inhibitors is lost. Understanding drug resistance through mutations in the binding pocket of Eg5 makes it possible to anticipate drug resistance in tumours when developing new Eg5 inhibitors. As all specific Eg5 inhibitors bind to the same allosteric pocket, studies have been performed to determine the key residues which are crucial for Eg5 inhibition. [110, 111] Eleven residues located in the binding pocket were mutated to alanine and the inhibitory effect of monastrol and STLC assessed against the recombinant mutated Eg5 and in HeLa and U2OS cells transfected with the mutant motor. Different inhibitory profiles were seen for the two inhibitors, which is down to their varying interactions with the amino acids in the binding pocket. R119A, D130A, P131A, I136A, V210A, Y211A, and L214A mutations conferred significant resistance to monastrol; the L214A mutation abolished the inhibitory effect of STLC, but R119A, P131A, Y211A and R221A mutations only converted STLC from a tight to a classic binder. Furthermore, the mutation of the key residue W127A on Loop5 did not confer significant resistance to either monastrol or STLC. Recently, cancer cells resistant to ispinesib were found to harbour a D130V substitution located in loop L5 of Eg5.[112] Based on these results, inhibition appears to be due to multiple interactions with residues located not only in loop5 but also in helices α2 and α3, and that drug mediated inhibition of Eg5 cannot be pinpointed to a single amino acid in the binding pocket. Rather, there are many different residues within the induced fit pocket of Eg5 that are equally important for ligand binding, and there will be other residues which have not yet been identified that could be important for binding.

1.6 Aims and objectives

Our aim was to optimise the structure of STLC against Eg5 using computer-aided drug design (CADD). The co-crystal structure of STLC-Eg5 that was recently solved by our co-workers at the Beatson Institute for Cancer Research, in association with other Eg5-inhibitor complexes, have provided us with rich information about binding to the allosteric site. This information was utilised to modify the scaffold and to assess the synthesised compounds against Eg5 basal ATP activity, in the absence of microtubules and different tumour cell lines.

The objectives were as follows:

- Optimise STLC using CADD.
- Synthesise the core scaffold and the structurally modified products.
- Assess the compounds *in vitro* in a specific ATPase inhibition activity test against the Eg5 motors.
- Assess the compounds against selected cell lines and evaluate their MDR activity.
- Correlate the results in order to develop an SAR profile

Chapter 2: Result and discussion

2.1 Establishing new active Eg5 inhibitors

The design of new compounds to specifically inhibit Eg5 was performed using computer aided drug design based on existing structure activity relationship (SAR) studies and the 3-dimensional crystal structure of the target protein. New inhibitors were designed and synthesised based on the geometry of the Eg5 binding site, the binding mode of STLC itself recently co-crystallised with Eg5 by our group, and through docking studies to evaluate the fitness of the designed compounds in the active site.

2.1.1 The binding site of Eg5

The protein crystal structure of Eg5 complexed with ADP and several different inhibitors has demonstrated that these compounds bind at an allosteric site 12 Å from the nucleotide binding site. Binding of the ligands at this pocket instigates a conformational change through the protein that prevents ADP release, thus locking the motor in an inhibited state. The allosteric pocket is lined with 20 amino acids forming three hydrophobic pockets of which pocket A is considered the most hydrophobic[70] (**Figure 2.1 and 2.2**). Any new inhibitor would be required to have a compatible size and properties to enable it to fit into the binding pocket and make the essential interactions with residues in the binding site.
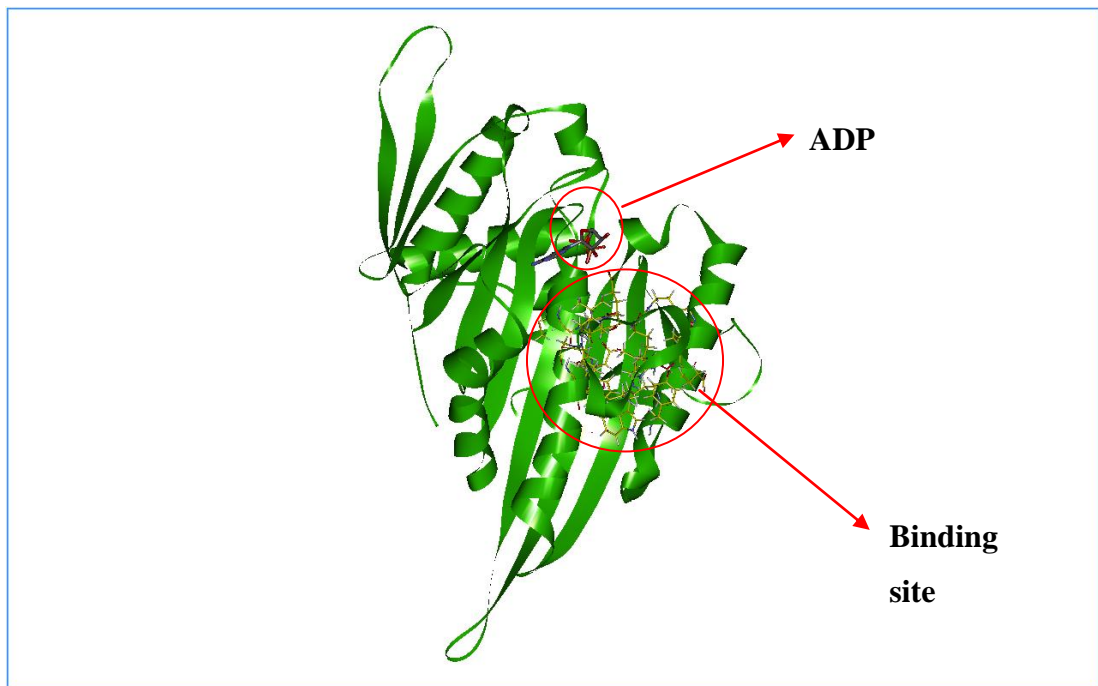
Figure 2.1: Eg5 allosteric pocket and the nucleotide binding site.
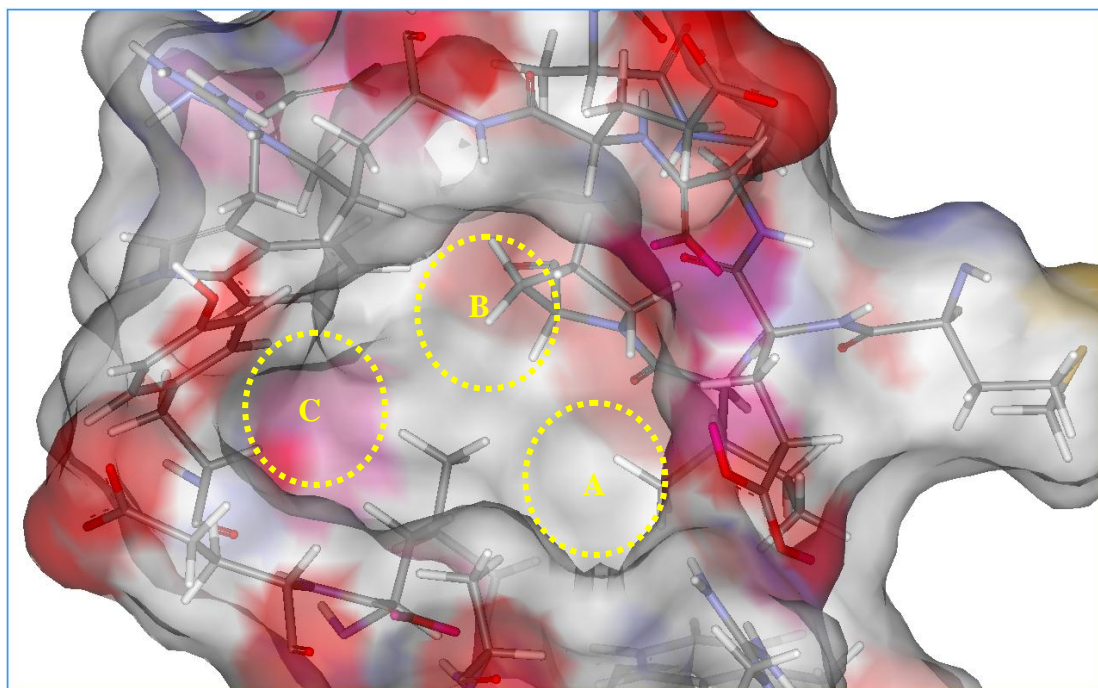
Figure 2.2: The three hydrophobic pockets of the Eg5 allosteric binding site.

2.1.2 Binding pattern of STLC

The recently published co-crystal structure of STLC-Eg5[68, 69] has provided useful information for consideration when designing new inhibitors. The crystal structure of the Eg5-STLC complex was solved at a resolution of 2.0 Å. The complex crystallised with one molecule of $Mg^{2+}ADP$ bound in the nucleotide binding pocket. The magnesium ion coordinated octahedrally with the nucleotide β-phosphate, the oxygen of the hydroxyl side chain of Thr112 and four water molecules. The allosteric pocket, bordered by helix α2, Loop L5 and helix α3, was occupied by STLC. The three phenyl rings of STLC were buried in the hydrophobic part of the pocket and displayed several hydrophobic interactions with the side chains of Glu215, Glu116 and Arg119. Also observed was an edge-to-face interaction between the first phenyl group of STLC and the indole ring of Trp127; a C—H---π interaction between the same phenyl group and the pyrrolidine ring of Pro137; stacked π-π interactions between the second phenyl group and Tyr211; and a C—H---π interaction between the third phenyl group and the side chain of Leu214. The hydrophilic cysteine moiety was solvent-exposed and formed several hydrogen bond interactions with the protein: the amino group with the main chain carbonyl oxygen of Gly117, the side chain oxygen of Glu116 and a structural water molecule; the carboxyl group of the cysteine moiety interacted with one of the side chain amino groups of Arg221 and five structural water molecules.

In a related study, our group has performed extended molecular dynamics (MD) simulations to examine and quantify which functionalities of the STLC structure are responsible for these specific inter-residue interactions. (**Figure 2.3**).[113] The phenyl headgroups (P1-P3) made a significant contribution to the binding free energy of the ligand (-6.42 Kcal/mol), which included hydrophobic interactions with the lipophilic pocket containing residues Tyr211 and Leu214 and, interestingly, through long-range electrostatic interactions with Glu116, Glu118, Glu128 and Asp130. Of most interest was the large stabilizing interaction by the cationic amino group (-10.29 Kcal/mol) with the acidic residues Glu116 and Glu118 and the backbone C=O of Gly117. Despite the distance between ADP and STLC, there was a long-range electrostatic interaction between the cationic amino group and the anionic

diphosphate (-9.12 Kcal/mol) of ADP itself, contributing to the inhibitor's ability to prevent the release of the nucleotide from the kinesin, which confirmed our earlier studies[70] that removal of this amino group produced a compound that did not inhibit Eg5. The same studies also suggested that the carboxylate moiety was not essential for binding – for example cysteamine could replace cysteine and retain inhibition. Our calculations showed that if anything, the carboxylate had a repulsive role, particularly with respect to the anionic diphosphate moiety of the nucleotide, which was compensated by its contribution to solvation through projection into the solvent-exposed region of the binding pocket
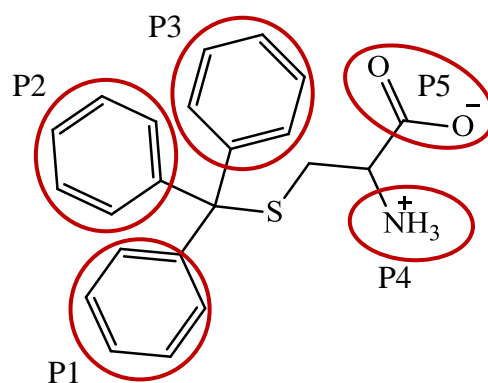
P1		P2		P3		P4	
Res. No.	**Kcal/mol**	**Res. No.**	**Kcal/mol**	**Res. No.**	**Kcal/mol**	**Res. No.**	**Kcal/mol**
Ala133	1.16	Leu214	0.64	Mg^{2+}	1.14	Lys111	2.16
Mg^{2+}	0.71	Glu215	-0.73	Pro137	0.75	Mg^{2+}	1.45
Gly117	0.62	Tyr211	-1.57	Asp265	-0.5	Met115	0.85
Glu128	-0.64	**Total**	**-1.66**	Glu215	-0.67	Arg221	0.79
Glu116	-1.12	**P5**		Glu116	-0.74	Ile136	0.69
Asp130	-1.34	ADP	5.71	Leu214	-1.8	Gln78	0.64
Glu118	-2.33	Glu116	0.96	**Total**	**-1.82**	Gly110	0.52
Total	**-2.94**	Glu118	0.6			Glu118	-1.02
		Arg221	-1.38			Glu116	-3.53
		Lys111	-1.49			Gly117	-3.72
		Total	**4.4**			ADP	-9.12
						Total	**-10.29**

Figure 2.3: The functional groups (subsites P1-P5) of STLC and the binding free energies (Kcal/mol) between residues in Eg5 and each subsite of STLC.[113]

Having established the key interactions between our hit compound, STLC with Eg5, we used the GOLD docking algorithm to re-dock STLC into the Eg5 crystal structure to establish a protocol that would aid our hit optimisation process. The algorithm was required to reproduce the conformation of the ligand determined experimentally, if we were to have confidence in translating any suggested structural modifications

into synthetic strategies. The docked pose of STLC was superimposed over the crystallised Eg5-STLC complex (**Figures 2.4**) and they showed high similarity in their poses with an RMSD of 0.4427: the docked STLC was placed inside the binding site, with the three phenyl rings positioned in three hydrophobic pockets and the cysteine moiety solvent-exposed. In addition to the interactions described above, one of the phenyl rings in the most hydrophobic pocket also interacts with the aromatic amino acid Phe239. The primary amine forms hydrogen bonds with Glu116 and Gly117 and the sulphur is near the Glu116 residue, but with no obvious interactions. The docking algorithm was run in the absence of water, so the carboxylic acid is observed outside the pocket, towards the solvent, forming no significant interactions.
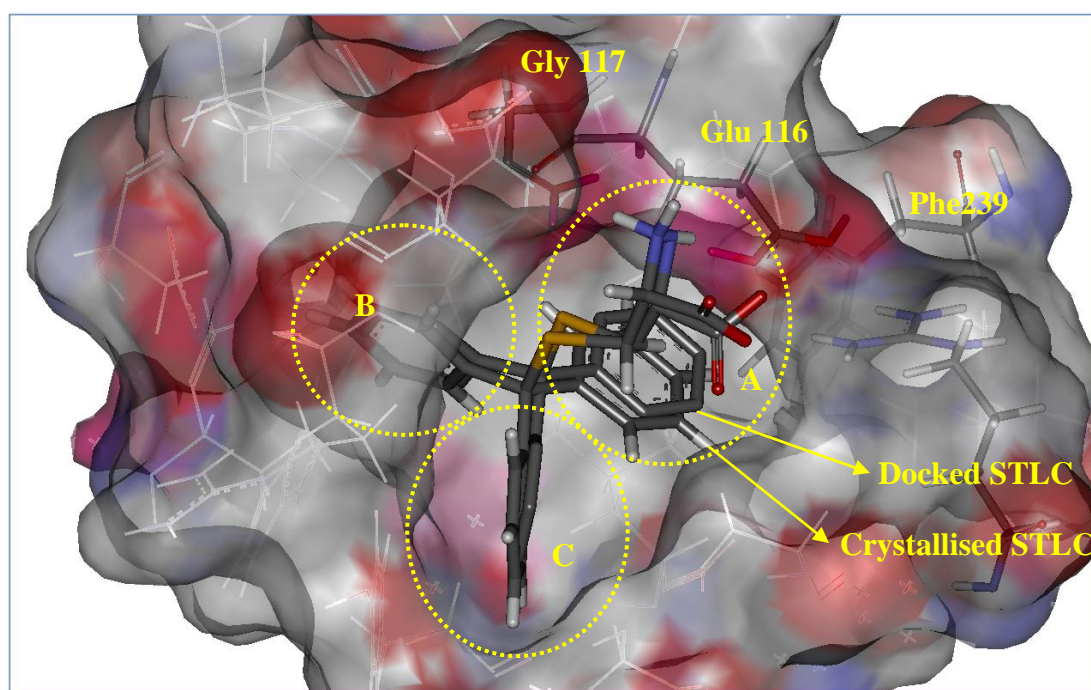
Figure 2.4: STLC pose and crystal structure inside the Eg5 binding pocket.

2.2 Hit optimisation of STLC

The different approaches we have adopted to optimise the structure of STLC can be summarised as follows:

Optimisation of the hydrophobic head group - a recent SAR study on STLC showed that Eg5 ATPase inhibitory activity and the inhibition of HeLa cancer cell growth

were significantly improved with a *para*-methyl substitution in one of the phenyl rings.[70] Reshuffling of the *para*-methyl group to a benzyl moiety (**Figure 2.5**) is a common approach in hit optimisation strategies because the lipophilic pocket that the *para*-methyl group occupies can often accommodate the benzyl ring more tightly. Substituents on the benzyl ring could further increase interactions with the pocket, as would substituents on the other phenyl rings. Finally, conformationally restraining the hydrophobic head group by fusing two of the ring systems could reduce the entropic penalty often seen with ligand binding when a conformationally flexible molecule is restrained in the binding site.

Optimisation of the hydrophilic tail group - the basic amine is an important group that should be retained in order to form H-bonds with Glu116 and Gly117, and secondary and tertiary amines at this position will be investigated. Our studies have shown that the carboxylic acid can be retained or removed. If retained, it could be modified to an ester or amide to either alter the zwitterionic nature of the molecule and the implications this has for absorption, or to enhance interactions with the protein rather than simply being solvent-exposed.
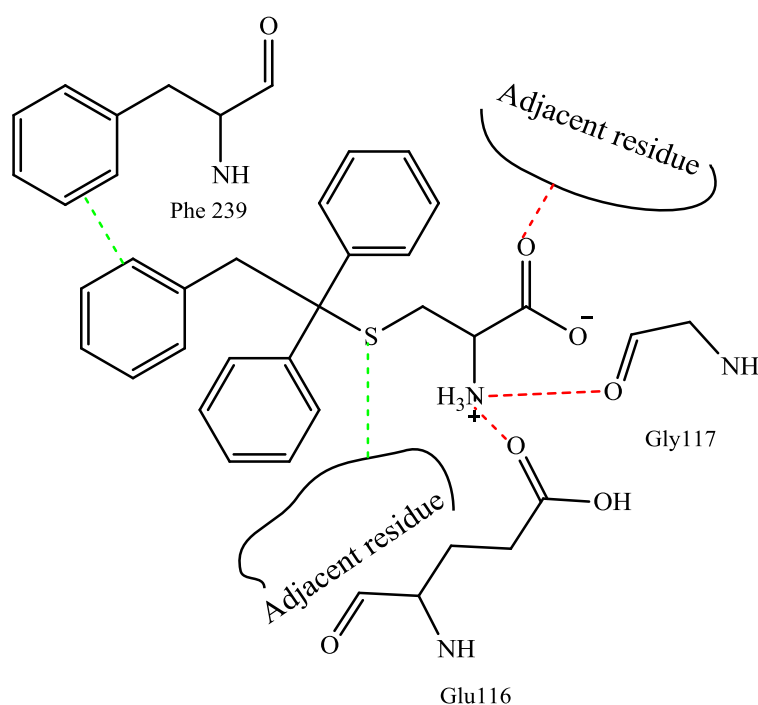
Figure 2.5: Schematic diagram of the proposed interactions of the benzyl derivative with Eg5 binding site

2.2.1 The core scaffold

The docked pose of benzyl analogue in the binding pocket is illustrated in **Figure 2.6**, and shows that the primary amine could still form the two important H-bonds with Glu116 and Gly117. Introducing a benzyl moiety into the structure appeared to change the angle of fit, enabling the sulphur atom to come closer to the neighbouring Glu116 to form a hydrophobic interaction, and to allow the carboxylic acid to interact with the protein, forming a hydrogen bond with the nearest residue Arg221. The phenyl groups occupied the hydrophobic pockets of the binding site seen with the STLC; however, the benzyl ring did not occupy the most hydrophobic pocket as expected, but flipped and occupied pocket B.
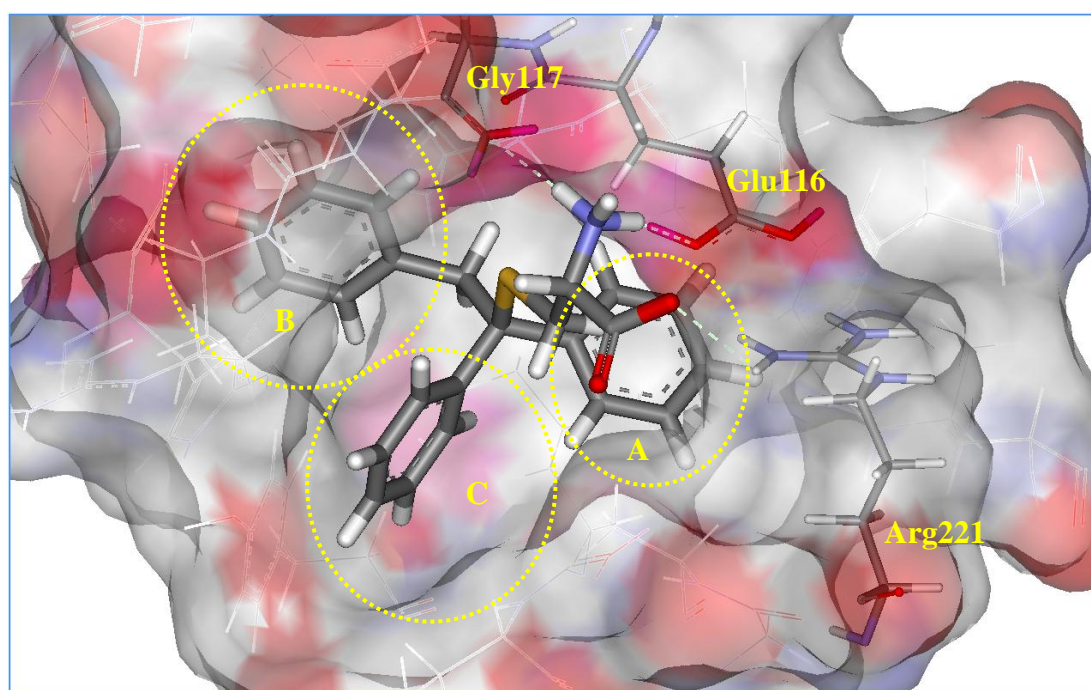
Figure 2.6: Docking pose of core scaffold.

The core scaffold compound was tested in two biological assays; for Eg5 ATPase inhibitory activity and in a cell based assay against the K562 leukaemia cell line (**Table 3.1**). The core scaffold compound had an IC_{50} of 130 nM against Eg5, which is an improvement on STLC (IC_{50} = 225 nM), although the EC_{50} result for the cell based assay was lower than STLC (3141 nM vs 700 nM). Accordingly the target compounds were synthesised as show in the next section.

2.3 Chemical synthesis

2.3.1 Synthesis of alcohols to couple with L-cysteine or cysteamine

The preparation of STLC analogues proceeded via the coupling of a suitable tertiary alcohol with either L-cysteine or cysteamine. Since the recommended alcohols were not commercially available, they were synthesised by reacting a suitable ketone with either a Grignard or aryllithium reagent. The alcohols prepared by this method are summarised in **Table 2.1.**
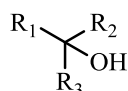
Compound	R$_1$	R$_2$	R$_3$	Yield (%)
79[‡]	benzyl	phenyl	phenyl	58
80[‡]	benzyl	H	phenyl	30
81[‡]	benzyl	methyl	phenyl	46
82[‡]	benzyl	ethyl	phenyl	37
83[*]	4-pyridyl	phenyl	phenyl	20
84[‡]	isopropyl	phenyl	phenyl	22
85[‡]	benzyl	3-hydroxyphenyl	phenyl	76
86[‡]	benzyl	4-hydroxyphenyl	phenyl	86
87[‡]	benzyl	3-chlorophenyl	phenyl	36
89[‡]	benzyl	4-chlorophenyl	phenyl	53
90[*]	benzyl	3,4-dichlorophenyl	phenyl	64
91[‡]	benzyl	4-chlorophenyl	4-chlorophenyl	21
92[‡]	benzyl	4-chlorophenyl	3-chlorophenyl	42
93[‡]	benzyl	4-methylphenyl	phenyl	45
94[‡]	benzyl	4-methylphenyl	4-methylphenyl	60
95[‡]	benzyl	2-fluorophenyl	phenyl	69
96[‡]	benzyl	4-fluorophenyl	phenyl	79
97[‡]	benzyl	4-fluorophenyl	4-fluorophenyl	32
98[‡]	3,4- dichlorobenzyl	phenyl	phenyl	37
99[‡]	4-chlorobenzyl	phenyl	phenyl	30
100[‡]	3-chlorobenzyl	phenyl	phenyl	49

Table 2.1: Synthesised Alcohols

Reagent used (‡) Grignard (*) aryllithium.

As an example of the structural elucidation of the achiral alcohol, the ^{1}H NMR spectrum of compound **79** (**Figure 2.7**) shows a singlet at δ 2.32 ppm, which corresponds to the hydroxyl proton. The singlet at δ 3.66 ppm represents the benzylic protons which are expected to be deshielded as they are attached to a phenyl group. The aromatic region for this compound as well as other related derivatives appear as multiplets, the two protons adjacent to the quaternary carbon of the benzyl ring appearing in the upfield region separated from the other aromatic protons at δ 6.90 ppm because they are the most shielded protons of the aromatic region.

The ^{13}C NMR spectrum of compound **79** (**Figure 2.8)** has a peak at δ 48.02 ppm which represent the deshielded benzylic carbon C2. The highly deshielded signal at δ 77.97 ppm corresponds to the quaternary carbon C1 due to the effect of the adjacent electronegative oxygen atom. The crowded aromatic region represents the three phenyl rings, with the quaternary carbons of the phenyl rings at δ 135.85 and 146.63 ppm, which corresponds to C3 and C5 and 5' respectively.
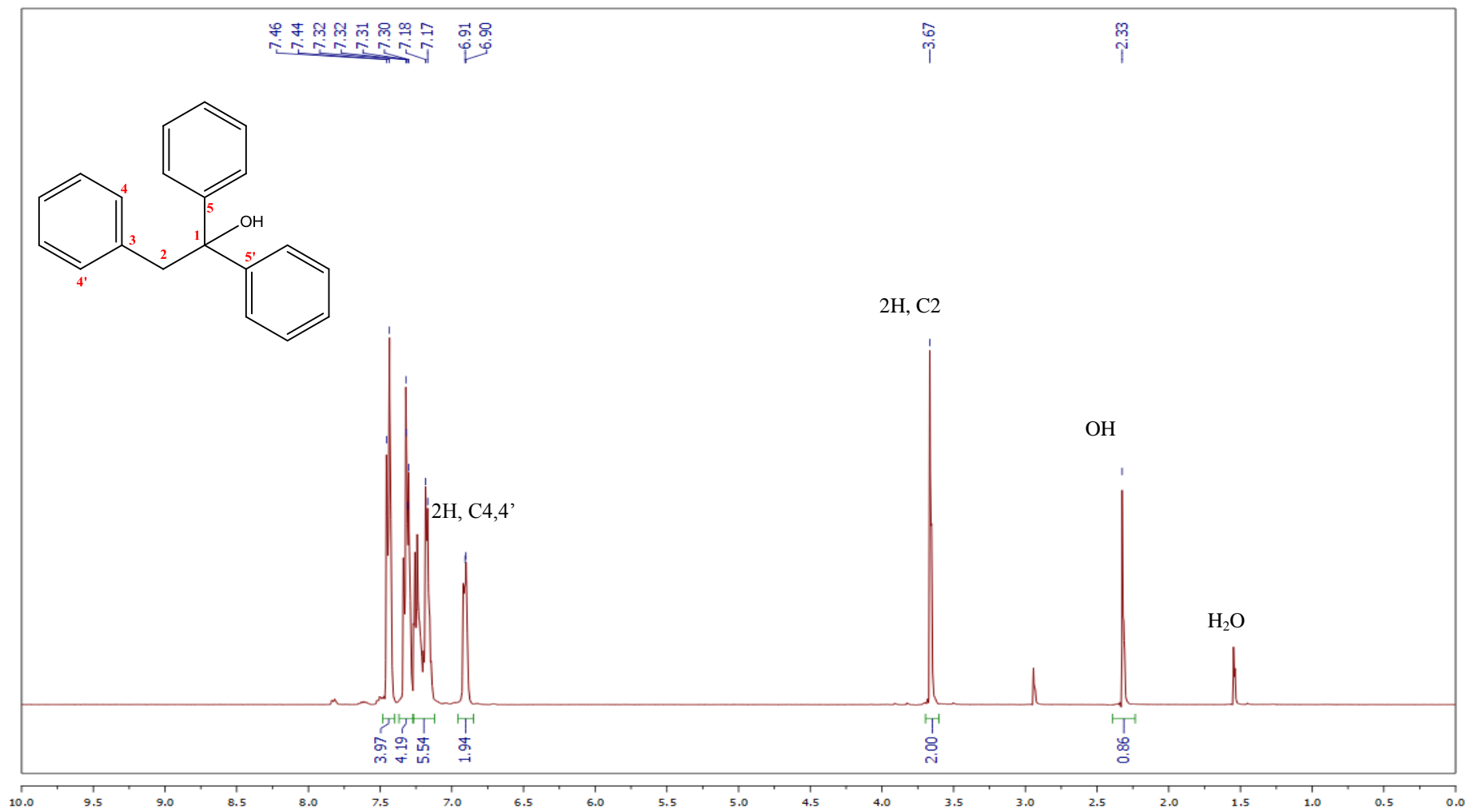
Figure 2.7: ^{1}H NMR (CDCl$_3$) spectrum of compound **79.**
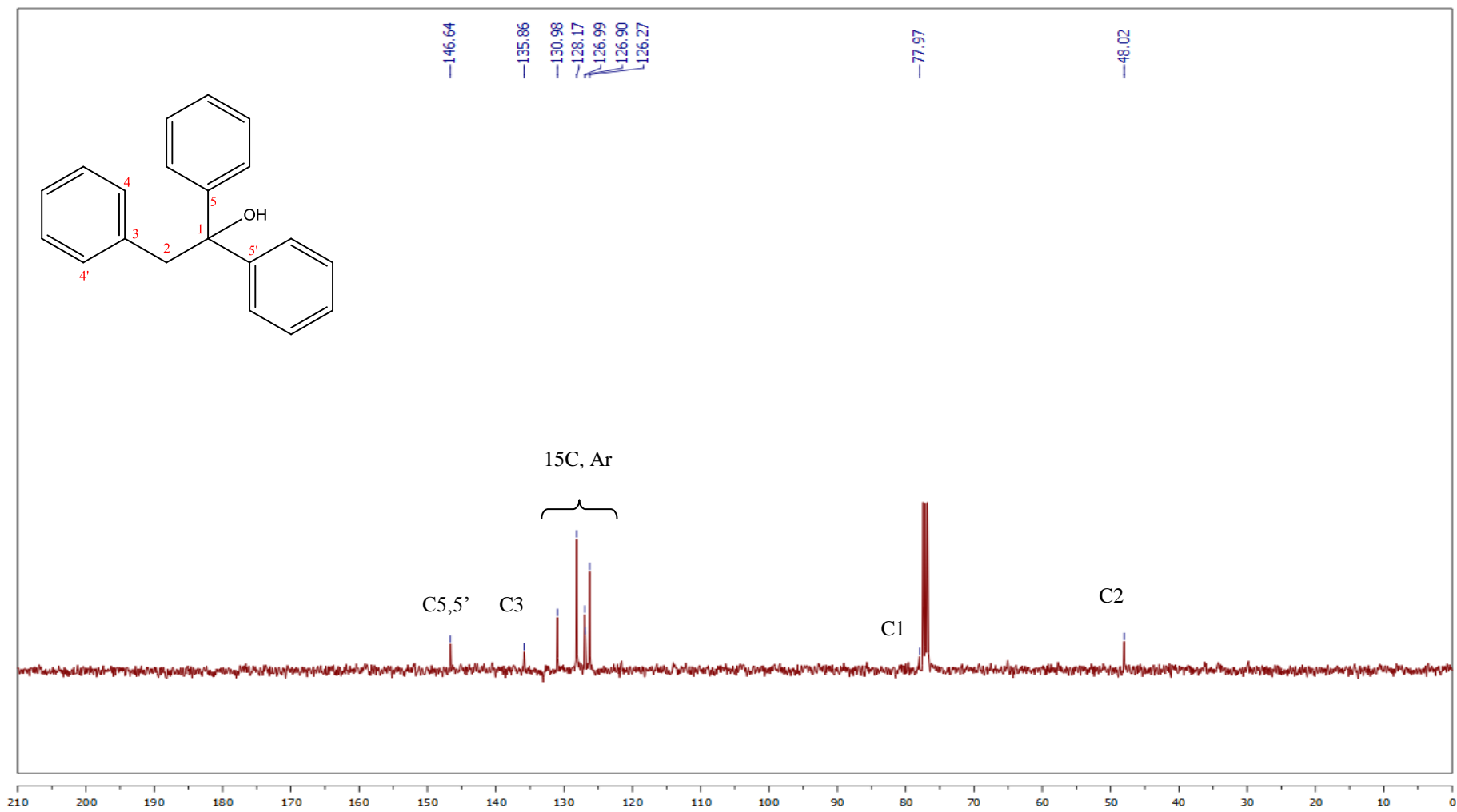
Figure 2.8: The ^{13}C NMR (CDCl$_3$) spectrum of compound 79.

As an example of an alcohol with a chiral carbon at C1, the ^{1}H NMR of compound **87** is shown in **Figure 2.9**, in which the non-equivalent protons at C2 appear as two adjacent doublets with a *J* value of 13.6 Hz that corresponds to geminal coupling.
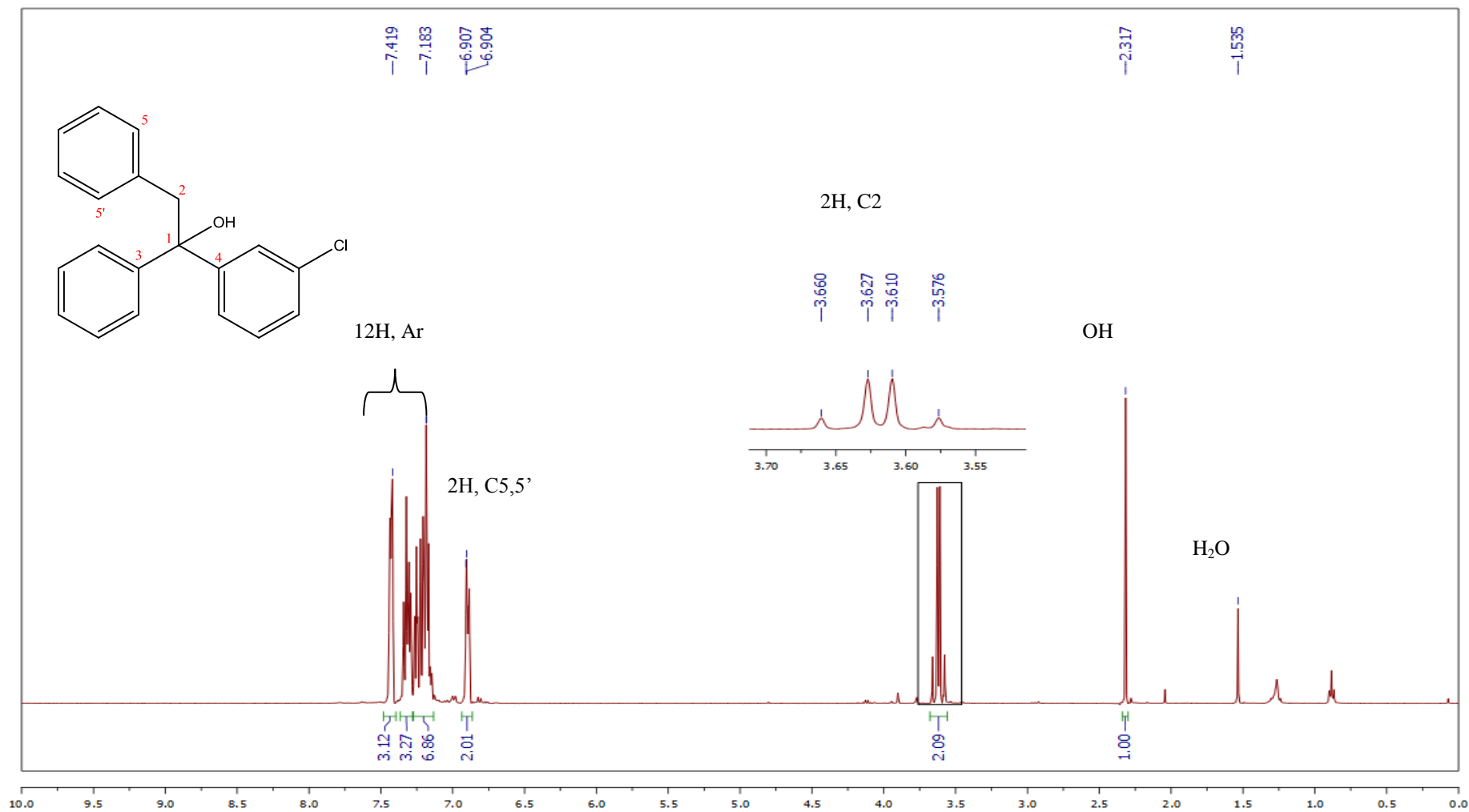
Figure 2.9: ^{1}H NMR (CDCl$_3$) of compound **87**.

2.3.1.1 Preparation of alcohol intermediates using Grignard reagents

This commonly used method to prepare tertiary alcohols involves the reaction of a Grignard reagent with the ketone under anhydrous conditions.[114] The crude product was either recrystallized or purified using column chromatography to give the required alcohol in varied yields.

The Grignard reagent was prepared *in situ* by mixing the corresponding halide with magnesium metal at room temperature if it was not commercially available (**Scheme 2.1**). [115, 116]

98 R= 3,4 dichlorbenzyl (37 %)
99 R= 4-chlorobenzyl (30 %)
100 R= 3-chlorobenzyl (40 %)
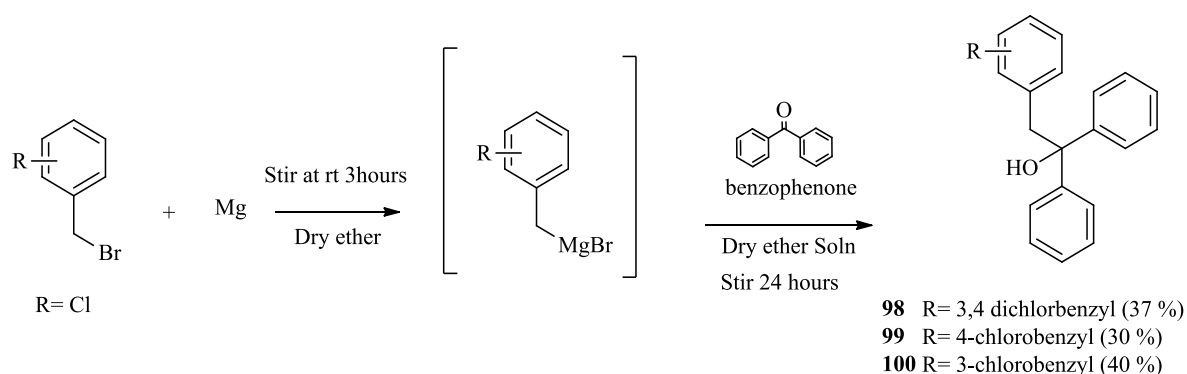
Scheme 2.1: Synthesis of compounds with chloro substituents in the benzyl ring

2.3.1.2 Preparation of alcohol intermediates using aryllithium reagents

Compound **92** was synthesised via the formation of the aryllithium reagent by treating the aryl bromide with (**Scheme 2.2**) *n*-butyllithium at low temperature (-78 ºC), [117-119] which was then reacted with the ketone to form the required alcohol in a moderate yield (42 %).

1- bromo 3- chlorobenzene   4-Chloro-2-phenylacetophenone   **92** (42 %)
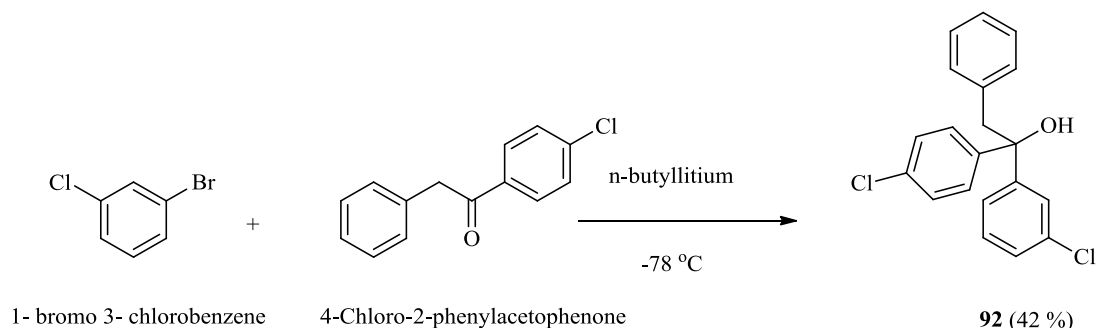
Scheme 2.2: Synthesis of compound 92 via an organolithium intermediate.

2.3.2 Synthesis of analogues of STLC with modified head groups

The alcohols were then coupled with L-cysteine (**Scheme 2.3**) via a nucleophilic S_N1 substitution of the hydroxyl group by the thiol sulfur of the L-cysteine. BF$_3$.etherate was used as a Lewis Acid to make the hydroxyl a good leaving group and form the tertiary carbocation intermediate, which then reacted with the sulfur nucleophile.[120] The L-cysteine derivatives produced by this method are listed in **Table 2.2**.
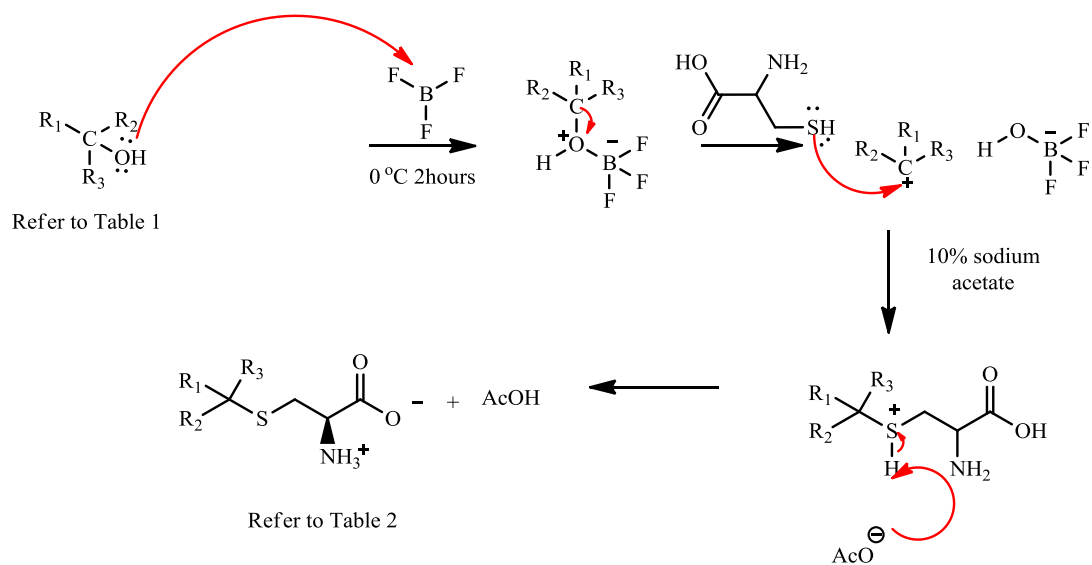
Scheme 2.3: Synthesis of L-cysteine derivatives
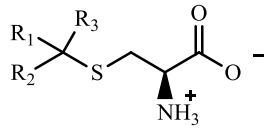
Compound	R₁	R₂	R₃	Yield %
101*	benzyl	phenyl	phenyl	37
102	benzyl	H	phenyl	19
103	benzyl	methyl	phenyl	32
104	benzyl	ethyl	phenyl	37
105	benzyl	3- hydroxyphenyl	phenyl	10
106	benzyl	4-hydroxyphenyl	phenyl	8
107	benzyl	3-cholrophenyl	phenyl	11
108	benzyl	4-cholrophenyl	phenyl	29
109	benzyl	3,4-dichlrophenyl	phenyl	13
110	benzyl	4-chlorophenyl	4-cholropheny	20
111	benzyl	3-chlorophenly	4-chlrophenyl	15
112	benzyl	4-methylphenyl	phenyl	22
113	benzyl	4-methylphenyl	4-methylphenyl	15
114	benzyl	2-fluorophenyl	phenyl	19
115	benzyl	4-fluorophenyl	phenyl	12
116	benzyl	4-fluorophenyl	4-fluorophenyl	17
117	3,4 dichlrobenzyl	phenyl	phenyl	21
118	4-cholrobenzyl	phenyl	phenyl	22
119	3-chlorobenzyl	phenyl	phenyl	24
120	pyridyl	phenyl	phenyl	28

Table 2.2: Analogues of STLC with modified head groups.

(*): The core scaffold compound

In general, the low yield of this reaction was due to the formation of the alkene bi-product which is formed through elimination under the acidic conditions of the general coupling procedure.

The ^{1}H NMR spectrum of the core scaffold (compound **101**) in **Figure 2.10** shows two doublets of doublets for the non-equivalent protons at C3 due to the effect of the adjacent chiral centre at C2; each proton couples with its geminal partner ($J = 12.4$ Hz) and also with the vicinal chiral proton at C2 ($J = 9.2$ and 4.0 Hz). The proton at the chiral C2 also is a doublet of doublets as it couples with the two non-equivalent methylene protons ($J = 4.0$ and 9.2 Hz). The singlet at δ 3.66 ppm represents the deshielded benzylic protons. The aromatic region has two singlets at δ 6.68 ppm

which represent the two deshielded protons at the C7 and 7' position of the benzyl group.

The ^{13}C NMR spectrum of compound **101** (**Figure 2.11)** confirms a successful coupling between L-cysteine and the alcohol, with an extra three peaks in the aliphatic region corresponding to the L-cysteine aliphatic carbons, and one highly shielded peak at δ 170 ppm for the carbonyl group of the carboxylic acid.
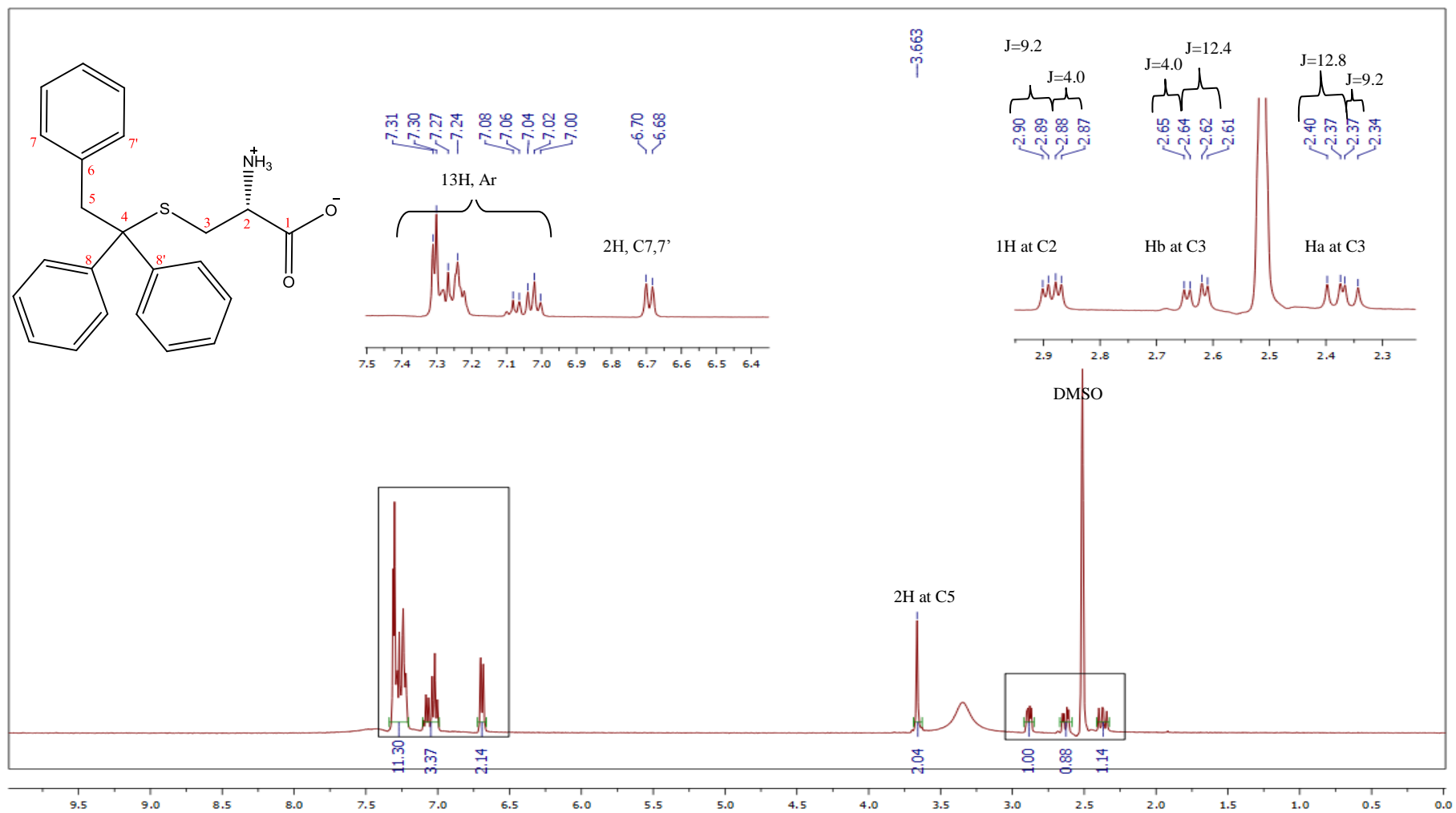
Figure 2.10: ^{1}H NMR (DMSO-*d6*) of L-cysteine coupled compound 101.
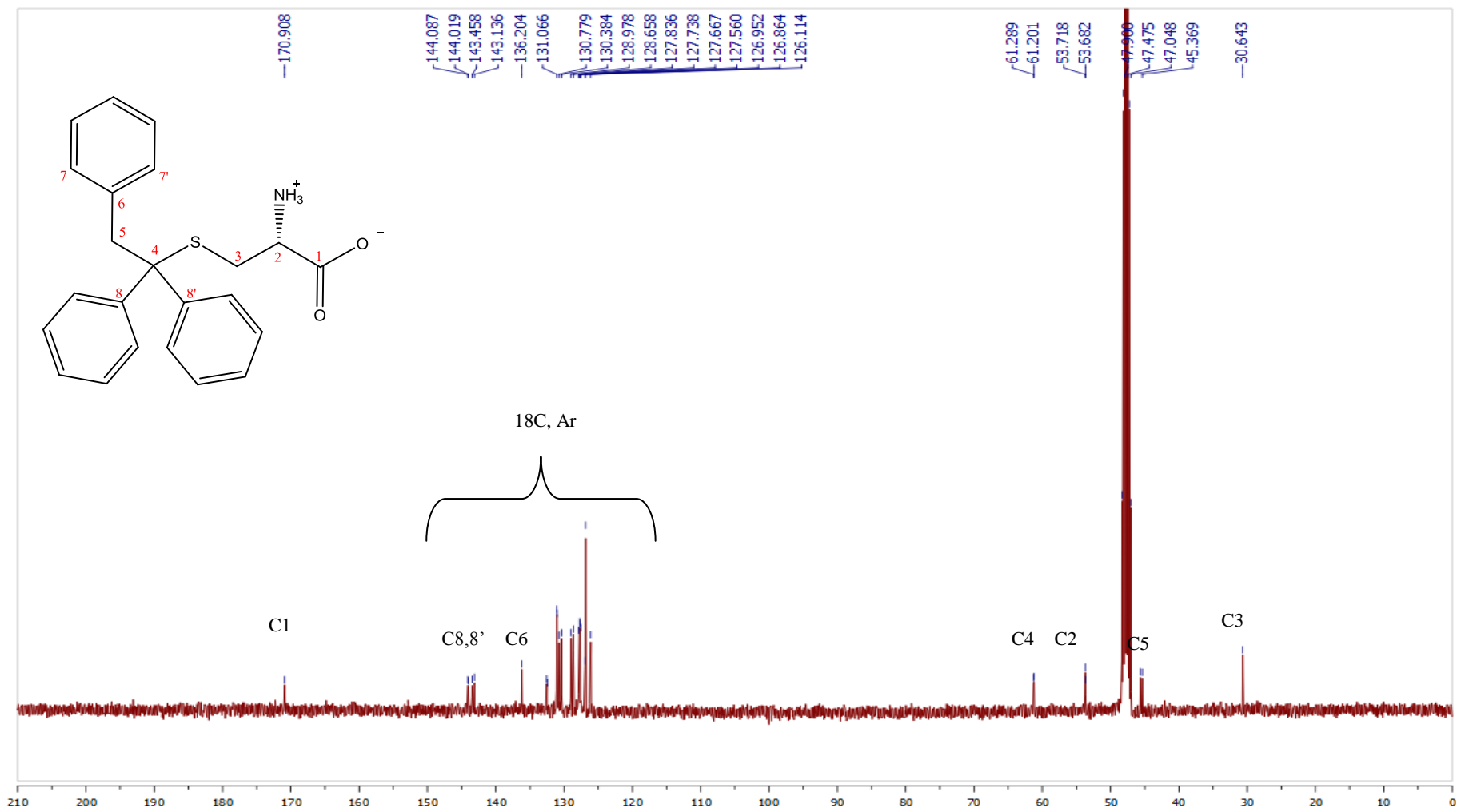
Figure 2.11: ^{13}C NMR (DMSO-*d6*) spectrum of L-cysteine coupled compound **101**.

Some of the derivatives were diastereomers as they have two chiral centres, which have characteristic peaks in their ^{1}H NMR spectra compared to those of the pure isomers. The ^{1}H NMR spectrum of the pure enantiomer (compound **116**) (**Figure 2.12A)** has three distinguished doublets of doublets for all the aliphatic protons, whereas the diastereomeric mixture of compound **115** (**Figure 2.12B**) has two doublets of doublets.
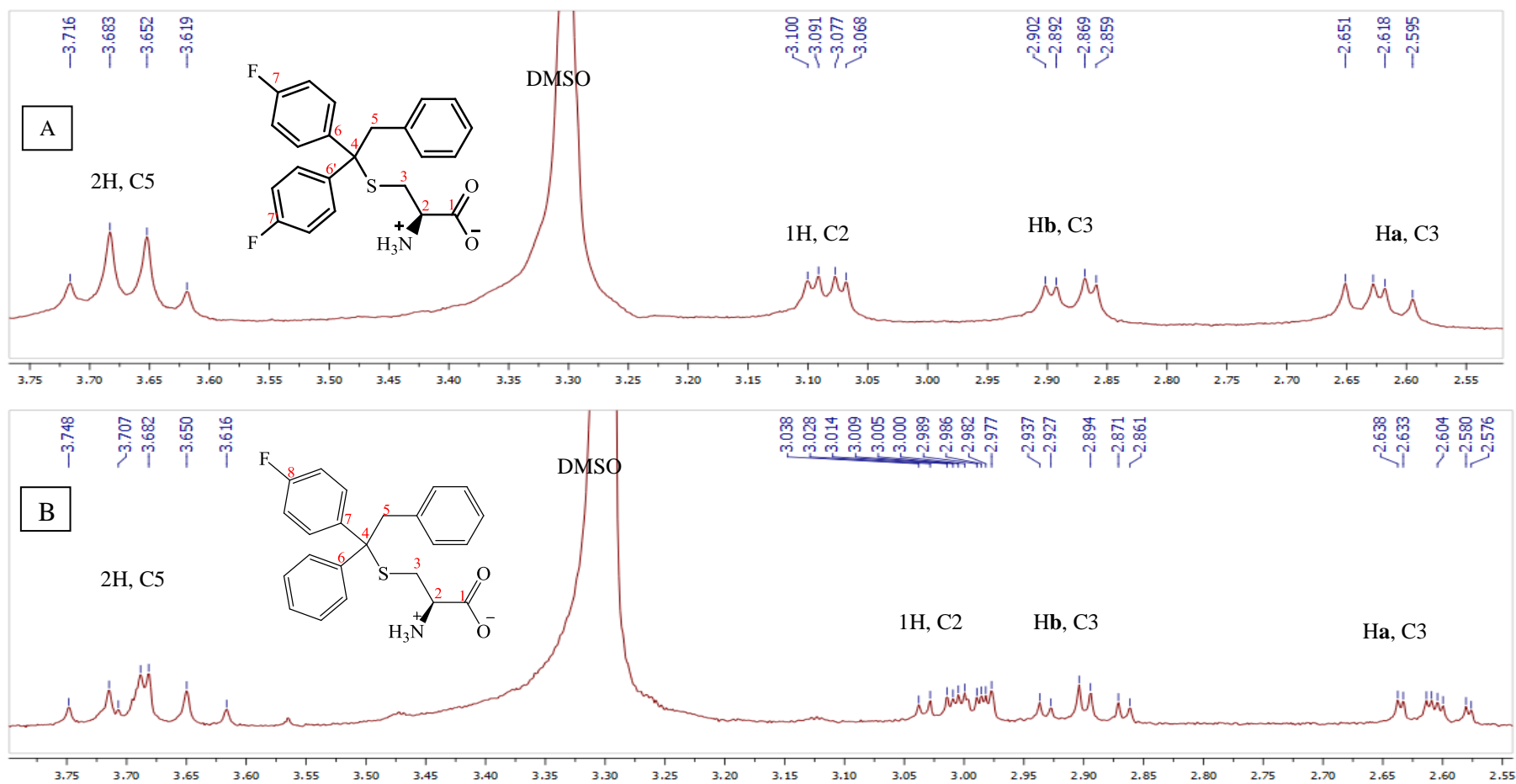
Figure 2.12: ^{1}H NMR (DMSO-*d6*) spectrum of (A) pure enantiomer (compound **116**), and (B) the diastereomeric mixture (compound **115**).

2.3.3 Synthesis of cysteamine derivatives with different head groups

The cysteamine derivatives listed in **Table 2.3** were synthesised using the same coupling procedure utilized for L-cysteine as shown in **Scheme 2.4**.
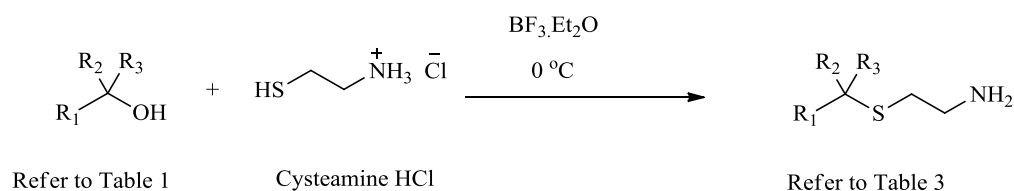
Scheme 2.4: Synthesis of cysteamine coupled compounds
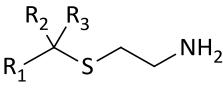
Compound	R$_1$	R$_2$	R$_3$	Yield%
121	benzyl	phenyl	phenyl	57
122	benzyl	3- hydroxyphenyl	phenyl	10
123	benzyl	4-hydroxyphenyl	phenyl	10
124	benzyl	3-chlorophenyl	phenyl	21
125	benzyl	4-chlorophenyl	phenyl	17
126	benzyl	3,4-dichlorophenyl	phenyl	13
127	benzyl	4-chlorophenyl	4-chlorophenyl	20
128	benzyl	3-chlorophenyl	4-chlorophenyl	9
129	benzyl	4-methylphenyl	phenyl	18
130	benzyl	4-methylphenyl	4-methylphenyl	8
131	benzyl	2-fluorophenyl	phenyl	11
132	benzyl	4-fluorophenyl	phenyl	9
133	benzyl	4-fluorophenyl	4-fluorophenyl	8
134	phenyl	H	phenyl	81
135	phenyl	methyl	phenyl	49
136	phenyl	isopropyl	phenyl	44
137	phenyl	phenyl	phenyl	60
138	pyridyl	phenyl	phenyl	18

Table 2.3: Cysteamine derivatives with modified head groups.

The ^{1}H NMR of the cysteamine analogue of compound **121** (**Figure 2.13**) has two triplets at δ 2.43 and 2.58 ppm which represent the four ethylene protons coupled to

71

each other ($J = 6.8$ Hz) and a singlet at δ 3.69 ppm that corresponds to the deshielded benzylic protons. The aromatic region was similar to the L-cysteine analogues, with two shielded protons adjacent to the benzyl quaternary carbon at δ 6.64 ppm, and the other three protons of the benzyl ring appearing as two triplets.

The ^{13}C NMR spectrum of compound **121** (**Figure 2.14**) shows two peaks at 26.7 and 39.6 ppm, which represent the aliphatic carbons of cysteamine. A deshielded carbon appears at δ 45.6 ppm, which represents the benzylic carbon C4. The highly deshielded signal at δ 61.8 ppm corresponds to the quaternary carbon C3. For the crowded aromatic region representing the three phenyl rings, we could assign the quaternary carbons of the phenyl rings at δ 136.8 ppm and 144.6 ppm, which corresponds to C5 and C7 and 7', respectively.
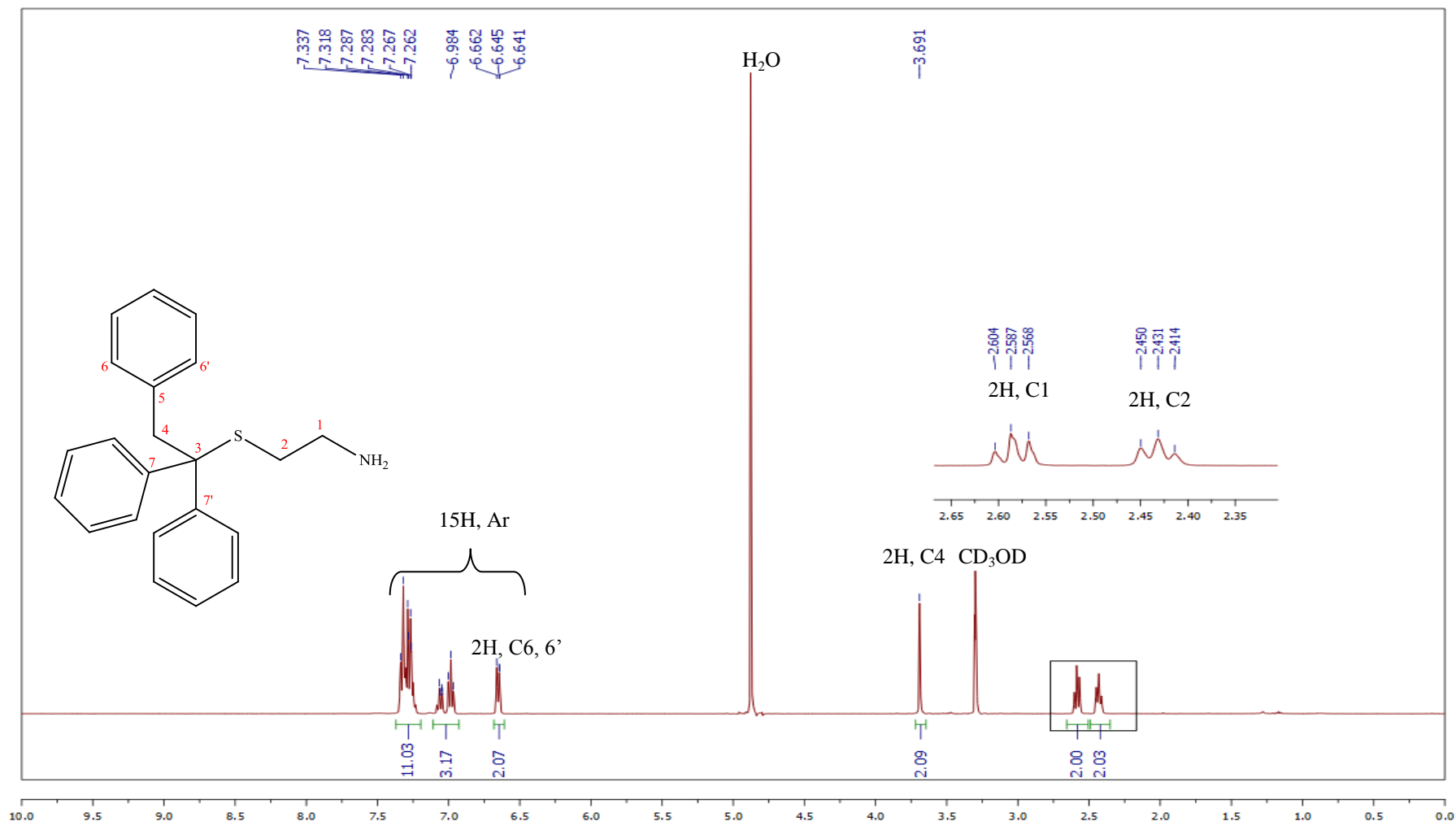
Figure 2.13: ^{1}H NMR (CD$_3$OD) spectrum of the cysteamine derivative (compound 121).
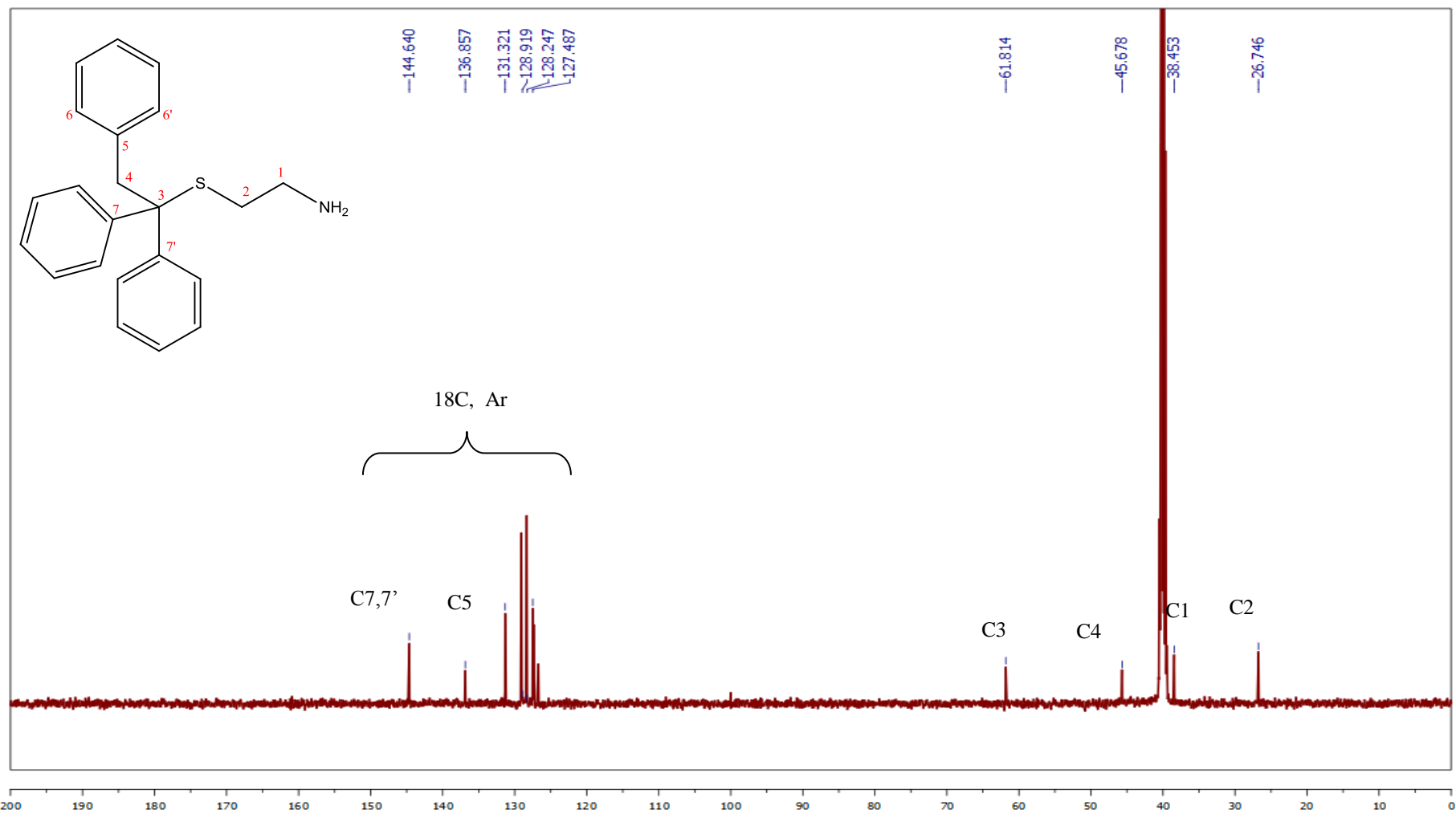
Figure 2.14: ^{13}C NMR(CD$_3$OD) of the cysteamine derivative (compound 121).

Another two L-cysteine and cysteamine derivatives where the benzyl was replaced with a benzoyl moiety, were synthesised in two steps; first α-phenylbenzoin was prepared by reacting benzil with phenyl lithium at room temperature, followed by reaction of the alcohol with cysteamine or L-cysteine at 70 °C for 12h to give the final compounds **140** and **141**, respectively (**Scheme 2.5**).
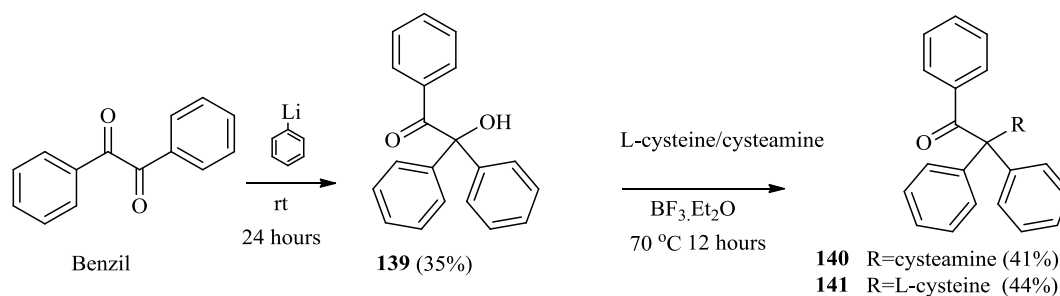
Scheme 2.5: Synthesis of the benzoyl analogues

2.3.4 Synthesis of ester analogues of STLC

A microwave method that employed a short run time of 5 minutes at 100 °C catalysed by 10% sulphuric acid[121] was used in the synthesis of the butyl esters (compounds **142** and **143**) and the hydroxyethyl and hydroxypropyl esters (compounds **144** and **145**) (**Scheme 2.6).**
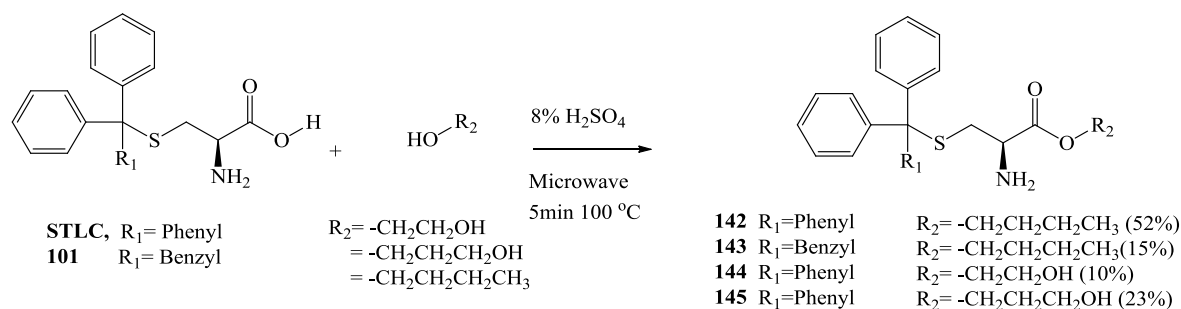
Scheme 2.6: Synthesis of esters

The ester (compound **147**) was synthesised using the Fischer procedure (**Scheme 2.7**) to prepare the butyl L-cysteine ester,[122] which was then coupled with the tertiary alcohol as previously described.
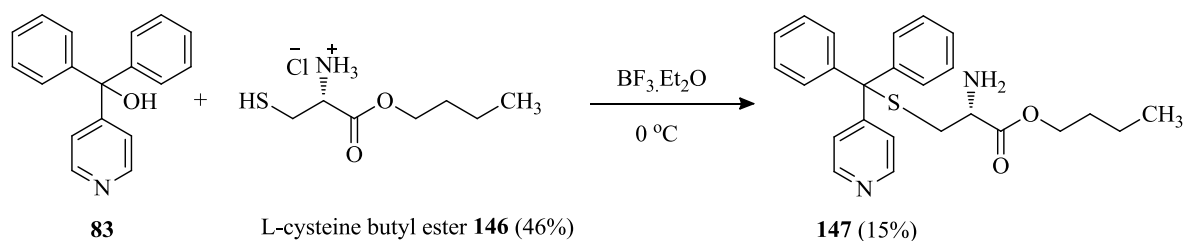
Scheme 2.7: Synthesis of compound 147 from L-cysteine butyl ester

The ^{1}H NMR spectrum of compound **142** (**Figure 2.15**) confirms successful esterification in which the butoxy protons at C9, C8, C7 and C6 appear as a triplet, sextet, pentet and triplet, respectively. The most deshielded protons were at C6 since they are attached to the electronegative oxygen. The spectrum shows two non-equivalent methylene protons (C3) adjacent to the chiral carbon appearing as two doublets of doublets.

The ^{13}C NMR of compound **142** (**Figure 2.16**) also confirms successful esterification with a deshielded signal at δ 65.07 ppm corresponding to C6 attached to the electronegative oxygen along with three other aliphatic carbons further upfield.
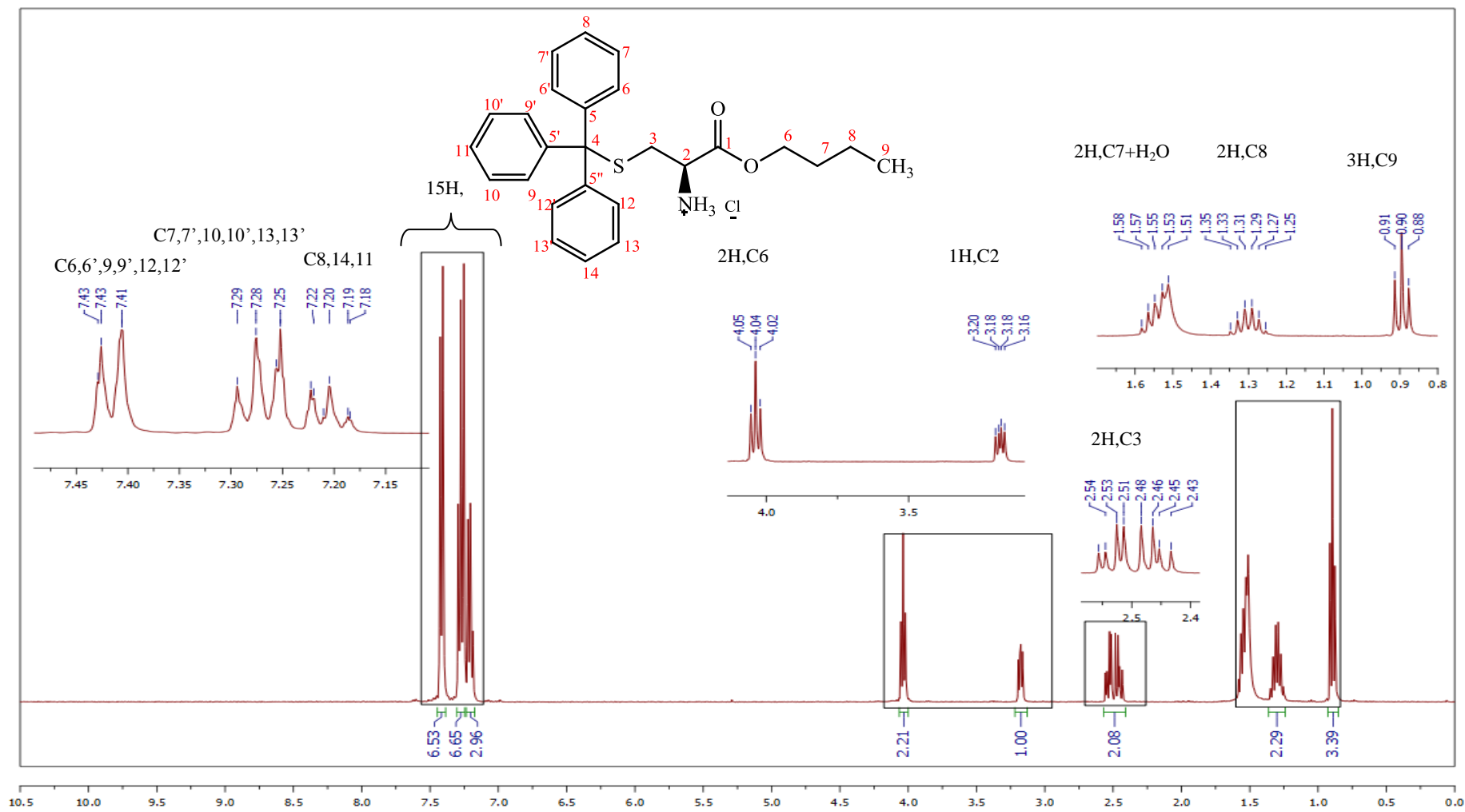
Figure 2.15: ^{1}H NMR (CDCl$_3$) of the STLC ester (compound 142).
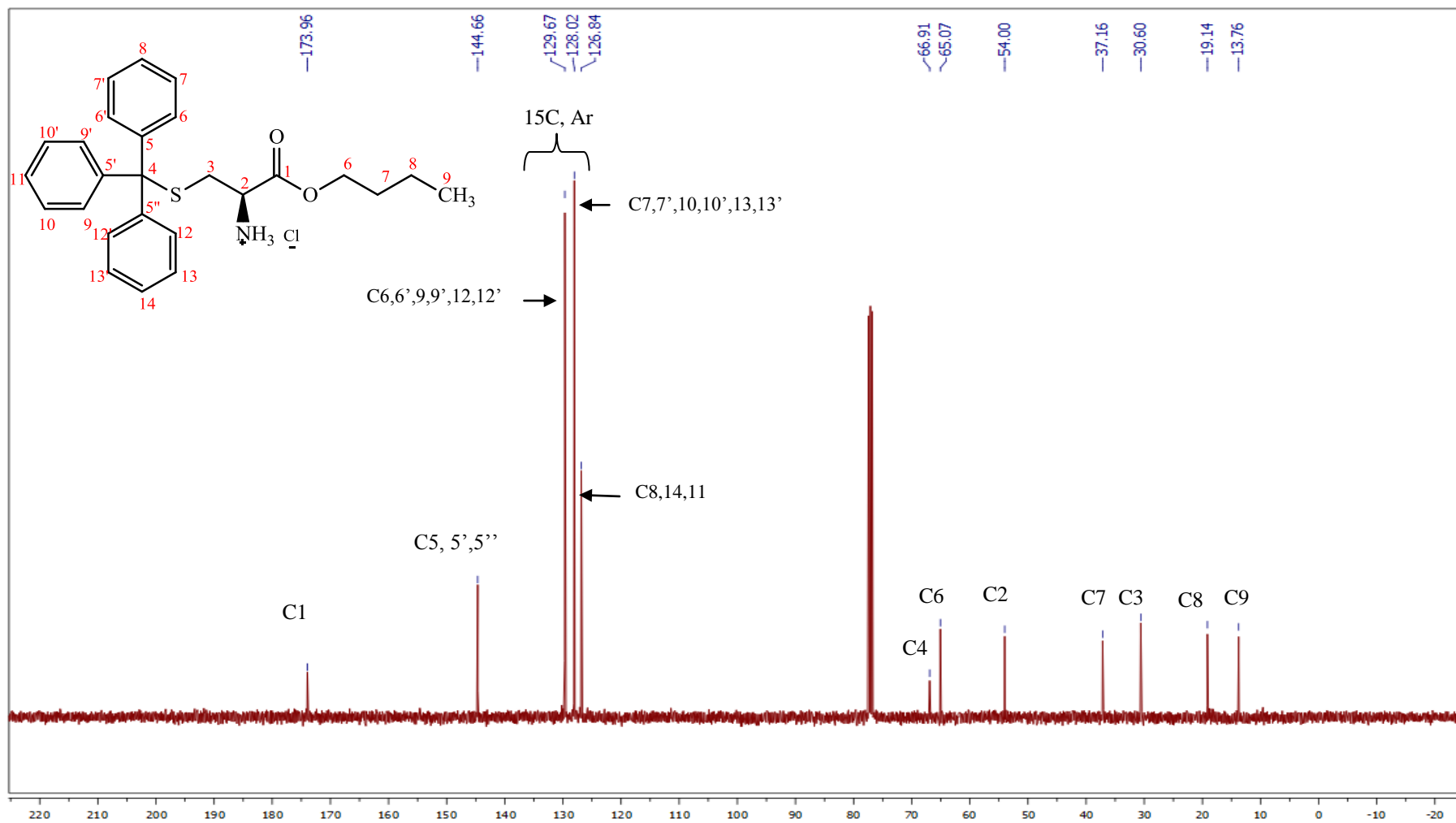
Figure 2.16: ^{13}C NMR (CDCl$_3$) of the STLC ester (compound 142).

2.3.5 Synthesis of amide analogues of STLC

Compounds with the carboxylic acid converted to an amide as opposed to an ester were synthesised in a relatively good yield by reacting STLC with thionyl chloride[123, 124] (**Scheme 2.8**) to form the corresponding acyl chloride, then with the primary amine (also as a solvent) at room temperature for 24h.[125]
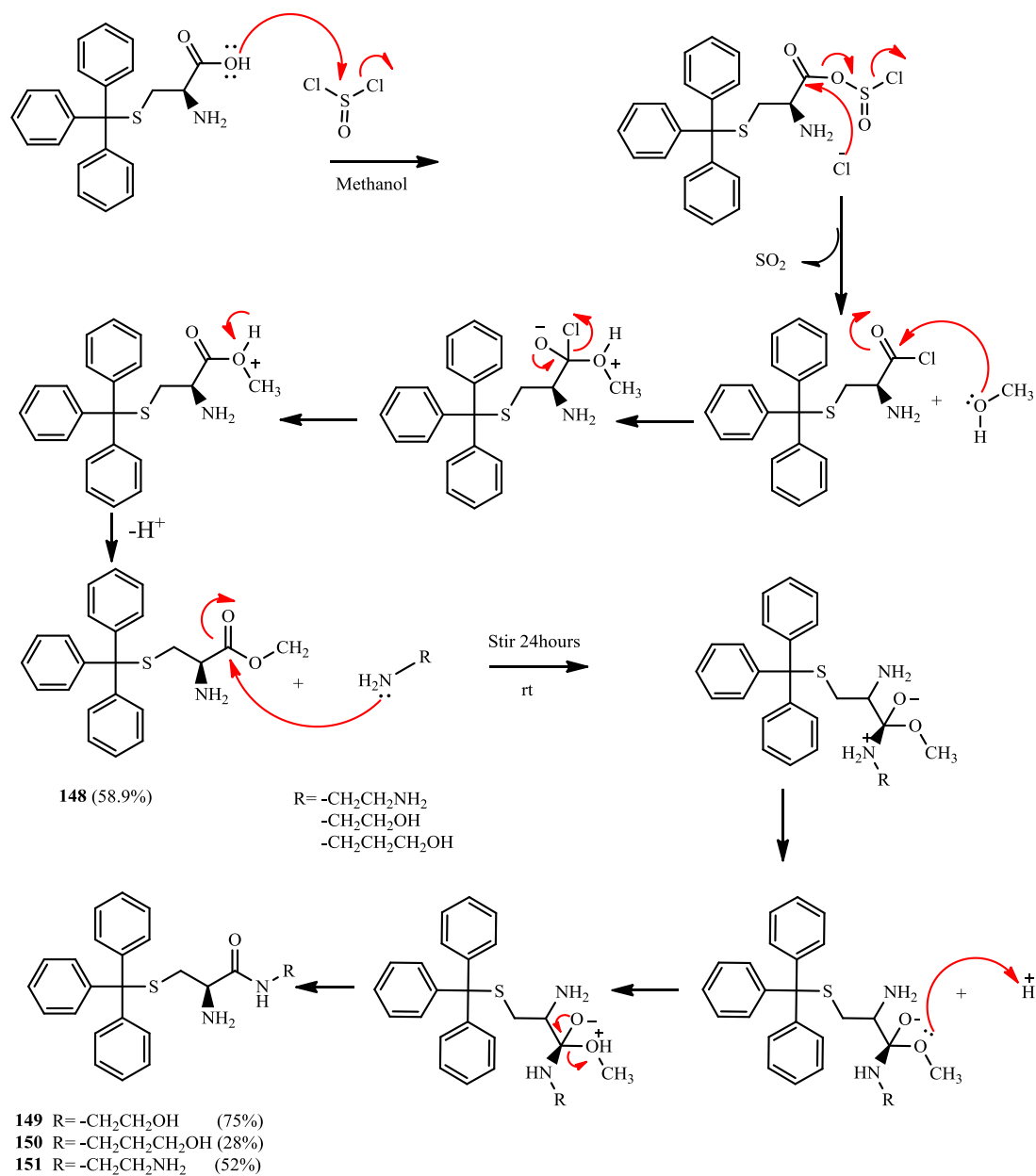
Scheme 2.8: Synthesis of amide analogues of STLC

2.3.6 Synthesis of the cyclic amine analogues

Compounds were prepared in which the primary amines of cysteine and cysteamine were replaced with cyclic amines such as piperidine and pyrrolidine (**Scheme 2.9**).

The *N*-protected pyrrolidine or piperidine methanol were converted to its corresponding thioether following the Mitsunobu reaction,[126] which was then hydrolysed to the thiol and coupled with the trityl alcohol using BF_3.etherate. The deprotection of the cyclic amine occurred simultaneously during the coupling step (compounds **158** and **159**). The *N*-protected derivatives (compound **160** and **161**) were prepared under alkaline conditions using TEA instead of using BF_3.etherate and trityl chloride in moderate yields.[127-129]
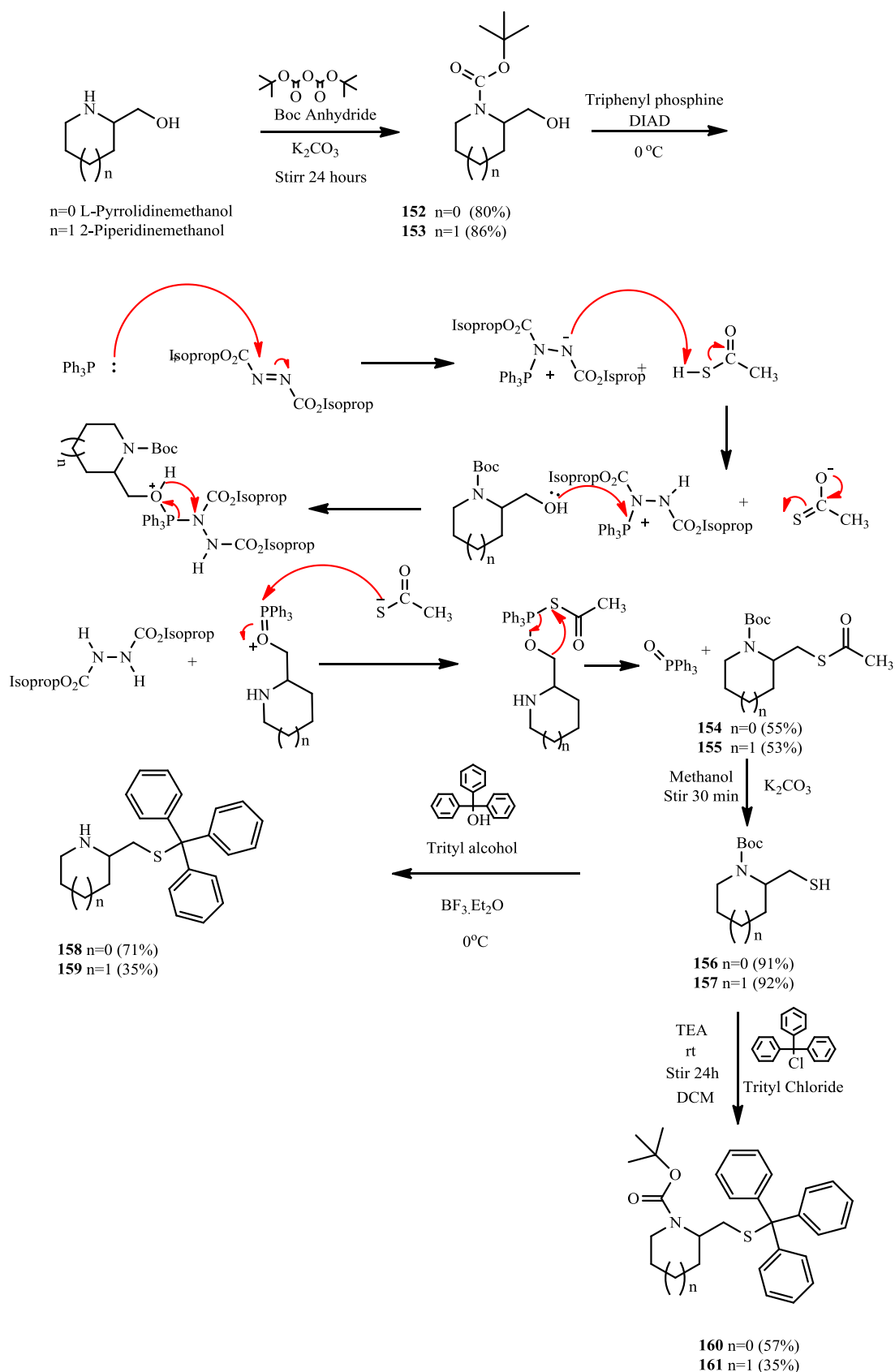
Scheme 2.9: Synthesis of the cyclic amine analogues

The ^{1}H NMR spectrum of compound **158** (**Figure 2.17)** shows five multiplets in the range δ 1.31- 2.97 ppm that correspond to the protons of the pyrrolidine and the two protons at C5. All the aliphatic protons appear as multiplets due to the presence of the chiral centre at C4 which makes all these protons non-equivalent and couple to each other in a complex way. However, we could assign the C5 protons adjacent to the chiral carbon at δ 2.32-2.40 ppm, which again appeared as a doublet of doublets.
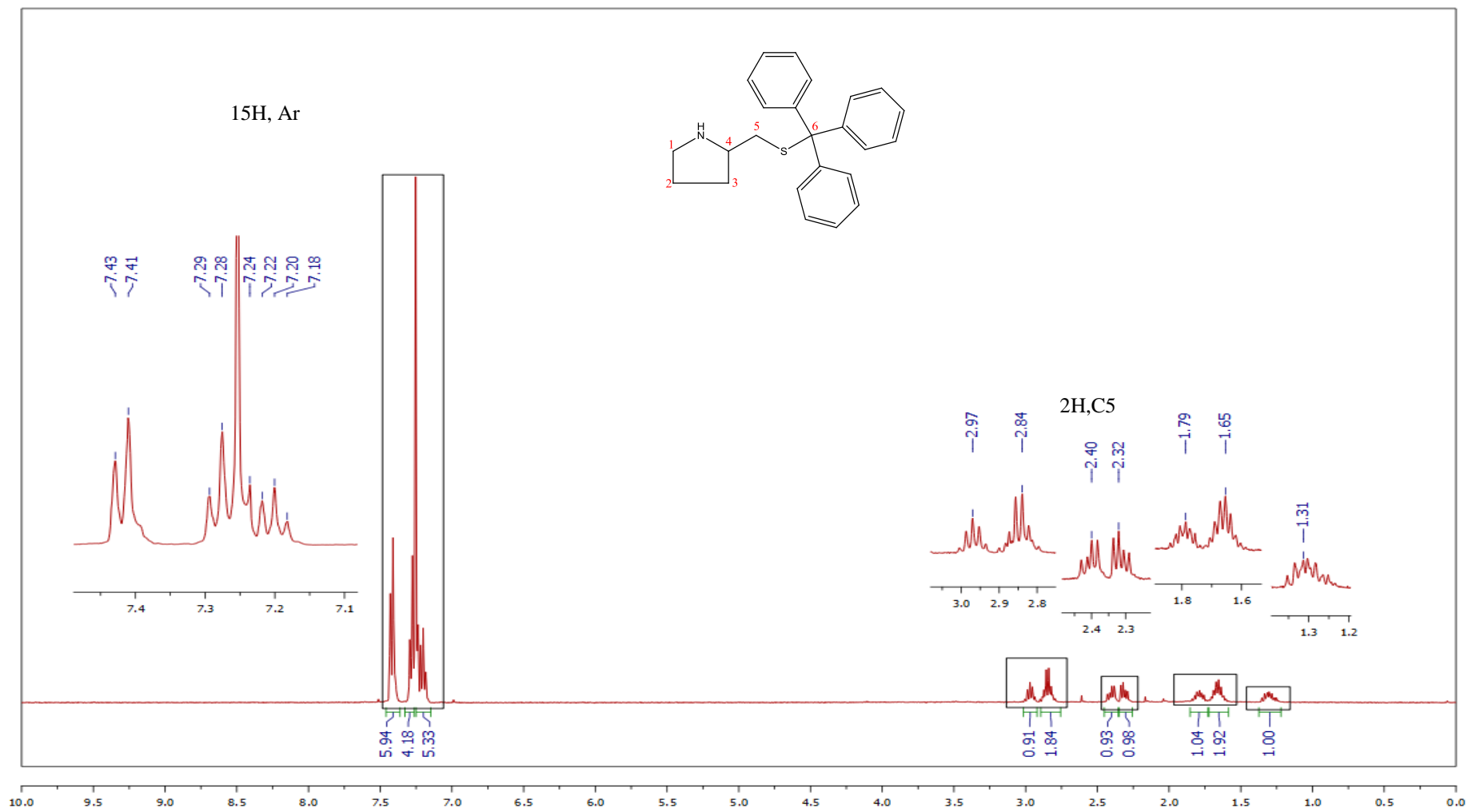
Figure 2.17: ^{1}H NMR (CDCl$_3$) of the cyclic amine (compound **158**).

2.3.7 Synthesis of xanthenes, thioxanthene, and fluorene analogues of STLC

The tricyclic analogues were synthesised (**Scheme 2.10**) by treating the commercially available ketones (fluorenone, xanthone and thioxanthone) with the phenyl and benzyl Grignard reagents[130] to give the corresponding alcohols (compounds **162** and **168**) (**Table 2.4**). The xanthone and thioxanthone were also reduced to the secondary alcohol using sodium borohydride[131-134] to afford compounds **166** and **167**.

Xanthone   X=O, n=1
Thioxanthone X=S, n=1
9-Fluorenone   n=0

Refer to Table 4

Refer to Table 4

Refer to Table 5
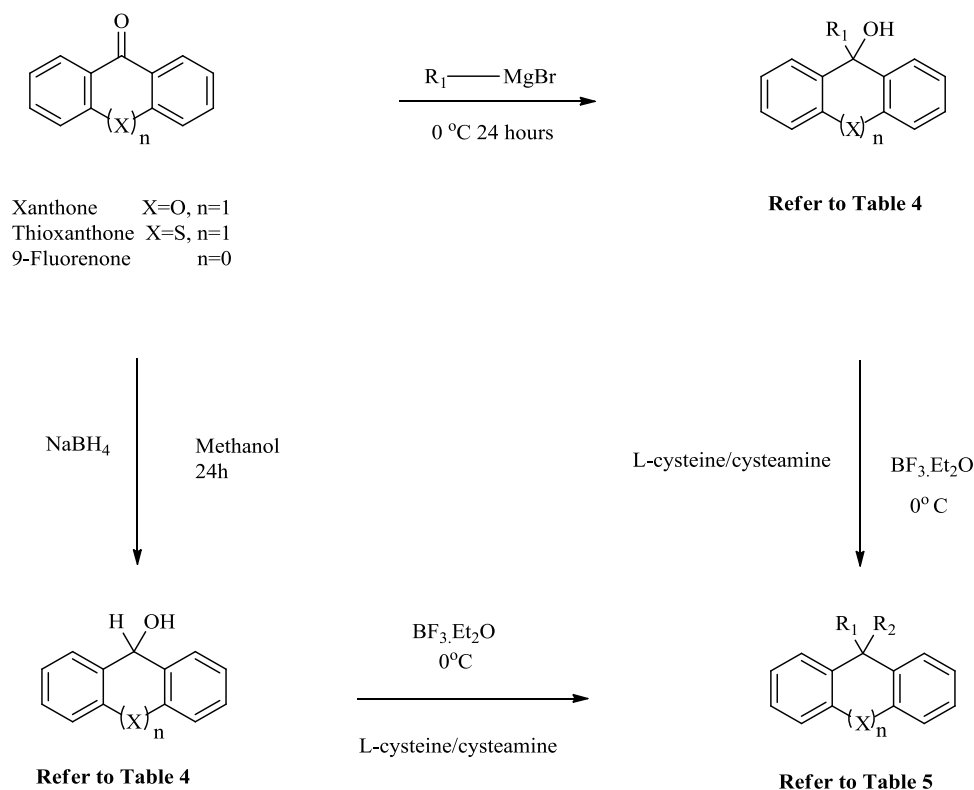
Scheme 2.10: Synthesis of the fluorene, xanthenes thioxanthene tricyclic compounds

Table 2.4: Alcohols used in the synthesis of fused rings
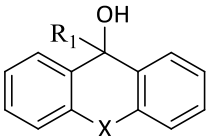
Compound	R$_1$	X	(n)	Yield %
162	phenyl	O	1	71
163	phenyl	S	1	32
164	benzyl	O	1	69
165	benzyl	S	1	66
166	H	O	1	25
167	H	S	1	47
168	benzyl	-	0	49

Table 2.4: Alcohols used in the synthesis of fused rings

The alcohols were then coupled with L-cysteine or cysteamine using the general coupling procedure previously described (**Table 2.5**).
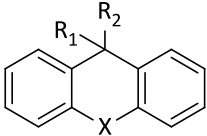
Compound	X	n	R$_1$	R$_2$	Yield %
169	O	1	H	L-cysteine	86
170	O	1	H	cysteamine	24
171	S	1	H	L-cysteine	77
172	S	1	H	cysteamine	52
173	O	1	phenyl	L-cysteine	80
174	O	1	phenyl	cysteamine	43
175	S	1	phenyl	L-cysteine	56
176	S	1	phenyl	cysteamine	62
177	O	1	benzyl	L-cysteine	84
178	O	1	benzyl	cysteamine	66
179	S	1	benzyl	L-cysteine	9
180	S	1	benzyl	cysteamine	44
181	-	0	benzyl	L-cysteine	53
182	-	0	benzyl	cysteamine	35

Table 2.5: Fused ring analogues of STLC.

The ^{1}H NMR spectra of the xanthene analogues, compound **169** (**Figure 2.18a**) and compound **170** (**Figure 2.18b**), show the aliphatic protons of the L-cysteine and cysteamine moieties having similar assignments to those described before. The proton attached to the tertiary carbon of the xanthene ring of compounds **169** and **170** appears at δ 5.5 ppm. The total aromatic protons of the xanthene group integrated to 8 protons. In compound **169**, the aromatic protons of C6, 6' and C7, 7' appear together at δ 7.15 ppm with an integration of 4, the triplet at δ 7.32 ppm (*J* =7.6 Hz) represent two protons of C8, 8' and the two protons at C9, 9' are non-equivalent due to the effect of the L-cysteine moiety and appear as a two separate doublets at δ 7.47 and 7.61 ppm (*J* =7.6 Hz). In compound **170,** the 4 aromatic protons of C5,5' and C6,6' appear together at δ 7.13 ppm, the protons of C7,7' appear as triplet at δ 7.30 ppm (*J* = 7.6 Hz) and the two protons at C8,8' are equivalent and appear as doublet at δ 7.49 (*J* = 7.6 Hz).
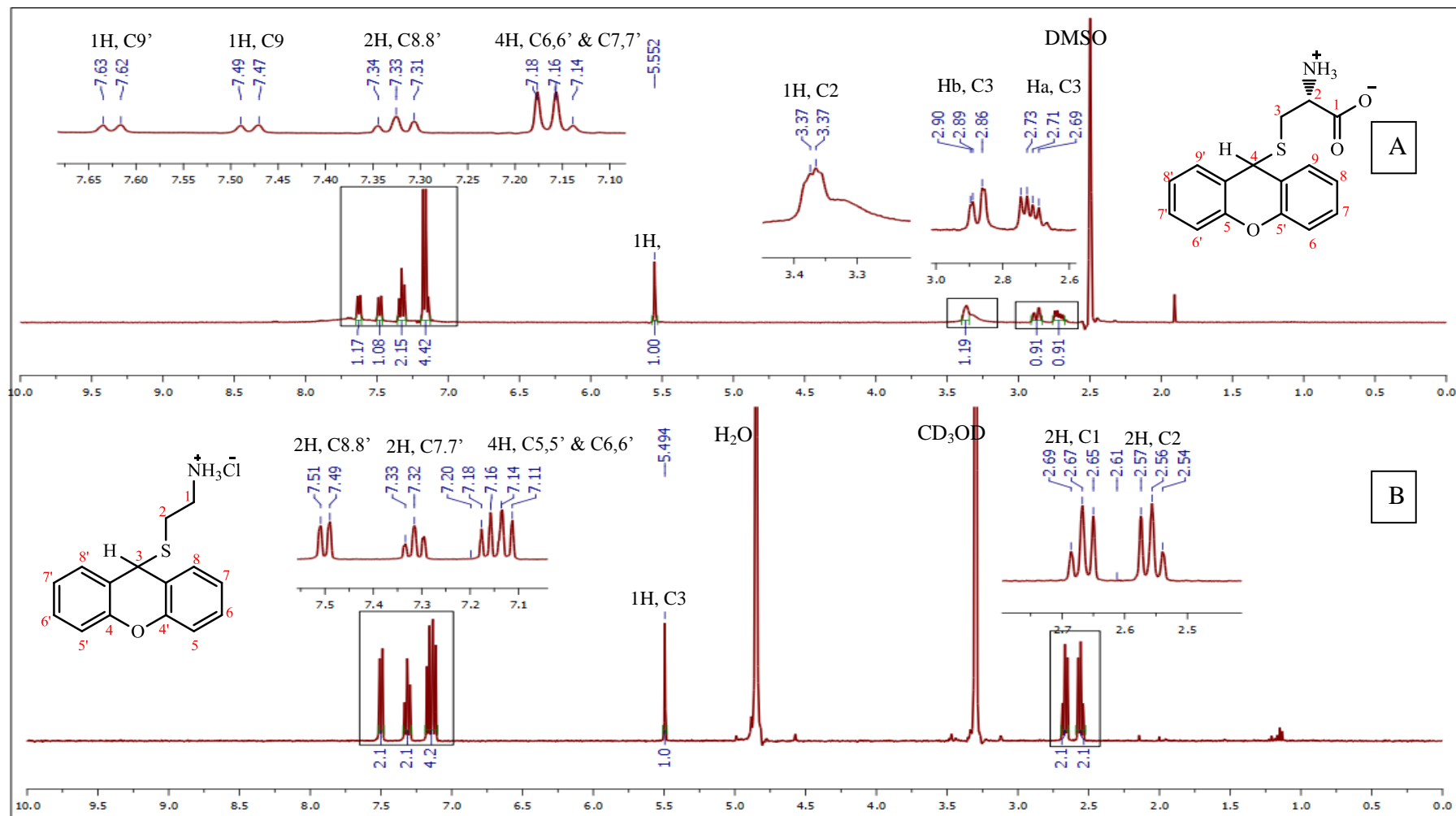
Figure 2.18: ^{1}H NMR (DMSO-*d6*) of (a) compound 169 (b) compound 170.

2.3.8 Attempted synthesis of 2-((2-aminoethyl)thio)-2,2-diphenylacetonitrile

The objective here was to replace one of the trityl phenyl groups with a nitrile to gain access to new STLC analogues through derivatisation of this moiety. The first step involved reacting benzophenone with trimethyl silyl cyanide (TMSCN) in the presence of KCN as a catalyst and 18-crown-6 for phase transfer.[135-137] BF_3.etherate was utilized as before to couple the intermediate alcohol with cysteamine, but instead of the desired compound, cysteamine reacted twice through the proposed mechanism illustrated in **Scheme 2.11** to produce compound **184**.
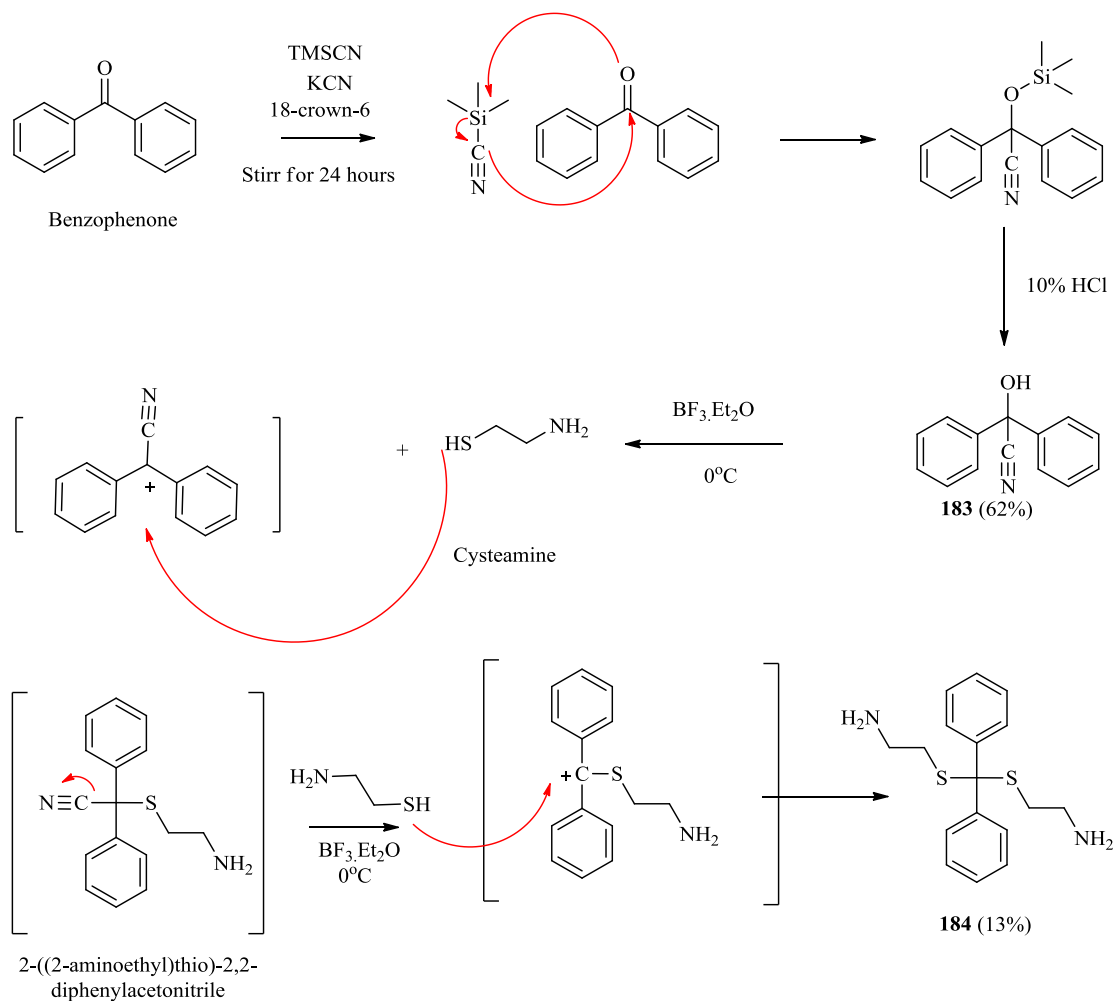
Scheme 2.11: Proposed mechanism for the formation of compound 184

The ^{1}H NMR spectrum of compound **184** (**Figure 2.19)** shows two triplets at δ 2.47 and 2.59 ppm that integrate to 8 protons, which confirms the presence of two cysteamine moieties in the structure. The peaks in the aromatic region integrate to 10 protons which represent the two phenyl rings. A broad peak at 1.14 ppm with an integration of 4 corresponds to the two primary amines, which exchanged when the proton NMR experiment was obtained in deuterated methanol.

The ^{13}C NMR of compound **184** (**Figure 2.20)** confirms coupling of cysteamine twice. The quaternary carbon appears at δ 69.4 ppm, whereas the nitrile carbon of the cyanohydrin starting material which appeared at 85 ppm was not present. The high resolution mass spectra further confirms the synthesis of compound **184** found (M+H=319.12918).
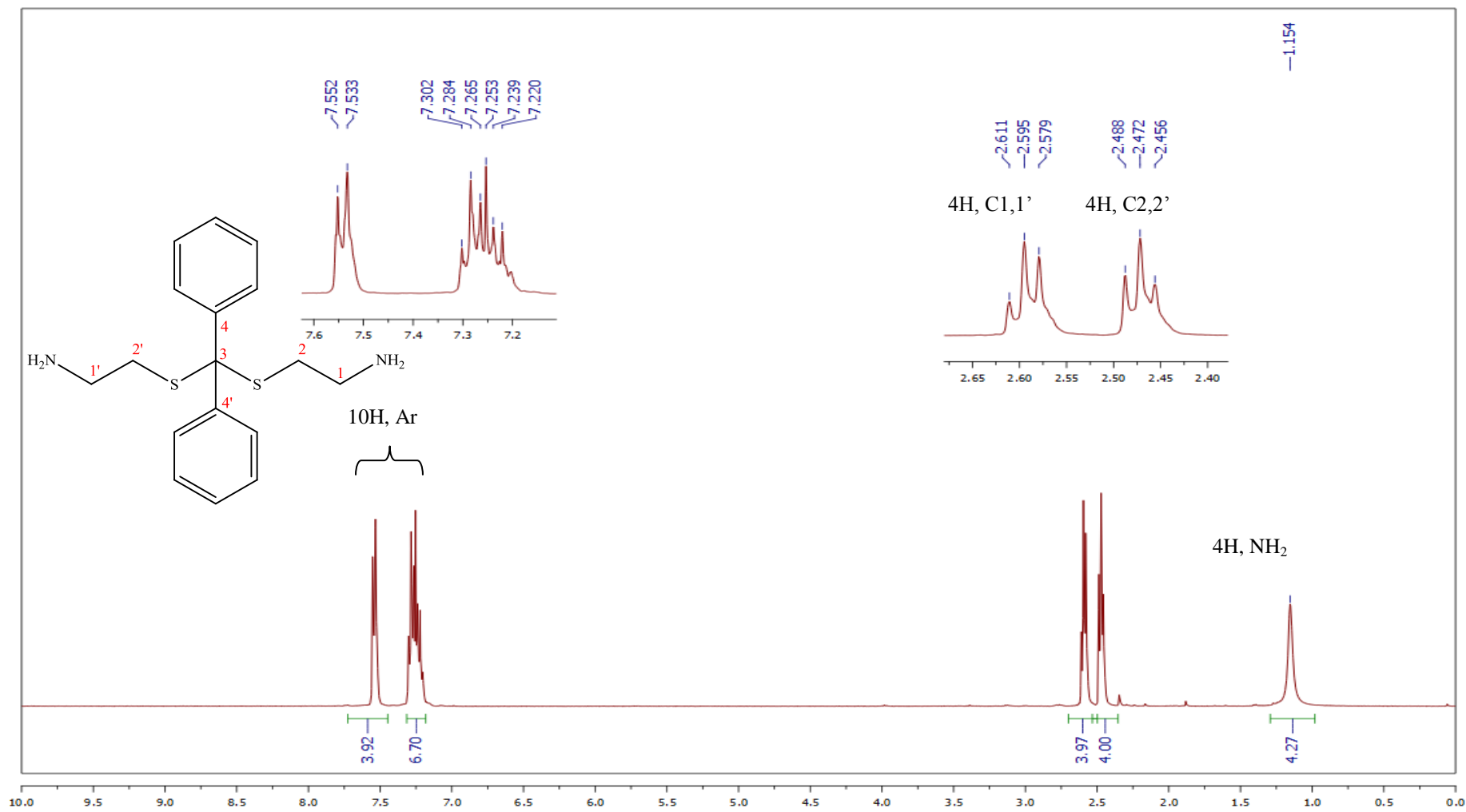
Figure 2.19: ¹H NMR (CDCl₃) spectrum of compound 184
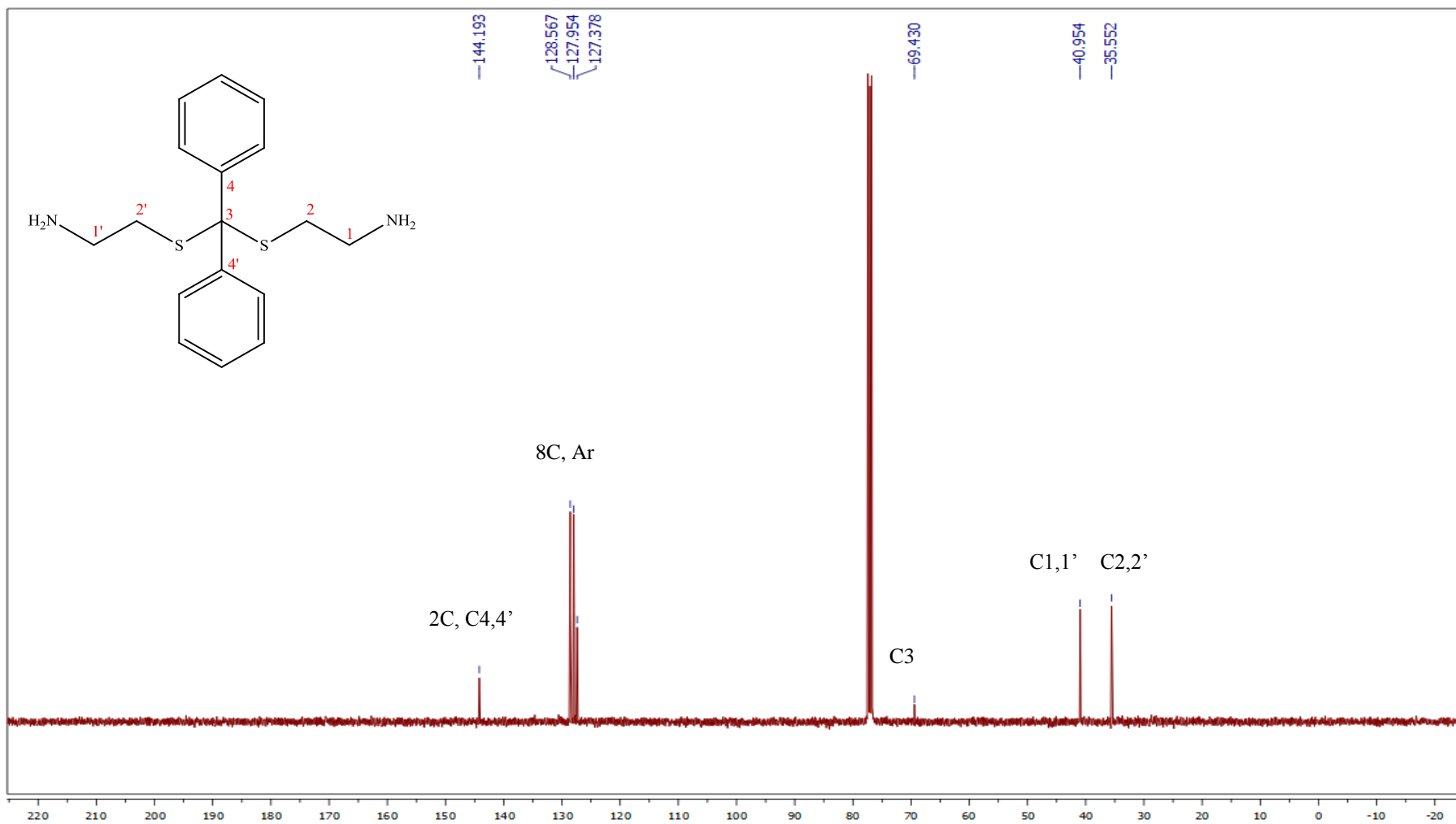
Figure 2.20: ^{13}C NMR (CDCl$_3$) spectrum of compound **184**.

2.3.9 Synthesis of analogues of STLC with extended head groups

The extension of one of the trityl phenyl rings by a two carbon moiety from the quaternary carbon initially required the synthesis of 1,1,3-triphenylprop-2-yn-1-ol (compound **185**) using commercially available lithium phenylacetylide solution to which benzophenone was added slowly at 0 °C. The two signals at δ 87 and 91 ppm in the ^{13}C NMR spectrum of the alcohol (**Figure 2.21**) represent the two acetylene carbons.
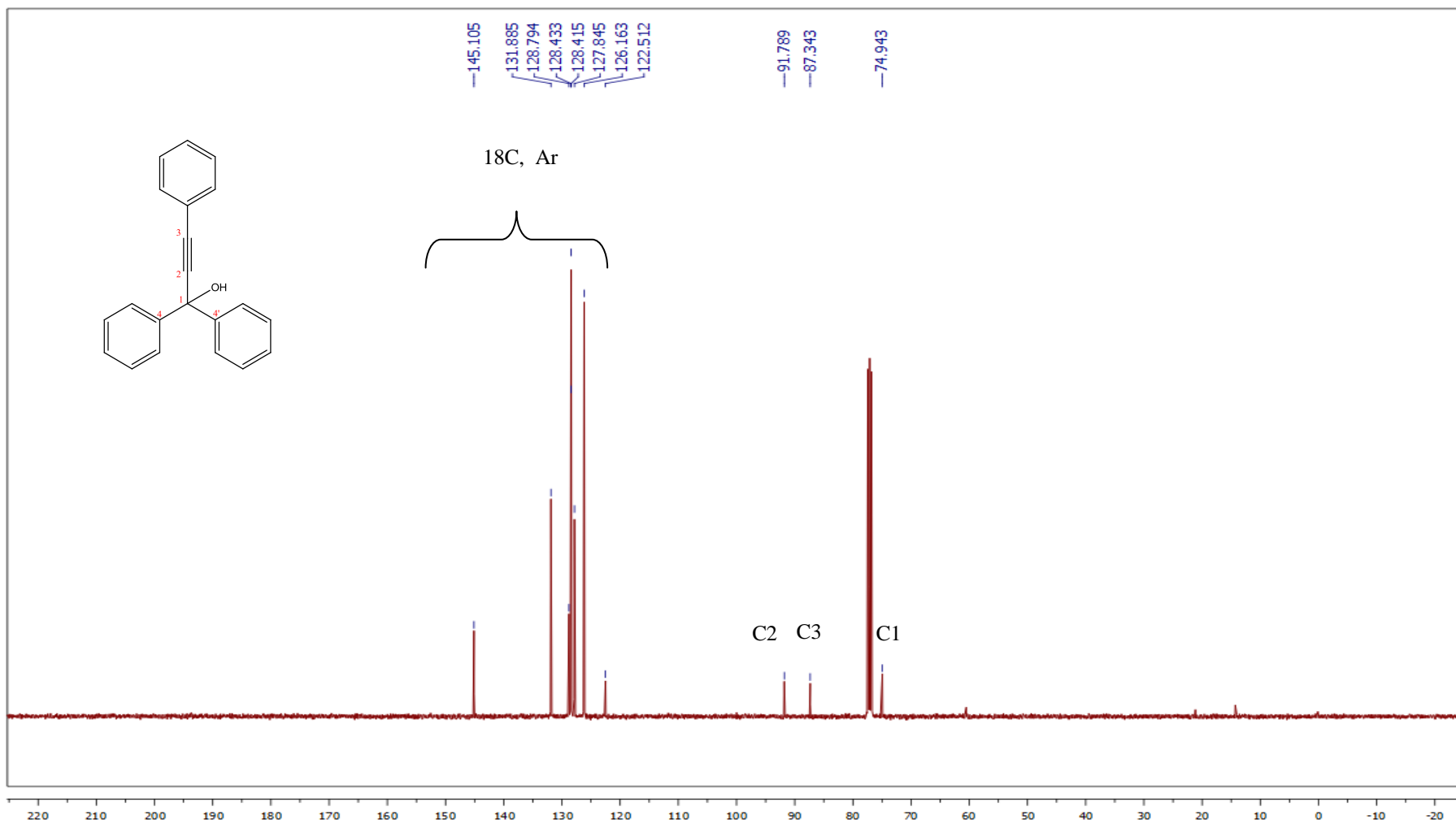
Figure 2.21: ^{13}C NMR (CDCl$_3$) spectrum of compound 185.

Reduction of compound **185** using lithium aluminium hydride (LAH) under atmospheric pressure yielded the *trans* alkene.[138] Attempted reduction to the cis-alkene using Lindlar's reagent resulted in complete reduction to the alkane. The ^{1}H NMR spectrum of compound **187** showed a multiplet at δ 2.8 ppm that integrated to 4 protons. The HMQC (Heteronuclear Multiple Quantum Coherence) spectrum confirmed the four protons were from the ethylene moiety (**Figure 2.22**).

The alcohols were coupled with L-cysteine using the established coupling procedure (**Scheme 2.12**). The ^{1}H NMR spectra with the assigned proton of compounds **188** and **189** are shown **Figure 2.23.** The ^{1}H NMR spectrum of compound **151** shows the protons of the alkane extended group (C6 and C5) as multiplets at δ 2.45 and 2.68 ppm, respectively. The proton of C5 is resonating with the one proton of C3. While in compound **152** the protons of the alkene extended group appear at δ 6.51 ppm, which corresponds to the C6 and the other highly shielded proton at δ 4.5 ppm corresponds to the C5, the multiplicity of the aliphatic and extended group protons indicate that the compound is a racemic mixture of stereoisomers. The successful coupling of compounds **188** and **189** were also confirmed by high resolution mass spectrometry (M+H= 390.1519 and 392.1676, respectively).
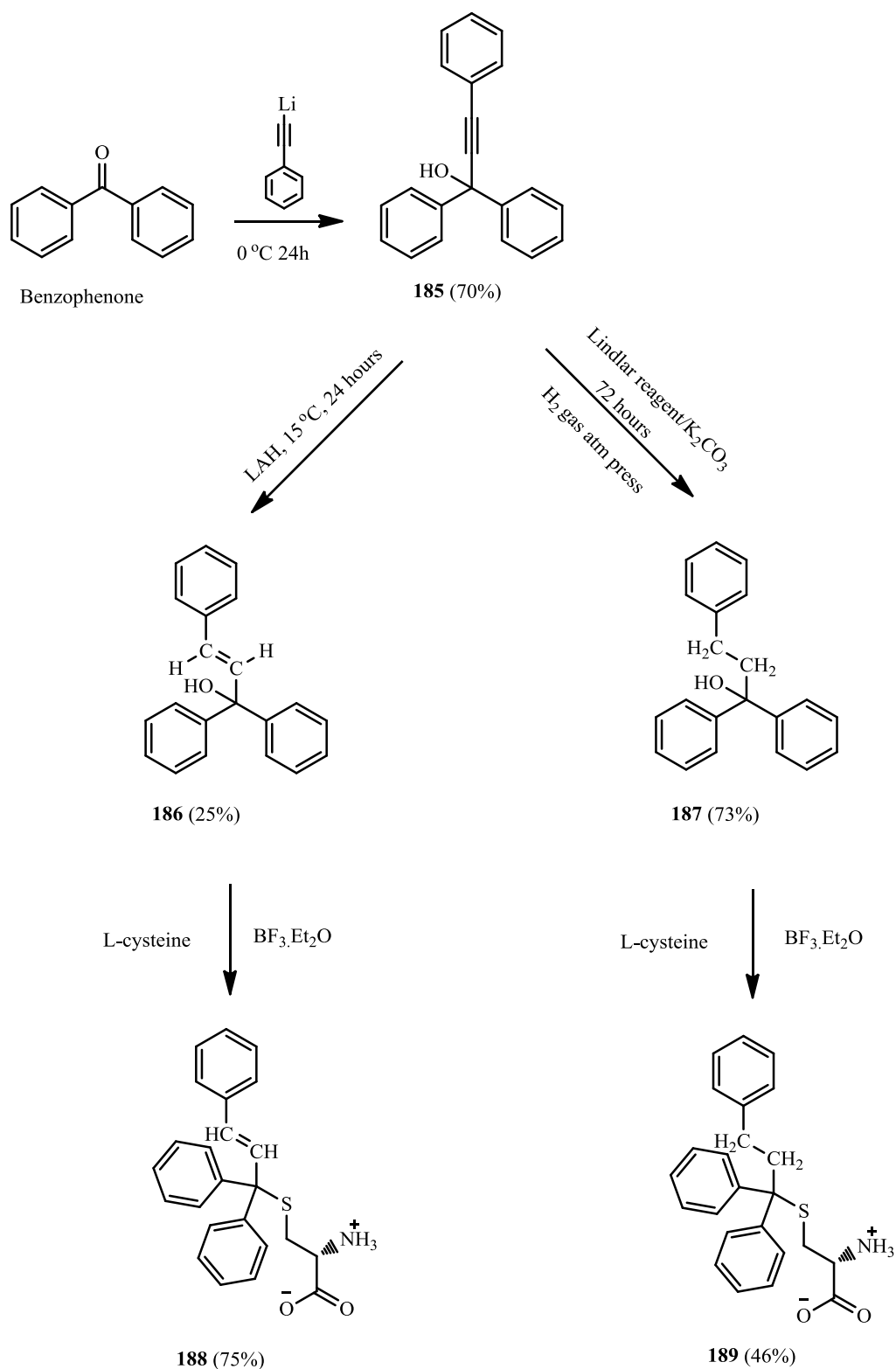
Scheme 2.12: Synthesis of alkane and alkene extended analogues of STLC
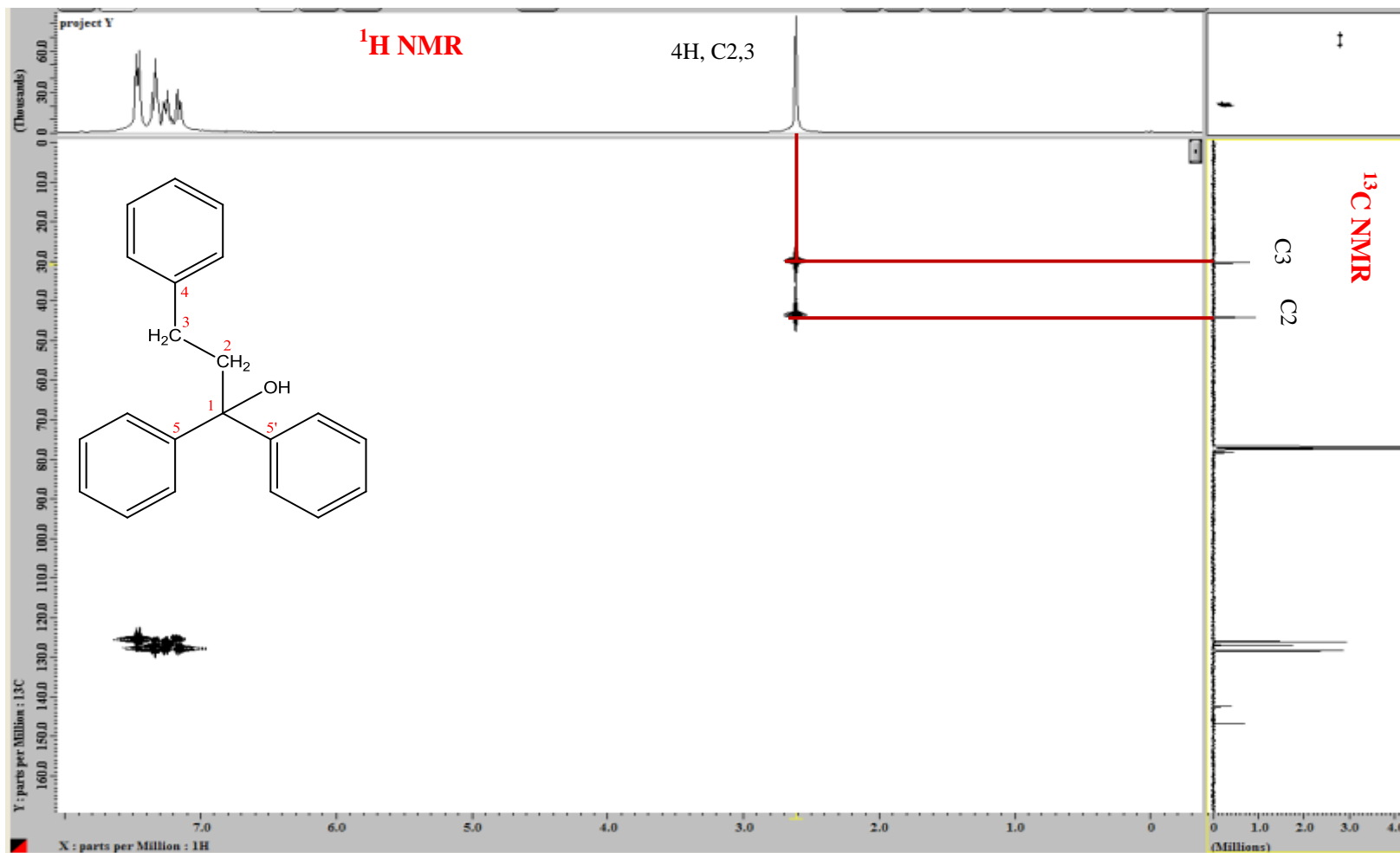
Figure 2.22: HMQC (DMSO-*d6*) of compound 187.
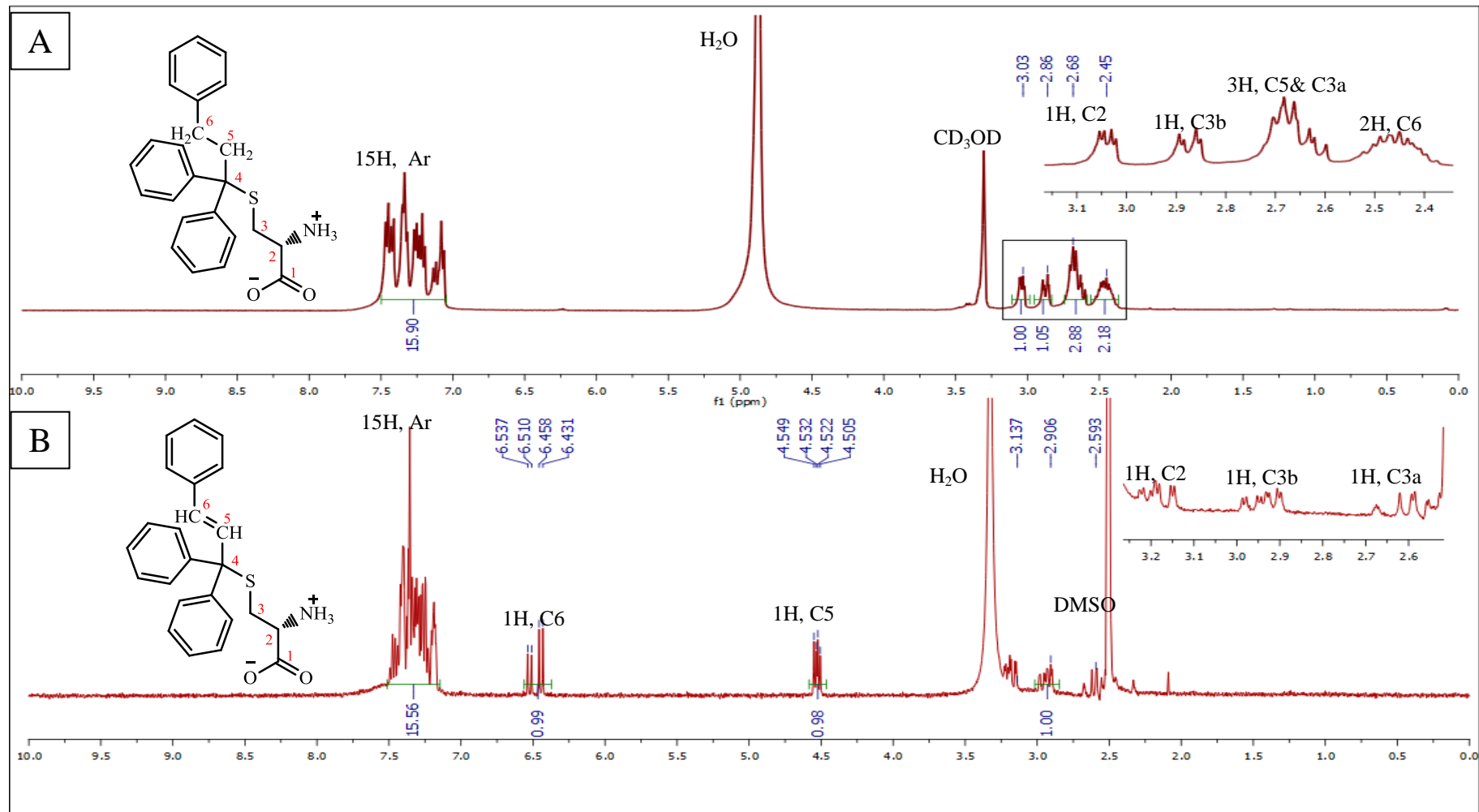
Figure 2.23: ^{1}H NMR (CD$_3$OD) spectrum of (A) compound **189** (B) compound **188.**

97

2.4 Modelling and biological results

2.4.1 Modification of the head group

2.4.1.1 Substituents on the phenyl rings

Substituents on the phenyl rings of core scaffold (compound **101)** can either enhance lipophilic or hydrophilic interactions with the target, the latter by including H-bond donor or acceptor groups to target specific residues in the pocket. Groups including OH, Cl, CH_3 and F were introduced into the phenyl rings at different positions and the docking studies indicate that, in general, substituents are favoured in ring A.

Monastrol has a *meta*-hydroxyl group that specifically makes H-bonds with the main chain carbonyl group of Glu118, the main chain amino group of Ala133, and the side chain nitrogen of Arg119 in the Eg5 allosteric binding site.[69] Compound **105** also has a *meta*-hydroxyl substituent, which was incorporated to increase H-bond donor/acceptor capability. Docking this compound into Eg5 suggested an additional H-bond inside the pocket with the backbone NH of Ala218 (**Figure 2.24**), whereas compound **106**, with a *para*-hydroxy substituent did not appear to form any H-bond (**Figure 2.25**). Interestingly, compound **105** had a better IC_{50} against Eg5 (67.6 nM) than compound **106** (159.4 nM), which was an improvement over compound **101** (138.0 nM), and suggests that a *meta*-hydroxyl facilitates binding with the allosteric pocket as our docking suggested. Goldscore was consistent with the biological results and scored slightly higher for compounds **105** (82.6) compared to **106** (82.2) while compound **101** scored 74.1. Unfortunately, both compounds were significantly less active in the cell-based assay compared to both STLC and compound **101**, which could be due to decreased cell permeability through introduction of the hydrophilic hydroxyl group.
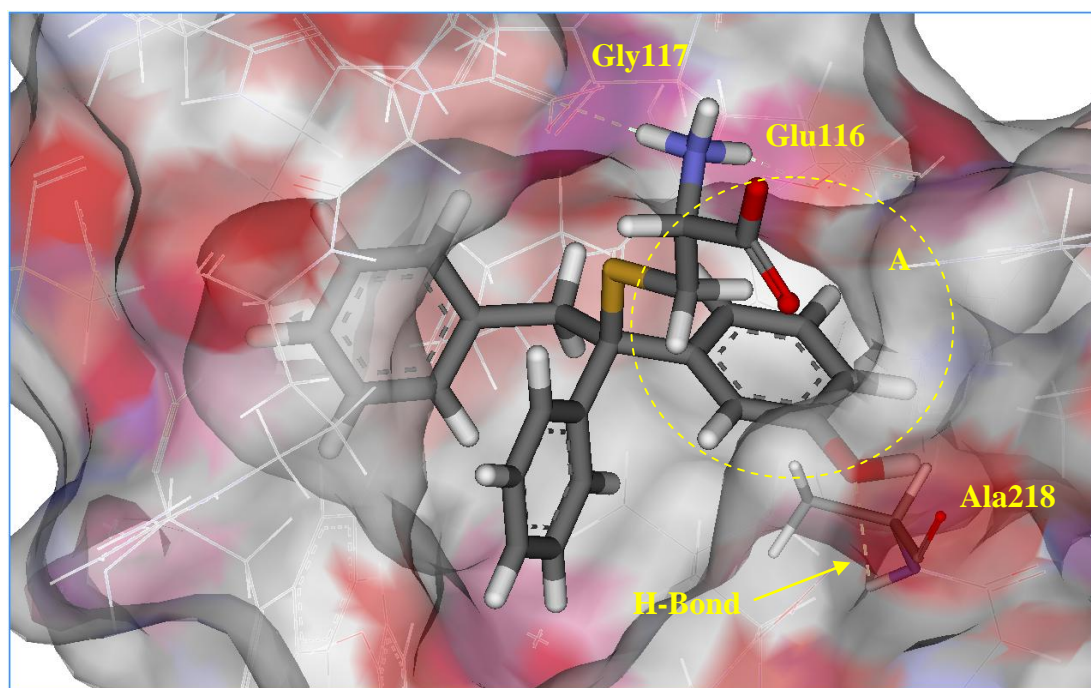
Figure 2.24: Docking pose of compound 105.
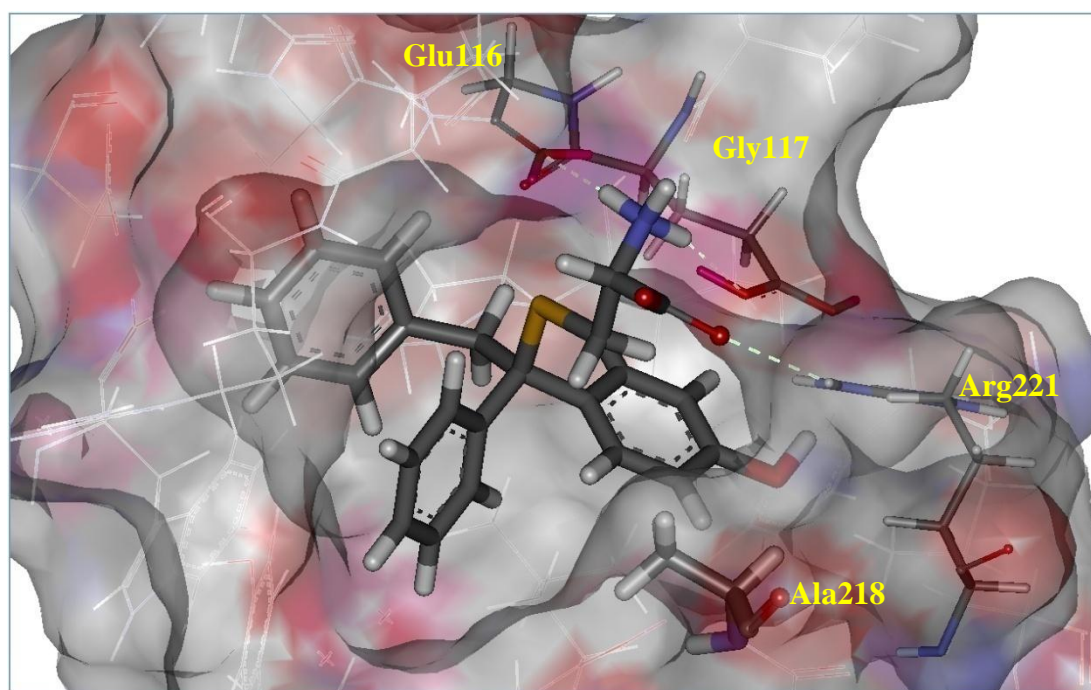
Figure 2.25: Docking pose of compound 106.

Our docking studies show that a methyl group on the phenyl ring (compounds **112** and **113**) should increase hydrophobic interactions with the binding pockets, with the Goldscore for both of them (80.06 and 81.50) being higher than STLC (78. 63) and

the core scaffold **101** (74.1). Compound **112** with a single *para*-methyl substituent fits deeply inside lipophilic pocket A, while compound **113**, with a *para*-methyl substituent in each phenyl ring reorientated the molecule (**Figure 2.26 and 2.27**). Each methylated aromatic ring occupied lipophilic pockets A and B with the benzyl substituent now positioned in the smallest of the three pockets C. The primary amine for both compounds maintains its two H-bonds with Glu116 and Gly117, and the carboxylate remains solvent-exposed. The dimethyl substituted derivative (compound **113**) had higher activity against Eg5 (IC_{50} = 106.5 nM) compared to compound **112** (IC_{50} = 167.6 nM), and demonstrated that enhanced hydrophobic contacts improved its activity compared with **101** (138 nM). Compound **112** had 2-fold higher cell activity (1442 nM) than compound **113** (2786 nM) and was an improvement over compound **101** (3141 nM) and comparable with STLC (1452 nM).
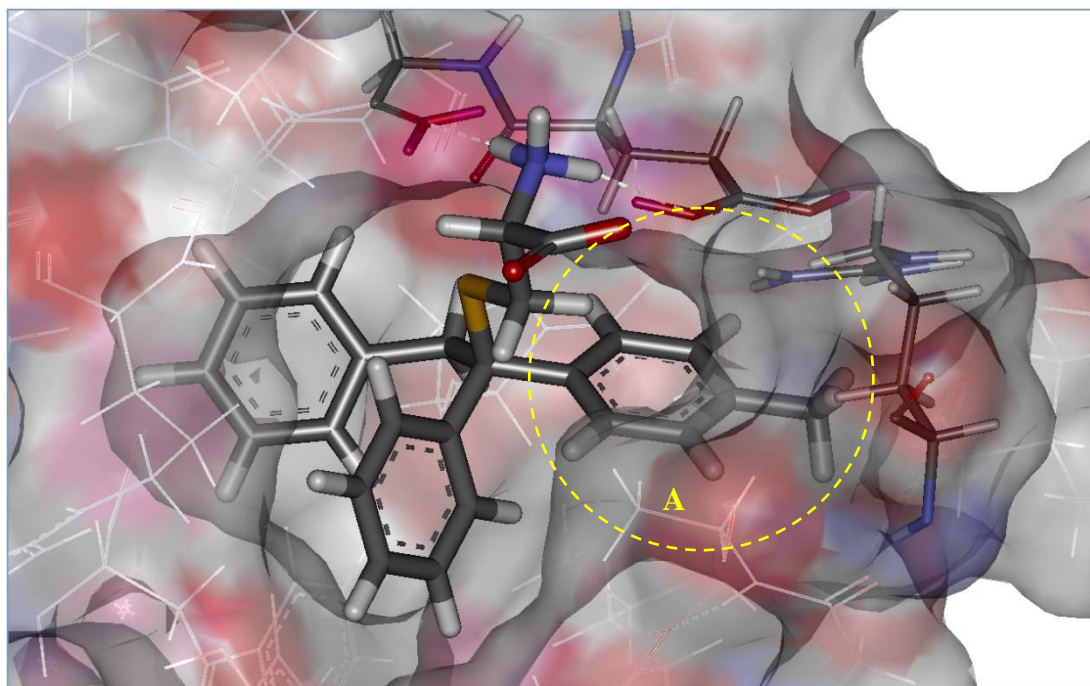
Figure 2.26: Docking pose of compound 112.
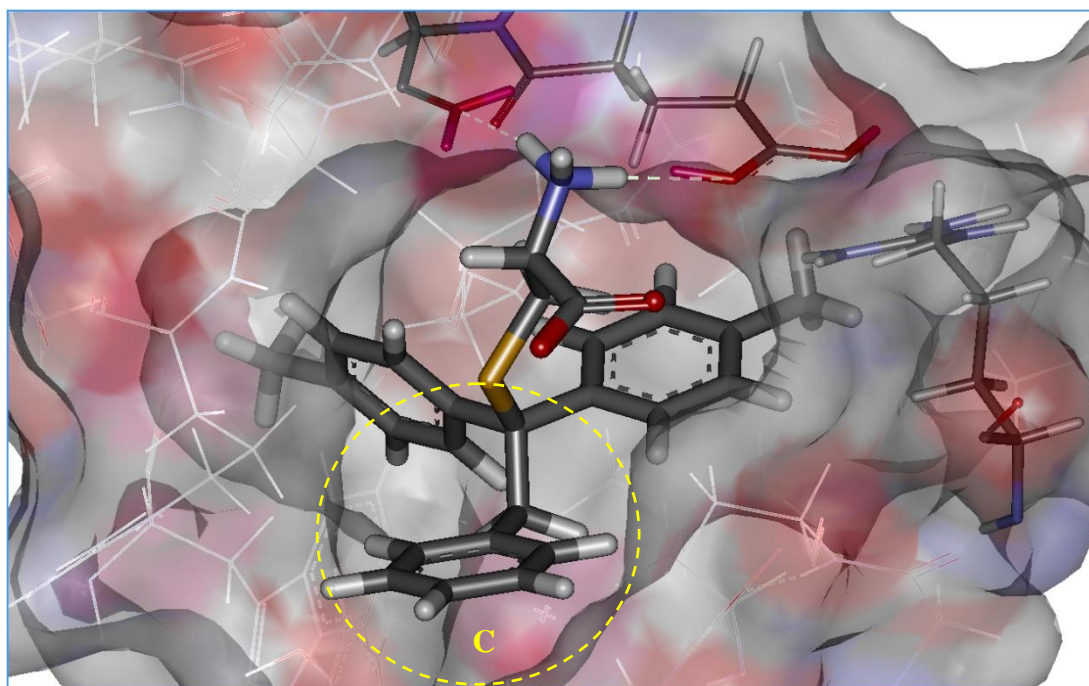
Figure 2.27: Docking pose of compound 113

Overall, compounds with substituents on the phenyl rings proved to be successful inhibitors of Eg5 ATPase activity (**Table 2.7**). Compound **108** with a *para*-chloro substituent in one ring was the most potent compound (58.6 nM), while compound **107**, with a *meta*-chloro substituent also showed good activity (128.9 nM). Goldscore was higher for the *para*-chloro (86.83) compared with the *meta*-chloro (82.8). A ring with two chloro substituents (compound **109**) had reduced activity (191.2 nM), which suggests that the *meta*-chloro group negates the positive lipophilic gain of the *para*-substituent which was reflected by the slightly lower Goldscore (84.37). The *para*-fluoro analogue (compound **115**) had almost a three-fold drop in activity compared with compound **108**; the Goldscore was also lower (80.27), which suggests that the larger lipophilic chloro substituent makes more favourable interactions with the hydrophobic pocket. Compounds in which both phenyl rings contained halide substituents (compounds **111**, **110** and **116**) consistently demonstrated less inhibitory activity against Eg5, which is possibly due to an increase in bulkiness that affects the pose of the carboxylic acid, as the docking study showed none of these compounds formed a hydrogen bond with Arg221. Unfortunately, as before, none of these compounds has cell activity against the K562 cell line comparable with STLC, and the most active compound **112** in the group did not correlate with the enzyme

101
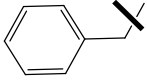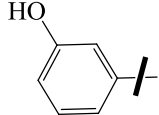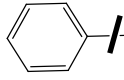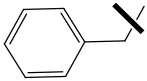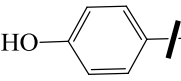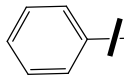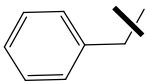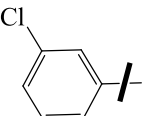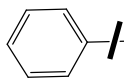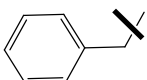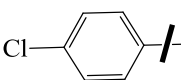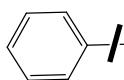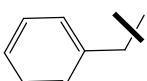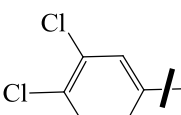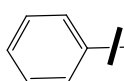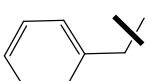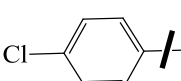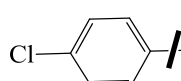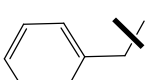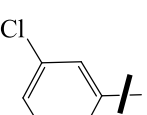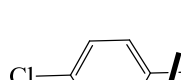
inhibitory activity. A possible explanation for this decreased activity is all the compounds were tested as racemic mixtures, and if one of the isomers was more active than the other, the effective concentration is essentially reduced. Our docking results suggest that the chirality of the head group for some of the compounds will have an influence on activity (**Table 2.6**).

Compound	*R*- diastereomere	*S*- diastereomere
102	68.62	71.48
103	60.58	63.68
104	67.26	70.54
105	82.66	82.84
106	82.21	78.54
107	79.59	86.37
108	80.95	82.84
109	84.37	77.06
111	80.89	81.65
112	80.06	78.49
114	77.34	82.88
115	75.24	80.28

Table 2.6: Docking Goldscores of the R and S diastereomeres of compounds with modified phenyl rings.

Compound	R_1	R_2	R_3	ATPase activity IC_{50} nM	Cell based assay EC_{50} nM
STLC	(phenyl)	(phenyl)	(phenyl)	$225 \pm 12^{*}$	1452 ± 76
101	(benzyl)	(phenyl)	(phenyl)	$138.0 \pm 11.2^{\ddagger}$	3141 ± 296
102	(benzyl)	H	(phenyl)	No inhibition	NT
103	(benzyl)	H_3C-	(phenyl)	No inhibition	NT
104	(benzyl)	H_3C-CH_2-	(phenyl)	No inhibition	NT

105				67.6 ± 7.4[‡]	17742 ± 3186
106				159.4 ± 15.7[‡]	18239 ± 3565
107				128.9 ± 15.8[‡]	4539 ± 191
108				58.6 ± 7.4[‡]	2471 ± 360
109				191.2 ± 20.1[‡]	2655 ± 217
110				251.8 ± 29.2[‡]	5224 ± 567
111				567.5 ± 56.9[‡]	4742 ± 420
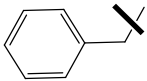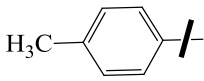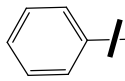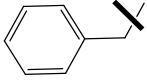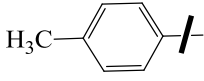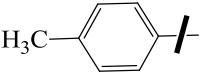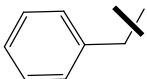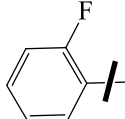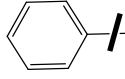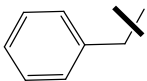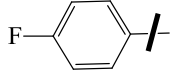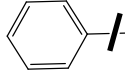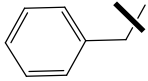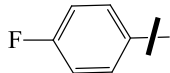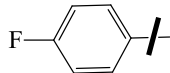
112		H₃C—		$167.6 \pm 18.1^{\ddagger}$	1442 ± 82
113		H₃C—	H₃C—	$106.5 \pm 16.1^{\ddagger}$	2786 ± 177
114		F		$216.8 \pm 19.2^{\ddagger}$	2317 ± 123
115		F—		$150.5 \pm 10.7^{\ddagger}$	6095 ± 587
116		F—	F—	$178.2 \pm 19.6^{\ddagger}$	5117 ± 719

Table 2.7: The results of inhibitory activity against Eg5 ATPase and K562 cancer cells for the ring substituted compounds.

Note: IC$_{50}$ results were measured by (*) testing once (‡) testing in triplicate.

2.4.1.2 Reducing the size of the third substituent in the hydrophobic head group

Having established that one phenyl ring could be replaced by a larger benzyl substituent, a series of compounds were prepared with a smaller substituent in this position: hydrogen, methyl, ethyl (compounds **102**-**104**). All compounds without an aromatic substituent were inactive against Eg5 (**Table 2.7**), and docking studies suggest that in the absence of a third phenyl ring; the cysteine tail docked into one of the hydrophobic pockets, and prevented the primary amine from forming H-bonds with Glu116 and Gly117 (**Figure 2.28**).
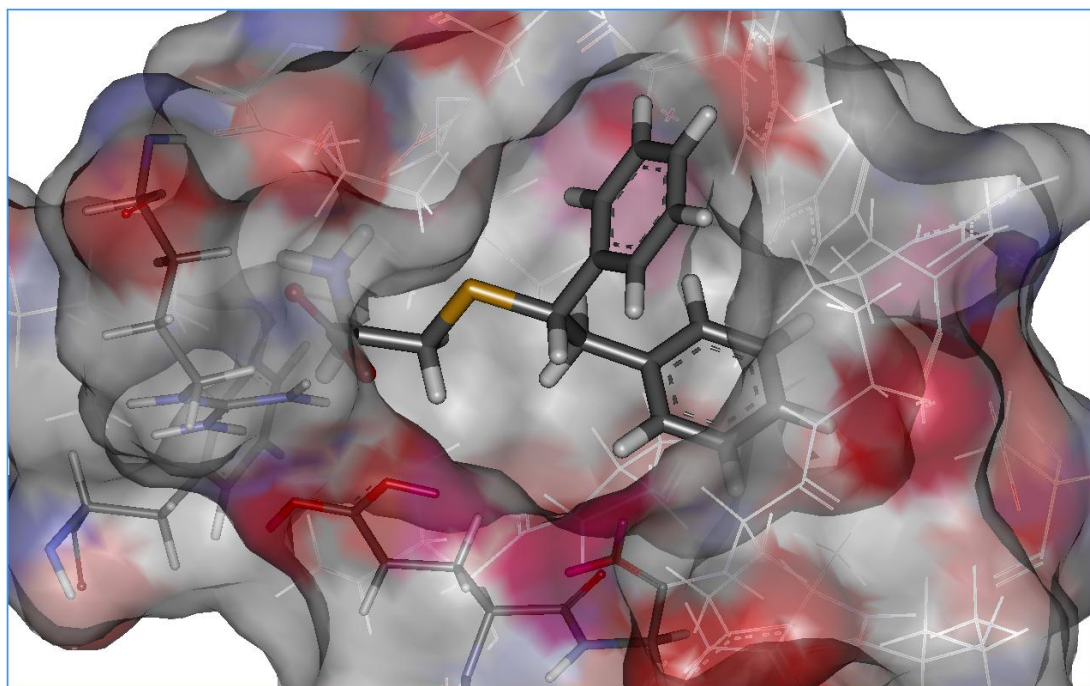
Figure 2.28: Docking pose of compound 102

The inactivity of these compounds could also be explained by another two reasons. Firstly, smaller substituents are unable to interact strongly with the hydrophobic pocket and the ligand does not associate with the protein with sufficient affinity to cause induced inhibition. The other possible reason why these particular compounds do not inhibit Eg5 is through the effect of the smaller substituent on the relative orientation of the remaining two phenyl rings, which in itself could impact on their ability to interact with the hydrophobic pockets. In order to investigate this possibility, we examined the relative orientation of the two phenyl rings with different sized substituents using a combination of X-ray diffraction and molecular modelling.

Four compounds were synthesised replacing one of the three phenyl rings of the trityl cysteamine with an increasing size of substituent, ie H, CH_3, isopropyl, phenyl. All the compounds were recrystallized from a supersaturated solution of actonitrile to determine the crystal structure (see Materials and Methods). The ATPase inhibitory activity against Eg5 for the crystalized compounds and the dihedral angle between the two phenyl rings were determined[139] from the solved crystal structures.

Results in **Table 2.8** show that compound **134** has the highest dihedral angle and the lowest inhibitory activites. The more bulky groups of methyl, isopropyl and phenyl substituents reduce the dihedral angle and there is a corresponding improvement in activity. The bulkiness of the third substituent reduces the dihedral angle between the two phenyl rings and restricts their rotation relative to one another to optimise their interation with the protein. Furthermore, an improved hydrophobic interaction with the third pocket is also possible with a larger substituent, as the activity difference between compounds **136** and **137** suggests. It would therefore appear that inhibition of the enzyme is due to a combination of factors and two phenyl rings alone are insufficient for inhibition.
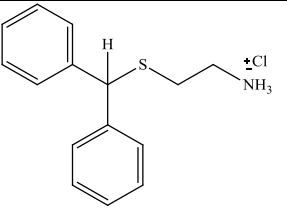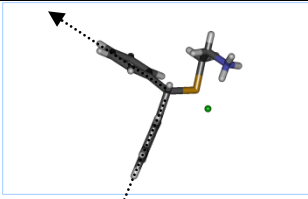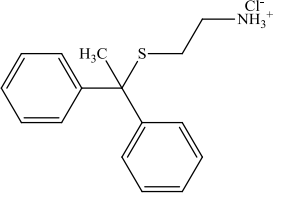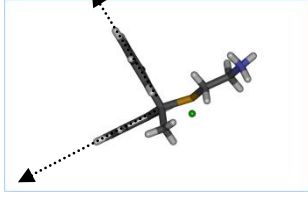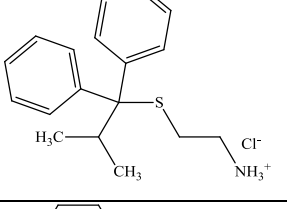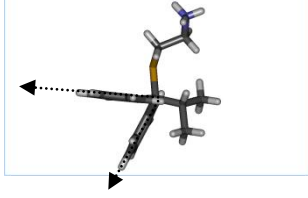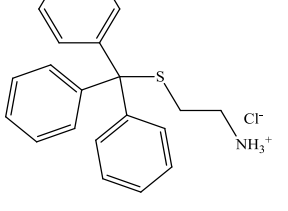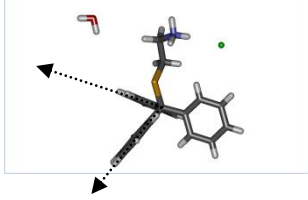
Comp	Structure	Crystal structure	Dihedral angle	IC$_{50}$ (nM)
134			125.94°	No inhibition[*]
135			88.77°	22186[*]
136			68.27°	222.5 ± 34.9[‡]
137			71.33°	150[*]

Table 2.8: Crystal structures, dihedral angles and ATPase inhibitory activity of analogues with head groups of varying flexibility.

Note: IC$_{50}$ results were measured by (*) testing once (‡) testing in triplicate.

2.4.1.3 Rigidification of the hydrophobic head group

Having established that a hydrophobic head group with limited flexibility was required for effective inhibition of Eg5, presumably through a reduced entropic penalty when binding, a series of compounds were prepared in which two of the phenyl moieties were restrained into fused ring systems as the planar fluorene, or the more angular xanthene and thioxanthene (**Figure 2.29**).
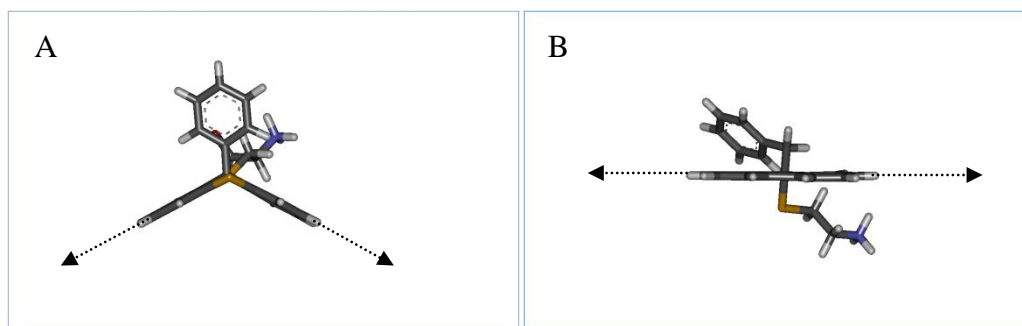
Figure 2.29: (A) tilted structure of thioxanthene derivative (B) and the flatter structure of fluorene derivative.

Fourteen compounds in the fused ring family were synthesised with benzyl, phenyl and H substitution, both with cysteine and cysteamine tails (**Table 2.5**). The docking Goldscores of these compounds were generally lower compared with those of the unrestrained head groups (**Table 2.9**).

Compound	Gold score
169	59.42
170	55.38
171	60.07
172	53.02
173	69.43
174	66.96
175	68.68
176	67.28
177	76.67
178	69.75
179	71.47
180	63.47
181	78.42
182	69.60

Table 2.9: Goldscores of fused ring family

Our modelling studies suggested that the xanthene and thioxanthene ring systems are more compatible with the three hydrophobic pockets, which is exemplified by the docking pose of compound **179,** which has an angular thioxanthene ring system. **Figure 2.30** shows the tilted structure of the fused rings fits into two pockets (A and

C), the benzyl moiety occupies pocket B and the primary amine was able to form the H-bonds with the Glu116 and Gly117.
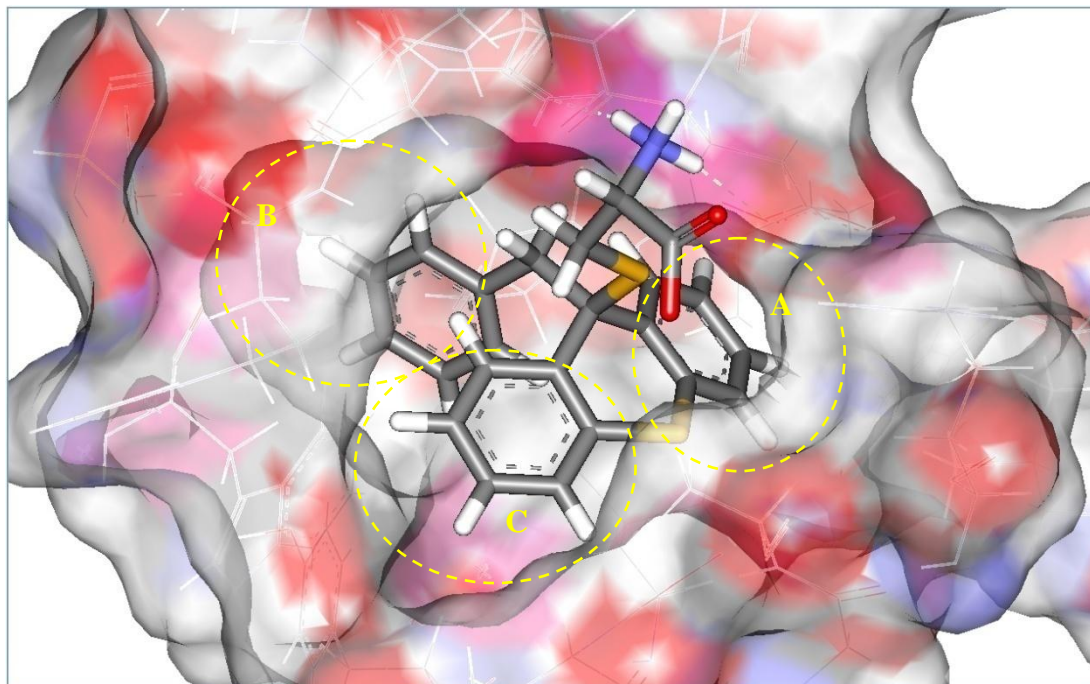
Figure 2.30: Docking pose of compound 179.

The inhibitory data against Eg5 (**Table 2.10**) showed that all compounds with no third aromatic ring (compounds **169**-**172**) were inactive, which is possibly through lost hydrophobic interactions inside the hydrophobic pocket. The thioxanthene and xanthenes with a phenyl moiety (compounds **173**-**176**) were more active than those with a benzyl moiety (compounds **177-180**), which may be due to the extended structure of the benzyl moiety pushing the rigid xanthenes and thioxanthenes further outside the binding pocket.

The flatter fluorene derivatives (compounds **181** and **182**) showed different docking poses, with the cysteine moiety occupying one of the hydrophobic pockets, the fused rings protruding outside the binding pocket and the benzyl moiety occuping pocket B (**Figure 2.31**).

110
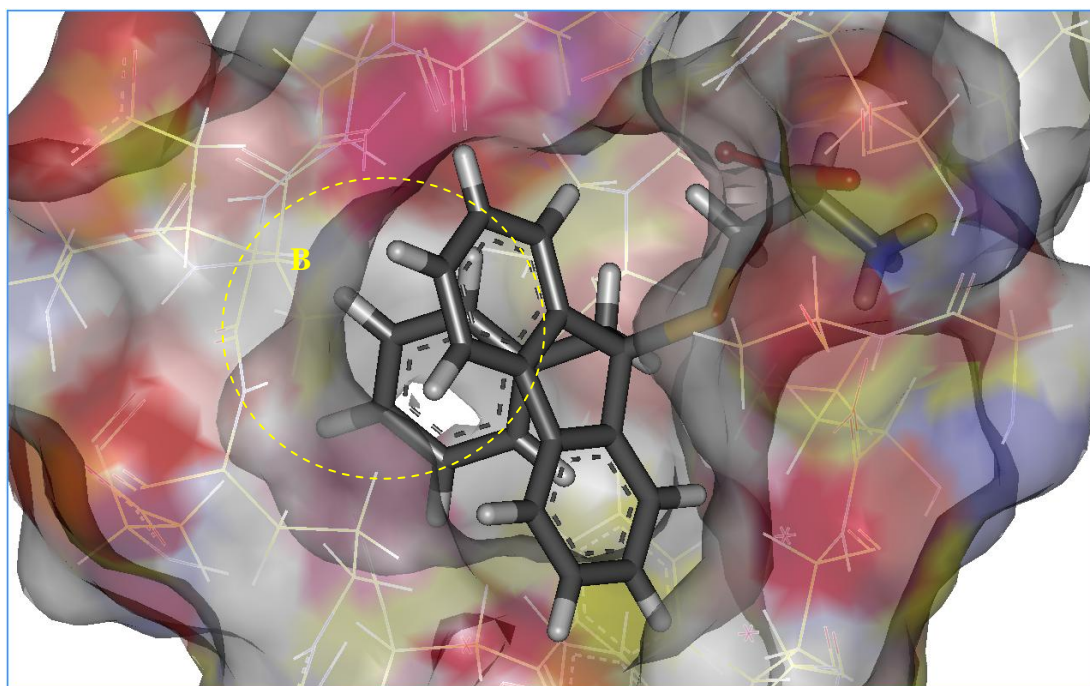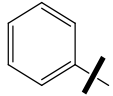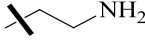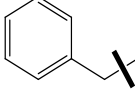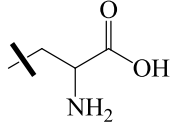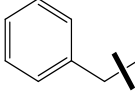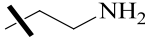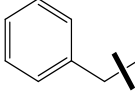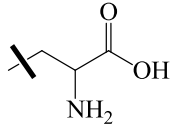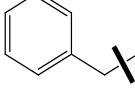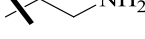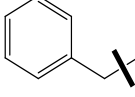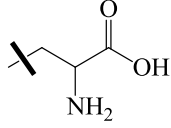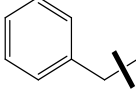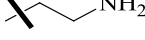
Figure 2.31: Docking pose of compound 181.

The fluorenes had very low activity for the phenyl substituted compound **181** (236110 nM) and no activity at all for the benzyl substituted analogue (compound **182**), which could be due to the inability of the flat fluorene to accommodate itself properly inside the hydrophobic pocket. The overall ATPase results in **Table 2.10** revealed that introducing rigidity into the head group of the structure lowers its inhibition.
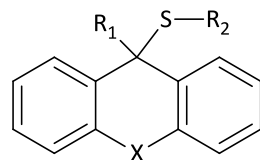
ID	X	R$_1$	R$_2$	ATPase activity IC$_{50}$ nM	Cell based assay EC$_{50}$ nM
169	O	H		No inhibition	NT
170	O	H		No inhibition	NT
171	S	H		No inhibition	NT
172	S	H		No inhibition	NT
173	O			25439	NT
174	O			16027	NT
175	S			12270	>50000

176	S			58632	NT
177	O			No inhibition	NT
178	O			No inhibition	NT
179	S			43595	NT
180	S			54197	NT
181	-*			236110	NT
182	-*			No inhibition	NT

*Fluorene structure derivative

Table 2.10: Biological results of xanthene, thioxanthene and flourene derivative compounds

Note: IC$_{50}$ for all compounds were measured by testing samples once.

2.4.1.4 Modification of the benzyl ring

Certain lipophilic substituents in the benzyl ring have the potential to enhance binding affinity and affect its orientation with respect to the three hydrophobic pockets and the binding of the core unsubstituted scaffold (compound **101**). To test this rationale, we docked three compounds with chloro substituents at different positions on the benzyl ring: compounds **117** (*meta/para*), **118** (*para*) and **119** (*meta*). The Goldscores for the three compounds were 82.07, 78.69, and 84.73, respectively, and higher than the unsubstituted core compound **101** (74.1), due to the increased hydrophobic interactions by the chlorine substituents. The docking pose of these compounds is exemplified by compound **119** (**Figure 2.32**). Similar to the docking pose of **101**, the *meta*-chloro substituted benzyl ring occupied pocket B, the primary amine retained the H-bond with Glu116 and Gly117, although the carboxylic acid of this group of compounds lost its ability to form H-bonds with Arg221.
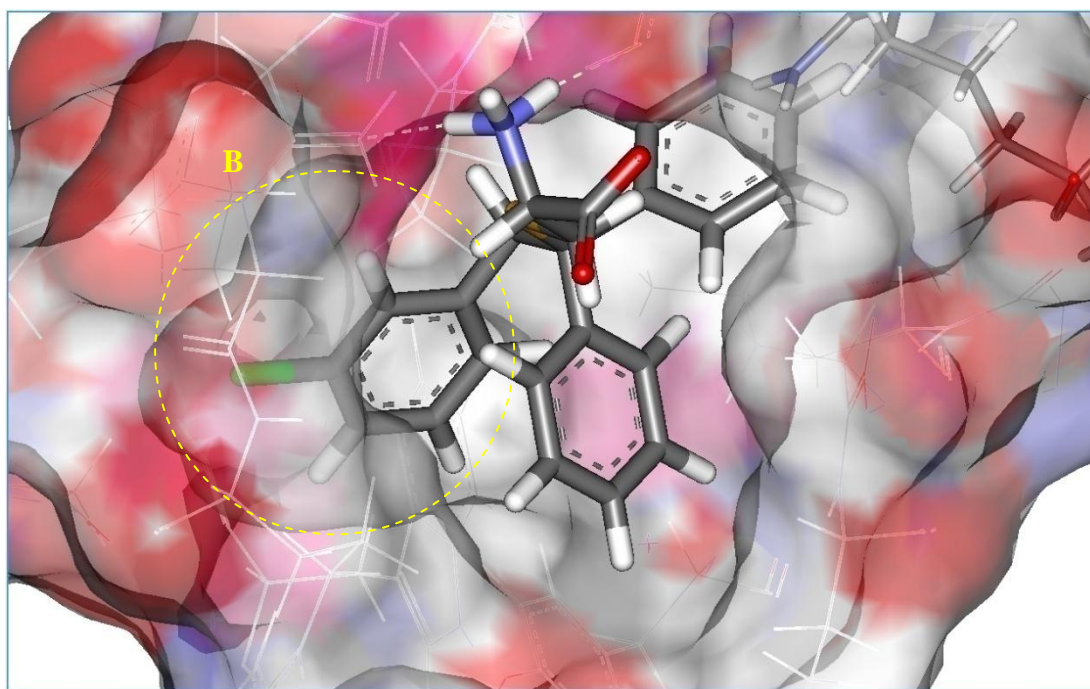
Figure 2.32: Docking pose of compound 119.

The biological results (**Table 2.11**) revealed that the mono *para*-chloro group produced a 1.5-fold loss in activity (237.5 nM), the *meta*-chloro group caused a 3-fold loss in inhibitory activity (455.8 nM), while the dichloro (*para*/*meta*) substitution (compound **117**) exhibited almost a 40-fold loss in activity compared to

the unsubstituted core scaffold (compound **101**). The inhibitory activity against Eg5 is in an increasing order of *para > meta > para/meta* chlorosubstitution in all the compounds with modified head groups. Dichlorosubstitution may produce a more pronounced decrease in activity through its displacement from the binding pocket.

Extending the benzyl group to an unsaturated styryl or saturated phenylethyl moiety (compounds **188** and **189**) was also investigated. The docking pose of compound **189** (**Figure 2.33**) showed the extended moiety occupied the same pocket B as compound **101**, the primary amine retained the H-bonds with Glu116 and Gly117, and furthermore, the carboxylic acid was able to form a H-bond with Arg221. We are awaiting Eg5 inhibitory data for these two compounds.
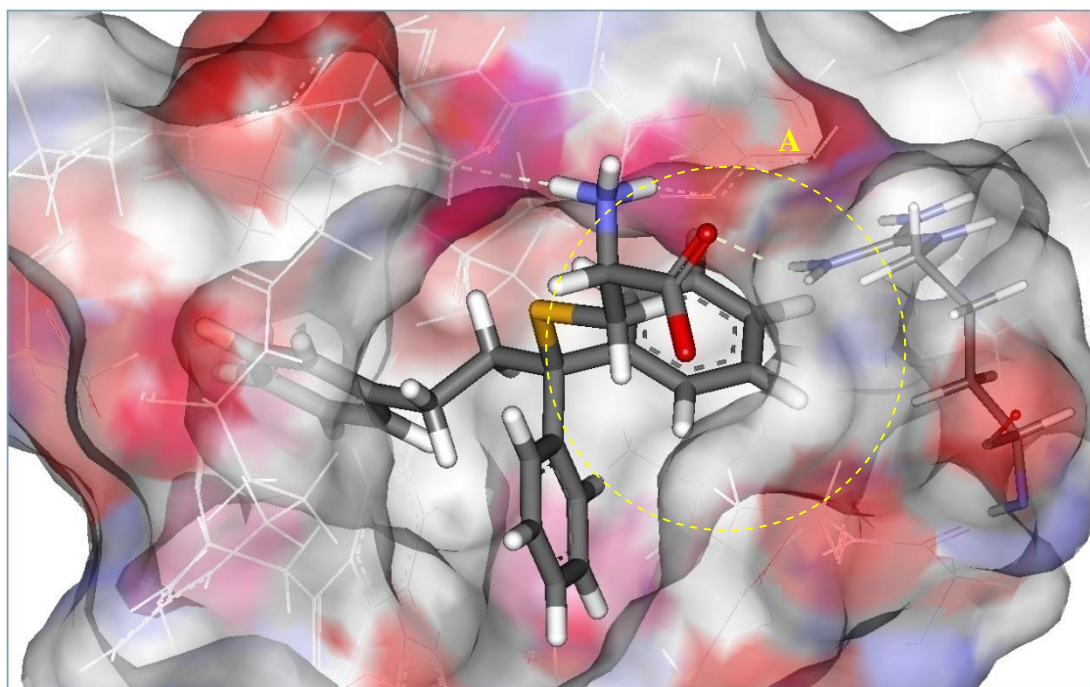
Figure 2.33: Docking pose of compound 189.

Replacement of the benzyl with a benzoyl moiety imparts rigidity into the head group and although offering the potential to form H-bonds inside the pocket through the ketone, the docking pose (**Figure 2.34**) suggests this is unlikely. Compounds **140** and **141** with cysteamine and cysteine tails, respectively, were synthesised and tested against Eg5; both were inactive. Although the docking score of compounds

140 and **141** was relatively high (80.76 and 74.44), the reason behind this total loss of activity is unclear.
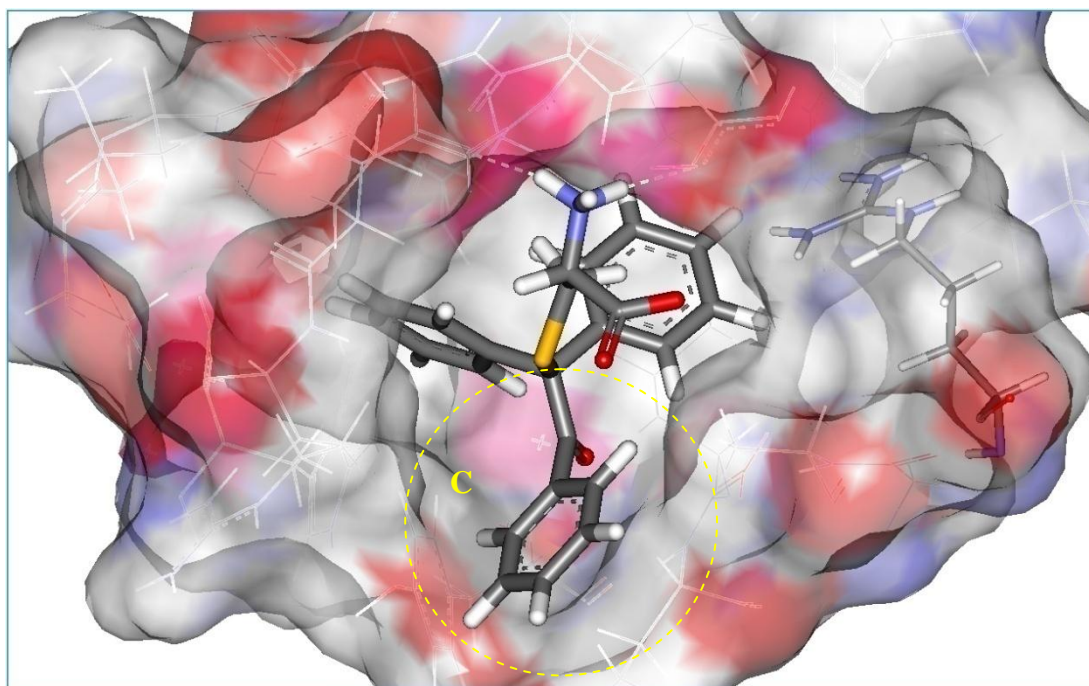
Figure 2.34: Docking pose of compound 141.

Compounds **120** and **138** had one of the phenyl rings replaced with a pyridine ring in order to lower the log P of the highly lipophilic trityl head group. However, the docking results showed lower Goldscores for both compounds (**120**: 76.36 and **138**: 73.46) compared to STLC (78.63). The docking poses had both primary amines forming H bonds with the Glu116 and Glu117 and the carboxylic acid of compound **120** forming an H bond with Arg221, but the pyridyl ring did not form any H bonds with the binding pocket. These lower scores were reflected by reduced Eg5 inhibitory activity: compound **120** had an IC$_{50}$ of 514.2 nM and compound **138** an IC$_{50}$ of 942.2 nM. However, the cell based assay data for these two compounds (**Table 2.11**) was comparable to STLC (EC$_{50}$= 1452 nM).
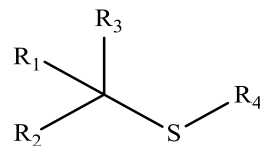
ID	R$_1$	R$_2$	R$_3$	R$_4$	ATPase activity IC$_{50}$ nM	Cell based assay EC$_{50}$ nM
117					5278.2 ± 376.2[‡]	> 50000
118					455.8 ± 86.5[‡]	15996 ± 1768
119					237.5 ± 11.6[‡]	18155 ± 1485
120					514.2 ± 66.6[‡]	1832 ± 134
138					942.2 ± 182.4[‡]	1742 ± 312

117
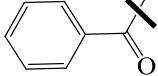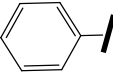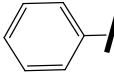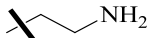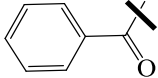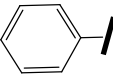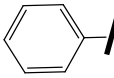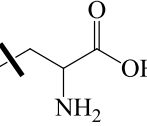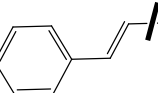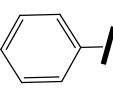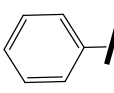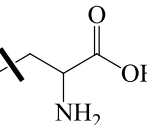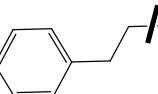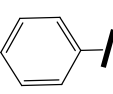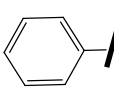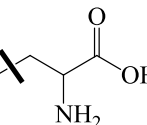
140					No inhibition[*]	NT
141					No inhibition[*]	NT
188					Not tested yet	> 50000
189					Not tested yet	19055 ± 1511

Table 2.11: Biological results of the analogues with a modified benzyl moiety.

Note: IC$_{50}$ results were measured by (*) testing once (‡) testing in triplicate.

2.4.2 Modification of the tail group

2.4.2.1 Cysteamine analogues

A tail group with a zwitterionic functionality has the potential to create problems for drug delivery and movement through biological barriers. Our crystallographic and modelling studies have revealed that the amino substituent is needed for inhibitory activity against the kinesin through the formation of essential hydrogen bonds with two glutamate residues. The carboxylate on the other hand, occupies a solvent-exposed position in the co-crystal structure. In terms of hit optimisation, this group could either be removed, as we have demonstrated with the cysteamine analogues of STLC, or be modified to a more lipophilic moiety, so that it does interact with the protein and enhance affinity for the target.

Docking studies on this group of compounds is exemplified by compound **121**, the cysteamine analogue of the core compound **101**. The Goldscore of this compound (75.94) was slightly lower than the cysteamine analogue of STLC (compound **137**: 78.34), but the inhibitory activity was 4 fold less active, which could be due to a higher entropic penalty associated with the more flexible benzyl moiety. When comparing the score of compound **121** with the core scaffold (compound **101)** the Goldscore was slightly higher and the docking pose (**Figure 2.35**) showed similar attributes: the aromatic rings of the hydrophobic head group occupied the lipophilic pockets, while the primary amine of the cysteamine still formed the essential H-bonds with Glu116 and Gly117.
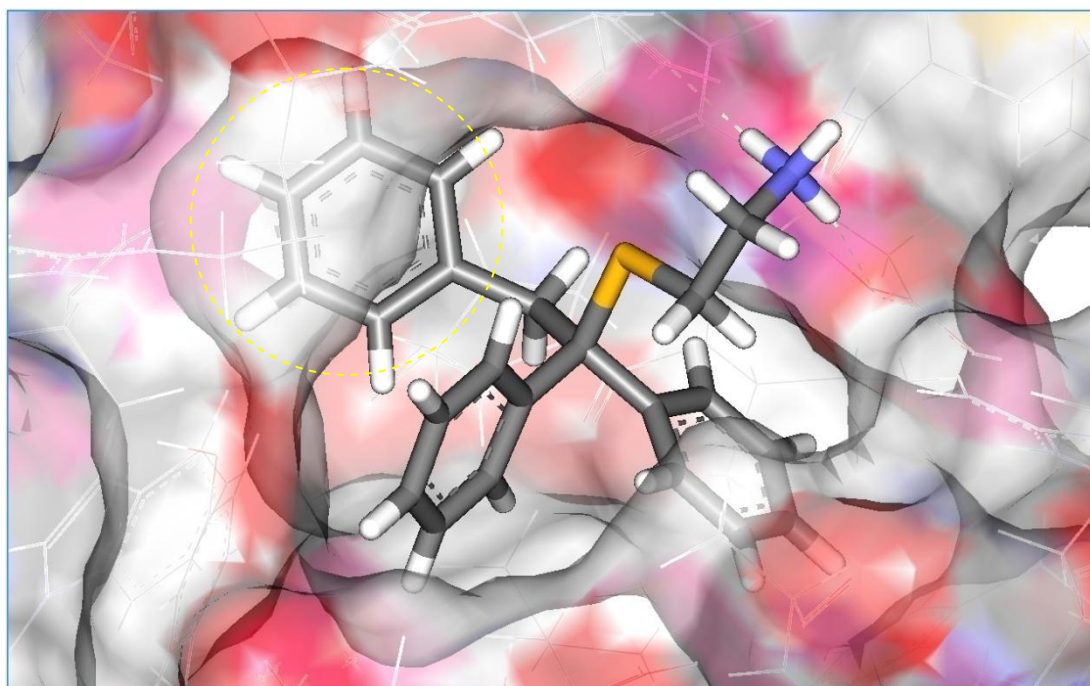
Figure 2.35: Docking pose of compound 121.
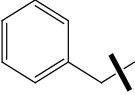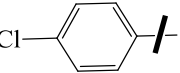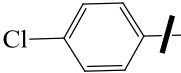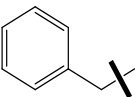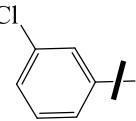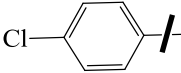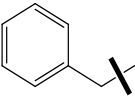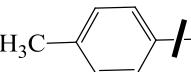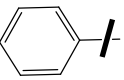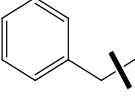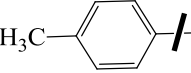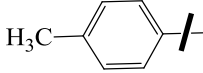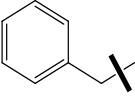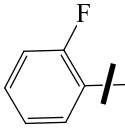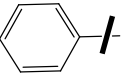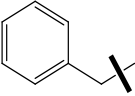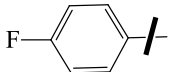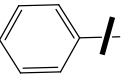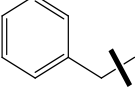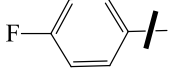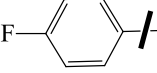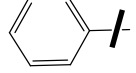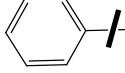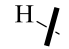
Similarly, all the docking poses of all the cysteamine analogues were almost identical to the poses of the cysteine-based compounds in which the benzyl group occupied pocket B and the cysteamine tail formed two hydrogen bonds with Glu116 and Gly117.

Surprisingly, the inhibitory activity of cysteamine analogue of compound **121** (684.5 nM) was 4.5-fold less active than the core compound **101** (138 nM), in common with all the cysteamine derivatives, which showed lower Eg5 inhibitory activity. A possible explanation for the consistent decrease in activity of these analogues is that the benzyl group has more of an influence on the positioning of the carboxyl group of the tail than the smaller phenyl substituent in the head group, to the extent where it forms more significant interactions with the protein rather than simply occupying a solvent-exposed position. Our earlier MD-based modelling studies suggested an electrostatic interaction with the side chain guanidine of Arg 221 and the side chain NH_2 of Lys111, and it is possible also that the carboxylic acid makes bridging H-bonds with water molecules present in the protein. The results shown in **Table 2.12** also revealed that the removal of the carboxylic acid did not improve the inhibition against the K562 cancer cell line. The racemic mixture of cysteamine analougues

120

could also lower relative activity; Table **2.13** shows the Goldscores of both the *R* and *S* enantiomers of the cysteamine analogues and clearly indicates that there is a difference in the interaction of the enantiomers with the Eg5 hydrophobic pocket.

ID	R_1	R_2	R_3	ATPase activity IC_{50} nM	Cell Based assay EC_{50} nM
121	benzyl	phenyl	phenyl	684.5 ± 81.0[‡]	2333 ± 247
122	benzyl	3-hydroxyphenyl	phenyl	256.1 ± 34.6[‡]	2729 ± 391
123	benzyl	4-hydroxyphenyl	phenyl	665.6 ± 179.9[‡]	> 50000
124	benzyl	3-chlorophenyl	phenyl	435.6[*]	5395 ± 613
125	benzyl	4-chlorophenyl	phenyl	140.9 ± 16.2[‡]	3724 ± 275
126	benzyl	3,4-dichlorophenyl	phenyl	229.3 ± 21.1[‡]	5534 ± 667

122

127		Cl—⬡—/	Cl—⬡—/	403.7 ± 19.6[‡]	5572 ± 207
128		Cl⬡—/	Cl—⬡—/	436.7 ± 36.0[‡]	5370 ± 1425
129		H₃C—⬡—/	⬡—/	171.9 ± 15.4[‡]	2393 ± 215
130		H₃C—⬡—/	H₃C—⬡—/	261.0 ± 12.5[‡]	2323 ± 148
131		F⬡—/	⬡—/	789.5 ± 42.8[‡]	2143 ± 226
132		F—⬡—/	⬡—/	577.9 ± 23.6[‡]	3540 ± 183
133		F—⬡—/	F—⬡—/	587.8 ± 649[‡]	NT
134	⬡—/	⬡—/	H—/	No inhibition[*]	NT
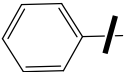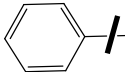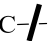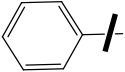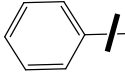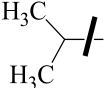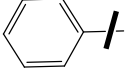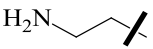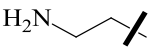
Compound				IC50	IC50
135	(phenyl)	(phenyl)	H₃C–	22186[*]	NT
136	(phenyl)	(phenyl)	(H₃C)₂CH–	222.5 ± 34.9[‡]	> 50000
184	(phenyl)	H₂N-CH₂CH₂–	H₂N-CH₂CH₂–	5351.6 ± 820.0[‡]	6818 ± 450

Table 2.12: Biological results for the cysteamine analogues.

Note: IC$_{50}$ results were measured by (*) testing once (‡) testing in triplicate.

Compound	*R*-enantiomer	*S*-enantiomer
122	76.21	83.08
123	73.62	81.83
124	75.74	85.65
125	72.55	80.98
126	74.82	86.31
128	82.98	80.54
129	74.32	82.34
131	81.50	77.87
132	78.50	78.62

Table 2.13: Goldscores of *R* and *S* enantiomers of the cysteamine analogues.

2.4.2.2 Amide and ester derivatives of the STLC series

Extending the carboxylic acid with an ester or amide linkage was proposed to increase the lipophilicity of the compounds and to potentially form extra H-bonds with the protein.

Compounds **149** and **150** are amides with a terminal primary alcohol, which was introduced to form additional H-bonds with residues or water molecules in the binding pocket. Goldscores were higher for these compounds (84.24 and 85.31, respectively) compared to STLC (78.63) due to the ability of the carbonyl amide to form an H-bond with the side chain NH_2 of Arg221. The terminal primary alcohol itself did not form any H-bond with residues in the binding site (**Figure 2.36**). In the case of compound **151,** which has a terminal primary amine, a H-bond with the backbone carbonyl of Ala218 was formed (Goldscore 84.21) (**Figure 2.37**). Unfortunately, this was not reflected by an improvement in Eg5 inhibitory activity for any of these amides (**Table 2.14**), possibly because of their greater flexibility, and their activity against the K562 cell line was also reduced, which may be due to the decreased cell permeability of these more polar compounds.
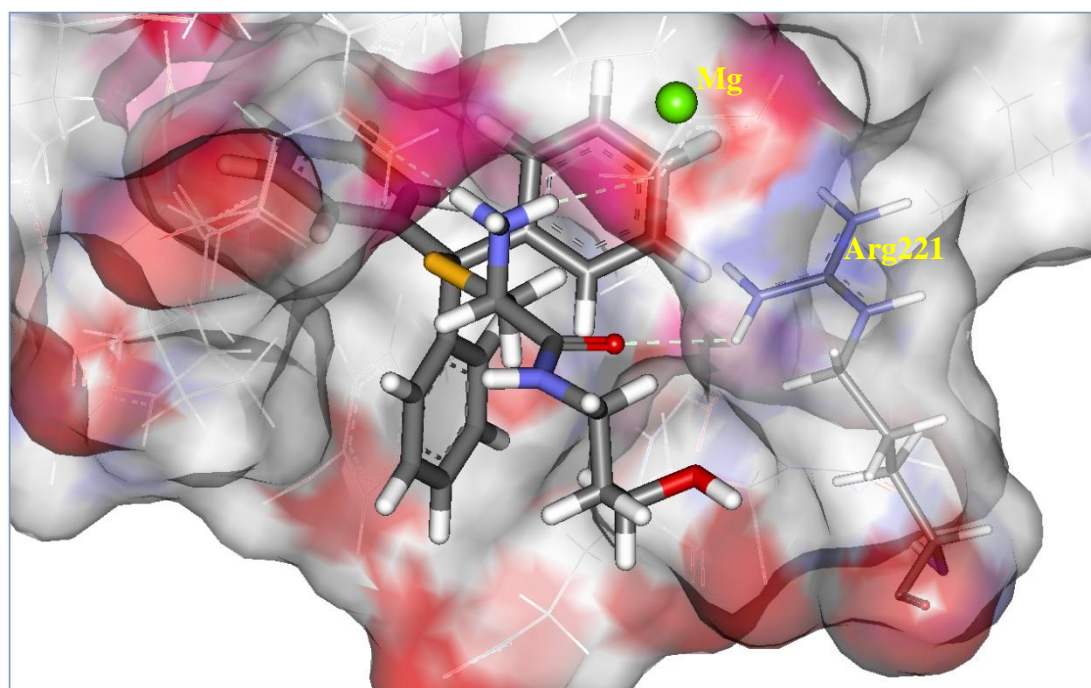
Figure 2.36: Docking pose of compound 150
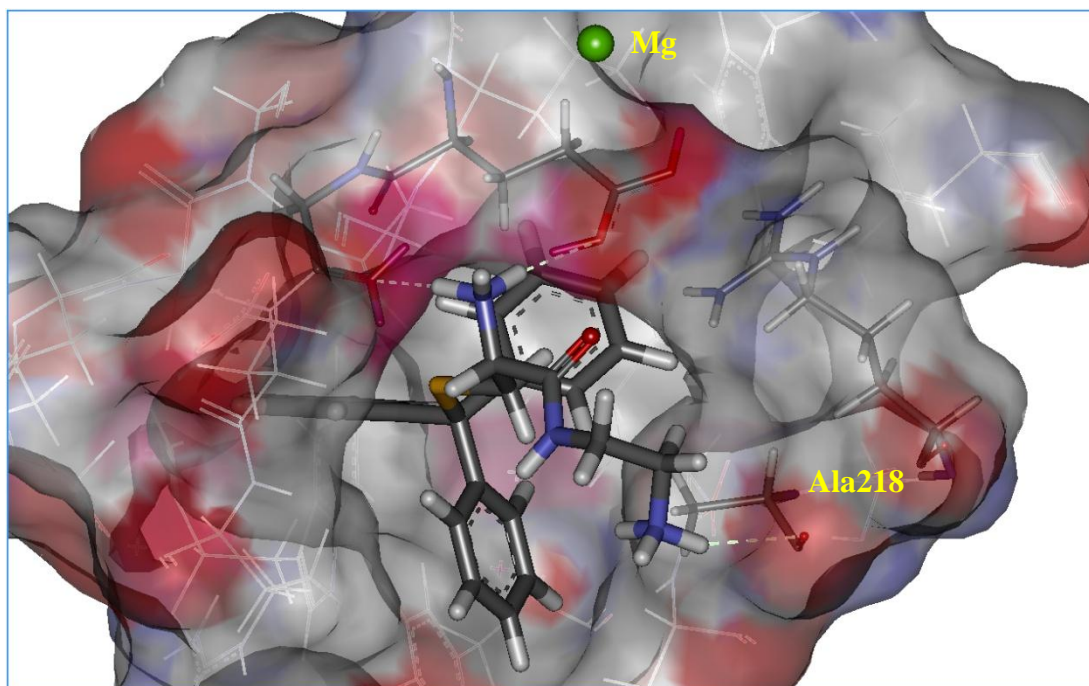
Figure 2.37: Docking pose of compound 151.

Compound **144** is an ester isostere of compound **149**, which had a slightly improved Goldscore (86.61) and slightly better Eg5 inhibitory activity (IC_{50} = 254.0 nM). The carbonyl of the ester formed a H-bond with the NH_2 of Arg221, and increasing the chain length by one methylene unit (compound **145**) led to a improved enzymatic inhibitory activity (IC_{50} = 183.3 nM). Both of the esters (compounds **144** and **145**) had better cell growth inhibitory activity compared to the amides, which could be explained by better cell permeability.

The butyl ester analogues (compounds **142**, **143** and **147**) are exemplified with the docking pose of compound **143** (**Figure 2.38**). The carbonyl ester of these compounds did not form a H-bond as before, which was reflected by a decrease in the Goldscores (68.23, 74.79 and 70.75, respectively). The biological activity of compound **143** in both the enzyme and cell assay was significantly less when the benzyl group replaced the phenyl ring (compound **142**), possibly because of a greater entropic penalty on binding. The poor cell inhibitory activity of this compound (IC_{50} = 13.9 μM), which is almost 10-fold less than STLC (IC_{50} = 1.44 μM), may be due to the very high log P value of **143** (5.089) compared to STLC (1.739) which may cause

the compound to accumulate in the lipophilic cell membrane rather than allowing it to reach the active site.
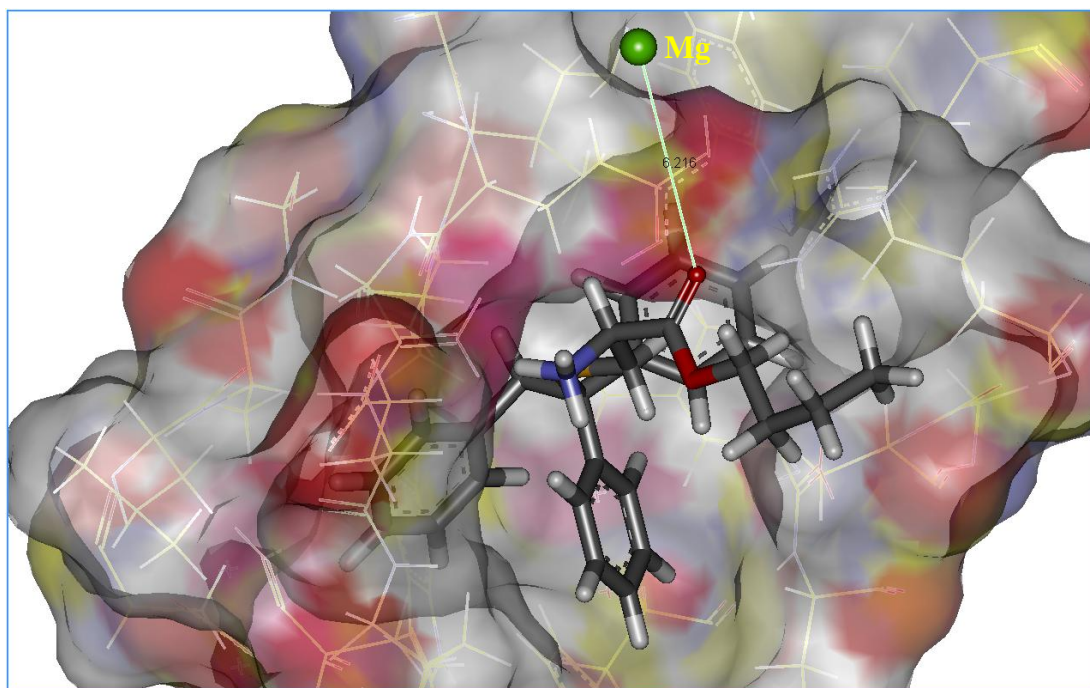
Figure 2.38: Docking pose of compound 143.
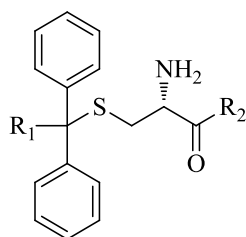
ID	R$_1$	R$_2$	ATPase activity IC$_{50}$ nM	Cell based assay EC$_{50}$ nM
142		O CH_3	$201.2 \pm 35.5^{\ddagger}$	6081 ± 928
143		O CH_3	5742^{*}	13900 ± 1210
144		O OH	$254.0 \pm 28.0^{\ddagger}$	3793 ± 179
145		O OH	$183.3 \pm 34.1^{\ddagger}$	2477 ± 193
147		O CH_3	$4170 \pm .690^{\ddagger}$	2198 ± 165
149		$\underset{H}{N}$ OH	1179^{*}	5117 ± 585
150		$\underset{H}{N}$ OH	$562.2 \pm 93.8^{\ddagger}$	9506 ± 565
151		$\underset{H}{N}$ NH_2	$332.6 \pm 83.3^{\ddagger}$	11508 ± 910

Table 2.14: Biological results of ester and amide derivatives.

Note: IC$_{50}$ results were measured by (*) testing once (‡) testing in triplicate.

2.4.2.3 Cyclic amines

Compounds where the amino group of the tail was incorporated into a cyclic amine (piperidyl or pyrrolidyl) were prepared as racemic mixtures via t-BOC protected intermediates (see section 2.6). The docking study showed a lower Goldscore for

both the enantiomers (**Table 2.15**) compared to the cysteamine tail with a triphenyl head group (compound **137**: 78.344; STLC: 78.63). The docking pose exemplified by compound **159** (**Figure 2.39**) showed that the three phenyls occupied the three binding pockets while the piperidyl and pyrrolidyl tail was located outside the pocket and did not make any H-bond with Glu116 or Gly117.

Compound	*R*-enantiomer	*S*-enantiomer
158	66.69	66.68
159	63.12	67.09
160	65.50	67.68
161	73.81	69.06

Table 2.15: Goldscore of the *R* and *S* enatiomers of the cyclic amine compounds.
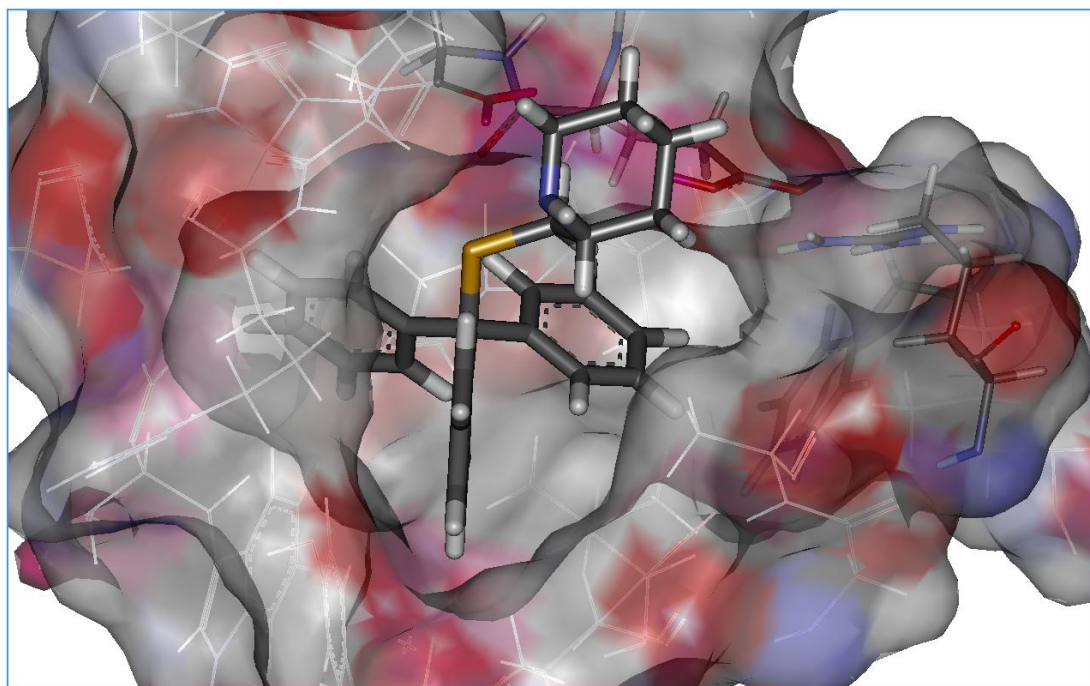
Figure 2.39: Docking pose of compound 159.

The biological results for these compounds (**Table 2.16**) show that the secondary amine analogue **159** was slightly less effective at inhibiting cells (1858 nM) than STLC (1452 nM), while kinesin inhibition was 1.5-fold less than STLC and 3.5-fold less than the STLC cysteamine analogue (compound **137**). The improved Eg5 inhibitory activity of compound **159** (IC_{50} = 498.1 nM) compared with compound

158 (IC_{50} = 617.6 nM) may be due to the increased hydrophobic interaction of the six membered piperidine ring as opposed to a pyrrolidine ring. Not unexpectedly, the bulky t-BOC protected intermediates (compounds **160** and **161**) were completely inactive.
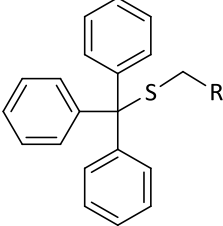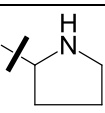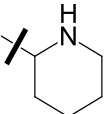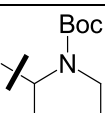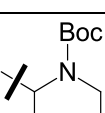
ID	R	ATPase activity IC_{50} nM	Cell based assay EC_{50} nM
158	(pyrrolidine, NH)	617.6 ± 253.6[‡]	4395 ± 408
159	(piperidine, NH)	498.1 ± 80.0[‡]	1858 ± 214
160	(pyrrolidine, Boc)	No inhibition[*]	NA
161	(piperidine, Boc)	No inhibition[*]	NA

Table 2.16: Biological results for the cyclic amino analogues

Note: IC_{50} results were measured by (*) testing once (‡) testing in triplicate.

2.5 Cell growth inhibition and resistance

All the compounds which showed Eg5 ATPase inhibitory activity were also assessed in the K562 leukemia cell line, and activities have been reported along with Eg5 inhibitory data. Compounds with very low ATPase inhibition or no inhibition activity at all were not tested. Cell-based inhibitory values were lower than the Eg5 ATPase inhibitory data, which is not unexpected given that many other proteins in the cell can sequester the ligand and lower its effective concentration at the site of action. Unfortunately, while some compounds were more efficient than STLC at inhibiting Eg5, this was not reproduced in the cell-based assays, and all consistently proved to be less effective to differing degrees. Most of our compounds are racemic mixtures, which also lowers the effective concentrations at the target in the cell. STLC analogues with modified tails such as the ester, amide and cyclic amine analogues have high log Ps, and could be sequestered by lipophilic elements within the cell and reduce concentrations at the target. For example, compound **142** (Log P = 4.166) has an Eg5 inhibitory activity (IC_{50} = 201.1 nM) equal to STLC (IC_{50} = 225.12 nM), but its cell growth inhibitory activity was 4-fold less active (6081 nM).

Five compounds were selected for further assessment in another three types of cancer cells; HCT116 (colon), H1299 (breast) and BxPC-3 (pancreatic). These compounds included the core scaffold (compound **101**), the most active compound in the enzyme assay (compound **108**) and its cysteamine analogue (compound **125**), and compound **112**, the most active against the K562 cell line and it its cysteamine analogue compound **129**. The results in **Table 2.17** show a consistent inhibitory pattern in all cell types, with HCT116 being the most responsive compared with the other cell lines.[140-142] The cysteamine analogues were less active, which is consistent with enzyme activity assays. Compound **112**, which had almost the same activity as STLC in the K562 cell line, had lower activity in the other cell lines, which we currently cannot explain.

Compound	EC$_{50}$ [nM]			
	K562 (5000 cells)	HCT116 (1250 cells)	NCI-H1299 (2500 cells)	BxPC3 (1250 cells)
STLC	1452 ± 76	553 ± 57	1549 ± 111	1563 ± 155
137*	2286 ± 213	471 ± 29	2301 ± 511	2463 ± 908
101	3141 ± 296	2371 ± 239	6871 ± 587	14322 ± 3938
108	2471 ± 360	2084 ± 188	3631 ± 331	3793 ± 643
112	1442 ± 82	1493 ± 117	2432 ± 263	4335 ± 824
125	3724 ± 275	2051 ± 270	6792 ± 363	4256 ± 454
129	2393 ± 215	1170 ± 78	2495 ± 216	4074 ± 550

Table 2.17: Growth inhibitory assays conducted in different tumour cell lines.

(*): STLC cysteamine analogue.

Note: Tests were performed in triplicates.

The same five compounds were assessed for multi-drug resistance (MDR) in Human Cervix Carcinoma KB-V1 cells that over-express mdr1 at both the mRNA and protein level compared with its parental KB-3-1 cell line. The MDR ratio was calculated by dividing the EC$_{50}$ value for a particular compound in the mdr1-overexpressing KB-V1 cells by the value obtained in the parental KB-3-1 cells. Thus, if an inhibitor is a substrate for mdr1, KB-V1 cells will be more resistant to its antiproliferative effects than parent KB-3-1 cells, resulting in an MDR ratio greater than 1. Results shown in **Table 2.18** clearly demonstrate that two of the compounds (**125** and **129**), which are cysteamine analogues, have an MDR ratio of 1, and suggest that these compounds have the potential to overcome MDR.[79, 143] It would therefore appear that the presence of the carboxylic acid has a significant effect on MDR, and there is nothing recorded in the literature that suggests that compounds with zwitterion functionality should become mdr1 substrates. However, amino acids are known substrates for the active transport by proteins, so this result is not totally unexpected.[144]

Compound	EC50 [nM]		
	KB-3-1	KB-V1	mdr ratio
101	5333 ± 731	> 50000	> 10
108	4887 ± 1492	> 50000	> 10
112	2443 ± 262	> 50000	> 20
125	5546 ± 1403	5781 ± 1016	1
129	1884 ± 381	1718 ± 408	1

Table 2.18: MDR ratios for selected inhibitors

2.6 HPLC method development for separation of diastereomers

Many of the compounds prepared have one or two chiral centres which mean they have been assessed as mixtures of compounds. Some cysteamine analogues are enantiomeric mixtures of two compounds, while a number of the STLC analogues are also mixtures of two diastereoisomers (*R* and *S* head groups and an *R* tail group). In theory the two diastereoisomers can be separated by HPLC reverse phase chromatography.

To assess the pure isomers in the biological assays, we attempted to develop a reverse HPLC method using a C18 column to separate the diastereomeric mixtures of those compounds listed in **Figure 2.40** using different mobile phases. An isocratic mobile phase of acetonitrile:water (40:60) with a C18 column was used and full separation of compound **102** was achieved, but only partial or no separation for compounds **103** and **104**, respectively (**Figure 2.41**). It would appear that an increase in hydrophobicity results in poorer separation and longer peak elution times.
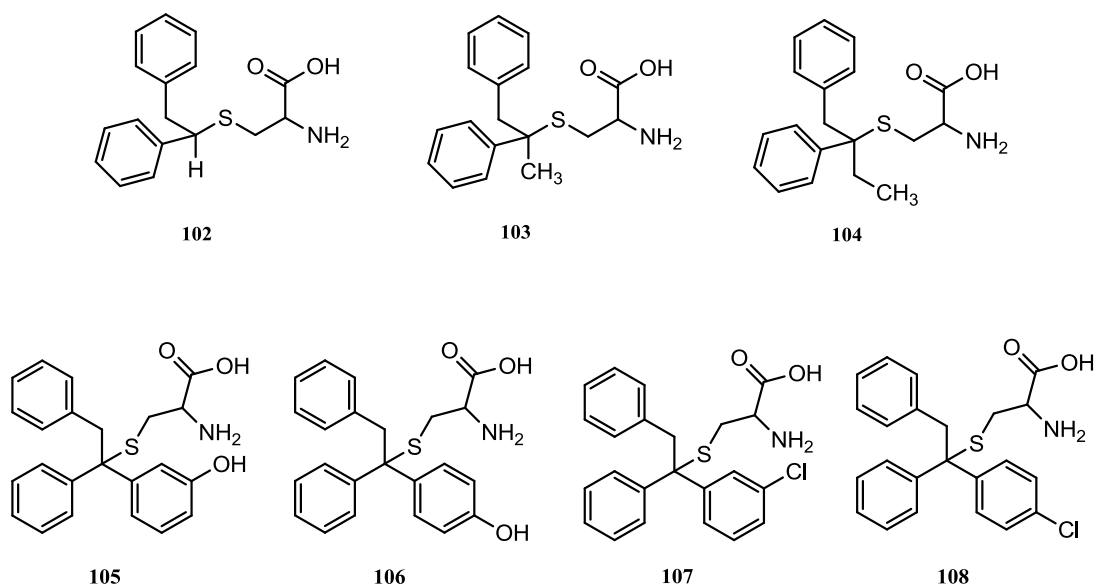
Figure 2.40: Compounds tested for HPLC method development.
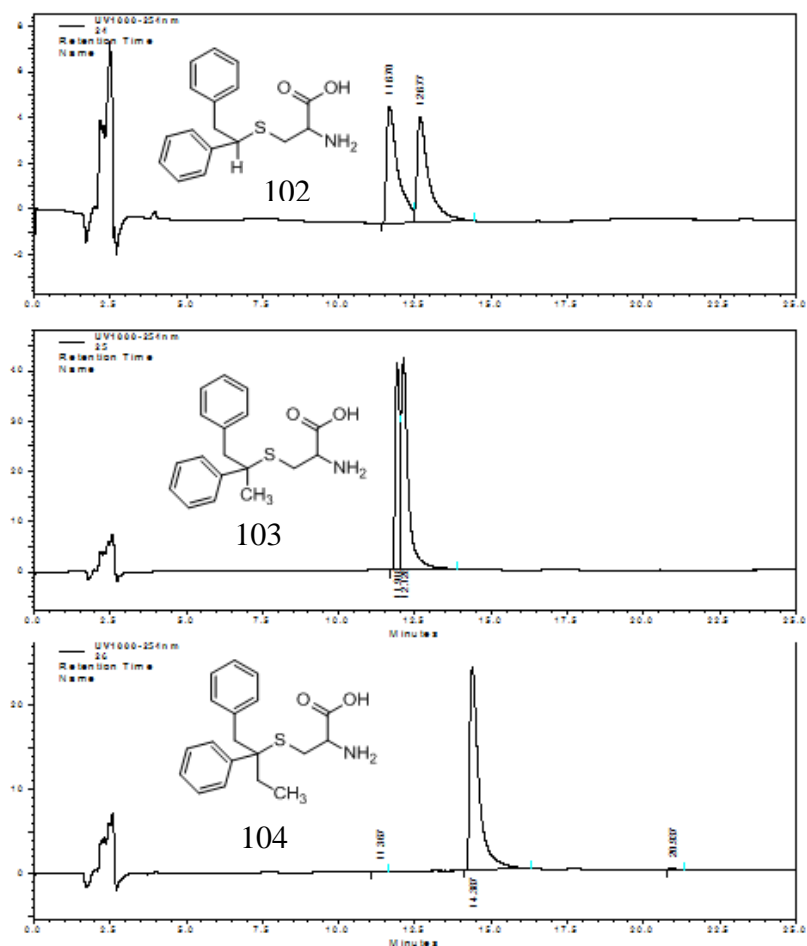
Figure 2.41: Chromatograms of compounds 102, 103 and 104.

134

The same method was applied to the separation of racemic mixtures of compounds **105-108** and separation was successful for the polar compounds **105** and **106** and, whereas the hydrophobic compounds **107** and **108** did not separate and took longer to elute **(Figure 2.42)**.
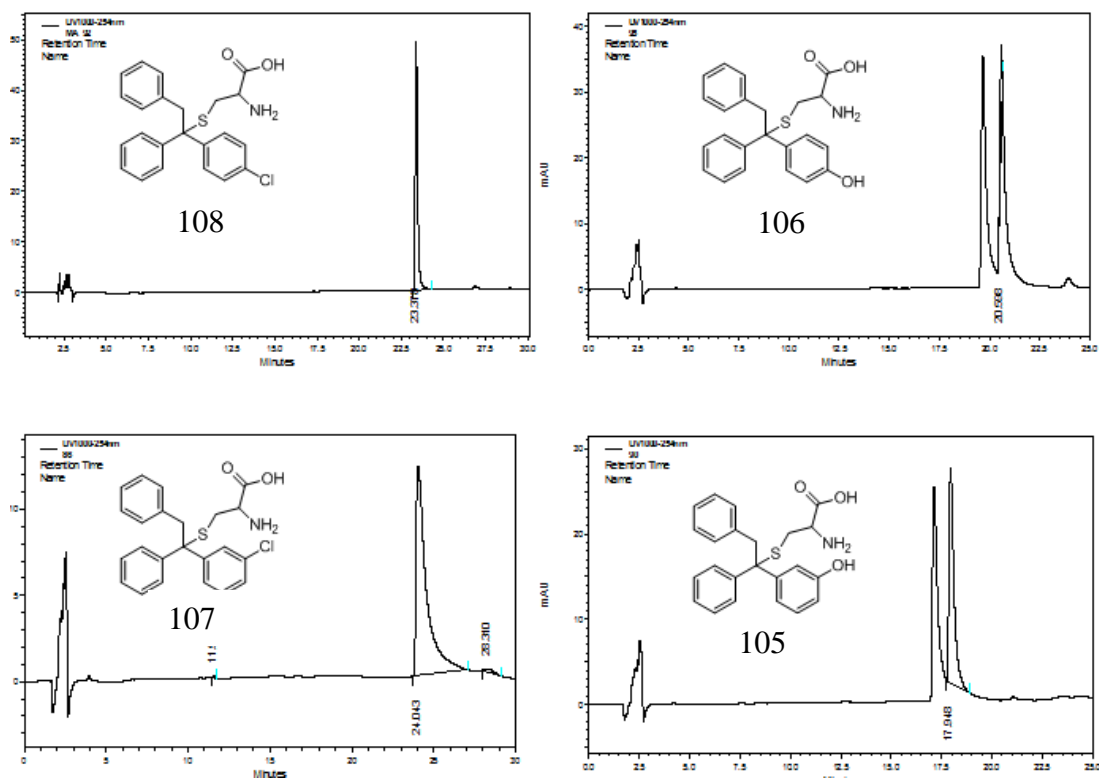
Figure 2.42: HPLC separation of compounds 105-108.

Chapter 3: Conclusions and future work

A number of the STLC analogues prepared proved to be reversible, tight binders and potent Eg5 inhibitors. The co-crystal structure of STLC with Eg5 provided useful insight into the binding properties of the ligand with the allosteric binding site of the target kinesin. Utilizing this information, with the aid of docking program GOLD we designed different groups of compounds which were then synthesised and tested *in vitro* against the Eg5 motor, as well as in K562 leukaemia cell line.

Replacing one of the phenyl rings of the hydrophobic trityl head group of STLC with a benzyl moiety provided our core scaffold and showed improved ATPase inhibitory activity (IC_{50} = 138 nM) compared to STLC (IC_{50} = 225 nM). Further modifications were performed on the head and tail groups of the ligand, and compounds with substituents on the phenyl rings showed the highest Eg5 inhibitory activity. Chloro, fluoro, hydroxyl and methyl groups improved activity against Eg5, with the position of the substituent proving vital. For example, a hydroxyl group at the *meta* position was 3-fold more active than the equivalent *para*-substituted analogue. The same trend was observed, but to a lesser extent, with the chloro and fluoro substituents. Growth inhibition activites in the K562 cell-based assays for these compounds did not correlate with kinesin inhibitory activity - the most potent compound was **112** (1442 ± 82 nM), which was less effective tham STLC itself.

Removal of one of the phenyl rings (compounds **102-104)** resulted in a total loss of inhibitory activity, which emphasizes the importance of having three ring systems to maximise interactions with the target protein. Whether this is through induced conformational rigidity, or simply through improved interactions with the protein, is unclear at present; for example, inducing rigidity into the head group by fusing two of the rings into xanthene, thioxanthene and fluorene systems significantly reduced or abolished activity.

Substitutions on the benzyl ring (compounds **117-119**) or extending the ring from the tail with an alkyl or alkenyl (compounds **188** and **189**) chain lowered activity.

Furthermore, replacing the benzyl group with a pyridyl ring lowered activity, while replacing it with a benzoyl moiety resulted in a total loss of inhibitory activity.

The primary amine in the tail was retained in most of our compounds. The importance of this group was confirmed by the lower activity of the cyclic pyrrolidinyl and piperidinyl secondary amine analogues, and emphasises the need for hydrogen bonds with Glu116 and Gly117 of Eg5.

To improve the cell membrane permeability, a group of compounds with the carboxylic acid functionalised as the ester or amide, or with the carboxylate group removed completely were prepared and assessed; all had lowered ATPase inhibitory activity, and cell inhibitory activity did not improve in comparison with those compounds with a free carboxylic acid.

The multi-drug resistance assay with human cervix carcinoma KB-3-1 cells showed that the cysteamine analogues (compounds **125** and **129**) were not substrates for Pgp efflux, and has promise as templates for future development, providing that the Eg5 inhibitory activity for these cysteamine-based compounds can be improved.

The first priority of such future work should focus on separating the diastereomer mixtures of the most active compounds to establish which absolute conformation of the head group is required. Earlier work has established that either the *R*- or *S*-configuration of the cysteine tail can interact with the protein, which, although surprising, can be explained by the solvent exposed nature of the tail-binding site. The hydrophobic pockets that bind the head group are much more likely to be stereoselective, as our docking studies suggest, and which enantiomer is preferred needs to be established. We have initiated the important step of developing an HPLC method which was successful in separating polar compounds, and can be applied when a preparative column is available. However, separating more lipophilic compounds has proved more challenging, and may require chemical derivatization prior to separation using normal or reverse phase chromatographic separation or by using specific chiral HPLC columns. Co-crystallisation of our most active compound

with Eg5 will also help establish the absolute stereochemistry of the head group – studies are underway to investigate this interaction, and MD studies on the complex will help quantify the interactions between the ligand and protein, to help direct further synthetic optimisations.

Parallel studies by our group have shown that the sulphur atom in the STLC tail is essential for activity – the oxygen and nitrogen isosteres are inactive. A sulfinyl or sulfonyl group would add H-bond acceptors to this moiety (**Figure 3.1**) and provide further interactions with H-bond donor containing residues in this region of the protein, and lower the Log P. They may also provide the modifications required for the cysteamine analogues to improve Eg5 inhibitory activity whilst overcoming MDR.
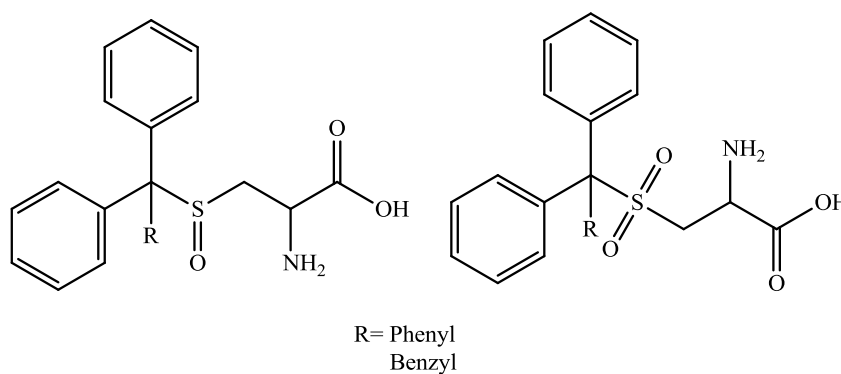
R= Phenyl
Benzyl

Figure 3.1: Suggested sulfinyl and sulfonyl derivatives of STLC.

Replacing one of the phenyl rings with a saturated heterocyclic ring would maintain the essential three ring system of the head group, and provide further opportunities for polar interactions with the protein, whilst reducing the Log P of the overall molecule (**Figure 3.2**).
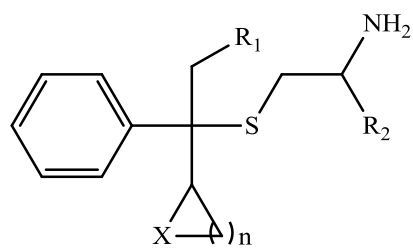
n=0,1,2,3,4 R_1= Phenyl R_2= H
X=C, O,S,N   =Benzyl   = COOH

Figure 3.2: Compounds with a third heterocyclic ring

Chapter 4: Materials and methods

4.1 General Experimental Details

Melting point determination: Melting points (Mpt) were determined on Stuart Scientific Melting Point apparatus SMP1 and are in degrees Celsius (°C) and are uncorrected.

Elemental analysis: Elemental analysis was performed on Perkin Elmer 2400 Analyser Series II elemental analyser. Standard methods of measuring the thermal conductivity for the combustion product were used to determine C, H, and N simultaneously and halogens and sulphur separately by titration with carium percholate solution.

Infrared spectroscopy: Infrared spectra for liquid samples were run on Jasco FT-IR-4200 ATR (Attenuated Total Reflection Mode) and solid samples compressed with KBr into disks and recorded with Mattson Genesis Series FT-IR spectrometers. Wavenumbers, ν_{max} (cm^{-1}) are quoted for appropriate functional groups.

Nuclear Magnetic Resonance (NMR) spectroscopy: Proton (^{1}H NMR) and carbon (^{13}C NMR) nuclear magnetic resonance spectra were run either on a JEOL Lambda Delta 400 (400 MHz) or Bruker AMX-400 (400 MHz) spectrometer. The deuterated solvent used for each of the compound is specified in the text. Chemical shifts are stated in parts per million (ppm) and multiplicity indicated as singlet (s), doublet (d), doublet of doublet (dd), triplet (t), quartet (q), pentet, sextet and multiplet (m). Coupling constants (J) are quoted in hertz (Hz).

Mass Spectrometry: High-resolution mass spectrometry (HRMS) was obtained using electron impact ionisation (ESI, 70 eV) in a Fourier transform analyser by Exactive$^®$ Thermo Scientific. Mass to charge ratio (m/z) molecular ion radical is given as [M$^+$].

Reagents and solvents: All commercially available reagents and solvents used were obtained (and used without further purification) from Sigma-Aldrich, Alfa-Aesar or Fisher Scientific, unless otherwise stated.

Purification of products: All compounds were purified by recrystallisation or by either gravity column chromatography or flash chromatography using a Biotage SP4 Automated Chromatography system. All chromatography was carried out on SiO_2 60A 6 μm-35 μm (Fisher-Scientific). Thin-Layer Chromatography (TLC) was carried out on aluminium-backed SiO_2 plates (Merck) and spots visualised using ultra-violet light (254 nm).

Microwave reactions: Some reactions were carried out in a Biotage Initiator-8 Microwave Synthesis system using standard Biotage microwave vials of volume capacity (0.2 − 20 mL) depending on the reaction-scale. The reaction time and temperature settings are detailed in the text. The pressure safety limit was set at 15 Bar.

Log P calculation: The (Log P) for compounds were calculated using Pipeline Pilot 8.0 (Accelrys) program[145].

4.2 Single crystal X-ray diffraction data collection

The X-ray crystal structure of compounds (**134-137**) was determined after recrystallization from a supersaturated solution of acetonitrile, to produce single crystals of sufficient size for data collection. Single crystal diffraction data were collected on a Bruker Apex II CCD diffractometer using graphite monochromated Mo Kα1 radiation of wavelength 0.71073Å. The data were collected in the 0 − 52° 2θ range at 123K. Samples were mounted under oil on a glass fibre situated on top of a goniometer head. Diffraction data were processed using Bruker SAINT software and structure solution carried out with SHELXS 97 using direct methods.[146]

4.3 HPLC method for the separation of diastereomeric compounds (102 – 108)

Compounds (**102** – **108**) were separated using an integrated Thermo-Fisher RP-HPLC system equipped with binary pump (P200), in-line degasser (SCM1000), auto-injector (AS300) and UV detector (UV1000). Data analysis was carried out using Chromquest software (Version 2.53). HPLC grade acetonitrile (MeCN) was obtained from Fisher-Scientific and HPLC grade water was obtained using a reverse osmosis (Millipore, Direct-Q) water purification system. The mobile phase (MeCN-H_2O, 40:60 v/v) was prepared, filtered through a 0.45 µm pore filter paper and degassed prior to use. Samples were prepared in mobile phase at a concentration of 50 µg/mL. The chromatographic conditions used are summarised in **Table 3.1**:

Table 4.1: Summary of RP-HPLC chromatographic conditions used in the separation of compounds (102 – 108).

Instrument	Thermo-Fisher RP-HPLC system
Mobile phase	Acetonitrile-water (40:60 v/v), isocratic
Column	ACE C18 analytical column (4.6 × 150 mm i.d., 5 µm), Hichrom
Flow rate	0.8 mL/min
Detection System	UV, 254 nm
Column Temperature	25 °C
Injection Volume	10 µL

4.4 Chemical synthesis of target compounds

4.4.1 Preparation of tertiary alcohols

4.4.1.1 General Procedure A: Preparation of tertiary alcohols using either a Grignard or organolithium reagent. Grignard (or organolithium) reagent solution (*circa.* 1.2 eq.) was added to a round bottom flask under a nitrogen atmosphere, at 0 °C. The required ketone or aldehyde (1.0 eq.) was added, the mixture stirred for 24h, and then quenched with saturated ammonium chloride (20 mL). The mixture was then extracted with ethyl acetate (3 x 10 mL), dried over magnesium sulphate and evaporated under reduced pressure. The residue was purified either by recrystallization or by silica gel chromatography.

1,1,2-Triphenylethanol (79)
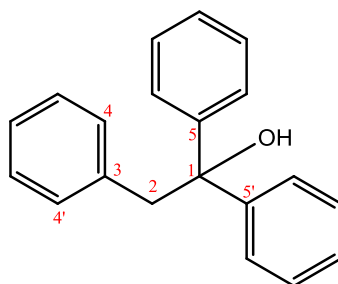
Using General Procedure A: Benzylmagnesium chloride 2M solution in THF (9.75 mL, 19.5 mmol) and benzophenone (2.73 g, 15 mmol) gave compound **79** (2.39 g, 58 %) as a white powder after recrystallisation from methanol. Mpt: 85-87 °C (literature: 87-88 °C).[147] ^{1}H NMR (400 MHz): δ (CDCl$_3$): 2.32 (1H, s, -O**H**); 3.67 (2H, s, -C**H$_2$**, C2); 6.90 (2H, C4,4'); 7.17-7.45 (13H, m, Ar). ^{13}C NMR (125 MHz): δ (CDCl$_3$): 48.03 (C2); 77.97 (C1); 126.26-130.90 (15C, Ar: 126.27, 126.90, 126.99, 128.17, 130.98); 135.85 (C3); 146.64 (2C, C5,5'). Elemental analysis: Found C, 87.52; H, 6.44 (Required for C$_{20}$H$_{18}$O: C, 87.52; H, 6.61). HRMS-ESI (+ve): Calculated for C$_{20}$H$_{17}$ (M-OH)$^+$ 257.1325, found 257.1322. IR: KBr disc, υ$_{max}$ (cm^{-1}): 3549.7 (-OH stretch of tertiary alcohol).

(±)-1,2-Diphenylethanol (80)
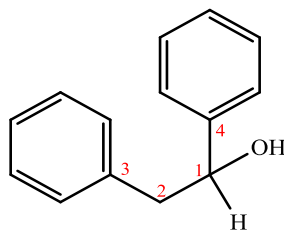
Using General Procedure A: Benzylmagnesium chloride 2M solution in THF (9.75 mL, 19.5 mmol) and benzaldehyde (1.59 g, 15 mmol) gave compound **80** (0.889 g, 30%) as a white powder after recrystallisation from methanol. Mpt:67-68 ℃ (literature: 67-68 °C).[148] ^{1}H NMR (400 MHz): δ (CDCl$_3$): 1.94 (1H, s, –O**H**); 3.01 (2H, m, -C**H$_2$**, C2); 4.89 (1H, m, -C**H**, C1); 7.25-7.36 (10H, m, Ar). ^{13}C NMR (125 MHz): δ (CDCl$_3$): 46.19 (C2); 75.43 (C1); 125.98-129.60 (10C, Ar); 138.12 (C3); 143.80 (C4). Elemental analysis: Found: C, 84.69; H, 6.82 (Required for C$_{14}$H$_{14}$O: C, 84.80; H, 7.12). HRMS-ESI (+ve): Calculated for C$_{14}$H$_{13}$ (M-OH)$^+$ 181.1012, found 181.1009. IR: KBr disc, υ_{max} (cm^{-1}): 3312.2 (-OH stretch of tertiary alcohol).

(±)-1,2-Diphenylpropan-2-ol (81)
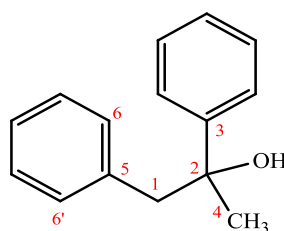
Using General Procedure A: Benzylmagnesium chloride 2M solution in THF (9.75 mL, 19.5 mmol) and acetophenone (1.802 g, 15 mmol) gave compound **81** (1.4 g, 46 %.) as a white powder after purification by gravity column chromatography [ethyl acetate:n-hexane (10:90)]. Mpt: 49-50 ℃ (literature: 49.5-51.0 °C).[149] ^{1}H NMR

(400 MHz): δ (CDCl$_3$): 1.54 (3H, d, J = 6.4 Hz, –**CH$_3$**, C4); 1.83 (1H, d, J = 6.0 Hz, –**OH**), 4.89 (2H, dd, J = 13.2, J = 6.0 Hz, -**CH$_2$**, C1); 6.92 (2H, C6,6'); 7.20-7.40 (8H, m, Ar). ^{13}C NMR (125 MHz): δ (CDCl$_3$): 29.38 (C4); 50.37 (C1); 75.50 (C2); 125.09-130.84 (10C, Ar); 136.84 (C5); 147.66 (C3). HRMS-ESI (+ve): Calculated for C$_{15}$H$_{15}$ (M-OH)$^+$ 195.1168, found 195.1275. IR: KBr disc, υ_{max} (cm^{-1}): 3322.2 (-OH stretch of tertiary alcohol).

(±)-1,2-Diphenylbutan-2-ol (82)
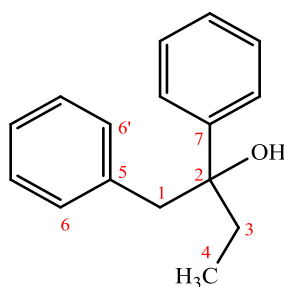
Using General Procedure A: Benzylmagnesium chloride 2M solution in THF (9.75 mL, 19.5 mmol) and propiophenone (2.01 g, 15 mmol) gave compound **82** (1.25 g, 37 %) as a pale yellow liquid after purification by gravity column chromatography [ethyl acetate:n-hexane (10:90)]. ^{1}H NMR (400 MHz): δ (CDCl$_3$): 0.776 (3H, t, J = 7.2 Hz, –**CH$_3$**, C4); 1.75 (1H, s, -**OH**); 1.81 (1H, p, J = 7.2 Hz, **CH$_a$**H$_b$, C3); 1.97 (1H, p, J = 7.2 Hz, -CH$_a$**H$_b$**, C3); 3.00-3.17 (2H, dd, J = 13.2 Hz, -**CH$_2$**, C1); 6.96 (2H, C6,6') 7.18-7.32 (8H, m, Ar). ^{13}C NMR (125 MHz): δ (CDCl$_3$): 8.09 (C4); 34.41 (C3); 49.69 (C1); 77.07 (C2); 125.42-130.78 (10C, Ar); 136.57 (C5); 145.58 (C6). HRMS-ESI (+ve): Calculated for C$_{16}$H$_{17}$ (M-OH)$^+$ 209.1325, found 209.1323. IR: ATR, υ_{max} (cm^{-1}): 3332.1 (-OH stretch of tertiary alcohol).

Diphenyl(pyridin-4-yl)methanol (83)

Using General Procedure A: Phenylmagnesium bromide 1M solution in THF (11.7 mL, 11.7 mmol) and 4-benzoylpyridine (1.69 g, 9 mmol) gave compound **83** (0.48 g, 20%) as pale yellow powder after recrystallisation from methanol Mpt: 238-239 °C (literature: 238-238.5 °C).[150] ^{1}H NMR (400 MHz): δ (CDCl$_3$): 2.96 (1H, s, −O**H**); 7.23-7.34 (12H, m, Ar); 8.54 (2H, dd, J = 4.8, 1.6 Hz, C4,4'). ^{13}C NMR (125 MHz): δ (CDCl$_3$): 79.90 (C1); 122.72-128.45 (12C, Ar: 122.72, 127.87, 127.93, 128.45); 146.36-149.15 (3C, C2, 5,5'); 155.94 (2C, C4,4'). Elemental analysis: Found: C, 82.17; H, 5.60; N, 5.15 (Required for C$_{18}$H$_{15}$NO: C, 82.73; H, 5.79; N, 5.15). HRMS-ESI (+ve): Calculated for C$_{18}$H$_{16}$NO (M+H) 262.1226, found 262.1226. IR: KBr disc, υ_{max} (cm^{-1}): 3429.3 (-OH stretch of tertiary alcohol).

2-Methyl-1,1-diphenylpropan-1-ol (84).

Using General Procedure A: Isopropylmagnesium chloride 2M solution (9.75 mL, 19.5 mmol) and benzophenone (2.73 g, 15 mmol) gave compound **84** (0.754 g, 22 %) as a pale yellow liquid after purification by gravity column chromatography [ethyl acetate:*n*-hexane (10:90)]. ^{1}H NMR (400 MHz): δ (CDCl$_3$): 0.89 (6H, d, J = 6.8 Hz, -C**H$_3$**, C3,3'); 2.02 (1H, s, -O**H**); 2.90 (1H, hept, J = 6.8 Hz, -C**H**, C2); 7.16 (2H, t, J = 7.6 Hz, C7, 10,Ar); 7.28 (4H, t, J = 8 Hz, C6,6',7,7', Ar), 7.48 (4H, d, J = 8.0 Hz, 5,5',8,8',Ar). ^{13}C NMR (125 MHz): δ (CDCl$_3$): 17.15 (2C, C3,3'); 34.58 (C2); 82.74 (C1); 125.62-127.63 (10C, Ar); 148.0 (2C, C4,4'). HRMS-ESI (+ve): Calculated for C$_{16}$H$_{19}$O (M+H) 227.1430, found 227.1424. IR: ATR, υ$_{max}$ (cm^{-1}): 3232.3 (-OH stretch of tertiary alcohol).

(±)-3-(1-Hydroxy-1,2-diphenylethyl)phenol (85)
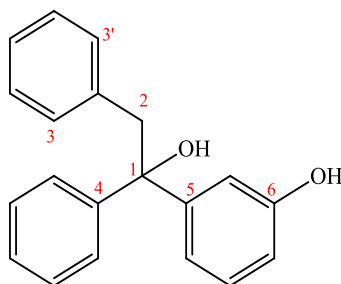
Using General Procedure A: Benzylmagnesium chloride 2M solution in THF (5 mL, 10 mmol) and 3-hydroxybenzophenone (450 mg, 2.27 mmol) gave compound **85** (0.5 g, 76 %) as a colourless oil after purification by flash chromatography (Biotage SP4) [ethyl acetate:*n*-hexane (10:90)]. ^{1}H NMR (400 MHz): δ (CDCl$_3$): 2.28 (1H, s, -O**H**); 3.58-3.64 (2H, s, C**H$_2$**, C2); 4.67 (1H, s, -O**H**); 6.67 (2H, C3,3') 6.89 -7.43 (12H, m, Ar). ^{13}C NMR (125 MHz): δ (CDCl$_3$): 47.90 (C2); 77.42 (C1); 113.54-135.70 (15C, Ar); 146.40 (C4); 48.63 (C3); 155.43 (C5). HRMS-ESI (-ve): Calculated for C$_{20}$H$_{17}$O$_2$ (M-H) 289.1234, found 289.1235. IR: ATR, υ$_{max}$ (cm^{-1}): 3563.7 (-OH stretch of tertiary alcohol).

(±)-1-(4-Hydroxyphenyl)-1,2-diphenylethanol (86).
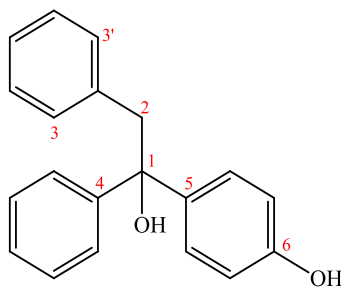
Using General Procedure A: Benzylmagnesium chloride 2M solution in THF (10 mL, 20 mmol) and 4-hydroxybenzophenone (1.98 g, 10 mmol) gave compound **86** (2.5 g, 86 %) as a white solid after purification by flash chromatography (Biotage SP4) [ethyl acetate:*n*-hexane (10:90)]. Mpt:82-84 °C (literature: 137-139 °C).[151] ^{1}H NMR (400 MHz): δ (CDCl$_3$): 2.30 (1H, s, -**OH**); 3.59 (2H, s, -**CH$_2$**, C2); 4.98 (1H, s, -**OH**); 6.72 (2H, d, *J* = 8.8 Hz, C3,3'); 7.15-7.46 (12H, m). ^{13}C NMR (400 MHz): δ (CDCl$_3$): 48.14 (C2); 77.42 (C1); 114.95-135.59 (15C, Ar); 139.05 (C5); 146.74 (C4); 154.50 (C6). HRMS-ESI (+ve): Calculated for C$_{20}$H$_{17}$O (M-OH)$^+$ 273.1274, found 273.0400. IR: ATR, υ$_{max}$ (cm^{-1}): 3385.9 (-OH stretch of tertiary alcohol).

(±)-1-(3-Chlorophenyl)-1,2-diphenylethanol (87)
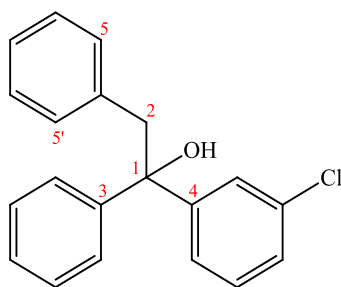
Using General Procedure A: Benzylmagnesium chloride 2M solution in THF (5 mL, 10 mmol) and 3-chlorobenzophenone (1083 mg, 5 mmol) gave compound **87** (0.55 g, 36 %) as a colourless liquid after purification by flash chromatography (Biotage

SP4) [ethyl acetate:*n*-hexane (10:90)]. ^{1}H NMR (400 MHz): δ (CDCl$_3$): 2.32 (1H, s, -O**H**); 3.58-3.66 (2H, d, *J* = 13.6 Hz, -C**H$_2$**, C2); 6.90 (2H, m, C5,5'); 7.18-7.42 (12H, m, Ar). ^{13}C NMR (125 MHz): δ (CDCl$_3$): 47.87 (C2); 77.43 (C1); 124.50 - 135.33 (16C, Ar); 146.02 (C4); 148.78 (C3). HRMS-ESI (+ve): Calculated for C$_{20}$H$_{16}$Cl (M-OH)[+] 291.0935, found 291.2013. IR: ATR, υ$_{max}$ (cm^{-1}): 3564.6 (-OH stretch of tertiary alcohol).

(±)-1-(4-Chlorophenyl)-1,2-diphenylethanol (89)
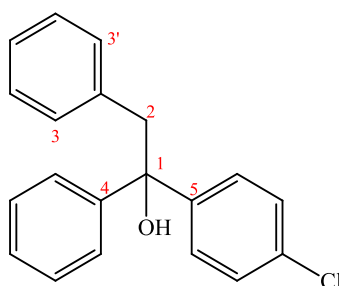
Using General Procedure A: Benzylmagnesium chloride 2M solution in THF (10 mL, 20 mmol) and 4-chlorobenzophenone (2 g, 9.25 mmol) gave compound **89** (1.5 g, 53 %) as pale yellow liquid after purification by flash chromatography (Biotage SP4) [ethyl acetate:*n*-hexane (10:90)]. ^{1}H NMR (400 MHz): δ (CDCl$_3$): 2.32 (1H, s, -O**H**); 3.58-3.65 (2H, d, *J* = 13.2 Hz, -C**H$_2$**, C2); 6.89 (2H, d, *J* = 8.8 Hz, C3,3'); 7.17-7.41 (12H, m, Ar). ^{13}C NMR (125 MHz): δ (CDCl$_3$): 47.91 (C2); 77.66 (C1); 126.16-135.80 (16C, Ar); 145.19 (C5); 146.30 (C4). HRMS-ESI (+ve): Calculated for C$_{20}$H$_{16}$Cl (M-OH)[+] 291.0935, found 291.0934. IR: ATR, υ$_{max}$ (cm^{-1}): 3275.9 (-OH stretch of tertiary alcohol).

(±)-1-(3,4-Dichlorophenyl)-1,2-diphenylethanol (90)
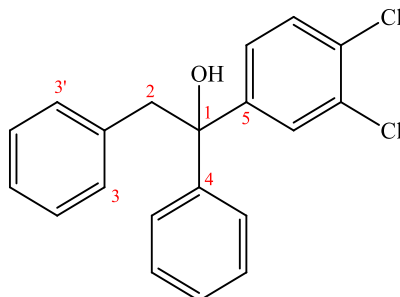
Using General Procedure A: Benzylmagnesium chloride 2M solution in THF (10 mL, 20 mmol) and 3,4-dichlorobenzophenone (2.5 g, 10 mmol) gave compound **90** (2.2 g, 64 %) as colourless liquid after purification by flash chromatography (Biotage SP4) [ethyl acetate:*n*-hexane (10:90)]. ^{1}H NMR (400 MHz): δ (CDCl$_3$): 2.34 (1H, s, -**OH**); 3.55-3.65 (2H, d, J = 13.6 Hz, **CH$_2$**, C2); 6.91 (2H, d, J = 7.6, C3.3'); 7.18-7.60 (11H, m, Ar). ^{13}C NMR (125 MHz): δ (CDCl$_3$): 47.79 (C2); 77.37 (C1); 125.85-135.07 (16C, Ar); 145.72 (C4); 147.04 (C3). HRMS-ESI (+ve): Calculated for C$_{20}$H$_{15}$Cl$_2$ (M-OH)$^+$ 325.0545, found 325.0543. IR: ATR, υ$_{max}$ (cm^{-1}): 3475.3 (-OH stretch of tertiary alcohol).

1,1-Bis(4-chlorophenyl)-2-phenylethanol (91)
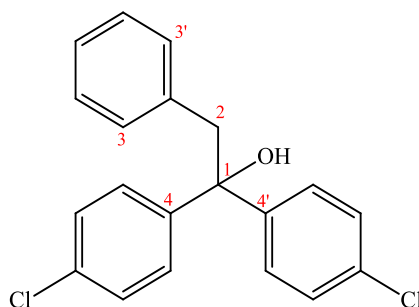
Using General Procedure A: Benzylmagnesium chloride solution 2M in THF (10 mL, 20 mmol) and 4,4'-dichlorobenzophenone (2.5 g, 10 mmol) gave compound **91**

(0.7 g, 20 %) as a pale yellow waxy solid after purification by flash chromatography (Biotage SP4) [ethyl acetate:n-hexane (10:90)]. Mpt:112-113°C (literature: 116-117 °C).[152] ^{1}H NMR (400 MHz): δ (CDCl$_3$): 2.31 (1H, s, -O**H**); 3.576 (2H, s, -C**H$_2$**, C2); 6.87 (2H, d, J = 7.6 Hz, C3,3'); 7.18-7.34 (11H, m, Ar). ^{13}C NMR (125 MHz): δ (CDCl$_3$): 47.80 (C2); 77.12 (C1); 127.24-135.05 (16C, Ar); 144.79 (2C, C4,4'). HRMS-ESI (+ve): Calculated for C$_{20}$H$_{15}$C$_{l2}$ (M-OH)$^+$ 325.0545, found 325.0545. IR: KBr disc, υ$_{max}$ (cm^{-1}): 3528.5 (-OH stretch of tertiary alcohol).

(±)-1-(3-Chlorophenyl)-1-(4-chlorophenyl)-2-phenylethanol (92)
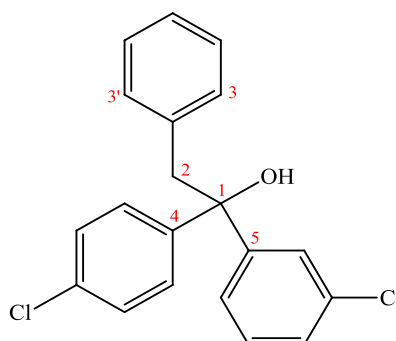
Using an adaptation of General Procedure A: 3-Chlorobromobenzene (0.574 g, 3 mmol) was dissolved in dry THF (5 mL). The solution was then cooled to -78 °C and n-butyllithium 2.7M solution in heptane (1.2 mL, 3.3 mmol) was added and stirred for half hour (white precipitate formed). 4-Chloro-2-benzophenone (0.690 g, 3 mmol) was dissolved in THF (10 mL) was then added dropwise to the mixture dropwise and the reaction was left stirred for a further 24 hours. The reaction was then quenched with saturated ammonium chloride (20 mL) and extracted with ethyl acetate (3 x 20 mL). The combined organic fractions were dried over anhydrous magnesium sulphate and evaporated under reduced pressure. The resulting residue was purified using flash column chromatography (Biotage SP4) [ethyl acetate:n-hexane, (10:90)] to give compound **92** as colourless liquid (0.43 g, 42%). ^{1}H NMR (400 MHz): δ (CDCl$_3$): 2.32 (1H, s, -O**H**); 3.58 (2H, s, -C**H$_2$**), 6.88 (2H, d, J =7.6, C3, 3'); 7.18-7.43 (11H, m, Ar). ^{13}C NMR (125 MHz): δ (CDCl$_3$): 47.76 (C1); 77.43 (C2); 114.89-134.93 (16C, Ar); 144.54 (C4/C5); 148.41(C4/C5). HRMS-ESI (+ve):

Calculated for $C_{20}H_{15}Cl_2$ (M-OH)$^+$ 325.0545, found 325.0545. IR: ATR, υ_{max} (cm^{-1}): 3552.2 (-OH stretch of tertiary alcohol).

(±)-1-(4-Methylphenyl)-1,2-diphenylethanol (93)
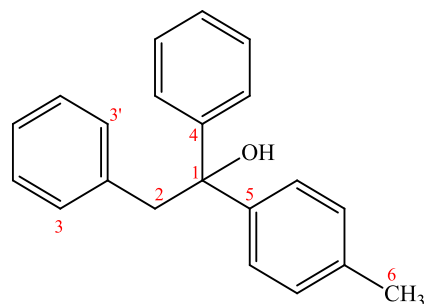
Using General Procedure A: Benzylmagnesium chloride 2M solution in THF (10 mL, 20 mmol) and 4-methylbenzophenone (1.96 g, 10 mmol) gave compound **93** (1.3 g, 46 %) as white waxy solid after purification by flash chromatography (Biotage SP4) [ethyl acetate:*n*-hexane (10:90)]. Mpt : 80-81 °C (literature: 92-93 °C).[153] ^{1}H NMR (400 MHz): δ (CDCl$_3$): 2.25 (1H, s, -O**H**); 2.30 (3H, s, -C**H$_3$**, C5); 3.61 (2H, s, -C**H$_2$**, C2); 6.90 (2H, m, C3.3'); 7.09-7.40 (12H, m, Ar). ^{13}C NMR (400 MHz): δ (CDCl$_3$): 21.08 (C6); 48.03 (C2); 77.42 (C1); 126.17-136.58 (16C, Ar); 143.80 (C5); 146.79 (C4). HRMS-ESI (+ve): Calculated for $C_{21}H_{19}O$ (M-OH)$^+$ 271.1481, found 271.1475. IR: KBr disc, υ_{max} (cm^{-1}): 3584.9 (-OH stretch of tertiary alcohol).

1,1-Bis(4-methylphenyl)-2-phenylethanol (94)
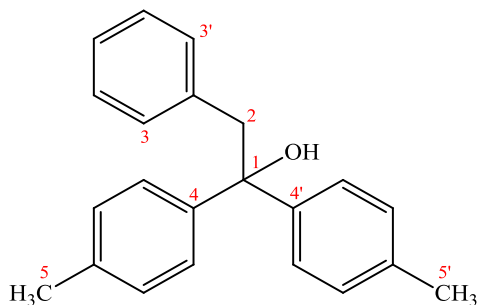
Using General Procedure A: Benzylmagnesium chloride 2M solution in THF (5 mL, 10 mmol) and 4,4'-dimethylbenzophenone (1.05 g, 5 mmol) gave compound **94** (0.9 g, 60 %) as colourless liquid after purification by flash chromatography (Biotage SP4) [ethyl acetate:*n*-hexane (10:90)]. ^{1}H NMR (400 MHz): δ (CDCl$_3$): 2.23(1H, s, -**OH**); (2.31 (6H, s, -**CH$_3$**, C5,5'); 3.60 (2H,s , -**CH$_2$**, C2); 6.90 (2H, m, C3,3', Ar); 7.09 (4H, d, *J* = 8.0 Hz, Ar); 7.15-7.17(3H, m, Ar); 7.30 (4H, d, *J* = 8.4 Hz, Ar). ^{13}C NMR (125 MHz): δ (CDCl$_3$): 21.07 (2C, C5,5'); 48.04 (C2); 77.78 (C1); 126.11-136.14 (16C, Ar); 143.95 (2C, C4,4'). HRMS-ESI (+ve): Calculated for C$_{22}$H$_{21}$ (M-OH)$^+$ 285.1638, found 285.1638. IR: ATR, υ$_{max}$ (cm^{-1}): 3566.2 (-OH stretch of tertiary alcohol).

(±)-1-(2-Fluorophenyl)-1,2-diphenylethanol (95)
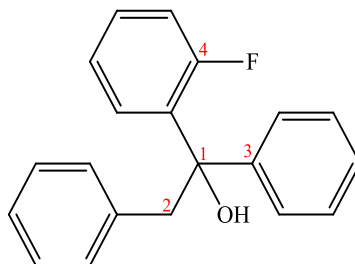
Using General Procedure A: Benzylmagnesium chloride 2M solution in THF (10 mL, 20 mmol) and 2-fluorobenzophenone (2 g, 10 mmol) gave compound **95** (2 g, 68 %) as a white waxy solid after purification by flash chromatography (Biotage SP4) [ethyl acetate:*n*-hexane (10:90)]. Mpt: 85-86 °C. ^{1}H NMR (400 MHz): δ (CDCl$_3$): 2.53 (1H, d, *J* = 3.2 Hz, -O**H**); 3.55-3.86 (2H, d, *J* = 13.2 Hz, -C**H$_2$**, C2); 6.92-7.30 (14H, m, Ar). ^{13}C NMR (125 MHz): δ (CDCl$_3$): 45.96 (C2); 77.33 (C1); 115.98-136.03 (16C, Ar); 146.79 (C3); 159.72 (d, *J$_{CF}$* = 305.38, C4). HRMS-ESI (+ve): Calculated for C$_{20}$H$_{16}$F (M-OH)$^+$ 275.1231, found 275.1232. IR: KBr disc, υ$_{max}$ (cm^{-1}): 3588.3 (-OH stretch of tertiary alcohol).

(±)-1-(4-Fluorophenyl)-1,2-diphenylethanol (96)
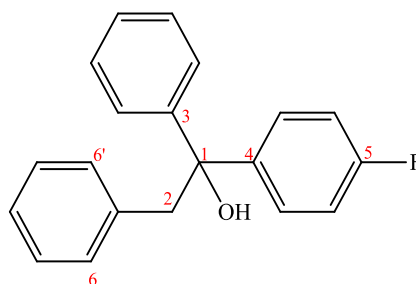
Using General Procedure A: Benzylmagnesium chloride 2M solution in THF (10 mL 20 mmol) and 4-fluorobenzophenone (2 g, 10 mmol) gave compound **96** (2.3 g, 79 %) as a white waxy solid after purification by flash chromatography (Biotage SP4)

[ethyl acetate:*n*-hexane (10:90)]. Mpt: 78-79 °C. ^{1}H NMR (400 MHz): δ (CDCl$_3$): 2.335 (1H, s, -O**H**); 3.59-3.64 (2H, d, *J* = 13.2,-C**H$_2$**, C2); 6.89 (2H, d, *J* = 8.8 Hz, C6,6'); 6.93-7.44 (12H, m, Ar). ^{13}C NMR (125 MHz): δ (CDCl$_3$): 48.138 (C2); 77.69 (C1); 114.78-135.6 (15C, Ar); 142.45 (C4); 146.51 (C3); 161.80 (d, *J$_{CF}$* = 305.5, C5). HRMS-ESI (+ve): Calculated for C$_{20}$H$_{16}$F (M-OH)$^+$ 275.1231, found 275.1231. IR: KBr disc, υ$_{max}$ (cm^{-1}): 3575.3 (-OH stretch of tertiary alcohol).

1,1-Bis(4-fluorophenyl)-2-phenylethanol (97)
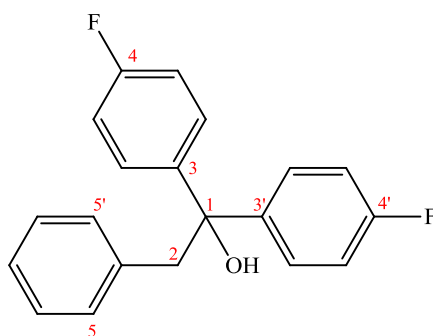
Using General Procedure A: Benzylmagnesium chloride 2M solution in THF (10 mL, 20 mmol) and 4,4'-difluorobenzophenone (2.18 g, 10 mmol) gave compound **97** (1 g, 32 %) as a white waxy solid after purification by flash chromatography (Biotage SP4) [ethyl acetate:*n*-hexane (10:90)]. Mpt: 88-89 °C. ^{1}H NMR (400 MHz): δ (CDCl$_3$): 2.32 (1H, s, -O**H**); 3.59 (2H, s, -C**H$_2$**, C2); 6.87 (2H, d, *J* = 7.6 Hz, C5,5'); 6.97-7.39 (11H, m, Ar). ^{13}C NMR (400 MHz): δ (CDCl$_3$): 48.22 (C2); 77.37 (C1); 114.89-135.37 (14C, Ar); 142.31 (2C, C5,5'); 161.86 (d, *J$_{CF}$* = 306.0, C4). HRMS-ESI (+ve): Calculated for C$_{20}$H$_{15}$F$_2$ (M-OH)$^+$ 293.1136, found 293.1138. IR: KBr disc, υ$_{max}$ (cm^{-1}): 3557.3 (-OH stretch of tertiary alcohol).

2-Hydroxy-1,2,2-triphenylethanone (139)
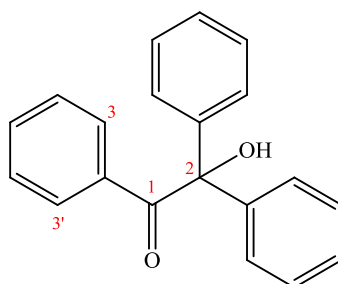
Using General Procedure A: Phenyllithium 1.8M solution in THF (5 mL, 9 mmol) and benzil (1.05 g, 5 mmol) gave compound **139** (1g, 35 %) as white waxy solid after purification by flash chromatography (Biotage SP4) [ethyl acetate:*n*-hexane (20:80)]. Mpt: 78-79 °C (literature: 81-83 °C).[154] ^{1}H NMR (400 MHz): δ (CDCl$_3$): 4.98 (1H, s, -O**H**); 7.27-7.44 (13H, m, Ar); 7.71 (2H, d, *J* = 7.6 Hz, C3, 3'). ^{13}C NMR (125 MHz): δ (CDCl$_3$): 85.13 (C2); 127.23-141.92 (18C, Ar); 200.90 (C1). HRMS-ESI (+ve): Calculated for C$_{20}$H$_{15}$O (M-OH)$^+$ 271.1117, found 271.1118. IR: KBr disc, υ$_{max}$ (cm^{-1}): 3468.2 (-OH stretch of tertiary alcohol), 1667.9 (C=O stretch of ketone).

9-Phenyl-9*H*-xanthen-9-ol (162)
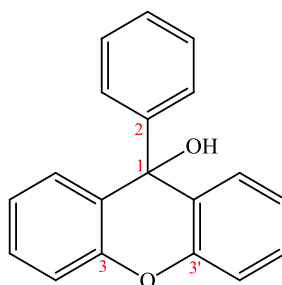
Using General Procedure A: Phenyllithium 2M solution in THF (5 mL, 10 mmol) and 9*H*-xanthen-9-one (0.980 g, 5 mmol) gave compound **162** (0.97 g, 71 %) as a white powder after purification by gravity column chromatography [ethyl acetate:*n*-hexane (10:90)]. Mpt: 155-158 ºC (literature: 157-158 °C).[155] ^{1}H NMR (400 MHz):

δ (CDCl$_3$): 2.59 (1H, s, -O**H**); 7.03 (2H, t, J = 8.0 Hz, Ar); 7.18 (3H, m, Ar), 7.27-7.40 (8H, m, Ar). ^{13}C NMR (125 MHz): δ (DMSO-d_6): 68.64 (C1); 115.78-128.76 (15C, Ar); 149.07-149.68 (3C, C2, 3, 3'). HRMS-ESI (+ve): Calculated for C$_{19}$H$_{13}$O (M-OH)$^+$ 257.0960, found 257.0959. IR: KBr disc, υ_{max} (cm^{-1}): 3547 (-OH stretch of tertiary alcohol).

9-Phenyl-9H-thioxanthen-9-ol (163)
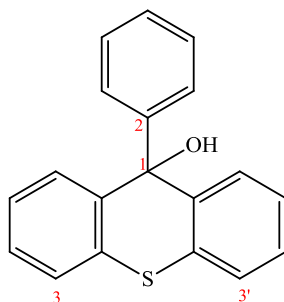
Using General Procedure A: Phenyllithium 2M solution in THF (5 mL, 10 mmol) and 9H-thioxanthen-9-one (1.06 g, 5 mmol) gave compound **163** (0.47 g, 32 %) as an orange colour powder after purification by gravity column chromatography [ethyl acetate:n-hexane (10:90)]. Mpt: 192-193 ºC (literature: 115-116 °C).[156] ^{1}H NMR (400 MHz): δ (CDCl$_3$): 2.71 (1H, s, -O**H**); 6.98 (2H, m, Ar); 7.17 (3H, m, Ar); 7.29 (2H, m, Ar); 7.42 (4H, m, Ar); 8.04 (2H, d, J = 8.4 Hz, C3,3',Ar). ^{13}C NMR (125 MHz): δ (DMSO-d_6): 75.32 (C1); 126.01-130.28 (15C, Ar); 140.64 (2C, Ar); 144.27 (C2). HRMS-ESI (+ve): Calculated for C$_{19}$H$_{13}$S (M-OH)$^+$ 273.0732, found 273.0733. IR: KBr disc, υ_{max} (cm^{-1}): 3287.6 (-OH stretch of tertiary alcohol).

9-Benzyl-9*H*-xanthen-9-ol (164)
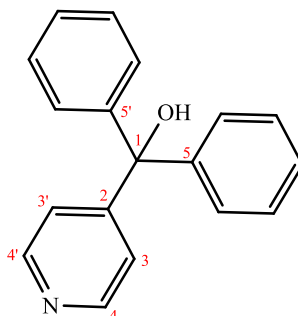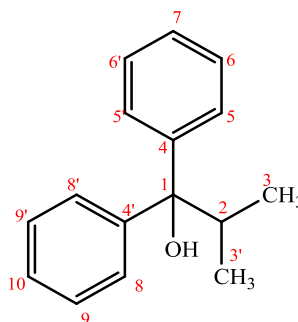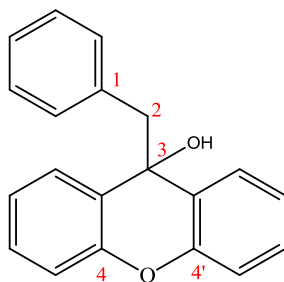

Using General Procedure A: Benzylmagnesium chloride 2M solution in THF (10 mL, 20 mmol) and 9*H*-xanthen-9-one (0.980 g, 5 mmol) gave compound **164** (1 g, 69 %) as a white powder after recrystallisation from methanol. Mpt: 165-167 ºC. ^{1}H NMR (400 MHz): δ (CD$_3$OD): 3.15 (2H,s,-C**H$_2$**, C2) 6.25-7.75 (13H, m, Ar). ^{13}C NMR (125 MHz): δ (DMSO-*d*$_6$): 73.84 (C3), 115.01-129.26 (15C, Ar), 137.24 (C1), 151.67 (2C, C4,4'). HRMS-ESI (+ve): Calculated for C$_{20}$H$_{15}$O (M-OH)$^+$ 271.1117, found 271.1113. IR: KBr disc, υ$_{max}$ (cm^{-1}): 3559.0 (-OH stretch of tertiary alcohol).

9-Benzyl-9*H*-thioxanthen-9-ol (165)
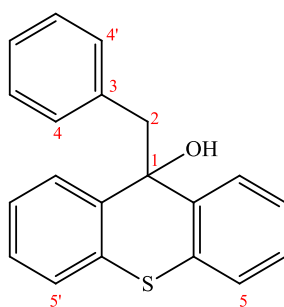
Using General Procedure A: Benzylmagnesium chloride 2M solution in THF (10 mL, 20 mmol) and 9*H*-thioxanthen-9-one (2.12 g, 10 mmol) gave compound **165** (2 g, 66 %) as a pale brown powder after purification by gravity column chromatography [ethyl acetate:*n*-hexane (10:90)]. Mpt: 172-174 ºC. ^{1}H NMR (400 MHz): δ (CDCl$_3$): 2.95 (1H, s, -O**H**); 3.30 (2H, s, -C**H$_2$**, C2); 6.66 (2H, d, *J* = 8.0 Hz,

C4,4'); 6.97 (3H, m, Ar); 7.15 (4H, m, Ar); 7.37 (2H, d, J = 7.6 Hz, Ar); 7.57 (2H, d, J = 7.6 Hz, C5,5', Ar). ^{13}C NMR (125 MHz): δ (DMSO-d_6): 43.37 (C2); 74.64 (C1); 125.64-126.92 (15C, Ar); 136.33 (1C, C3); 140.34 (2C, Ar). HRMS-ESI (+ve): Calculated for $C_{20}H_{15}S$ (M-OH)$^+$ 287.0889, found 287.0887. IR: KBr disc, υ_{max} (cm^{-1}): 3450.0 (-OH stretch of tertiary alcohol).

9-Benzyl-9H-fluoren-9-ol (168)
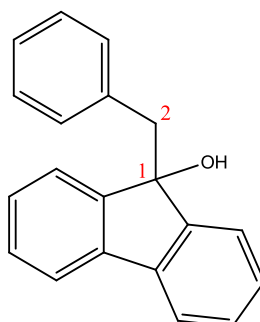
Using General Procedure A: Benzylmagnesium chloride 2M solution in THF (9.75 mL, 19.5 mmol) and 9H-fluoren-9-one (0.720 g, 4 mmol) gave compound **168** (0.53 g, 50%) as a white powder after recrystallisation from methanol. Mpt: 140-141 ºC (literature: 143-144 °C).[157] ^{1}H NMR (400 MHz): δ (DMSO-d$_6$): 2.13 (1H, s, -O**H**); 3.30 (2H, s, -C**H$_2$**, C2), 6.96-7.55 (13H, m, Ar). HRMS-ESI (+ve): Calculated for $C_{20}H_{15}$ (M-OH)$^+$ 255.1168 found 255.1165. IR: KBr disc, υ_{max} (cm^{-1}): 3520.5 (-OH stretch of tertiary alcohol).

1,1,3-Triphenylprop-2-yn-1-ol (185)
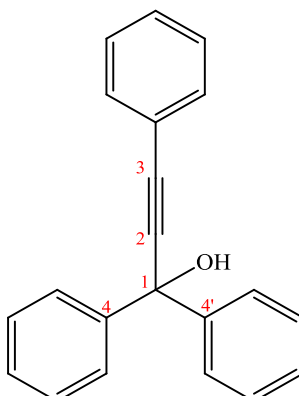
Using General Procedure A: Lithium phenylacetylide 1M solution in THF (15 mL, 15 mmol) and benzophenone (1.8 g, 10 mmol) gave compound **185** (2 g, 70 %) as pale yellow waxy solid after purification by flash chromatography (Biotage SP4) [ethyl acetate:*n*-hexane (15:85)]. Mpt: 76-77 °C. (literature: 78-80 °C).[158] ^{1}H NMR (400 MHz): δ (CDCl$_3$): 2.91 (1H, s, -O**H**); 7.34-7.70 (15H, m, Ar). ^{13}C NMR (125 MHz): δ (CDCl$_3$): 74.94 (C1); 87.3 (C3); 91.7 (C2); 122.51-131.87 (16C, Ar; 122.51, 126.16, 127.85, 128.43, 128.79, 131.89); 145.11 (2C, C4,4'). HRMS-ESI (+ve): Calculated for C$_{21}$H$_{15}$ (M-OH)$^+$ 267.1168, found 267.1166. IR: KBr disc, υ_{max} (cm^{-1}): 3546.4 (-OH stretch of tertiary alcohol).

4.4.1.2 General Procedure B: Preparation of tertiary alcohols via *in-situ* generation of Grignard reagent. Magnesium turnings (150 mg) were heated to 50 °C for 1 hour under a nitrogen atmosphere and two chips of iodine were then added. The mixture was cooled to room temperature, anhydrous diethyl ether (10 mL) added, followed by a solution of the substituted benzylbromide derivative (3 mmol in anhydrous diethyl ether (10 mL) and the mixture was stirred for 3 hours. A solution of benzophenone (0.375 g, 3 mmol in anhydrous diethyl ether (10 mL) was added and the mixture was stirred at room temperature under nitrogen for a further 24 hours. The reaction was quenched with saturated ammonium chloride (20 mL) and then extracted with ethyl acetate (3 x 20 mL). The combined organic fractions were dried (MgSO$_4$), evaporated under reduced pressure, and residue purified using flash

column chromatography (Biotage SP4) [ethyl acetate:*n*-hexane (10:90)] to give the desired tertiary alcohol product.

2-(3,4-Dichlorophenyl)-1,1-diphenylethanol (98).
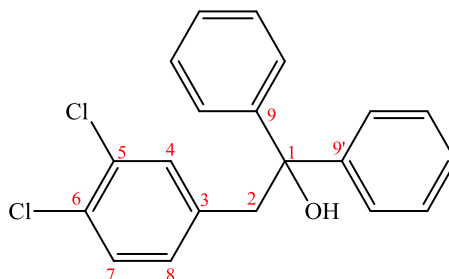
Using the General Procedure B: 3,4-Dichlorobromobenzyl bromide (0.717 g, 3 mmol) gave compound **98** (0.375 g, 37 %) as a white waxy solid. Mpt**:** 65-66 °C. ^{1}H NMR (400 MHz): δ (CDCl$_3$): 2.17 (1H, s -O**H**); 3.55 (2H, s, -C**H$_2$**); 6.66-6.69 (1H, dd, J = 8.4, J = 2 Hz, C8); 6.99 (1H, d, J = 2 Hz, C4); 7.16 (1H, d, J = 8.4, C7); 7.16-7.37 (10H, m, Ar). ^{13}C NMR (125 MHz): δ (CDCl$_3$): 47.20 (C1); 78.12 (C2); 126.27- 136.65 (16C, Ar); 146.06 (2C, C9,9'). HRMS-ESI (+ve): Calculated for C$_{20}$H$_{15}$Cl$_2$ (M-OH)$^+$ 325.0545, found 352.0544. IR: KBr disc, υ_{max} (cm^{-1}): 3566.9 (-OH stretch of tertiary alcohol).

2-(4-Chlorophenyl)-1,1-diphenylethanol (99)
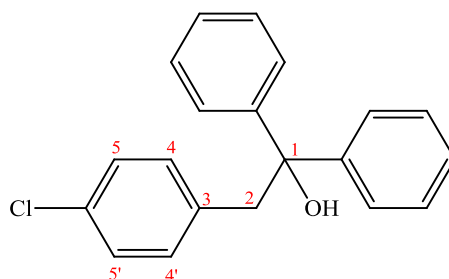
Using the General Procedure B: 4-Chlorobromobenzyl bromide (0.6 g, 3 mmol) gave compound **99** (0.275 g, 30 %) as a white waxy solid. Mpt: 115-117 °C (literature: 153-154 °C) .[159] ^{1}H NMR (400 MHz): δ (CDCl$_3$): 2.1978 (1H, s, -O**H**); 3.5938 (2H, s, -C**H$_2$**, C2); 6.79-6.81 (2H, dd, J = 8.4, J = 2 Hz, C4,4'); 7.09-7.11 (2H, dd, J = 8.4, J = 2 Hz, C5,5'); 7.22-7.40 (10H, m, Ar). ^{13}C NMR (125 MHz): δ (CDCl$_3$): 47.37 (C1); 78.23 (C2); 126.26-146.33 (18C, Ar). HRMS-ESI (+ve): Calculated for C$_{20}$H$_{16}$Cl (M-OH)$^+$ 291.0935, found 291.0934. IR: KBr disc, υ_{max} (cm^{-1}): 3530.1 (-OH stretch of tertiary alcohol).

2-(3-chlorophenyl)-1,1-diphenylethanol (100)
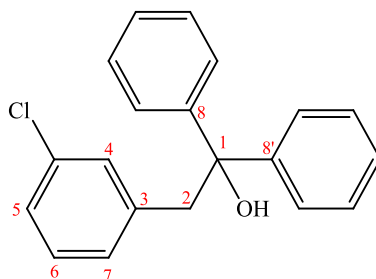
Using the General Procedure B: 3-Chlorobromobenzyl bromide (0.60 g, 3 mmol) gave compound **100** (0.6 g, 49 %) as a white waxy solid. Mpt: 162-163 °C. ^{1}H NMR (400 MHz): δ (CDCl$_3$): 2.249 (1H, s, -O**H**); 3.64 (2H, s, -C**H$_2$**, C2); 6.74 (1H, d, J = 7.6 Hz, C7); 6.90 (1H, s, C4); 7.05 (1H, t, J = 7.6 Hz, C6); 7.14 (1H, d, J = 7.6 Hz, C5); 7.24-7.40 (10H, m, Ar). ^{13}C NMR(400 MHz): δ (CDCl$_3$): 47.75 (C2); 78.21 (C1); 126.29-138.25 (16C, Ar); 146.3 (2C, C8,8').   HRMS-ESI (+ve): Calculated for C$_{20}$H$_{16}$Cl (M-OH) $^+$ 291.0935, found 291.0935. IR: KBr disc, υ_{max} (cm^{-1}): 3560.4 (-OH stretch of tertiary alcohol).

4.4.1.3 General Procedure C: Preparation of tertiary alcohols by reduction ketones using sodium borohydride. The required ketone (8 mmol) was dissolved in methanol (20 mL) and NaBH$_4$ (15 mmol) was added gradually. The reaction was stirred for 24h, filtered and concentrated *in vacuo*. The sticky residue was purified

using gravity column chromatography [ethyl acetate:*n*-hexane (20:80)] to give the desired tertiary alcohol product.

9*H*-Xanthen-9-ol (165)
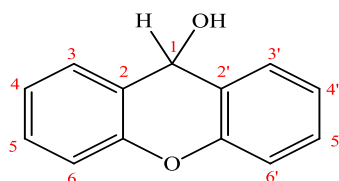
Using General Procedure C: Xanthone (1.569 g, 8 mmol) gave compound **165** (0.5 g, 25) as white powder. Mpt: 122-124 °C (literature: 127-128 °C).[160] ^{1}H NMR (400 MHz): δ (CDCl$_3$): 2.20 (1H, d, J = 8.8 Hz, -O**H**); 5.82 (1H, d, J = 8.8 Hz, -C**H**, C1); 7.15 (4H, t, J = 8.0 Hz, C4,4',5',5', Ar); 7.35(2H, t, J = 7.2 Hz, Ar); 7.5 (2H, d, J = 8.0 Hz, C3,3', Ar). ^{13}C NMR (125 MHz): δ (DMSO-d_6): 69.25 (C1); 125.24-136.53 (12C, Ar). HRMS-ESI (+ve): Calculated for C$_{13}$H$_9$O (M-OH)$^+$ 181.0648, found 181.0645. IR: KBr disc, υ_{max} (cm^{-1}): 3336.4 (-OH stretch of tertiary alcohol).

9*H*-Thioxanthen-9-ol (167)
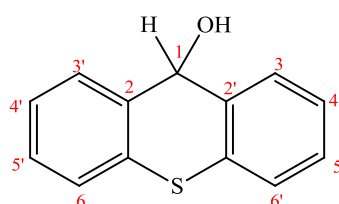
Using General Procedure C: Thioxanthone (1.698 g, 8 mmol) gave compound **167** (1 g, 47 %) as a white powder. Mpt: 105-107 °C (literature: 104-105 °C). ^{1}H NMR (400 MHz): δ (CDCl$_3$): 2.29 (1H, d, J = 6.8 Hz, -O**H**); 5.5 (1H, d, J = 6.8 Hz -C**H**, C1); 7.25-7.34 (4H, m, Ar); 7.48 (2H, d, J = 7.6 Hz,C6,6', Ar); 7.63 (2H, d, J = 7.2 Hz, C5,5', Ar). ^{13}C NMR (125 MHz): δ (DMSO-d_6): 69.25 (C1); 125.24-136.53

(10C, Ar); 153.58 (2C, C2,2'). HRMS-ESI (+ve): Calculated for $C_{13}H_9S$ (M-OH)$^+$ 197.0419, found 197.0417. IR: KBr disc, υ_{max} (cm^{-1}): 3566.5 (-OH stretch of tertiary alcohol).

4.4.1.4 Preparation of tertiary alcohols (183, 186 and 187):

2-Hydroxy-2,2-diphenylacetonitrile (183)
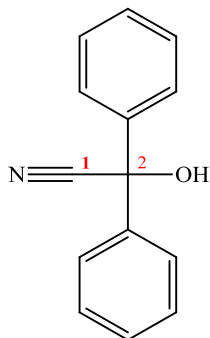
Potassium cyanide (50 mg, 0.77 mmol), 18-crown-6 (100 mg, 0.38 mmol) and trimethylsilyl cyanide (2 g, 20 mmol) was added to a solution of benzophenone (1.82 g, 10 mmol) in anhydrous dichloromethane (50 mL) and the mixture stirred for 24 hours. A mixture of 10% hydrochloric acid solution (15 mL) and THF (20 mL) was added to the reaction mixture and stirred for 2 hours. The mixture was extracted with ethyl acetate (3 x 20 mL); the organic fractions were dried (MgSO$_4$) and evaporated under reduced pressure. The residue was purified using flash column chromatography (Biotage SP4) [ethyl acetate:*n*-hexane (10:90)] to give compound **183** (1.3 g, 62 %) as a white waxy solid. Mpt: 112-113 °C (literature:116-119 °C).[161] ^{1}H NMR (400 MHz): δ (CDCl$_3$): 3.27 (1H, s, -O**H**); 7.38-7.55 (10H, m, Ar). ^{13}C NMR (125 MHz): δ (CDCl$_3$): 75.61 (C2); 120.69 (C1); 125.93-140.29 (12C, Ar). HRMS-ESI (+ve): Calculated for $C_{14}H_{10}N$ (M-OH)$^+$ 192.0808, found 192.1001. IR: KBr disc, υ_{max} (cm^{-1}): 3368.88 (-OH stretch of tertiary alcohol), 2247.66 (C≡N stretch of cyano group).

(*E*)-1,1,3-Triphenylprop-2-en-1-ol (186)
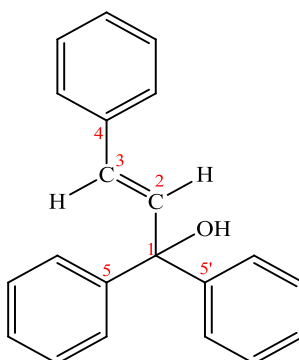
1,1,3-Triphenylprop-2-yn-1-ol (**185**) (288 mg, 1 mmol) was dissolved in dry THF (10 mL) and added dropwise to a solution of lithium aluminium hydride (59 mg, 1.5 mmol) in dry THF (20 mL) at 15 °C. The reaction was stirred for 24 hours then quenched with ethanol (10 mL). The reaction solvent was then evaporated under reduced pressure and water (20 mL) was added to the residue. The mixture was extracted with dichloromethane (3 x 25 mL) and the combined organic fractions dried (MgSO$_4$). Evaporation of the solvent under reduced pressure gave compound **186** (0.70 g, 25%) as a white solid. Mpt:106-108 °C (literature: 106-108).[162] ^{1}H NMR (400 MHz): δ (CDCl$_3$): 2.39 (1H, s, -O**H**); 6.67 (1H, d, *J* = 14.0 Hz, -C**H**, C3); 6.85 (1H, d, *J* = 14.0 Hz, -C**H**, C2); 7.28-7.43 (15H, m, Ar). ^{13}C NMR (125 MHz): δ (CDCl$_3$): 78.85 (C1); 125.91-131.29 (15C, Ar); 135.78 (C4); 146.67 (C5, 5'). HRMS-ESI (+ve): Calculated for C$_{21}$H$_{17}$ (M-OH)$^{+}$ 269.1325, found 269.1323.

1,1,3-Triphenylpropan-1-ol (187)
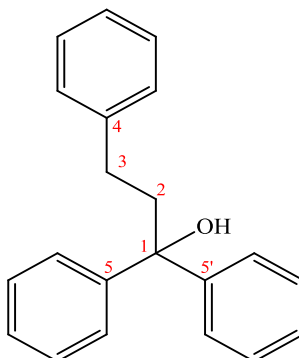
1,1,3-Triphenylprop-2-yn-1-ol (**185**) (586   mg, 2   mmol) was dissolved in ethyl acetate (20 mL) and a mixure of Lindlar's catalyst (80 mg) and potassium carbonate (80 mg) were added to the solution. The reaction flask was purged, filled with H_2 gas and the mixture was stirred at atmospheric pressure at room temperature for 72 hours. The reaction was then filtered and evaporated under reduced pressure, the residue was then purified by flash column chromatography (Biotage SP4) [ethyl acetate:*n*-hexane(10:90)] to give compound **187** (0.432 g, 73 %) as a white powder. Mpt: 85-87 °C (Literature: 85-86 °C)[163] ^{1}H NMR (400 MHz): δ (CDCl$_3$): 2.14 (1H, s, -O**H**); 2.61 (4H, s, -C**H$_2$**, C2,3); 7.15-7.47 (15H, m, Ar). ^{13}C NMR (125 MHz): δ (CDCl$_3$): 30.37 (C1); 44.10 (C3); 78.38 (C2); 125.93-128.53 (15C, Ar); 142.43 (C4); 146.90 (2C, C5,5'). HRMS-ESI (+ve): Calculated for $C_{21}H_{19}$ (M-OH)$^+$ 271.1481, found 271.1480. IR: KBr disc, υ_{max} (cm^{-1}): 3553.5 (-OH stretch of tertiary alcohol).

4.4.2 General Procedure D: Synthesis of L-cysteine analogues. L-Cysteine (58.4 mg, 0.48 mmol) and the required tertiary alcohol (0.48 mmol) were dissolved in acetic acid (0.5 mL). Boron trifluoride etherate (0.09 mL, 0.82 mmol) was added dropwise under nitrogen atmosphere at 0 °C. The reaction mixture was stirred at at 0 °C for 2h and 10 % sodium acetate (1.5 mL) and water (1.5 mL) was then added. The

resulting precipitate was filtered, washed with water and diethyl ether and then dried in a vacuum oven (40 °C for 24 h) to give the corresponding L-cysteine derivatives.

(*R*)-2-Amino-3-((1,1,2-triphenylethyl)thio)propanoic acid (101)
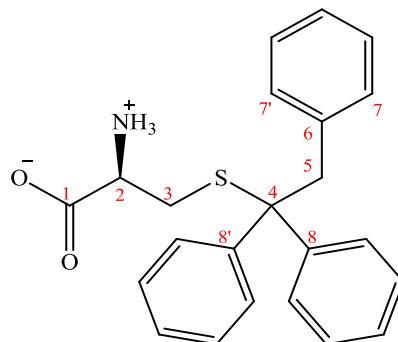
Using General Procedure D: 1,1,2-Triphenylethanol (**79**) (0.658 g, 2.4 mmol) and L-cysteine (0.292 mg, 2.4 mmol) gave compound **101** (0.335 g, 37 %) as a white powder. Mpt: 169-170 °C. ^{1}H NMR (400 MHz): δ (DMSO-d_6): 2.34 (1H, dd, $J = 12.8$, $J = 9.2$ Hz, -C**Ha**Hb**,** C3); 2.61 (1H, dd, $J = 12.4$, $J = 4.0$ Hz, -CHa**Hb,** C3); 2.87 (1H, dd, $J = 9.2$, $J = 4.0$ Hz, –C**H,** C2); 3.66 (2H, s, -C**H$_2$**, C5); 6.68 (2H, d, $J = 7.2$ Hz, C7,7') 7.00-7.31 (13H, m, Ar). ^{13}C NMR (125 MHz): δ (CD$_3$OD): 30.64 (C3); 45.64 (C5); 53.68 (C2); 61.20 (C4); 126.14-131.07 (15C, Ar); 136.63 (C6); 144.08 (2C, C8,8'); 170.90 (C1). Elemental analysis: Found: C, 73.41; H, 5.93; N, 3.81; S, 8.14 (Required for C$_{23}$H$_{23}$NO$_2$S: C, 73.18; H, 6.14; N, 3.71; S, 8.49). HRMS-ESI (+ve): Calculated for C$_{23}$H$_{24}$NO$_2$S (M+H) 378.1522, found 378.1527. IR: KBr disc, υ_{max} (cm^{-1}): 1617.2 (C=O stretch for carboxylic acid).

(*R*)-2-Amino-3-(((±)-1,2-diphenylethyl)thio)propanoic acid (102)
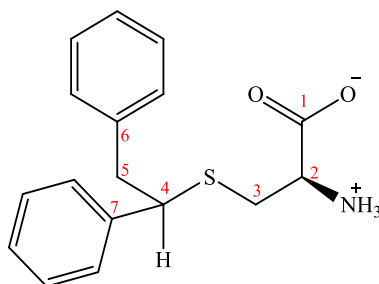
Using General Procedure D: 1,2-Diphenylethanol (**80**) (0.383.5 g, 1.92 mmol) and L-cysteine (0.232 g, 1.92 mmol) gave compound **102** (0.105 g, 18 %) as a white powder. Mpt: 184-185 ℃. ^{1}H NMR (400 MHz): δ (DMSO-d_6): 2.60-3.31 (5H, m, C5,3,2); 4.29 (1H, m, -C**H,** C4); 7.05-7.34 (10H, m, Ar). ^{13}C NMR (125 MHz): δ (DMSO-d_6): 32.19 (C3); 41.55 (C5); 49.92 (C4); 53.63 (C2); 126.037-129.31 (10C, Ar); 138.74 (C6); 141.53 (C7); 168.40 (C1). Elemental analysis: Found: C, 67.92; H, 6.01; N, 4.17; S, 10.87 (Required for $C_{17}H_{19}NO_2S$: C, 67.74; H, 6.35; N, 4.65; S, 10.64). HRMS-ESI (+ve): Calculated for $C_{17}H_{20}NO_2S$ (M+H) 302.1209 found, 302.1206. IR: KBr disc, υ_{max} (cm^{-1}): 1618.0 (C=O stretch for carboxylic acid).

(*R*)-2-Amino-3-(((±)-1,2-diphenylpropan-2-yl)thio)propanoic acid (103)
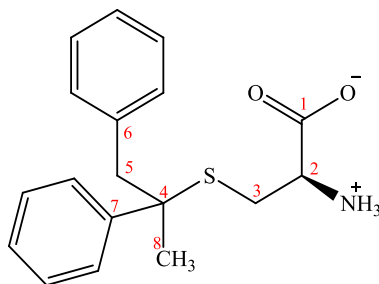
Using General Procedure D: 1,2-Diphenylpropan-2-ol (**81**) (0.407 g, 1.92 mmol) and L-cysteine (0.232 g, 1.92 mmol) gave compound **103** (0.229 g, 20 %) as a white powder. Mpt: 178-179 ℃. ^{1}H NMR (400 MHz): δ (DMSO-d_6): 1.607 (3H, -C**H₃**, C8); 2.47-3.29 (5H, C5,3,2); 6.83-7.48 (10H, Ar). ^{13}C NMR (125 MHz): δ (DMSO-

d_6): 25.17 (C8); 30.86 (C3); 48.49 (C5); 52.42 (C2); 54.54 (C4); 126.32-130.42 (10C, Ar); 136.66 (C6); 144.02 (C7); 168.26 (C1). Elemental analysis: Found: C, 67.47; H, 6.58; N, 4.44; S, 9.95 (Required for $C_{18}H_{21}NO_2S.1/2H_2O$: C, 66.64; H, 6.83; N, 4.32; S, 9.88). HRMS-ESI (-ve): Calculated for $C_{18}H_{20}NO_2S$ (M-H) 314.1220, found 314.1226. IR: KBr disc, υ_{max} (cm^{-1}): 1601.7 (C=O stretch for carboxylic acid).

(*R*)-2-Amino-3-(((±)-1,2-diphenylbutan-2-yl)thio)propanoic acid (104).
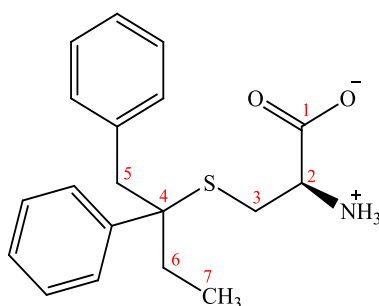
Using General Procedure D: 1,2-Diphenylbutan-2-ol (**82**) (0.434 g, 1.92 mmol) and L-cysteine (0.232 g, 1.92 mmol) gave compound **104** (0.139 g, 22 %) as a white powder. Mpt: 176-177 ºC. ^{1}H NMR (400 MHz): δ (DMSO-d_6): 0.96-1.03 (3H, m , -**CH$_3$**, C7); 1.78-1.88 (2H, -**CH$_2$**, m, C6); 2.36-3.33 (5H, m, C5,3,2); 6.77-7.50 (10H, Ar). ^{13}C NMR (125 MHz): δ (DMSO-d_6): 9.72 (C7); 27.50 (C6); 30.72 (C3); 43.89 (C5); 54.39 (C2); 57.65 (C4); 126.83-143.85 (12C, Ar); 168.68 (C1). Elemental analysis: Found: C, 69.73; H, 6.91; N, 4.28; S, 9.40 (Required for $C_{19}H_{23}NO_2S$: C, 69.27; H, 7.04; N, 4.25; S, 9.73). HRMS-ESI (+ve): Calculated for $C_{19}H_{24}NO_2S$ (M+H) 330.1522, found 330.1519. IR: KBr disc, υ_{max} (cm^{-1}): 1635.6 (C=O stretch for carboxylic acid).

(*R*)-2-Amino-3-(((±)-1-(3-hydroxyphenyl)-1,2-diphenylethyl)thio)propanoic acid (105).
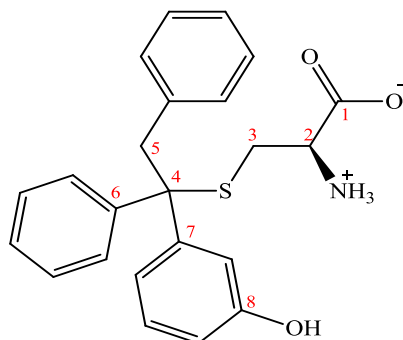
Using General Procedure D: 3-(1-Hydroxy-1,2-diphenylethyl)phenol (**85**) (0.320 g, 1.1 mmol) and L-cysteine (0.133 g, 1.1 mmol) gave compound **105** (0.045 g, 10 %) as a white powder. Mpt:186-187 °C. ^{1}H NMR (400 MHz): δ (CD$_3$OD): 2.59-2.67 (1H, m, -C**Ha**Hb, C3); 2.89-2.95 (1H, m, -CHa**Hb**, C3), 3.09-3.06 (1H, m, -C**H**, C2); 3.65-3.68 (2H, m, -C**H₂**, C5); 6.69-7.37 (14H, m, Ar). ^{13}C NMR (125 MHz): δ (CD$_3$OD): 30.78 (C3); 45.50 (C5); 53.79 (C2); 61.51 (C4); 113.57-136.51 (15C, Ar); 144.59 (C7/6); 146.14 (C6/7); 156.86 (C8); 171.27 (C1). Elemental analysis: Found: C, 67.94; H, 6.08; N, 3.45; S, 8.02 (Required for C$_{23}$H$_{23}$NO$_3$S. H$_2$O: C, 67.13; H, 6.12; N, 3.40; S, 7.79). HRMS-ESI (-ve): Calculated for C$_{23}$H$_{22}$NO$_3$S (M-H) 392.1326, found 392.1324. IR: KBr disc, v_{max} (cm^{-1}): 1598.6 (C=O stretch for carboxylic acid).

172

(*R*)-2-Amino-3-(((±)-1-(4-hydroxyphenyl)-1,2-diphenylethyl)thio)propanoic acid (106)
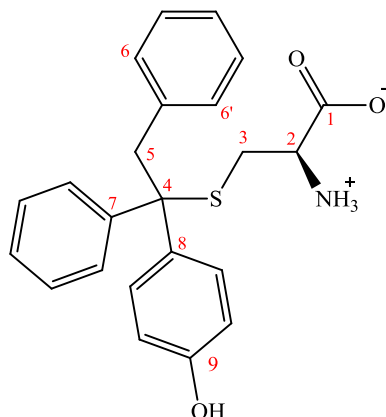
Using General Procedure D: 1-(4-Hydroxyphenyl)-1,2-diphenylethanol (**86**-MA94) (0.870 g, 3 mmol) and L-cysteine (0.360 g, 3 mmol) gave compound **106** (0.090 g, 8 %) as a white powder. Mpt: 170-171 °C. ^{1}H NMR (400 MHz): δ (CD$_3$OD): 2.55-2.60 (1H, m, -C**Ha**Hb, C3), 2.91-2.93 (2H, m, -CHa**Hb,** C3,and -C**H**, C2); 3.63-3.65 (2H, s, -C**H$_2$**, C5), 6.68-7.23 (14H, m, Ar). ^{13}C NMR (125 MHz): δ (CD$_3$OD): 30.59 (C3); 45.86 (C5); 53.50 (C2); 61.52 (C4); 113.98-136.68 (15C, Ar); 143.42 (C7/8); 144.58 (C7/8); 156.01 (C9); 170.63 (C1). Elemental analysis: Found: C, 66.00; H, 6.27; N, 3.22; S, 8.00 (Required for C$_{23}$H$_{23}$NO$_3$S.H$_2$O C, 66.97; H, 6.35; N, 3.40; S, 7.77). HRMS-ESI (+ve): Calculated for C$_{23}$H$_{24}$NO$_3$S (M+H) 394.1471, found 394.1470. IR: KBr disc, υ_{max} (cm^{-1}): 1614.1 (C=O stretch for carboxylic acid).

(R)-2-Amino-3-((±)-1-(3-chlorophenyl)-1,2-diphenylethyl)thio)propanoic   acid (107)
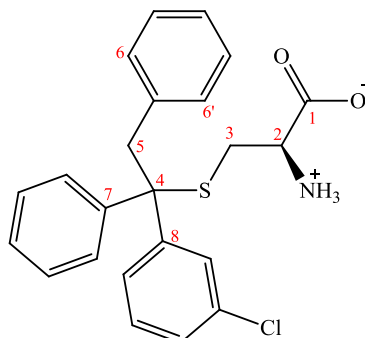
Using General Procedure D: 1-(3-Chlorophenyl)-1,2-diphenylethanol (**87**) (0.275 g, 0.892 mmol) and L-cysteine (108.03 g, 0.892 mmol) gave compound **107** (0.04 g, 11%) as a white powder. Mpt: 152-153 °C. ^{1}H NMR (400 MHz): δ (CD$_3$OD): 2.56-2.66 (1H, m, - **CHa**Hb, C3); 2.87-2.93 (1H, m, -CHa**Hb,** C3); 3.02-3.11 (1H, m, –**CH**, C2); 3.61-3.7 (2H, m,-**CH$_2$**, C5); 6.70 (2H, d, J = 7.6 Hz, C6,6'); 6.99 -7.39 (12H, m, Ar). ^{13}C NMR (125 MHz): δ (CD$_3$OD): 30.94 (C3); 45.50 (C5); 53.85 (C2); 61.33 (C4);   126.12-133.55 (16C, Ar); 143.95 (1C, C8); 146.78 (1C,C7); 171.36 (C1). Elemental analysis: Found: C, 61.48; H, 5.18; N, 3.01; Cl, 7.62; S, 7.69 (Required for C$_{23}$H$_{22}$ClNO$_2$S.2H$_2$O: C, 61.67; H, 5.85; Cl, 7.91; N, 3.13; S, 7.16). HRMS-ESI (+ve): Calculated C$_{23}$H$_{23}$ClNO$_2$S (M+H) 412.1133, found 412.1140. IR: KBr disc, υ_{max} (cm^{-1}): 1615.9 (C=O stretch for carboxylic acid).

(*R*)-2-Amino-3-(((±)-1-(4-chlorophenyl)-1,2-diphenylethyl)thio)propanoic   acid (108)
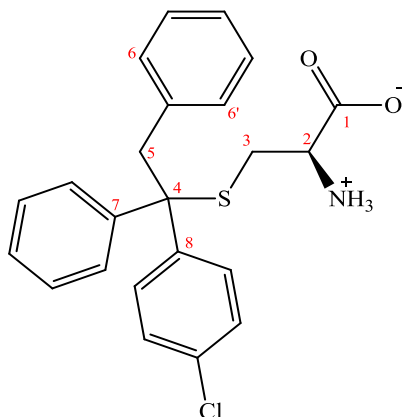
Using General Procedure D: 1-(4-Chlorophenyl)-1,2-diphenylethanol (**89**) (0.750 g, 2.43 mmol) and L-cysteine (0.296 g, 2.43 mmol) gave compound **108** (0.29 g, 29 %) as a white powder. Mpt: 165-166 °C. ^{1}H NMR (400 MHz): δ (CD$_3$OD): 2.60-2.65 (1H, m, -C**Ha**Hb, C3); 2.86-2.90 (1H, m, -CHa**Hb**, C3); 3.01-3.30 (1H, m, –C**H**, C2); 3.64-3.70 (2H, m, -C**H$_2$**, C5), 6.70 (2H, d, *J* = 7.2 Hz, C6,6'); 7.00-7.37 (12H, m, Ar). ^{13}C NMR (125 MHz): δ (CD$_3$OD): 30.65 (C3); 47.26.08 (C2); 53.72 (C5); 61.21 (C4); 126.86-136.20 (16C, Ar); 143.13 (C8); 144.09 (C7); 170.90 (C1). Elemental analysis: Found: C, 67.83; H, 5.39; N, 3.32; S, 7.95 (Required for C$_{23}$H$_{22}$ClNO$_2$S C, 67.06; H, 5.38; N, 3.40; S, 7.92). HRMS-ESI (+ve): Calculated for C$_{23}$H$_{23}$ClNO$_2$S (M+H) 412.1133, found 412.1129. IR: KBr disc, υ_{max} (cm^{-1}): 1615.3 (C=O stretch for carboxylic acid).

(*R*)-2-Amino-3-(((±)-1-(3,4-dichlorophenyl)-1,2-diphenylethyl)thio)propanoic acid (109).
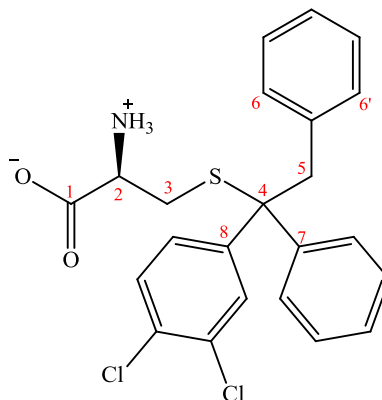
Using General Procedure D: 1-(3,4-Dichlorophenyl)-1,2-diphenylethanol (**90**) (0.668 g, 2 mmol) and L-cysteine (0.242 g, 2 mmol) gave compound **109** (0.119 g, 13 %) as a white powder. Mpt:163-164 °C. ^{1}H NMR (400 MHz): δ (CD$_3$OD): 2.60-2.67 (1H, m, -C**Ha**Hb, C3); 2.84-2.94 (1H, m, -CHa**Hb**, C3); 3.08-3.18 (1H, m, –C**H**, C2), 3.61-3.74 (2H, m, -C**H$_2$**, C5); 6.72 (2H, d, *J* = 6.8 Hz, C6,6'); 7.02-7.45 (11H, m, Ar). ^{13}C NMR (125 MHz): δ (CD$_3$OD): 30.69 (C3); 45.18 (C5); 53.72 (C2); 60.82 (C4); 126.28-131.06 (16C, Ar); 143.44 (C8); 145.57 (C7); 170.79 (C1). Elemental analysis: Found: C, 61.37; H, 4.80; N, 3.07; Cl, 14.99; S, 7.01 (Required for C$_{23}$H$_{21}$Cl$_2$NO$_2$S.1/2H$_2$O 60.66; H, 4.87; Cl, 15.57; N, 3.08; S, 7.04). HRMS-ESI (+ve): Calculated for C$_{23}$H$_{22}$Cl$_2$NO$_2$S (M+H) 446.0743, found 446.0739. IR: KBr disc, υ_{max} (cm^{-1}): 1617.3 (C=O stretch for carboxylic acid).

(*R*)-2-Amino-3-((1,1-bis(4-chlorophenyl)-2-phenylethyl)thio)propanoic acid (110).
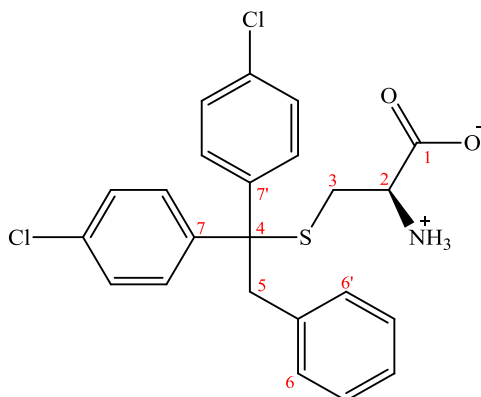
Using General Procedure D: 1,1-Bis(4-chlorophenyl)-2-phenylethanol (**91**) (0.342 g, 1 mmol) and L-cysteine (0.121 g, 1 mmol) gave compound **110** (0.087 g, 20%) as a white powder. Mpt: 170-171 °C. ^{1}H NMR (400 MHz): δ (CD$_3$OD): 2.617-2.650 (1H, dd, *J* = 13.2, *J* = 9.2 Hz, –**CHa**Hb**,** C3); 2.841-2.883 (1H, dd, *J* = 13.2, *J* = 3.6 Hz, –CHa**Hb**, C3**)**, 3.13-3.15 (1H, dd, *J* = 9.2, *J* = 4.0 –**CH**, C2); 3.30-3.67 (2H, d, *J* = 13.2 Hz, -CH$_2$, C5); 6.73 (2H, d, *J* = 7.2 Hz, C6.6'); 7.01-7.32 (11H, m, Ar). ^{13}C NMR (125 MHz): δ (CD$_3$OD): 30.67 (C3); 45.43 (C5); 53.65 (C2); 60.81 (C4); 126.24-135.92 (16C, Ar); 142.92 (2C, C7,7'); 170.75 (C1). Elemental analysis: Found: C, 61.78; H, 4.24; N, 2.87; Cl, 6.98; S, 7.39 (Required for C$_{23}$H$_{21}$Cl$_2$NO$_2$S C, 61.88; H, 4.74; N, 3.14; Cl, 7.17; S, 7.18). HRMS-ESI (+ve): Calculated for C$_{23}$H$_{22}$Cl$_2$NO$_2$S (M+H) 446.0743, found 446.07428. IR: KBr disc, υ_{max} (cm^{-1}): 1618.3 (C=O stretch for carboxylic acid).

(*R*)-2-Amino-3-(((±)-1-(3-chlorophenyl)-1-(4-chlorophenyl)-2-phenylethyl)thio)-propanoic acid (111)
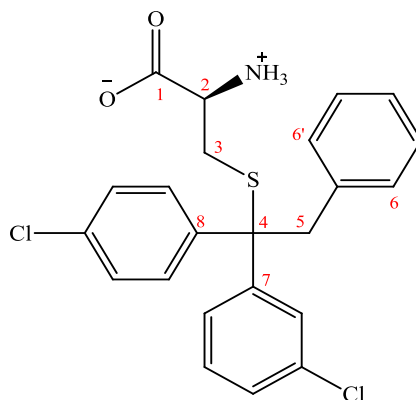
Using General Procedure D: 1-(3-Chlorophenyl)-1-(4-chlorophenyl)-2-phenylethanol (**92**) (0.340 g, 1.25 mmol) and L-cysteine (0.151g, 1.25 mmol) gave compound **111** (0.083 g, 15 %) as a white powder. Mpt:163-164°C. ^{1}H NMR (400 MHz): δ (CD$_3$OD): 2.58-2.68 (1H, m, -C**Ha**Hb, C3); 2.85-2.91(1H, m, -CHa**Hb**, C3); 3.16-3.21 (1H, m, –C**H**, C2); 3.62-3.72 (2H, m, -C**H$_2$**, C5); 6.72 (2H, d, *J* = 6.8 Hz, C6,6'); 7.02 -7.37 (11H, m, Ar). ^{13}C NMR (125 MHz): δ (CD$_3$OD): 32.16 (C3); 46.69 (C5); 55.20 (C2); 62.34 (C4); 127.76-137.31 (16C, Ar); 144.22 (C8); 148.01 (C7); 172.22 (C1). Elemental analysis: Found: C, 60.89; H, 4.69; N, 3.0; Cl, 15.24; S, 6.98 (Required for C$_{23}$H$_{21}$Cl$_2$NO$_2$S C, 60.66; H, 4.87; Cl, 15.57; N, 3.08; S, 7.04). HRMS-ESI (+ve): Calculated for C$_{23}$H$_{22}$Cl$_2$NO$_2$S (M+H) 446.0743, found 446.0740. IR: KBr disc, υ$_{max}$ (cm^{-1}): 1617.3 (C=O stretch for carboxylic acid).

(*R*)-2-Amino-3-((±)-1,2-diphenyl-1-(4-methylphenyl)ethyl)thio)propanoic   acid (112)
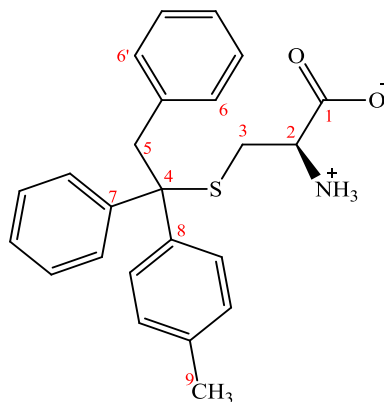
Using General Procedure D: 1-(4-Methylphenyl)-1,2-diphenylethanol (**93**) (0.272 g, 0.94 mmol) and L-cysteine (0.113 g, 0.94 mmol) gave compound **112** (0.20 g, 21%) as a white powder. Mpt: 148-149 °C. ^{1}H NMR (400 MHz): δ (CD$_3$OD): 2.30-2.32 (3H, m, -C**H$_3$**, C8); 2.59-2.62 (1H, m, -C**Ha**Hb, C3); 2.90-2.92 (2H, m, -CHa**Hb**, C3 and –**CH**, C2); 3.64-3.68 (2H, s, -C**H$_2$**, C5); 6.67 (2H, d, *J* = 7.2 Hz, C6,6'); 6.93-7.37 (12H, m, Ar). ^{13}C NMR (125 MHz): δ (CD3OD): 19.57 (C8); 30.56 (C3); 45.56 (C5); 53.70 (C2); 61.39 (C4); 125.48-136.39 (16C, Ar); 141.11 (C7/8); 144.59 (C7/8); 170.94 (C1). Elemental analysis: Found: C, 72.65; H, 7.52; N, 4.04; S, 8.09 (Required for C$_{24}$H$_{25}$NO$_2$S C, 73.62; H, 6.44; N, 3.58; S, 8.19). HRMS-ESI (+ve): Calculated for C$_{24}$H$_{26}$NO$_2$S (M+H) 392.1679, found 392.16824. IR: KBr disc, υ$_{max}$ (cm^{-1}): 1608.0 (C=O stretch for carboxylic acid).

(*R*)-2-Amino-3-((1,1-bis(4-methylphenyl)-2-phenylethyl)thio)propanoic   acid (113)
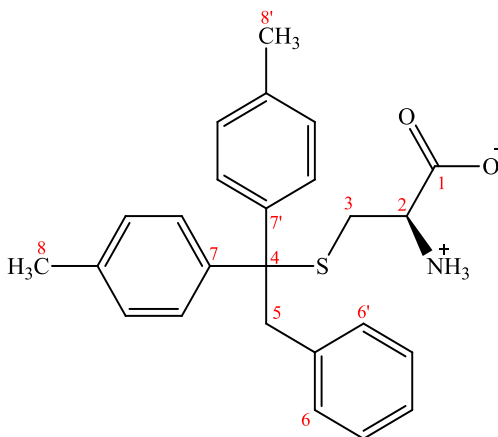
Using General Procedure D: 1,1-Bis(4-methylphenyl)-2-phenylethanol (**94**) (0.302 g, 1 mmol) and L-cysteine (0.121 g, 1 mmol) gave compound **113** (0.060 g, 15 %) as a white powder. Mpt: 162-164 °C. ^{1}H NMR (400 MHz): δ (CD$_3$OD): 2.29-2.31 (6H, d, *J* = 7.2Hz, -C**H$_3$**, C8,8'); 2.56-2.62 (1H, dd, *J* = 14.4, *J* = 10.8 Hz,-S**Ha**Hb, C3); 2.90-2.2.94 (2H, m, -CHa**Hb,** C3 and **-CH**, C2**)**, 3.58-3.70 (2H, d, *J* = 13.6 Hz, -C**H$_2$**, C5); 6.69 (2H, d, *J* = 7.2 Hz, C6,6'); 6.96-7.25 (11H, m, Ar). ^{13}C NMR (125 MHz): δ (CD$_3$OD): 19.68 (2C, C8,8'); 30.70 (C3); 45.61 (C5); 53.76 (C2); 61.28 (C4);   125.88-136.36 (16C, Ar); 141.71 (2C, C7,7'); 171.19 (C1).   Elemental analysis: Found: C, 74.59; H, 6.55; N, 3.36; S, 7.82 (Required for C$_{25}$H$_{27}$NO$_2$S C, 74.04; H, 6.71; N, 3.45; S, 7.91). HRMS-ESI (-ve): Calculated for C$_{25}$H$_{26}$NO$_2$S (M-H) 404.1690, found 404.16941. IR: KBr disc, υ_{max} (cm^{-1}): 1616.3 (C=O stretch for carboxylic acid).

(*R*)-2-Amino-3-(((±)-1-(2-fluorophenyl)-1,2-diphenylethyl)thio)propanoic acid (114).
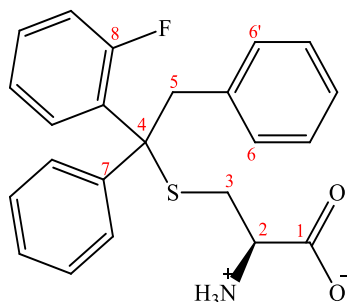
Using General Procedure D: 1-(2-Fluorophenyl)-1,2-diphenylethanol (**95**) (0.592 g, 2 mmol) and L-cysteine (0.242 g, 2 mmol) gave compound **114** (0.14 g, 19 %) as a white powder. Mpt: 160-161 °C. ^{1}H NMR (400 MHz): δ (CD$_3$OD): 2.54-2.65(1H, m, -C**Ha**Hb**,** C3); 2.73-2.79 (1H, m, -CHa**Hb**; C3); 2.90-3.02 (1H, –C**H**, C2); 3.82-3.85 (2H, d, *J* = 13.6 Hz, -C**H$_2$**, C5); 6.83 (2H, m, C6,6'); 6.97-7.37(12H, m, Ar). ^{13}C NMR (125 MHz): δ (CD$_3$OD): 32.35 (C3); 45.94 (C5); 55.08 (C2); 61.63 (C4); 117.28-137.87 (16C, Ar); 146.26 (C7); 162.27 (d, J_{CF} = 246.62, C8); 172.28 (C5). Elemental analysis: Found: C, 69.37; H, 5.60; N, 3.49; S, 7.95 (Required for C$_{23}$H$_{22}$FNO$_2$S C, 69.85; H, 5.61; N, 3.54; S, 8.11). HRMS-ESI (+ve): Calculated for C$_{23}$H$_{23}$FNO$_2$S (M+H) 396.1428, found 396.1427. IR: KBr disc, υ_{max} (cm^{-1}): 1636.0 (C=O stretch for carboxylic acid).

(*R*)-2-Amino-3-(((±)-1-(4-fluorophenyl)-1,2-diphenylethyl)thio)propanoic acid (115)
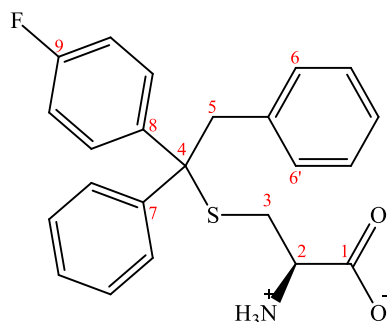
Using General Procedure D: 1-(4-Fluorophenyl)-1,2-diphenylethanol (**96**) (0.592 g, 2 mmol) and L-cysteine (0.242 g, 2 mmol) gave compound **115** (0.090 g, 12 %) as a white powder. Mpt: 171-172 °C. ^{1}H NMR (400 MHz): δ (CD$_3$OD): 2.58-2.64 (1H, m, -C**Ha**Hb,C3); 2.86-2.89 (1H, m, -CHa**Hb**, C3); 2.98-3.04 (1H, m, − C**H**, C2); 3.62-3.75 (2H, m, -C**H$_2$**, C5); 6.69 (2H, d, *J* = 7.2 Hz, C6,6'); 6.95-7.38 (12H, m, Ar). ^{13}C NMR (125 MHz): δ (CD$_3$OD): 32.15 (C3); 47.03 (C5); 55.21 (C2); 62.63 (C4); 115.47-137.79 (15C, Ar); 141.69 (C8); 145.88 (C7); 163.18 (d, J_{CF} = 243.63, C9); 172.35 (C1). Elemental analysis: Found: C, 69.40; H, 5.45; N, 3.32; S, 7.79 (Required for C$_{23}$H$_{22}$FNO$_2$S, C, 69.85; H, 5.61; N, 3.54; S, 8.11). HRMS-ESI (+ve): Calculated for C$_{23}$H$_{23}$FNO$_2$S (M+H) 396.14283, found 96.1429. IR: KBr disc, υ_{max} (cm^{-1}): 1603.7 (C=O stretch for carboxylic acid).

(*R*)-2-Amino-3-((1,1-bis(4-fluorophenyl)-2-phenylethyl)thio)propanoic **acid** **(116)**
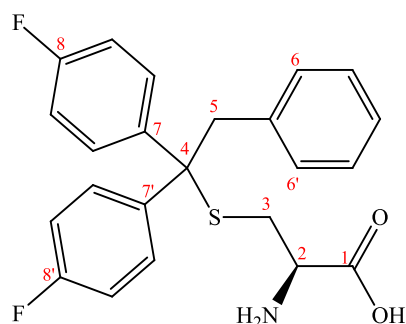
Using General Procedure D: 1,1-Bis(4-fluorophenyl)-2-phenylethanol (**97**) (0.7 g, 2.25 mmol) and L-cysteine (0.273 g, 2.25 mmol) gave compound **116** (0.09 g, 10 %) as a white powder. Mpt: 168-170 °C. ^{1}H NMR (400 MHz): δ (CD$_3$OD): 2.60-2.65 (1H, dd, J = 13.2, J = 9.2 Hz, -C**Ha**Hb, C3); 2.85-2.90 (1H, dd, J = 13.2, J = 4.0 Hz, –CHa**Hb**, C3); 3.07-3.10 (1H, dd, J = 9.2, J = 3.6 Hz, -C**H**, C2); 3.62-3.72 (2H, d, J = 13.2 Hz, -C**H$_2$**, C5); 6.71 (2H, d, J = 7.2 Hz, C6,6'); 6.97-7.37 (11H, m, Ar). ^{13}C NMR (125 MHz): δ (CD$_3$OD): 32.20 (C3); 47.30 (C5); 55.24 (C2); 62.20 (C4); 115.61-137.64 (14C, Ar); 141.62 (2C, C7, 7'); 163.23 (d, J_{CF} = 245.0, C8, 8'); 172.29 (C1). Elemental analysis: Found: C, 63.69; H, 5.38; N, 3.22; S, 7.12 (Required for C$_{23}$H$_{21}$F$_2$NO$_2$S.H$_2$O C, 64.02; H, 5.37; N, 3.25; S, 7.43). HRMS-ESI (+ve): Calculated for C$_{23}$H$_{22}$F$_2$NO$_2$S (M+H) 414.1334, found 414.1333. IR: KBr disc, υ$_{max}$ (cm^{-1}): 1603.7 (C=O stretch for carboxylic acid).

(*R*)-2-Amino-3-((2-(3,4-dichlorophenyl)-1,1-diphenylethyl)thio)propanoic   acid (117)
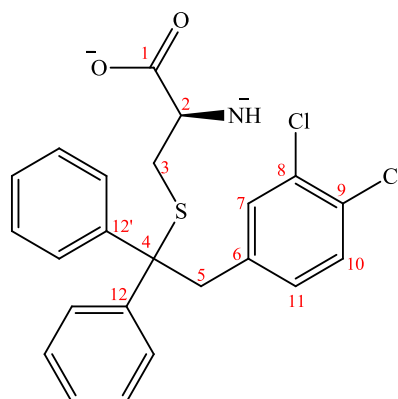
Using General Procedure D: 2-(3,4-dichlorophenyl)-1,1-diphenylethanol (**98**) (0.375 mg, 1.1 mmol) and L-cysteine (0.133 mg, 1.1 mmol) gave compound **117** (0.1g, 20 %) as a white powder. Mpt: 162-164 °C. ^{1}H NMR (400 MHz): δ (CD$_3$OD): 2.61-2.65 (1H, dd, J = 13.2, J = 9.2 Hz , -**CHa**Hb, C3); 2.89-2.92 (1H, dd, J = 13.2, J = 4.0 Hz, -CHa**Hb**, C3); 2.95-2.97 (1H, dd, J = 9.2 J = 4.0 Hz, -C**H**, C2); 3.63-3.77 (2H, d, J = 13.6 Hz, -**CH$_2$**, C5); 6.68 (1H, d, J = 2 Hz, C7); 6.70-6.72 (1H, dd, J = 8.4, J = 2 Hz, C11); 7.15 (1H, d, J = 8.4 Hz, C10); 7.25-7.38 (10H, m, Ar). ^{13}C NMR (125 MHz): δ (CD$_3$OD): 30.49 (C3); 44.39 (C5); 53.01 (C2); 61.25 (C4); 126.95-137.43 (116C, Ar); 144.14 (2C, C12,12'); 170.83 (C1). Elemental analysis: Found: C, 61.65; H, 4.87; N, 3.02; Cl, 15.70; S, 7.09 (Required for C$_{23}$H$_{21}$Cl$_2$NO$_2$S, C, 61.88; H, 4.74; N, 3.14; Cl, 15.88; S, 7.18).   HRMS-ESI (+ve): Calculated for C$_{23}$H$_{22}$Cl$_2$NO$_2$S (M+H) 446.0743, found 446.0743. IR: KBr disc, υ$_{max}$ (cm^{-1}): 1628.3 (C=O stretch for carboxylic acid).

**(*R*)-2-Amino-3-((2-(4-chlorophenyl)-1,1-diphenylethyl)thio)propanoic acid (118)**
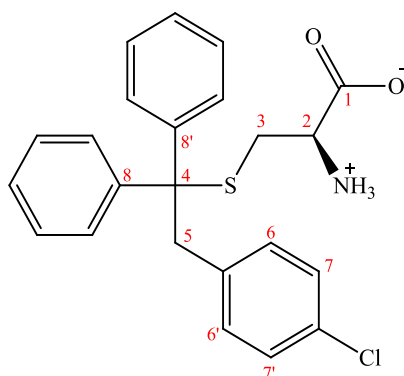
Using General Procedure D: 2-(4-Chlorophenyl)-1,1-diphenylethanol (**99**) (0.275 g, 0.89 mmol) and L-cysteine (0.108 g, 0.89 mmol) gave compound **118** (0.082 g, 22 %) as a white powder. Mpt: 163-165 °C. ^{1}H NMR (400 MHz): δ (CD$_3$OD): 2.63-2.67 (1H, dd, *J* = 13.2, *J* = 9.6, -C**Ha**Hb, C3); 2.88-2.92 (1H, dd, *J* = 13.2, *J* = 4.0 Hz, -CHa**Hb**,C3); 2.97-2.99 (1H, dd, *J* = 9.6, *J* = 4.0 Hz, –C**H**, C2); 3.62-3.73(2H, dd, *J* = 13.6 Hz, -C**H$_2$**, C5); 6.65-6.67 (2H, dt, *J* = 8.4, *J* = 2, C6,6'); 6.97-6.99 (2H, dt, *J* = 8.4, *J* = 2 Hz, C7,7'); 7.24-7.38 (10H, m, Ar). ^{13}C NMR (125 MHz): δ (CD$_3$OD): 30.33 (C3); 44.55 (C5); 53.77 (C2); 61.50 (C4); 126.75-135.33 (16C, Ar); 144.46 (2C, C8,8'); 171.03 (C1). Elemental analysis: Found: C, 67.14; H, 5.38; N, 3.25; Cl, 8.02; S, 7.39 (Required for C$_{23}$H$_{22}$ClNO$_2$S, C, 67.06; H, 5.38; N, 3.40; Cl, 8.61; S, 7.78). HRMS-ESI (+ve): Calculated for C$_{23}$H$_{23}$ClNO$_2$S (M+H) 412.1133, found 412.1130. IR: KBr disc, υ$_{max}$ (cm^{-1}): 1612.1 (C=O stretch for carboxylic acid).

**(*R*)-2-Amino-3-((2-(3-chlorophenyl)-1,1-diphenylethyl)thio)propanoic acid (119)**
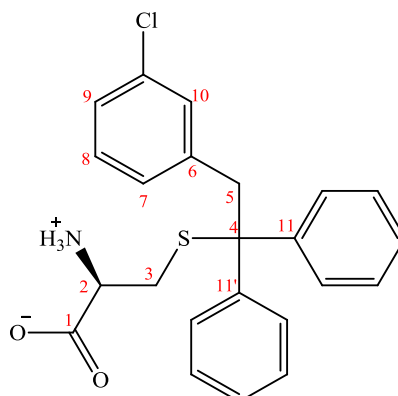
Using General Procedure D: 2-(3-Chlorophenyl)-1,1-diphenylethanol (**100**) (0.6 g, 1.94 mmol) and L-cysteine (0.235 g, 1.94 mmol) gave compound **119** (0.190 g, 24 %) as a white powder. Mpt:160-161 °C. ^{1}H NMR (400 MHz): δ (CD$_3$OD): 2.59-2.642 (1H, m, -C**Ha** Hb, C3); 2.89-2.95 (2H, m, -CHa**Hb**, C3 and –C**H**, C2); 3.65-3.75 (2H, dd, J = 13.6 Hz, -C**H$_2$**, C5); 6.58 (1H, s, C10); 6.68 (1H, d, J = 7.6 Hz, C7); 6.99 (1H, t, J = 7.6 Hz, C8); 7.06 (1H, d, J = 7.6 Hz, C9); 7.25-7.40 (10H, m, Ar). ^{13}C NMR (125 MHz): δ (CD$_3$OD): 30.58 (C3); 45.16 (C5); 53.71 (C2); 61.41 (C4); 126.05-138.84 (16C, Ar); 144.20 (C11, 11'); 171.03 (C1). Elemental analysis: Found: C, 67.58; H, 5.40; N, 3.32; Cl, 8.44; S, 7.29 (Required for C$_{23}$H$_{22}$ClNO$_2$S C, 67.06; H, 5.38; N, 3.40; Cl, 8.61; S, 7.78). HRMS-ESI (+ve): Calculated for C$_{23}$H$_{23}$ClNO$_2$S (M+H) 412.1133, found 412.1130. IR: KBr disc, υ_{max} (cm^{-1}): 1617.3 (C=O stretch for carboxylic acid).

(*R*)-2-Amino-3-(((±)-diphenyl(pyridin-4-yl)methyl)thio) propanoic acid ditetra-fluoroborate (120).
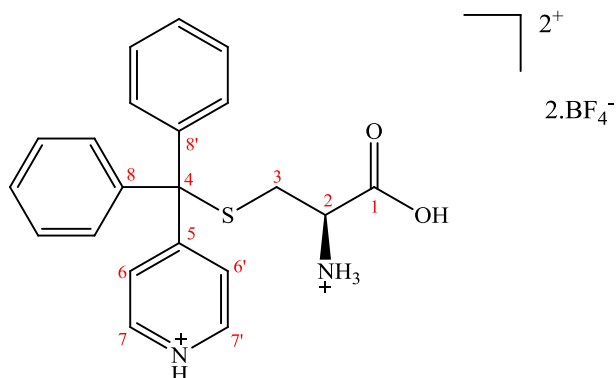
Using General Procedure D: Diphenyl(pyridin-4-yl)methanol (**83**) (0.522 g, 2 mmol) and L- cysteine (0.242 g, 2 mmol) gave compound **120** (0.3 g, 28 %) as a white powder after recrystallisation form diethyl ether. Mpt: 164-166 °C. ^{1}H NMR (400 MHz): δ (CD$_3$OD): 2.74-2.85 (2H, m, -**CH$_2$**, C3); 3.59 (1H, t, *J* = 5.2 Hz, –**CH**, C2); 7.29-7.50 (10, m, Ar); 8.19 (2H, d, *J* = 6.8 Hz, C6, 6'); 8.76 (2H, d, *J* = 6.8 Hz, C7, 7'). ^{13}C NMR (125 MHz): δ (DMSO-d_6): 31.60 (C3); 51.41 (C2); 65.47 (C4); 123.92-128.91 (12C, Ar); 142.43 (C7, 7'); 149.74 (2C, C8, 8'); 152.25 (C5); 168.87 (C1). Elemental analysis: Found: C, 46.31; H, 4.37; N, 4.47; (Required for: C$_{21}$H$_{22}$B$_2$F$_8$N$_2$O$_2$S C, 46.70; H, 4.11; N, 5.19; S, 5.94). HRMS-ESI (+ve): Calculated for C$_{21}$H$_{21}$N$_2$O$_2$S (M+H) 365.1318, found 365.1321. IR: KBr disc, υ$_{max}$ (cm^{-1}): 1635.8 (C=O stretch for carboxylic acid), 3032.1 (OH stretch for carboxylic acid).

2-((2-Aminoethyl)thio)-1,2,2-triphenylethanone (141)
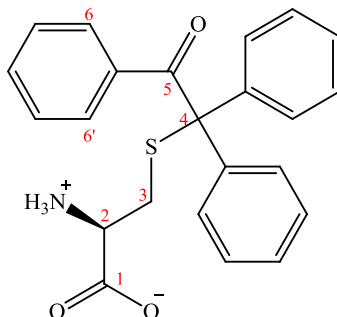
Using General Procedure D: 2-Hydroxy-1,2,2-triphenylethanone (**139**) (0.1 g, 1.1mmol) and L-cysteine (0.042 g, 0.347 mmol) gave compound **141** (0.060 g, 44 %) as a pale yellow powder. Mpt:85-86 °C. ^{1}H NMR (400 MHz): δ (CD$_3$OD): 2.61-2.67 (1H, dd, J = 13.6, J = 8.4 Hz, -C**Ha**Hb,C3); 2.69-2.71 (1H, dd, - J = 13.6, J = 4.4 Hz, -CHa**Hb**, C3); 3.45-4.47 (1H, m, –C**H**, C2); 7.19- 7.54 (13H, m, Ar); 7.66-7.7.68 (2H, C6,6'). ^{13}C NMR (125 MHz): δ (CD$_3$OD): 32.97 (C3); 53.86 (C2); 71.87 (C4); 126.98-139.71 (18C, Ar); 174.03 (C1); 197.31 (C5). Elemental analysis Found: C, 70.98; H, 5.41; N, 3.60; S, 7.98 (Required for C$_{23}$H$_{21}$NO$_3$S C, 70.56; H, 5.41; N, 3.58; S, 8.19). HRMS-ESI (+ve): Calculated for C$_{23}$H$_{22}$NO$_3$S (M+H) 392.1315, found 392.13168. IR: KBr disc, υ_{max} (cm^{-1}): 1627.4 (C=O stretch for carboxylic acid), 1680.3 (C=O stretch for keone).

(*R*)-3-((9*H*-Xanthen-9-yl)thio)-2-aminopropanoic acid (169)
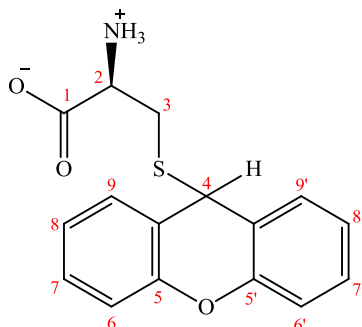
Using General Procedure D: 9*H*-Xanthen-9-ol (**166**) (0.197g, 1 mmol) and L-cysteine (0.121 g, 1 mmol) gave compound **169** (0.26 g, 86 %) as a white powder. Mpt: 218-219 °C. ^{1}H NMR (400 MHz): δ (DMSO-d_6): 2.72 (1H, dd, *J* = 14.0, *J* = 7.6 Hz, -**CHa**Hb, C3); 2.89 (1H, dd, *J* = 14.0, *J* = 3.2 Hz, -CHa**Hb**, C3); 3.36 (1H, dd, *J* = 7.6, *J* = 3.2 Hz, –C**H**, C2); 5.55 (1H, s, -C**H**, C4); 7.15 (4H, t, *J* = 7.2 Hz, C6,6' and C7,7'); 7.33 (2H, t, *J* = 7.6 Hz, C8,8'); 7.47 (1H, d, *J* = 7.6, C9); 7.62 (1H, d, *J* = 7.6 Hz,C9'). ^{13}C NMR (125 MHz): δ (DMSO-d_6): 32.35 (C3); 40.80 (C4); 53.73 (C2); 116.20-130.0 (10C, Ar); 152.26 (2C, C5, 5'); 168.87 (C1). Elemental analysis: Found: C, 62.33; H, 5.45; N4.02; S, 10.32 (Required for $C_{16}H_{15}NO_3S.1/2H_2O$: C, 61.92; H, 5.20; N, 4.51; S, 10.33). HRMS-ESI (+ve): Calculated $C_{16}H_{16}NO_3S$ (M+H) 302.0845, found 302.0851. IR: KBr disc, υ_{max} (cm^{-1}): 1639.6 (C=O stretch for carboxylic acid).

(R)-3-((9H-Thioxanthen-9-yl)thio)-2-aminopropanoic acid (171).
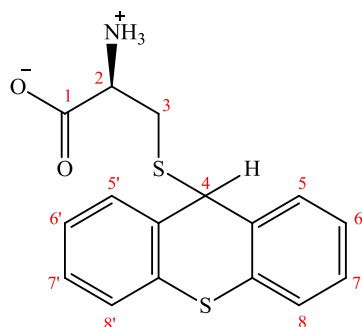
Using General Procedure D: 9H-Thioxanthen-9-ol (**167**) (0.213 g, 1 mmol) and L-cysteine (0.121 g, 1 mmol) gave compound **171** (0.25 g, 79%) as a pale yellow powder. Mpt: 170-172 °C. ^{1}H NMR (400 MHz): δ (DMSO-d_6): 2.66 (1H, dd, J = 14.4, J = 6.8 Hz, -C**Ha**Hb, C3); 2.71 (1H, dd, J = 14.4, J = 4.0 Hz, -CHa**Hb**, C3); 3.41 (1H, dd, J = 6.8, J = 4.0 Hz, –C**H**, C2); 5.67 (1H, s, -C**H**, C4); 7.28 (4H, m, C6,6',7,7', Ar); 7.49 (2H, m, C5,5', Ar); 7.66 (2H, m, C8,8', Ar). ^{13}C NMR (125 MHz): δ (DMSO-d_6): 33.30 (C3); 48.65 (C4); 54.17 (C2); 126.26-134.42 (12C, Ar); 168.40 (C1). Elemental analysis: Found: C, 60.36; H, 4.69; N4.20; S, 19.75 (Required for $C_{16}H_{15}NO_2S_2$: C, 60.54; H, 4.76; N, 4.41; S, 20.20). HRMS-ESI (+ve): Calculated $C_{16}H_{16}NO_2S_2$ (M+H) 318.0617, found 318.0623. IR: KBr disc, υ_{max} (cm^{-1}): 1617.29 (C=O stretch for carboxylic acid).

(*R*)-2-Amino-3-((9-phenyl-9*H*-xanthen-9-yl)thio)propanoic acid (173)
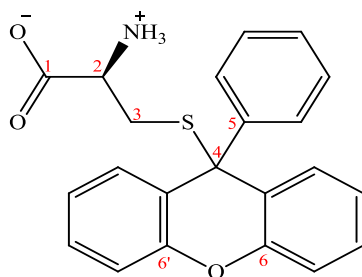
Using General Procedure D: 9-Phenyl-9*H*-xanthen-9-ol (**162**) (0.2743 g, 1 mmol) and L-cysteine (0.121 g, 1 mmol) gave compound **173** (0.3 g, 80 %) as a white powder. Mpt: 212-214 °C. ^{1}H NMR (400 MHz): δ (DMSO-d_6): 2.38 (1H, dd, J = 12.0, J = 10.0 Hz, –C**Ha**Hb, C3); 2.63 (1H, dd, J = 12.0 Hz, J = 4.0 Hz, -CHa**Hb**,C3); 2.83 (1H, dd, J = 9.6, J = 4.0 Hz, -C**H**, C2); 7.06 (2H, m, Ar); 7.17-7.38 (11H, m, Ar). The protons of the NH$_2$ and –OH were too broad to be observed. ^{13}C NMR (125 MHz): δ (DMSO-d_6): 32.29 (C3); 53.08 (C2); 55.15 (C4); 116.01-130.04 (15C, Ar); 145.32 (C5); 150.25 (2C, C6,6'); 167.86 (C1). Elemental analysis: Found: C, 70.02; H, 5.18; N, 3.28; S, 8.96 (Required for C$_{22}$H$_{19}$NO$_3$S: C, 70.0; H, 5.07; N, 3.71; S, 8.50). HRMS-ESI (+ve): Calculated C$_{22}$H$_{20}$NO$_3$S (M+H) 378.1158, found 378.1155. IR: KBr disc, $υ_{max}$ (cm^{-1}): 1629.45 (C=O stretch for carboxylic acid).

(*R*)-2-Amino-3-((9-phenyl-9*H*-thioxanthen-9-yl)thio) propanoic acid (175)
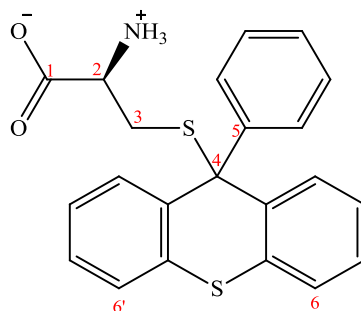
Using General Procedure D: 9-Phenyl-9*H*-thioxanthen-9-ol (**163**) (0.2904 g, 1 mmol) and L-cysteine (0.121 g, 1 mmol) gave compound **175** (0.22 g, 56 %) as a white powder. Mpt: 220-221 °C. ^{1}H NMR (400 MHz): δ(DMSO-d_6): 2.48 (1H, dd, J = 12.8 Hz J = 8.8 Hz, –C**Ha**Hb, C3); 2.60 (1H, dd, J = 12.8, J = 4.8 Hz, -CHa**Hb**, C3); 2.98 (1H, dd, J = 8.8, J = 4.8 Hz, -C**H**, C2); 7.21-7.36 (11H, m, Ar); 7.46 (2H, d, J = 7.6 Hz, C6,6', Ar). The protons of the NH$_2$ and –OH were too broad to be observed. ^{13}C NMR (125 MHz): δ(DMSO-d_6): 33.51 (C3); 53.12 (C2); 62.35 (C4); 126.59-132.09 (15C, Ar); 136.42 (2C, Ar); 142.44 (C5); 167.89 (C1). Elemental analysis: Found: C, 67.91; H, 5.02; N, 3.05; S, 16.03 (Required for $C_{22}H_{19}NO_2S_2$: C, 67.15; H, 4.87; N, 3.56; S16.30). HRMS-ESI (+ve): Calculated $C_{22}H_{20}NO_2S_2$ 394.0930, found 394.0933. IR: KBr disc, υ_{max} (cm^{-1}): 1633.18 (C=O stretch for carboxylic acid).

(*R*)-2-Amino-3-((9-benzyl-9*H*-xanthen-9-yl)thio)propanoic acid (177)
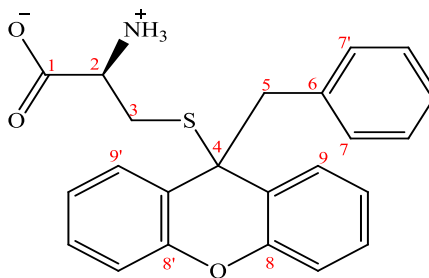
Using General Procedure D: 9-Benzyl-9*H*-xanthen-9-ol (**164**) (0.2904 g, 1 mmol) and L-cysteine (0.121 g, 1 mmol) gave compound **177** (0.33 g, 84 %) as a pale yellow powder. Mpt: 187-188 °C. ^{1}H NMR (400 MHz): δ (DMSO-d_6): 2.29 (1H, dd, *J* = 12.8, *J* = 10.0 Hz, –C**Ha**Hb**,** C3); 2.56 (1H, dd, *J* = 12.8, *J* = 4.4 Hz, -CHa**Hb,** C3); 2.79 (1H, dd, *J* = 9.6, *J* = 4.4 Hz, –C**H**, C2); 3.40 (2H, s, -C**H₂**, C5); 6.30 (2H, d, *J* = 7.6 Hz, C7,7'); 6.83-7.28 (9H, m, Ar); 7.94 (1H, d, *J* = 7.6 Hz, C9, Ar); 8.02 (1H, d, *J* = 7.6 Hz, C9', Ar). ^{13}C NMR (125 MHz): δ (DMSO-d_6): 32.24 (C3); 51.39 (C5); 53.49 (C2); 53.84 (C4); 116.01-130.26 (15C, Ar); 136.24 (C6); 150.67 (2C, C8,8'); 168.46 (C1). Elemental analysis: Found: C, 70.74; H, 5.57; N, 3.30; S, 7.95 (Required for $C_{23}H_{21}NO_3S$: C, 70.56; H, 5.41; N, 3.58; S, 8.19). HRMS-ESI (+ve): Calculated $C_{23}H_{22}NO_3S$ (M+H) 392.1315, found 392.1319. IR: KBr disc, $υ_{max}$ (cm^{-1}): 1629.47 (C=O stretch for carboxylic acid).

(*R*)-2-Amino-3-((9-benzyl-9*H*-thioxanthen-9-yl)thio)propanoic acid (179)
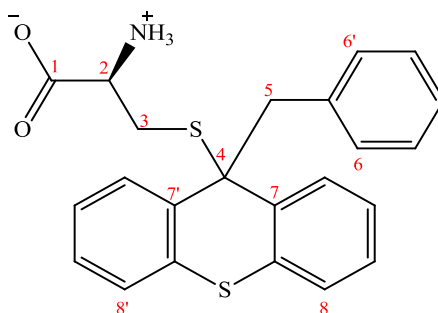
Using General Procedure D: 9-Benzyl-9*H*-thioxanthen-9-ol (**165**) (0.3044 g, 1 mmol) and L-cysteine (0.121 g, 1 mmol) gave compound **179** (0.037g, 9 %) as a white powder. Mpt: 190-192 °C. ^{1}H NMR (400 MHz): δ (DMSO-d_6): 2.32 (1H, dd, *J* = 12.8, *J* = 8.4 Hz, -C**Ha**Hb, C3); 2.52 (1H, dd, *J* = 12.8, *J* = 4.8 Hz, -CHa**Hb**, C3); 3.08 (1H, dd, *J* = 8.8, J = 4.4 Hz, –C**H**, C2); 3.43 (2H, s, -C**H₂**, C5); 6.44 (2H, d, J = 7.6 Hz, C6,6'); 6.96-7.30(9H, m, Ar); 8.06 (2H, m, C8,8', Ar). ^{13}C NMR (125 MHz): δ (DMSO-d_6): 31.19 (C3); 46.84(C5); 46.92 (C4); 53.31 (C2); 125.13-134.5 (15C, Ar); 135.25-145.30 (3C, C6, 6', 5); 167.50 (C1). Elemental analysis: Found: C, 66.96; H, 5.04; N 2.95; S, 15.43 (Required for $C_{23}H_{21}NO_2S_2.1/2H_2O$: C, 66.32; H, 5.32; N, 3.36; S, 15.40). HRMS-ESI (+ve): Calculated for $C_{23}H_{22}NO_2S_2$ (M+H) 408.1086, found 408.1088. IR: KBr disc, $υ_{max}$ (cm^{-1}): 1633.44 (C=O stretch for carboxylic acid).

(*R*)-2-Amino-3-((9-benzyl-9*H*-fluoren-9-yl)thio)propanoic acid (181)
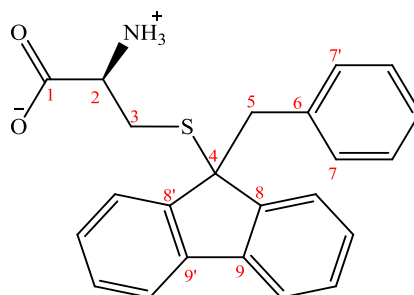
Using General Procedure D: 9-Benzyl-9*H*-fluoren-9-ol (**168**) (0.136 g, 0.5 mmol) and L-cysteine (0.062 g, 0.5 mmol) gave compound **181** (0.1 g, 53 %) as a white powder. Mpt: 195-197 °C. ^{1}H NMR (400 MHz): δ (DMSO-d_6): 2.09 (1H, dd, J = 12.6, J = 10.4 Hz , -C**Ha**Hb, C3); 2.34 (1H, dd, J = 12.8, J = 3.6 Hz, –CHa**Hb**, C3); 2.69 (1H, dd, J = 10.0, J = 4.0, –C**H**, C2); 3.54 (2H, s, -C**H$_2$**, C5); 6.61 (2H, d, J = 7.6 Hz, C7,7'); 7.30-7.50 (11H, m, Ar). ^{13}C NMR (125 MHz): δ (DMSO-d_6): 30.64 (C3); 43.42 (C5); 53.39 (C2); 59.91 (C4); 119.92-129.90 (13C, Ar); 135.5 (C6); 139.55 (2C, C9,9'); 146.65 (2C, C8,8'); 167.90 (C1). Elemental analysis: Found: C, 72.97; H, 5.27; N, 3.65; S, 8.49 (Required for $C_{23}H_{21}NO_2S$: C, 73.57; H, 5.64; N, 3.73; S, 8.54). HRMS-ESI (+ve): Calculated for $C_{23}H_{22}NO_2S$ (M+H) 376.1293, found 376.1400. IR: KBr disc, υ_{max} (cm^{-1}): 1635.74 (C=O stretch for carboxylic acid).

(*E/Z*)-(*R*)-2-Amino-3-((1,1,3-triphenylallyl)thio)propanoic acid (188)
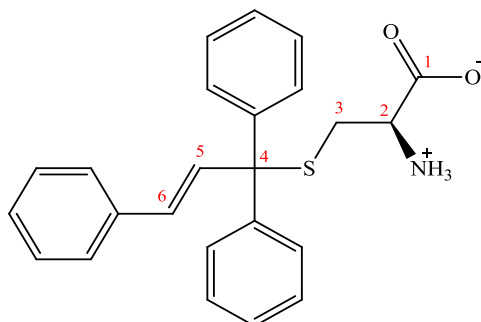
Using General Procedure D: (E)-1,1,3-Triphenylprop-2-en-1-ol (**186**) (0.07 g, 0.24 mmol) and L-cysteine (0.030 g, 0.24 mmol) gave compound **188** (: 0.70 g, 75 % mixture of *E/Z* isomers) as a white powder. Mpt: 132-134 °C. ^{1}H NMR (400 MHz): δ (CD$_3$OD): 2.62-353 (3H, m, C2,3); 4.65-4.67(1H, d, *J* = 10.8 Hz, =C**H**, C5); 6.39-6.42 (1H, d, *J* = 10.8 , =C**H** , C6); 7.18-7.45 (15H, m, Ar). ^{13}C NMR (125 MHz): δ (CD$_3$OD): 32.71 (C3); 48.82 (C2); 53.70 (C4); 126.35-143.40 (18C, Ar); 170.125(C1). Elemental analysis: Found: C, 74.20; H, 5.95; N, 2.93; S, 8.33 (Required for C$_{24}$H$_{23}$NO$_2$S: C, 74.00; H, 5.95; N, 3.60; S, 8.23). HRMS-ESI (+ve): Calculated for C$_{24}$H$_{24}$NO$_2$S (M+H) 390.1522, found 390.1519. IR: KBr disc, υ$_{max}$ (cm^{-1}): 1636.3 (C=O stretch for carboxylic acid).

(*R*)-2-Amino-3-((1,1,3-triphenylpropyl)thio)propanoic acid (189)
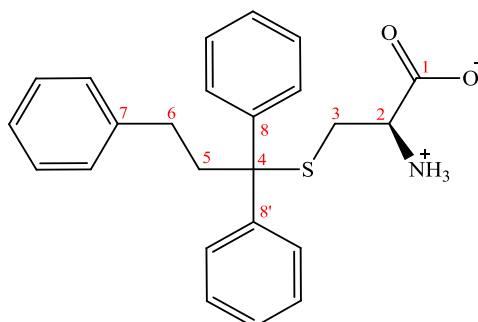
Using General Procedure D: 1,1,3-Triphenylpropan-1-ol (**187**) (0.422 g, 1.46 mmol) and L-cysteine (0.176 g, 1.46 mmol) gave compound **189** (0.25 g, 46 %) as a white powder. Mpt: 170-172 °C. ^{1}H NMR (400 MHz): δ (CD$_3$OD): 2.38-2.47 (2H, m, -**CH$_2$**, C6); 2.59-2.71 (3H, m, -C**Ha**Hb, C3 **and** –**CH$_2$**, C5); 2.85-2.89 (1H, dd, *J* = 13.6, *J* = 3.6 Hz, -C**Ha**Hb, C3); 3.01-3.05 (1H, dd, *J* = 9.6, *J* = 3.6 Hz, -C**H**, C2**);** 7.07-7.47 (15H, m, Ar). ^{13}C NMR (125 MHz): δ (CD$_3$OD): 32.71 (C6); 33.78 (C5); 44.56 (C3); 56.32 (C2); 63.08 (C4); 127.99-130.86 (15C, Ar); 144.41 (C7); 147.27 (2C, C8,8'); 173.33 (C1). Elemental analysis: Found: C, 73.29; H, 6.03; N, 3.07; S, 8.02 (Required for C$_{24}$H$_{25}$NO$_2$S: C, 73.62; H, 6.44; N, 3.58; S, 8.19). HRMS-ESI (+ve): Calculated for C$_{24}$H$_{26}$NO$_2$S (M+H) 392.1679, found 392.1676. IR: KBr disc, $υ_{max}$ (cm^{-1}): 1628.9 (C=O stretch for carboxylic acid).

4.4.3 Synthesis of cysteamine analogues

4.4.3.1 General Procedure E: Preparation of cysteamine derivatives using trifluoroacetic acid (TFA).[164, 165] The requisite tertiary alcohol (35 mmol) was added gradually to a mixture of trifluoroacetic acid (10 mL) and cysteamine hydrochloride (35 mmol). The mixture was allowed to stir for 1h and water (400 mL) was added to the mixture and the pH was adjusted to pH (10) with triethylamine. The resulting precipitate was filtered, washed with aqueous triethylamine and dried in an oven (40 °C for 24 h). The dried white precipitate was dissolved in acetonitrile (250 mL) and concentrated hydrochloric acid was to it then immediately diethyl ether (2

litres) was added to the solution to precipitate crystals of the pure hydrochloride salt. The product was filtered, washed with diethyl ether and dried in a vacuum oven (40 °C for 24 h) to give the desired cysteamine derivative.

2-(Benzhydrylthio)ethanamine hydrochloride (134)
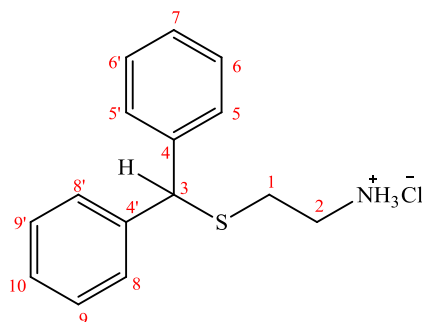
Using General Procedure E: Diphenylmethanol (1.62 g, 8.8 mmol) and cysteamine hydrochloride (1 g, 8.8 mmol) gave compound **134** (2 g, 81 %) as white crystals. Mpt: 110-115 °C. ^{1}H NMR (400 MHz): δ (DMSO-d_6): 2.56 (2H, t, J = 8 Hz, -C**H$_2$**, C1); 2.94 (2H, t, J = 7.6 -C**H$_2$**, C2); 5.15 (1H, s, -C**H**, C3); 7.24 (2H, t, J = 7.6 Hz, C7,10, Ar); 7.360 (4H, t, J = 8.0 Hz,C6,6'9,9', Ar); 7.49 (4H, d, J = 8.0 Hz, C5,5',8,8'Ar). ^{13}C NMR (125 MHz): δ (DMSO-d_6): 28.59 (C1); 38.0 (C2); 51.98 (C3); 127.2-128.58 (10C, Ar); 141.26 (2C, C4.4'). Elemental analysis: Found: C, 62.80; H, 6.54; N, 4.85; Cl, 12.89; S, 10.87(Required for $C_{15}H_{18}ClNS.1/2H_2O$: C, 62.37; H, 6.63; Cl, 12.27; N, 4.85; S, 11.10). HRMS-ESI (+ve): Calculated for $C_{15}H_{18}NS$ (M+H) 244.1154, found 244.1155.

Table 4.2: Crystal data and structure refinement for 134

Empirical formula	$C_{15}H_{18}ClNS$
Formula weight	279.8
Temperature	123(2)K
Wavelength	0.71073 Å
Crystal system	Monoclinic
Space group	$P2_1/n$
Unit cell dimensions	a = 5.9530(4) Å
	b = 14.1200(10) Å
	c = 17.0680(12) Å
	α= 90°.
	β= 96.539(4)°.
	γ = 90°.
Volume	1425.34(7) Å^3
Z	4
Density (calculated)	1.30 Mg/m^3
Absorption coefficient	0.397 mm^{-1}
F(000)	591.9
Crystal size	0.06 x 0.06 x 0.2 mm^3
Theta range for data collection	1.9 to 34.2°.
Index ranges	-9<=h<=6, -22<=k<=22, -26<=l<=26
Reflections collected	26400
Independent reflections	5840 [R(int) = 0.053]
Completeness to theta = 34.2°	99.3 %
Absorption correction	Semi-empirical from equivalents
Max. and min. transmission	0.6890 and 0.7467
Refinement method	Full-matrix least-squares on F^2
Data / restraints / parameters	5840 / 0 / 175
Goodness-of-fit on F^2	1.026
Final R indices [I>2sigma(I)]	R1 = 0.042, wR2 = 0.087
R indices (all data)	R1 = 0.081, wR2 = 0.099
Largest diff. peak and hole	0.449 and -0.262 e.Å^{-3}

2-((1,1-Diphenylethyl)thio)ethanamine hydrochloride (135)
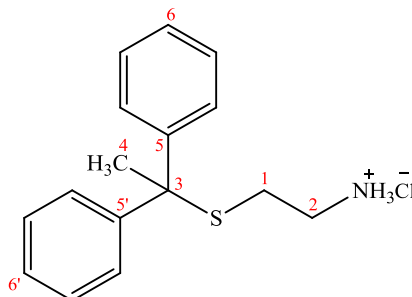
Using General Procedure E: Diphenylethanol (1.74 g, 8.8 mmol) and cysteamine hydrochloride (1 g, 8.8 mmol) gave compound **135** (1.27g, 49%) as white crystals. Mpt: 151-152 °C. ^{1}H NMR (400 MHz): δ (DMSO-d_6): 2.08 (3H, s, -C**H$_3$**, C4); 2.57 (2H, t, J = 7.2 Hz, -C**H$_2$**, C1); 2.70 (2H, t, J = 7.2 Hz, -C**H$_2$**, C2); 7.26 (2H, t, J = 7.2 Hz, C6,6', Ar); 7.34-7.41 (8H, m, Ar). ^{13}C NMR (125 MHz): δ (DMSO-d_6): 26.87 (C4); 29.69 (C1); 38.6 (C2); 56.35 (C3); 126.80-128.20 (10C, Ar); 145.49 (2C, C5,5'). Elemental analysis: Found: C, 65.15; H, 7.08; N, 5.13; Cl, 11.89; S, 11.02 (Required for $C_{16}H_{20}ClNS$: C, 65.40; H, 6.86; N, 4.77; Cl, 12.06; S, 10.91). HRMS-ESI (+ve): Calculated for $C_{16}H_{20}NS$ (M+H) 258.1311, found 258.1309.

Table 4.3: Crystal data and structure refinement for 135

Empirical formula	$C_{16}H_{20}ClNS$
Formula weight	293.9
Temperature	123(2)K
Wavelength	0.71073 Å
Crystal system	Orthorhombic
Space group	$Pca2_1$
Unit cell dimensions	a = 10.0050(13) Å
	b = 16.1330(22) Å
	c = 9.4170(12) Å
	α= 90°.
	β= 90°.
	γ= 90°.
Volume	1520.00(3) $Å^3$
Z	4
Density (calculated)	1.28 Mg/m^3
Absorption coefficient	0.375 mm^{-1}
F(000)	623.9
Crystal size	0.05 x 0.2 x 0.3 mm^3
Theta range for data collection	2.4 to 36.3°.
Index ranges	-10<=h<=16, -19<=k<=26, -8<=l<=15
Reflections collected	18105
Independent reflections	5397 [R(int) = 0.063]
Completeness to theta= 36.3°	99.6 %
Absorption correction	Semi-empirical from equivalents
Max. and min. transmission	0.6257 and 0.7471
Refinement method	Full-matrix least-squares on F^2
Data / restraints / parameters	5397 / 0 / 185
Goodness-of-fit on F^2	0.995
Final R indices	[I>2sigma(I)] R1 = 0.047, wR2 =
R indices (all data)	R1 = 0.134, wR2 = 0.082
Largest diff. peak and hole	0.387 and -0.455 e.$Å^{-3}$

2-(Tritylthio)ethanamine hydrochloride (137)
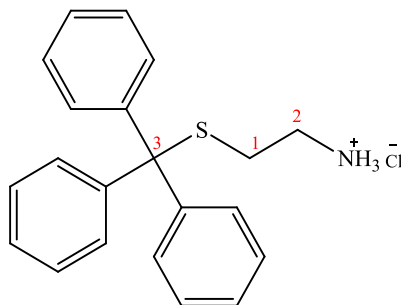
Using General Procedure E: Trityl alcohol (9.11 g, 35 mmol) and cysteamine hydrochloride (3.955 g, 35 mmol) gave compound **137** (7.5 g, 60 %) as white crystals. Mpt: 112-110 °C (literature: 94-97 °C).[136] ^{1}H NMR (400 MHz): δ (CD$_3$OD): 2.46 (2H, t, J = 7.6 Hz, -C**H$_2$**, C1); 2.58 (2H, t, J = 7.6 Hz, -C**H$_2$**, C2); 7.22-7.44 (15, m, Ar). ^{13}C NMR (125 MHz): δ (CD$_3$OD): 28.73 (C2); 38.26 (C1); 67.08 (C3); 126.01-144.03 (18C Ar). Elemental analysis: Found: C, 67.22; H, 6.56; N, 3.85; Cl, 9.78; S, 8.78 (Required for C$_{21}$H$_{22}$ClNS.H$_2$O C, 67.45; H, 6.47; N, 3.75; Cl, 9.48; S, 8.57). HRMS-ESI (+ve): Calculated for C$_{21}$H$_{22}$NS (M+H) 320.1467, found 320.1468.

Table 4.4: Crystal data and structure refinement for 137

Empirical formula	$C_{21}H_{24}ClNOS$
Formula weight	373.9
Temperature	123(2)K
Wavelength	0.71073 Å
Crystal system	Orthorhombic
Space group	Iba2
Unit cell dimensions	a = 14.7884(11) Å
	b = 36.4225(34) Å
	c = 7.2889(6) Å
	$\alpha = 90°$.
	$\beta = 90°$.
	$\gamma = 90°$.
Volume	3926.02(6) $Å^3$
Z	8
Density (calculated)	1.27 Mg/m^3
Absorption coefficient	0.309 mm^{-1}
F(000)	1583.8
Crystal size	0.03 x 0.1 x 0.5 mm^3
Theta range for data collection	1.5 to 29.8°.
Index ranges	-20<=h<=19, -50<=k<=50, -6<=l<=10
Reflections collected	19757
Independent reflections	4872 [R(int) = 0.056]
Completeness to theta = 29.8°	99.8 %
Absorption correction	Semi-empirical from equivalents
Max. and min. transmission	0.6420 and 0.7463
Refinement method	Full-matrix least-squares on F^2
Data / restraints / parameters	4872 / 2 / 244
Goodness-of-fit on F^2	1.026
Final R indices [I>2sigma(I)]	R1 = 0.039, wR2 = 0.074
R indices (all data)	R1 = 0.061, wR2 = 0.082
Largest diff. peak and hole	0.285 and -0.266 e.$Å^{-3}$

4.4.3.2 Using General Procedure F: Preparation of cysteamine derivatives using boron trifluoride etherate. Cysteamine hydrochloride (54.24 mg, 0.48 mmol) and the requisite tertiary alcohol (0.48 mmol) were dissolved in acetic acid (0.5 mL). Boron trifluoride etherate (0.82 mmol) was then slowly added dropwise at 0 °C under a nitrogen atmosphere. The reaction mixture was stirred for 2h and 10 % aqueous sodium acetate (1.5 mL) was added followed by water (1.5 mL). The mixture was then neutralized by saturated aqueous sodium bicarbonate solution (10 mL), extracted with ethyl acetate (3 x 20 mL); the combined organic fractions were dried over anhydrous magnesium sulphate and evaporated under reduced pressure, the residue was then purified either by flash column chromatography [methanol: dichloromethane (10:90)] or by crystallisation through hydrochloride salt formation. The crystal salts were formed from the resulting oil by dissolving it in anhydrous diethyl ether (10 mL) and then adding etheral HCl (2 eq.) until the hydrochloride salt precipitated. The precipitate was filtered, washed with diethyl ether and dried in a vacuum oven (40 °C for 24 h) to give the desired cysteamine derivative.

2-((1,1,2-Triphenylethyl)thio)ethanamine tetrafluoroborate (121).
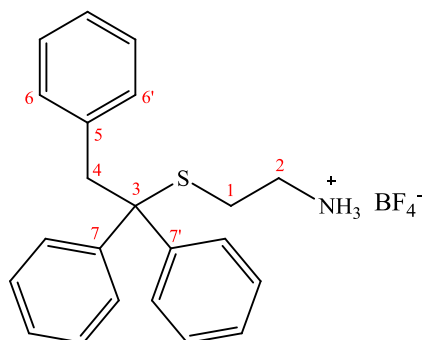
Using an adaptation of General Procedure F: 1,1,2-Triphenylethanol (**79**) (0.754 g, 2.75 mmol) and cysteamine hydrochloride (0.310 g, 2.75 mmol) were combined and after 2h the reaction mixture was extracted with ethyl acetate and the organic layer dried (MgSO$_4$). The organic layer was evaporated under reduced pressure to give compound **121** (0.335 g, 29 %) as a white powder after recrystallisation from diethyl ether. Mpt: 201-202 °C. ^{1}H NMR (400 MHz): δ (CD$_3$OD): 2.41 (2H, t, J = 7.6 Hz, -C**H$_2$**, C1); 2.57 (2H, t, J = 7.6 Hz, -C**H$_2$**, C2); 3.69 (2H, s, -C**H$_2$**, C4); 6.64

(2H, d, J = 7.6 Hz, C6, 6'); 6.98-7.33 (13H, m, Ar). ^{13}C NMR (125 MHz): δ (DMSO-d_6): 26.74 (C1); 38.45 (C2); 45.68 (C4); 61.81 (C3); 126.71-131.32 (15C Ar; 126.71, 127.49, 128.92, 13.32); 136.35 (C5); 144.14 (2C, C7,7'). Elemental analysis: Found: C, 61.18; H, 5.46; N, 3.36; S, 7.56 (Required for $C_{22}H_{24}BF_4NS.H_2O$: C, 61.41; H, 5.86; N, 3.26; S, 7.45). HRMS-ESI (+ve): Calculated for $C_{22}H_{24}NS$ (M+H) 334.1624, found 334.1618.

(±)-3-(1-((2-Aminoethyl)thio)-1,2-diphenylethyl)phenol (122)
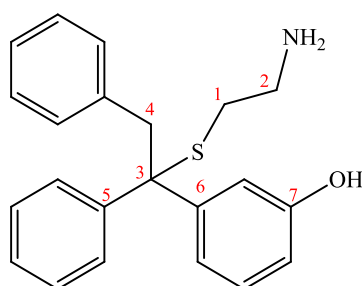
Using General Procedure F: 3-(1-Hydroxy-1,2-diphenylethyl)phenol (**85**) (0.150 g, 0.861 mmol) and cysteamine hydrochloride (0.097g, 0.861 mmol) gave compound **122** (0.030 g, 10 %) as a white solid after purification with flash column chromatography (Biotage SP4). Mpt: 160-161 °C. ^{1}H NMR (400 MHz): δ (CD$_3$OD): 2.44 (2H, t, J = 6.4 Hz, -C**H$_2$**, C1); 2.52 (2H, t, J = 6.4Hz, -C**H$_2$**, C2); 3.63 (2H, s, -C**H$_2$**, C4); 6.67 (3H, m, Ar); 6.79 (2H, m, Ar); 6.97-7.32 (9H, m, Ar). ^{13}C NMR (125 MHz): δ (CD3OD): 28.33 (C1); 39.2 (C2); 45.86 (C4); 61.43 (C4); 113.55-136.54 (15C, Ar); 144.56 (C6); 146.26 (C5); 156.82 (C7). Elemental analysis: Found: C, 76.86; H, 6.13; N, 3.94; S, 9.83 (Required for $C_{22}H_{23}NOS$ C, 75.61; H, 6.63; N, 4.01; S, 9.17). HRMS-ESI (-ve): Calculated for $C_{22}H_{22}NOS$ (M-H) 348.1428, found 348.1428. IR: KBr disc, υ_{max} (cm^{-1}): 3326.5 (OH phenol), 3457.2 (NH stretch for primary amine).

(±)-2-((1-(4-Hydroxyphenyl)-1,2-diphenylethyl)thio)ethanamine (123).
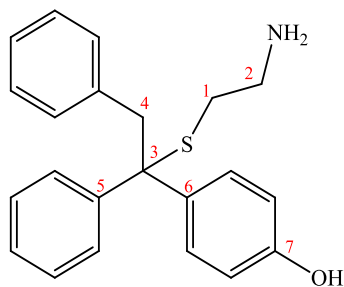
Using General Procedure F: 1-(4-Hydroxyphenyl)-1,2-diphenylethanol (**86**) (0.870 g, 3 mmol) and cysteamine hydrochloride (0.340 g, 3 mmol) gave compound **123** (0.1g, 10 %) as a pale yellow gum after purification with flash column chromatography (Biotage SP4). ^{1}H NMR (400 MHz): δ (CD$_3$OD): 2.40-2.43 (2H, t, J = 6.8 Hz, -**CH$_2$**, C1); 2.49-2.52 (2H, t, 6.8 Hz, -**CH$_2$**, C2); 3.61-3.62 (2H, d , J = 13.3 Hz, -**CH$_2$**, C4); 6.65-7.32 (14H, m, Ar). ^{13}C NMR (125 MHz): δ (CD$_3$OD): 28.33 (C1); 39.2 (C2); 45.86 (C4); 61.43 (C3); 113.55-136.65 (16C, Ar); 144.81 (C5); 156.82 (C7). HRMS-ESI (+ve): Calculated for C$_{22}$H$_{24}$NOS (M+H) 350.1573, found 350.1576. IR: KBr disc, υ_{max} (cm^{-1}): 3233.3 (OH phenol), 3399.8 (NH stretch for primary amine).

(±)-2-((1-(3-Chlorophenyl)-1,2-diphenylethyl)thio)ethanamine (124)
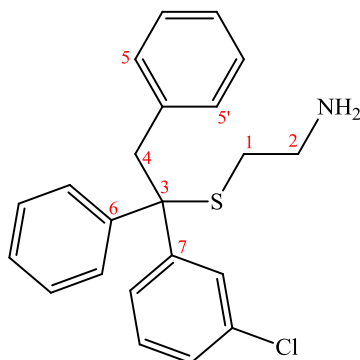
Using General Procedure F: 1-(3-Chlorophenyl)-1,2-diphenylethanol (**87**) (0.275 g, 0.89 mmol) and cysteamine hydrochloride (0.101g, 0.892 mmol) gave compound **124** (0.070 g, 21 %) as a pale yellow gum after purification with flash column chromatography (Biotage SP4). ^{1}H NMR (400 MHz): δ (CDCl$_3$): 1.80 (2H, s, N**H$_2$**); 2.38 (2H,t , J = 6.4 Hz, -C**H$_2$**, C1); 2.49 (2H, t, J = 6.8 Hz, -C**H$_2$**, C2); 3.39-3.62 (2H, d, J = 13.2 Hz, -C**H$_2$**, C4); 6.64 (2H, d, J = 7.2 Hz, C5,5'); 7.04-7.29 (12H, m, Ar). ^{13}C NMR (125 MHz): δ (CDCl$_3$): 32.05 (C1); 40.17 (C2); 46.60 (C4); 61.28 (C3); 126.69-135.95 (16C, Ar); 143.93 (1C, C7); 146.80 (1C, C6). Elemental analysis: Found: C, 68.65; H, 5.99; N, 3.64; Cl, 9.08; S, 8.43 (Required for C$_{22}$H$_{22}$ClNS. H$_2$O C, 68.46; H, 6.27; Cl, 9.19; N, 3.63; S, 8.31). HRMS-ESI (+ve): Calculated for C$_{22}$H$_{23}$ClNS 368.1234, found 368.1233. IR: KBr disc, υ_{max} (cm^{-1}): 3459.1 (NH stretch for primary amine).

(±)-2-((1-(4-Chlorophenyl)-1,2-diphenylethyl)thio)ethanamine (125)
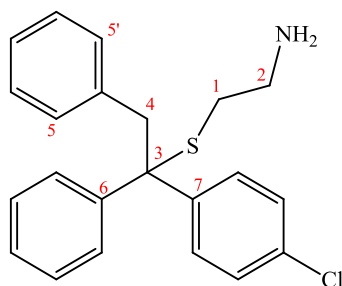
Using General Procedure F: 1-(4-Chlorophenyl)-1,2-diphenylethanol (**89**) (750 mg, 2.43 mmol) and cysteamine hydrochloride (274 mg, 2.43 mmol) gave compound **125** (0.15 g, 17 %) as a dark yellow gum after purification with flash column chromatography (Biotage SP4). ^{1}H NMR (400 MHz): δ (CDCl$_3$): 2.30 (2H, t, *J* = 6.8 Hz, -C**H$_2$**, C1); 2.55 (2H, t, *J* = 6.8 Hz, -C**H$_2$**, C1); 3.53-3.61 (2H, d, *J* = 13.2 Hz, -C**H$_2$**, C4); 2.27 (2H, s, -N**H$_2$**); 6.63 (2H, d, *J* = 7.6 Hz, C5, 5'); 7.04-7.27 (12H, m, Ar). ^{13}C NMR (125 MHz): δ (CDCl$_3$): 33.33 (C1); 40.69 (C2); 46.64 (C4); 60.98 (C3); 126.61-136.16 (16C Ar); 143.32 (C7); 144.34 (C6). Elemental analysis: Found: C, 66.24; H, 5.72; Cl, 8.65; N, 3.25; S, 8.53 (Required for C$_{22}$H$_{22}$ClNS.2 H$_2$O C, 65.41; H, 6.49; Cl, 8.78; N, 3.47; O, 7.92; S, 7.94). HRMS-ESI (+ve): Calculated for C$_{22}$H$_{23}$ClNS (M+H) 368.1234, found 368.1235. IR: ATR, υ$_{max}$ (cm^{-1}): 3545.5 (NH stretch for primary amine).

(±)-2-((1-(3,4-Dichlorophenyl)-1,2-diphenylethyl)thio)ethanamine (126).
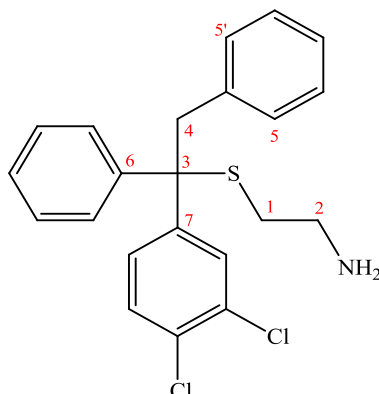
Using General Procedure F: 1-(3,4-Dichlorophenyl)-1,2-diphenylethanol (**90**) (1.4 g, 4 mmol) and cysteamine hydrochloride (0.454 g, 4 mmol) gave compound **126** (0.205g, 13 %) as a pale yellow gum after purification with flash column chromatography (Biotage SP4). ^{1}H NMR (400 MHz): δ (CDCl$_3$): 2.21 (2H, s, -N**H$_2$**); 2.30-2.2.34 (2H, t, J = 6.4 Hz, -C**H$_2$**, C1); 2.57-2.60 (2H, t, J = 6.4 Hz, -C**H$_2$**, C2); 3.52-3.60 (2H, s, -C**H$_2$**, C4); 6.63 (2H, d, J = 7.2 Hz, C5,5'); 7.06-7.39 (11H, m, Ar). ^{13}C NMR (125 MHz): δ (CDCl3): 33.26 (C1), 40.72 (C2); 46.53 (C4); 60.75 (C3) 127.42-135.81 (16C, Ar); 143.66 (C6) 145.27 (C7). Elemental analysis: Found: C, 65.31; H, 5.07; N, 3.07; Cl, 16.42; S, 7.53 (Required for C$_{22}$H$_{21}$Cl$_2$NS C, 65.67; H, 5.26; N, 3.48; Cl, 17.62; S, 7.79). HRMS-ESI (+ve): Calculated for C$_{22}$H$_{22}$Cl$_2$NS (M+H) 402.0845, found 402.0846. IR: ATR, υ$_{max}$ (cm^{-1}): 3449.6 (NH stretch for primary amine).

2-((1,1-Bis(4-chlorophenyl)-2-phenylethyl)thio)ethanamine (127)
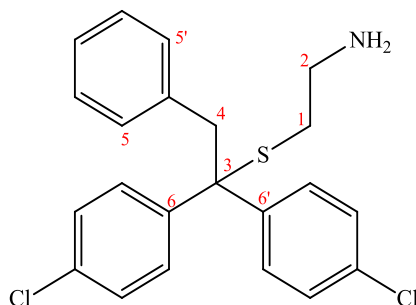
Using General Procedure F: 1,1-Bis(4-chlorophenyl)-2-phenylethanol (**91**) (0.342 g, 1 mmol) and cysteamine hydrochloride (0.113 g, 1 mmol) gave compound **127** (0.060 g, 20.4 %) as a white powder after purification with flash column chromatography (Biotage SP4). Mpt: 220-221 °C. ^{1}H NMR (400 MHz): δ (CD$_3$OD): 2.55-2.60 (4H, m, -C**H$_2$**, C1,2); 3.65 (2H, s, -C**H$_2$**, C4); 6.69 (2H, d, J = 7.2 Hz, 5,5'); 7.02-7.31 (11H, m, Ar). ^{13}C NMR (125 MHz): δ (CD$_3$OD): 26.90 (C1); 38.51 (C2); 45.60 (C4); 60.87 (C3); 126.34-135.85 (16C, Ar); 142.88 (2C, C6,6'). Elemental analysis: Found: C, 66.41; H, 4.58; N, 3.23; S, 7.35 (Required for C$_{22}$H$_{21}$Cl$_2$NS C, 65.67; H, 5.26; N, 3.48; S, 7.97). HRMS-ESI (+ve): Calculated for C$_{22}$H$_{22}$Cl$_2$NS (M+H) 402.0845, found 402.0841. IR: KBr disc, υ$_{max}$ (cm^{-1}): 3412.4 (NH stretch for primary amine).

(±)-2-((1-(3-Chlorophenyl)-1-(4-chlorophenyl)-2-phenylethyl)thio)ethanamine (128).
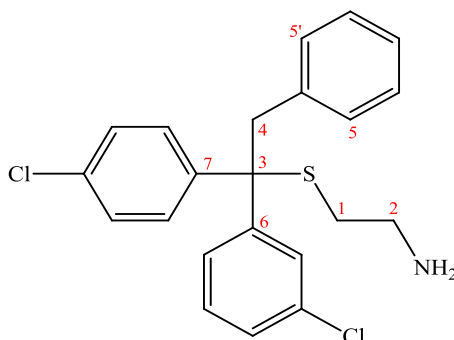
Using General Procedure F: 1-(3-Chlorophenyl)-1-(4-chlorophenyl)-2-phenylethanol (**92**) (0.519 g, 1.5 mmol) and cysteamine hydrochloride (0.170 g, 1.5 mmol) gave compound **128** (0.057 g, 9 %) as a pale yellow gum after purification with flash column chromatography (Biotage SP4). ^{1}H NMR (400 MHz): δ (CDCl$_3$): 2.38-2.60 (2H, t, J = 6.8 Hz, -C**H$_2$**, C1); 2.57-2.60 (2H, t, J = 6.8 Hz, -C**H$_2$**, C2), 3.54 (2H, s, -C**H$_2$**, C4); 3.65 (2H, s, -N**H$_2$**); 6.64 (2H, d, J = 7.6 Hz, C5,5'); 6.92-7.29 (11H, m, Ar). ^{13}C NMR (125 MHz): δ (CDCl$_3$): 32.91 (C1); 40.62 (C2); 46.53 (C4); 60.69 (C3); 127.28-135.69 (16C, Ar); 142.57 (C7); 146.22 (C6). Elemental analysis: Found: C, 65.08; H, 5.23; N, 3.02; Cl, 17.96; S, 7.24 (Required for C$_{22}$H$_{21}$Cl$_2$NS C, 65.67; H, 5.26; N, 3.48; Cl, 17.62; S, 7.79). HRMS-ESI (+ve): Calculated for C$_{22}$H$_{22}$Cl$_2$NS (M+H) 402.0845, found 402.0845. IR**:** KBr disc, υ$_{max}$ (cm^{-1}): 3434.6 (NH stretch for primary amine).

(±)-2-((1,2-Diphenyl-1-(p-tolyl)ethyl)thio)ethanamine (129)
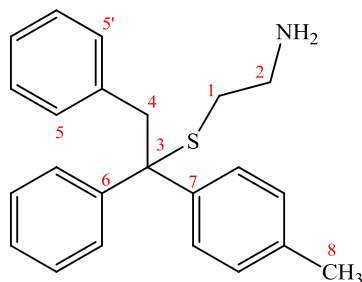
Using General Procedure F: 1-(4-Methylphenyl)-1,2-diphenylethanol (**93**) (0.205 g, 0.76 mmol) and cysteamine hydrochloride (0.086 g, 0.76 mmol) gave compound **129** (0.085 g, 18 %) as a brown gum after purification with flash column chromatography (Biotage SP4). ^{1}H NMR (400 MHz): δ (CDCl$_3$): 2.32 (3H, s, -C**H$_3$**, C8), 2.42-2.46 (4H, m, -C**H$_2$**, C1,2); 3.59 (2H, s, -C**H$_2$**, C4); 6.64 (2H,d, J = 7.2 Hz, C5,5'); 7.01-7.30 (12H, m, Ar). The protons of the NH$_2$ were too broad to be observed. ^{13}C NMR (125 MHz): δ (CDCl$_3$): 20.98 (C8); 31.20 (C1); 40.05 (C2); 46.71 (C4); 61.49 (C3); 127.12-136.74 (16C, Ar); 141.90 (C7); 144.48 (C6). Elemental analysis: Found: C, 75.87; H, 7.42; N, 3.07; S, 8.99 (Required for C$_{23}$H$_{25}$NS.H$_2$O C, 75.57; H, 7.45; N, 3.83; S, 8.77. HRMS-ESI (+ve): Calculated for C$_{23}$H$_{26}$NS (M+H) 348.1780, found 348.1781. IR: KBr disc, υ_{max} (cm^{-1}): 3434.8 (NH stretch for primary amine).

2-((2-Phenyl-1,1-di-p-tolylethyl)thio)ethanamine (130).
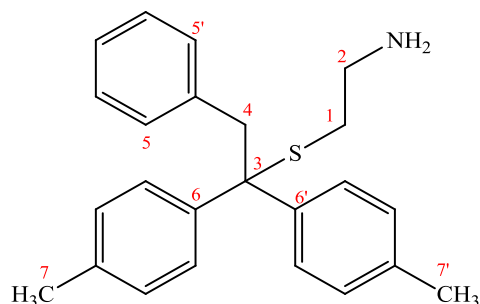
Using General Procedure F: 1,1-Bis(4-methylphenyl)-2-phenylethanol (**94**) (0.302 g, 1 mmol) and cysteamine hydrochloride (0.113 g, 1 mmol) gave compound **130** (0.030 g, 8 %) as a pale yellow gum after purification with flash column chromatography (Biotage SP4). ^{1}H NMR (400 MHz): δ (CDCl$_3$): 2.32(6H, s, -C**H$_3$**, C7,7'); 2.39 (2H, t, J = 5.6 Hz, -C**H$_2$**, C1); 2.45 (2H,t, J = 5.6 Hz, -C**H$_2$**, C2); 3.57 (2H,s ,-C**H$_2$**, C4); 3.98 (2H, s, N**H$_2$**); 6.61 (2H, d, J = 7.2 Hz, C5,5'); 7.02-.18 (11H, m, Ar). ^{13}C NMR (125 MHz): δ (CDCl3): 21.05 (2C, C7, 7'); 31.33 (C1); 40.09 (C2); 46.78 (C4); 61.35 (C3); 126.41-136.55 (16C, Ar); 141.60 (2C, C6, 6'). Elemental analysis: Found: C, 79.30; H, 7.82; N, 3.89; S, 8.70 (Required for C$_{24}$H$_{27}$NS C, 79.73; H, 7.53; N, 3.87; S, 8.87). HRMS-ESI (+ve): Calculated for C$_{24}$H$_{28}$NS (M+H) 362.1937, found 362.19343. IR: KBr disc, υ_{max} (cm^{-1}): 3412.4 (NH stretch for primary amine).

(±)-2-((1-(2-Fluorophenyl)-1,2-diphenylethyl)thio)ethanamine (131).
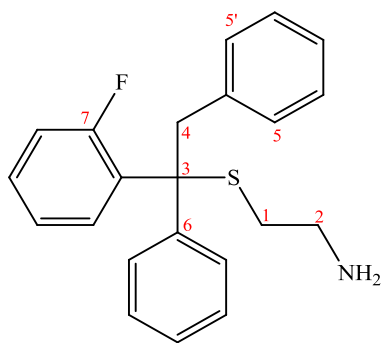
Using General Procedure F: 1-(2-Fluorophenyl)-1,2-diphenylethanol (**95**) (1 g, 3.42 mmol) and cysteamine hydrochloride (0.386 g, 3.42 mmol) gave compound **131** (0.143 g, 12 %) as a pale yellow gum after purification with flash column chromatography (Biotage SP4). ^{1}H NMR (400 MHz): δ (CDCl$_3$): 2.22-2.42 (4H, m, -C**H$_2$**, C1,2); 3.70 (2H, s, -N**H$_2$**); 3.72-3.83 (2H, d, J = 13.6 Hz, -C**H$_2$**, C4); 6.78 (2H, d, J = 7.2, C5,5'); 6.97-7.49 (12H, m, Ar). ^{13}C NMR (125 MHz): δ (CDCl$_3$): 31.84 (C1); 40.19 (C2); 44.59 (C4); 59.95 (C3); 116.12-136.41 (16C, Ar); 144.81 (C6); 160.69 (d, J_{CF} = 309.75, C7). Elemental analysis: Found: C, 75.72; H, 5.82; N, 3.50; S, 9.10 (Required for C$_{22}$H$_{22}$FNS, C, 75.18; H, 6.31; N, 3.99; S, 9.12). HRMS-ESI (+ve): Calculated for C$_{22}$H$_{23}$FNS (M+H) 352.1530, found 352.1530. IR: ATR, υ_{max} (cm^{-1}): 3410.4 (NH stretch for primary amine).

(±)-2-((1-(4-Fluorophenyl)-1,2-diphenylethyl)thio)ethanamine (132).
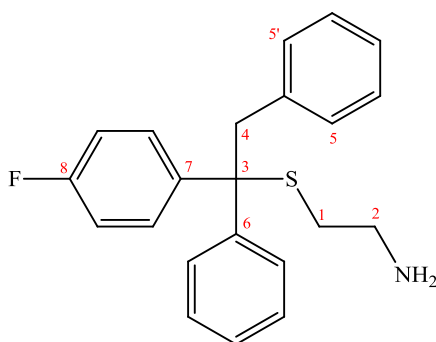
Using General Procedure F: 1-(4-Fluorophenyl)-1,2-diphenylethanol (**96**) (0.800 mg, 2.74 mmol) and cysteamine hydrochloride (0.310 g, 2.74 mmol) gave compound **132** (0.085 g, 9 %) as a pale yellow gum after purification with flash column chromatography (Biotage SP4). ^{1}H NMR (400 MHz): δ (CDCl$_3$): 1.94 (2H, s, -N**H$_2$**) 2.32-2.34 (2H, t, *J* = 6.4 Hz, -**CH$_2$**, C1); 2.52-2.56 (2H, t, *J* = 6.4 Hz, -**CH$_2$**, C2); 3.53-3.62 (2H, d, *J* = 13.2 Hz-, **CH$_2$**, C4); 6.63 (2H, d, *J* = 7.2 Hz, C5,5'); 6.91-7.32 (12H, m, Ar). ^{13}C NMR (125 MHz): δ (CDCl$_3$): 31.03 (C1); 40.90 (C2); 46.85 (C4); 60.91 (C3); 114.43-136.34 (15C, Ar); 140.48 (C7); 144.72 (C6); 161.51 (d, *J$_{CF}$* = 306.25, C8). Elemental analysis: Found: C, 71.58; H, 6.11; N, 3.91; S, 8.22 (Required for C$_{22}$H$_{22}$FNS.H$_2$O C, 71.51; H, 6.55; N, 3.79; S, 8.68). HRMS-ESI (+ve): Calculated for C$_{22}$H$_{23}$FNS (M+H) 352.1530, found 352.1526. IR: ATR, υ_{max} (cm^{-1}): 3395.4 (NH stretch for primary amine).

**2-((1,1-Bis(4-fluorophenyl)-2-phenylethyl)thio)ethanamine (133)**
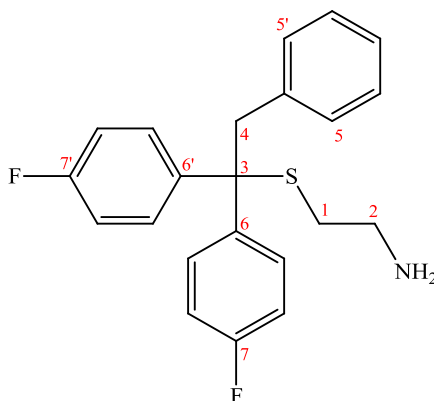
Using General Procedure F: 1,1-Bis(4-fluorophenyl)-2-phenylethanol (**97**) (1.09 g, 3.5 mmol) and cysteamine hydrochloride (0.398 g, 3.5 mmol) gave compound **133** (0.101 g, 8 %) as a pale yellow gum after purification with flash column chromatography (Biotage SP4). ^{1}H NMR (400 MHz): δ (CDCl$_3$): 1.47 (2H, s, -N**H$_2$**), 2.27-2.30 (2H, t, J = 6.8 Hz, -C**H$_2$**, C1); 2.58-2.61 (2H, t, J = 6.8 Hz, -C**H$_2$**, C2); 3.54 (2H, s, -C**H$_2$**, C4); 6.64 (2H, d, J = 7.6 Hz, C5,5'); 6.92-7.26 (11H, m, Ar). ^{13}C NMR (125 MHz): δ (CDCl$_3$): 33.89 (C1); 40.98 (C2); 46.94 (C4); 60.33 (C3); 114.54-136.13 (14C, Ar); 140.46 (2C, C6,6'); 161.55 (d, J_{CF} = 307.25, C7,7'). Elemental analysis: Found: C, 70.85; H, 5.33; N, 3.46; S, 8.32 (Required for C$_{22}$H$_{21}$F$_2$NS, C, 71.52; H, 5.73; N, 3.79; S, 8.68). HRMS-ESI (+ve): Calculated for C$_{22}$H$_{22}$F$_2$NS (M+H) 370.1436, found 370.1432. IR: ATR, $υ_{max}$ (cm^{-1}): 3420.5 (NH stretch for primary amine).

2-((2-Methyl-1,1-diphenylpropyl)thio)ethanamine hydrochloride (136)
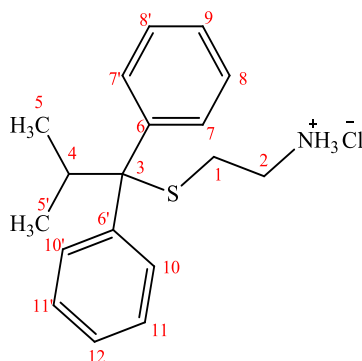
Using General Procedure F: 2-Methyl-1,1-diphenylpropan-1-ol (**84**) (1 g, 4 mmol) and cysteamine hydrochloride (0.354 g, 4.0 mmol) gave compound **136** (0.56 g, 44 %) as a white powder after crystallisation as the corresponding hydrochloride salt. Mpt: 208-209 °C. ^{1}H NMR (400 MHz): δ (CD$_3$OD): 1.12 (6H, d, *J* = 6.8 Hz, -CH$_3$, C5,5'); 1.51 (2H, t, *J* = 7.6 Hz, -CH$_2$, C1); 1.62 (2H, t, *J* = 7.6 Hz, -CH$_2$, C2); (1H, hept, *J* = 6.8 Hz, -CH, C4); 6.48 (2H, t, *J* = 7.2 Hz, C9,12, Ar); 6.56 (4H, t, *J* = 8.0 Hz, C8,8',11,11', Ar); 6.68 (4H, d, *J* = 8.0 Hz, C7,7', 10,10', Ar). ^{13}C NMR (125 MHz): δ (DMSO-d_6): 18.78 (2C, C5,5'); 26.28 (C1); 33.27 (C4); 37.90 (C2); 65.79 (C3); 126.90-129.58 (10C, Ar); 140.85 (2C, C6,6'). Elemental analysis: Found: C, 67.37; H, 7.67; N, 4.08; Cl, 10.93; S, 9.35 (Required for C$_{18}$H$_{24}$ClNS: C, 67.16; H, 7.51; N, 4.35; Cl, 11.01; S, 9.96). HRMS-ESI (+ve): Calculated for C$_{18}$H$_{24}$NS (M+H) 286.1624, found 286.1624.

Table 4.5: Crystal data and structure refinement for 136

Empirical formula	$C_{18}H_{24}ClNS$
Formula weight	321.9
Temperature	123(2)K
Wavelength	0.71073 Å
Crystal system	Orthorhombic
Space group	Iba2
Unit cell dimensions	a = 10.5820(3) Å
	b = 18.3920(6) Å
	c = 9.1110(3) Å
	α= 90°.
	β= 90°.
	γ = 90°.
Volume	1773.22(1) $Å^3$
Z	4
Density (calculated)	1.21 Mg/m^3
Absorption coefficient	0.327 mm^{-1}
F(000)	687.9
Crystal size	0.05 x 0.2 x 0.7 mm^3
Theta range for data collection	2.2 to 30.5°.
Index ranges	-15<=h<=8, -22<=k<=26, -13<=l<=10
Reflections collected	13037
Independent reflections	4837 [R(int) = 0.024]
Completeness to theta = 30.5°	99.5 %
Absorption correction	Semi-empirical from equivalents
Max. and min. transmission	0.6501 and 0.7461
Refinement method	Full-matrix least-squares on F^2
Data / restraints / parameters	4837 / 1 / 202
Goodness-of-fit on F^2	1.038
Final R indices [I>2sigma(I)]	R1 = 0.027, wR2 = 0.064
R indices (all data)	R1 = 0.032, wR2 = 0.067
Largest diff. peak and hole	0.298 and -0.165 e.$Å^{-3}$

2-((Diphenyl(pyridin-4-yl)methyl)thio)ethanamine di tetrafloriborate (138)
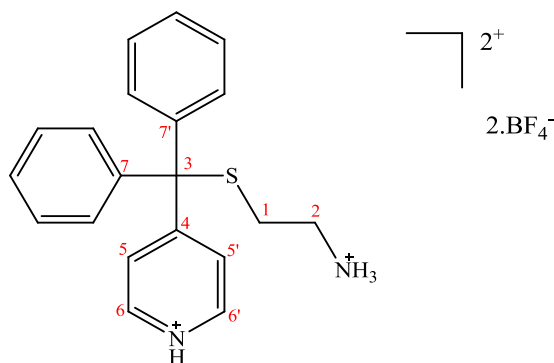
Using an adaptation of General Procedure F: Diphenyl(pyridin-4-yl)methanol (**83**) (0.522 g, 2.75 mmol) and cysteamine hydrochloride (0.310 mg, 2.75 mmol) were combined and after 2h the reaction mixture was extracted with ethyl acetate and the organic layer dried ($MgSO_4$). The organic layer was evaporated under reduced pressure to give compound **138** (0.2 g, 18 %) as a white powder after recrystallisation from diethyl ether. Mpt: 178-180 ºC. ^{1}H NMR (400 MHz): δ (DMSO-d_6): 2.38 (2H, t, J = 8.4 Hz, -C**H$_2$**, C1); 2.60 (2H, t, J = 8.0 Hz, -C**H$_2$**, C2); 7.30-7.42 (12H, m, Ar); 8.58 (2H, d, J = 5.2 Hz, C6, 6'). ^{13}C NMR (125 MHz): δ (DMSO-d_6): 29.09 (C1); 37.92 (C2); 79.15 (C3); 123.83-128.88 (13C, Ar); 142.71 (2C, C6, 6'); 149.77 (2C, C7,7'); 152.52 (C4). Elemental analysis: Found: C, 48.40; H, 4.82; N, 6.16; S, 6.51 (Required for $C_{20}H_{20}B_2F_8N_2S_2$ C, 48.42; H, 4.47; N, 5.65; S, 6.46). HRMS-ESI (+ve): Calculated for $C_{20}H_{21}N_2S$ 321.1420, found 321.1416.

2-((2-Aminoethyl)thio)-1,2,2-triphenylethanone (140)
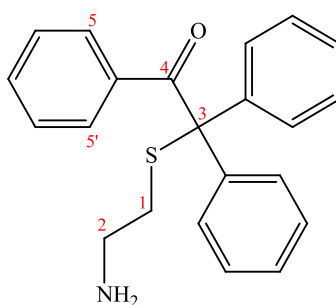
Using General Procedure F: 2-Hydroxy-1,2,2-triphenylethanone (**139**) (0.1584 g, 0.75 mmol) and cysteamine hydrochloride (0.085 g, 0.75 mmol) gave compound **140** (0.1 g, 41 %) as a yellow gum after purification with flash column chromatography (Biotage SP4). ^{1}H NMR (400 MHz): δ (CDCl$_3$): 2.41 (2H, t, J = 6.0 Hz, -**CH$_2$**, C1); 2.81 (2H, t, J = 6.0 Hz, -**CH$_2$**, C2); 6.21 (2H, s, -N**H$_2$**); 7.14-7.49 (13H, m, Ar); 7.64-7.66 (2H, C5,5'). ^{13}C NMR (125 MHz): δ (CDCl3): 25.46 (C1); 39.03 (C2); 48.96 (C3); 127.26-142.02 (18C, Ar); 198.65 (C1). Elemental analysis: Found: C, 76.80; H, 6.08; N, 4.32; S, 8.89 (Required for C$_{22}$H$_{21}$NOS C, 76.04; H, 6.09; N, 4.03; S, 9.23). HRMS-ESI (+ve): Calculated for C$_{22}$H$_{22}$NOS (M+H) 348.1417, found 348.1408. IR: KBr disc, υ_{max} (cm^{-1}): 1684.8 (C=O stretch for ketone), 3434.6 (NH stretch for primary amine).

2-((9*H***-Xanthen-9-yl)thio)ethanaminium chloride hydrochloride (170)**
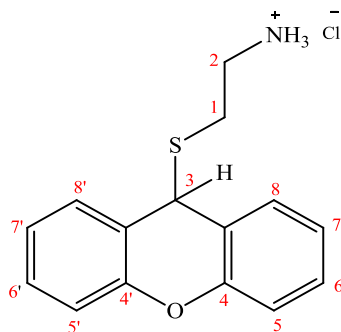
Using General Procedure F: 9*H*-Xanthen-9-ol (**166**) (0.198 g, 1 mmol) and cysteamine hydrochloride (0.113 g, 1 mmol) gave compound **170** (0.070 g, 24 %) as a white powder after crystallisation as the corresponding hydrochloride salt. Mpt: 194-196 °C. ^{1}H NMR (400 MHz): δ (CD$_3$OD): 2.56 (2H, t, *J* = 7.2 Hz, -C**H$_2$**, C1); 2.67 (2H, t, *J* = 7.2 Hz, -C**H$_2$**, C2); 5.49 (1H, s, -C**H**, C3); 7.11-7.20 (4H, m, C5,5' and C6,6'); 7.32 (2H, t, *J* = 7.6.0 Hz, C7,7'); 7.49 (2H, d, *J* = 7.6 Hz, C8,8'). ^{13}C NMR (125 MHz): δ (DMSO-*d$_6$*): 27.2 (C1); 38.79 (C2); 40.69 (C3); 116.28-130.0 (10C, Ar); 152.22 (2C, C4,4'). Elemental analysis: Found: C, 60.56; H, 5.47; N4.67; Cl, 11.95; S, 10.88 (Required for C$_{15}$H$_{16}$ClNOS: C, 61.32; H, 5.49; N, 4.77; Cl, 12.07; S, 10.91). HRMS-ESI (+ve): Calculated for C$_{15}$H$_{16}$NOS (M+H) 258.0947, found 258.0951.

2-((9H-Thioxanthen-9-yl)thio)ethanaminium chloride hydrochloride (172)
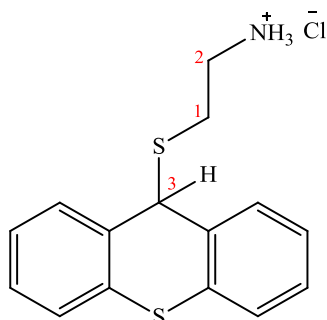
Using General Procedure F: 9*H*-Thioxanthen-9-ol (**167**) (0.198 g, 1 mmol) and cysteamine hydrochloride (0.113 g, 1 mmol) gave compound **172** (0.16 g, 52 %) as a white powder after crystallisation as the corresponding hydrochloride salt. Mpt: 222-224 °C. ^{1}H NMR (400 MHz): δ (CD$_3$OD): 2.59 (2H, t, *J* = 6.8 Hz, -C**H$_2$**, C1); 2.84 (2H, t, *J* = 6.8 Hz, -C**H$_2$**, C2); 5.56 (1H, s, -C**H**, C3); 7.28-7.31 (2H, m, Ar); 7.44-7.48 (6H, m, Ar). ^{13}C NMR (125 MHz): δ (DMSO-*d$_6$*): 28.40 (C1); 39.50 (C2); 48.72 (C3); 127.19-137.75 (12C, Ar). Elemental analysis: Found: C, 60.42; H, 4.95; N,3.56; Cl, 10.99; S, 19.80 (Required for C$_{15}$H$_{16}$ClNOS: C, 58.14; H, 5.20; N, 4.52; Cl, 11.44; S, 20.70). HRMS-ESI (+ve): Calculated for C$_{15}$H$_{16}$NS$_2$ (M+H) 274.0719, found 274.0724.

2-((9-Phenyl-9H-xanthen-9-yl)thio)ethanaminium chloride hydrochloride (174)
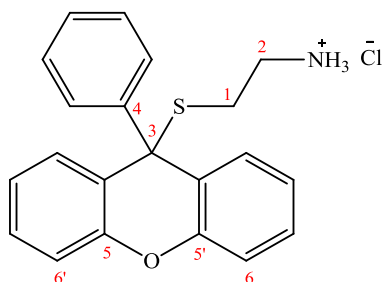
Using General Procedure F: 9-Phenyl-9*H*-xanthen-9-ol (**162**) (0.274 g, 1 mmol) and cysteamine hydrochloride (0.113 g, 1 mmol) gave compound **174** (0.160 g, 43 %) as a red powder after crystallisation as the corresponding hydrochloride salt. Mpt: 135-136 °C. ^{1}H NMR (400 MHz): δ (DMSO-d_6): 2.35 (2H, t, J = 6.0 Hz, -C**H$_2$**, C1); 2.52 (2H, t, J = 6.4 Hz, -C**H$_2$**, C2); 5.10 (2H, s, -N**H$_2$**); 6.94 (2H, t, J = 7.6 H, Ar); 7.06- 7.30 (9H, m, Ar); 7.51 (2H, d, J = 7.6 Hz, C6,6', Ar). ^{13}C NMR (125 MHz): δ (DMSO-d_6): 27.18 (C1); 37.78 (C2); 55.34 (C3); 116.45-128.99 (15C, Ar); 145.78 (C4); 150.13 (2C, C5,5'). Elemental analysis: Found: C, 67.03; H, 5.47; N, 3.42; Cl, 9.30; S, 9.05 (Required for $C_{21}H_{20}ClNOS$ C, 68.19; H, 5.45; N, 3.79; Cl, 9.58; S8.67).   HRMS-ESI (+ve): Calculated for $C_{21}H_{20}NOS$ (M+H) 334.1260, found 334.1263.

2-((9-Phenyl-9*H*-thioxanthen-9-yl)thio)ethanaminium   chloride   hydrochloride (176)
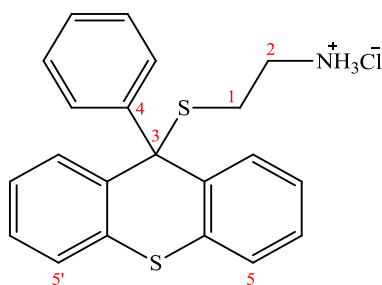
Using General Procedure F: 9-Phenyl-9*H*-thioxanthen-9-ol (**163**) (0.290 g, 1 mmol) and cysteamine hydrochloride (0.113 g, 1 mmol) gave compound **176** (0.240 g, 62 %) as a red powder after crystallisation as the corresponding hydrochloride salt. Mpt: 80-81°C. ^{1}H NMR (400 MHz): δ (DMSO-d_6): 2.07 (2H, t, J = 6.4 Hz, -C**H$_2$**, C1); 2.62 (2H, t, J = 6.4 Hz, -C**H$_2$**, C2); 6.03 (2H, s, -N**H$_2$**); 6.75 (2H, d, J = 8.0 Hz, Ar); 7.02 (2H, t, J = 7.6 Hz, Ar); 7.18 (2H, t, J = 7.6 Hz, Ar); 7.388 (5H, t, 7.6 Hz); 7.56 (2H, d, J = 6.8 Hz, C5,5', Ar). ^{13}C NMR (125 MHz): δ (DMSO-d_6): 28.38 (C1); 37.72 (C2); 62.36 (C3); 125.95-131.78 (15C, Ar); 136.47 (2C, Ar); 141.88 (C4). Elemental analysis: Found: C, 65.68; H, 5.26; N, 3.16; Cl, 9.30; S, 17.05 (Required

for $C_{21}H_{20}ClNS_2$ C, 65.35; H, 5.22; N, 3.63; Cl, 9.19; S, 16.62). HRMS-ESI (+ve): Calculated for $C_{21}H_{20}NS_2$ (M+H) 350.1032, found 350.1037.

2-((9-Benzyl-9*H*-xanthen-9-yl)thio) ethanamine (178)
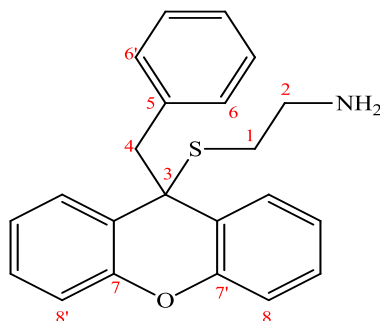
Using General Procedure F: 9-Benzyl-9*H*-xanthen-9-ol (**164**) (0.288 g, 1 mmol) and cysteamine hydrochloride (0.113 g, 1 mmol) gave compound **178** (0.230 g, 66 %) as a brown gum after purification by gravity column chromatography. ^{1}H NMR (400 MHz): δ (CDCl$_3$): 1.96 (2H, s, -N**H$_2$**); 2.30 (2H, t, *J* = 6.4 Hz, -C**H$_2$**, C1); 2.45 (2H, t, *J* = 6.4 Hz, -C**H$_2$**, C2); 3.36 (2H, s, -C**H$_2$**, C4); 6.32 (2H, d, 7.2 Hz, C6,6'); 6.77 (2H, m, Ar); 6.87(2H, t, *J* = 7.6 Hz, Ar); 6.99 (1H, t, *J* = 7.6 Hz, Ar); 7.15 (4H, m, Ar); 7.96 (2H, dd, *J* = 7.2, *J* = 2.4 Hz, C8,8', Ar). ^{13}C NMR (125 MHz): δ (DMSO-*d$_6$*): 34.40 (C1); 40.73(C2); 52.74(C4); 53.47 (C3); 116.0-130.21 (15C, Ar); 135.87 (C5); 151.70 (2C, C7,7'). Elemental analysis: Found: C, 76.32; H, 5.85; N, 4.32; S, 8.89 (Required for $C_{22}H_{21}NOS$ C, 76.04; H, 6.09; N, 4.03; S, 9.23). HRMS-ESI (+ve): Calculated for $C_{22}H_{22}NOS$ (M+H) 348.1417, found 348.1425. IR: KBr disc, υ_{max} (cm^{-1}): 3433.37 (NH stretch for primary amine).

2-((9-Benzyl-9*H*-thioxanthen-9-yl)thio)ethanamine (180)
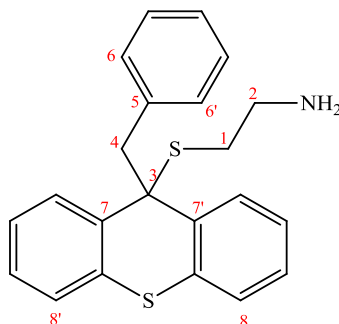
Using General Procedure F: 9-Benzyl-9*H*-thioxanthen-9-ol (**165**) (0.304 g, 1 mmol) and cysteamine hydrochloride (0.113 g, 1 mmol) gave compound **180** (0.160 g, 44 %) as a brown gum after purification by gravity column chromatography. ^{1}H NMR (400 MHz): δ (CDCl$_3$): 1.887 (2H, s, -N**H$_2$**); 2.30 (2H, t, *J* = 6.4 Hz, -C**H$_2$**, C1); 2.60 (2H,t, *J* = 6.4 Hz, -C**H$_2$**, C2); 3.37 (2H, s, -C**H$_2$**, C4); 6.47 (2H, d, *J* = 7.2 Hz, C6,6'); 6.92-7.23(9H, m, Ar); 8.10 (2H, d, *J* = 8.0 Hz, C8,8', Ar). ^{13}C NMR (125 MHz): δ (CDCl$_3$): 34.5 (C1); 40.9 (C2); 49.4 (C4); 59.98 (C3); 125.44-135.8 (18C, Ar). Elemental analysis: Found: C, 72.55; H, 5.73; N, 3.32; S, 17.52 (Required for C$_{22}$H$_{21}$NS$_2$ C, 72.68; H, 5.82; N, 3.85; S, 17.64). HRMS-ESI (+ve): Calculated for C$_{22}$H$_{22}$NS$_2$ (M+H) 364.1188, found 364.1198. IR: ATR, υ$_{max}$ (cm^{-1}): 3365.2 (NH stretch for primary amine).

2-((9-Benzyl-9H-fluoren-9-yl)thio)ethanaminehydrochloride (182)
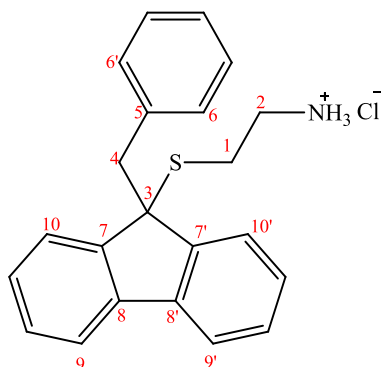
Using General Procedure F: 9-Benzyl-9H-fluoren-9-ol (**168**) (0.272 g, 1 mmol) and cysteamine hydrochloride (0.113 g, 1 mmol) gave compound **182** (0.135 g, 35 %) as a white powder after crystallisation as the corresponding hydrochloride salt. Mpt: 138-139 °C. ^{1}H NMR (400 MHz): δ (CDCl$_3$): 1.84 (2H, t, J = 6.4 Hz, -**CH$_2$**, C1); 2.21 (2H, t, J = 6.4 Hz, -**CH$_2$**, C2); 3.42 (2H, s, -**CH$_2$**, C4); 6.69 (2H, d, J = 7.2 Hz, C6,6'); 6.92 (3H, m, Ar); 7.30 (2H, m, Ar); 7.49 (2H, d, J = 7.2 Hz, C10,10', Ar); 7.57 (2H, d, J = 7.2 Hz, C9,9', Ar). ^{13}C NMR (125 MHz): δ (DMSO-d_6): 25.88 (C1); 38.36 (C2); 43.10 (C4); 60.14 (C3); 120.13-129.85 (13C, Ar); 135.34 (C5); 139.65 (2C, C8,8'); 146.38 (2C, C7,7'). Elemental analysis: Found: C, 72.04; H, 6.16; N, 3.60; Cl, 10.03; S, 7.82 (Required for C$_{22}$H$_{22}$ClNS: C, 71.82; H, 6.03; N, 3.81; Cl, 9.64; S, 8.71). HRMS-ESI (+ve): Calculated for C$_{22}$H$_{22}$NS (M+H) 332.1467, found 332.1470.

2,2'-((Diphenylmethylene)bis(sulfanediyl))diethanamine (184).
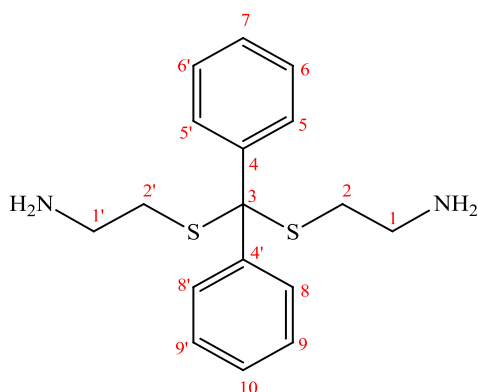
Using General Procedure F: 2-Hydroxy-2,2-diphenylacetonitrile (**183**) (0.982 g, 4.7 mmol) and cysteamine hydrochloride (0.531g, 4.7 mmol) gave compound **184** (0.080 g, 13 %) as a pale yellow gum after purification with flash column chromatography (Biotage SP4). ^{1}H NMR (400 MHz): δ (CDCl$_3$): 1.15 (4H, s, -N**H$_2$**); 2.45-2.2.48 (4H, t, J = 6.4 Hz, -C**H$_2$**, C2,2'); 2.58-2.61 (4H, t, J = 6.4 Hz, -C**H$_2$**, C1,1'); 7.22-7.30 (6H, m, C5,5',8,8',7,10, Ar); 7.53-7.55 (4H, d, J = 7.6, C6,6'9,9', Ar). ^{13}C NMR (125 MHz): δ (CDCl$_3$): 35.55 (2C, C2, 2'); 40.95 (2C, C1, 1'); 69.43 (C3); 127.38-128.56 (10C, Ar; 127.38, 127.95, 128.57); 144.19 (2C, C4, 4'). Elemental analysis: Found: C, 64.18; H, 6.88; N, 8.39; S, 19.98 (Required for C$_{17}$H$_{22}$N$_2$S$_2$ C, 64.11; H, 6.98; N, 8.80; S, 20.40). HRMS-ESI (+ve): Calculated for C$_{17}$H$_{23}$N$_2$S$_2$ (M+H) 319.1297, found 319.1292. IR: ATR, υ_{max} (cm^{-1}): 3347.8 (NH stretch for primary amine).

227

4.4.4 Synthesis of amide analogues (149-150).

(*R*)-Methyl 2-amino-3-(tritylthio)propanoate (148)
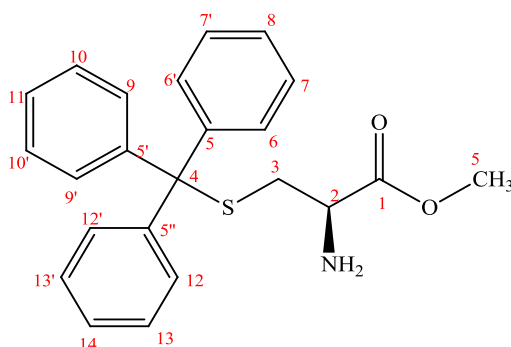
S-Trityl-L-cysteine (STLC, 180 mg, 0.5 mmol) dissolved in dry methanol (5 mL). was cooled to 0 °C and thionyl chloride (0.365 g, 5 mmol) was added slowly. The mixture was stirred for 1h at 0 °C, warmed to room temperature, stirred for a further stirred for 2h and finally refluxed for 18h. The mixture was evaporated under reduced pressure, the residue dissolved in aqueous saturated sodium carbonate (20 mL) and extracted with ethyl acetate (3 x 20 mL). The organic layer was dried over anhydrous magnesium sulphate, evaporated under reduced pressure and the residue purified flash column chromatography (Biotage SP4) [ethyl acetate:*n*-hexane (50:50)] to give compound **148** (0.120 g, 63 %) as pale green powder. Mpt: 75-76 °C (literature: 76 °C).[166] ^{1}H NMR (400 MHz): δ (CDCl$_3$): 2.47-2.52 (1H, dd, *J* =12.4, *J* = 7.6 Hz, -C**Ha**Hb, C3); 2.59-2.64 (1H, dd, *J* = 12.4, *J* = 4.8 Hz, -CHa**Hb**, C3); 3.24 (1H, m, -C**H**, C2); 3.67 (3H, s, -C**H₃**, C5); 7.22 (3H, t, *J* = 7.2 Hz, C8,11,14, Ar); 7.30 (6H, t, *J* = 8.0 Hz, C7,7'10,10',13,13', Ar); 7.46 (6H, d, *J* = 7.6 Hz, C6,6',9,9',12,12' Ar). The protons of the NH$_2$ were too broad to be observed. ^{13}C NMR (125 MHz): δ (CDCl$_3$): 37.09 (C3); 52.35 (C5); 53.96 (C2); 67.05 (C4); 126.96-144.70 (18C, Ar); 174.33 (C1).   HRMS-ESI (+ve): Calculated for C$_{23}$H$_{24}$NO$_2$S (M+H) 378.1522, found 378.1526. IR: KBr disc, υ$_{max}$ (cm^{-1}): 1748.4 (C=O stretch for ester), 3441.2 (NH stretch for primary amine).

4.4.4.1 General Procedure G: Preparation of amides *via* the STLC methyl ester (148). (*R*)-Methyl 2-amino-3-(tritylthio)propanoate (**148**) (50 mg, 0.13 mmol) was dissolved in the required primary amine (1 mL) and the mixture stirred at room temperature for 24 hours. To the mixture was purified by flash column chromatography (Biotage SP4) [methanol: chloroform (15:85)] to give the desired amide derivatives.

(*R*)-2-Amino-N-(2-hydroxyethyl)-3-(tritylthio)propanamide (149)
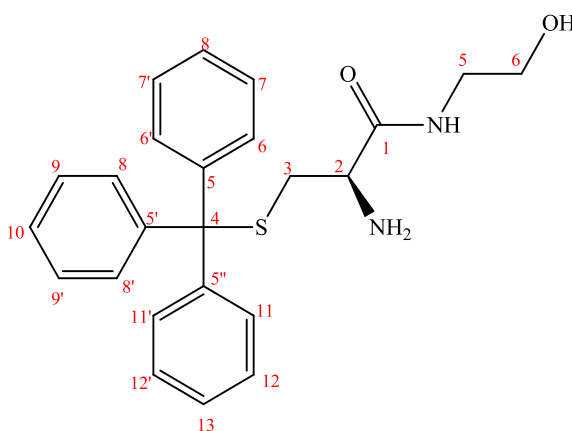
Using General Procedure G: (*R*)-Methyl 2-amino-3-(tritylthio)propanoate (**148**) (50 mg, 0.13 mmol) and ethanolamine (1 mL) gave compound **149** (0.044 g, 82 %) as a pale yellow gum. ^{1}H NMR (400 MHz): δ (CDCl$_3$):1.89 (2H, N**H$_2$**); 2.56-2.62 (1H, dd, *J* = 12.8 *J* = 8 Hz, -C**Ha**Hb, C3); 2.69-2.74 (1H, dd, *J* = 12.8, *J* = 4 Hz, − CHa**Hb,** C3); 3.03-3.06 (1H, dd, *J* = 8.0, *J* = 4 Hz, -C**H** , C2); 3.32-3.35 (2H, q, *J* = 5.6 Hz, -C**H$_2$,** C5); 3.64-3.67(2H, t, *J* = 5.2 Hz, -C**H$_2$**, C6); 7.21 (3H, t, *J* = 7.2 Hz, C8,10,13, Ar); 7.30 (6H, t, *J* = 8.0 Hz, C7,7',9,9'12,12', Ar); 7.44 (6H, d, *J* = 7.2 Hz, C6,6',8,8',11,11', Ar). ^{13}C NMR (125 MHz): δ (CDCl$_3$): 37.49 (C3); 42.55 (C5); 54.16 (C2); 62.55 (C6); 67.22 (C4); 127.01-144.7 (18C, Ar); 174.499 (C1). Elemental analysis: Found: C, 67.80; H, 6.98; N, 6.58; S, 7.39 (Required for C$_{24}$H$_{26}$N$_2$O$_2$S.H$_2$O C, 67.74; H, 6.87; N, 6.58; O, 11.28; S, 7.53). HRMS-ESI (+ve): Calculated for C$_{24}$H$_{27}$N$_2$O$_2$S (M+H) 407.1788, found 407.17813. IR: KBr disc, υ$_{max}$ (cm^{-1}): 1651.7 (C=O stretch for amide), 3368.5 (NH stretch for primary amine).

(*R*)-2-Amino-N-(3-hydroxypropyl)-3-(tritylthio)propanamide (150)
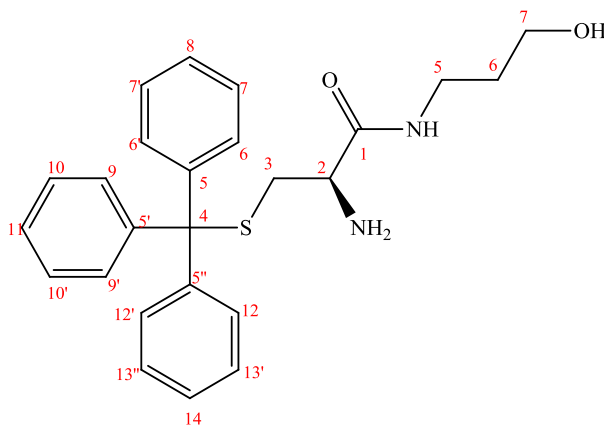
Using General Procedure G: (*R*)-Methyl 2-amino-3-(tritylthio)propanoate (**148**) (50 mg, 0.13 mmol) and 3-aminopropanol (1 mL) gave compound **150** (0.040 g, 71 %) as a dark yellow gum. ^{1}H NMR (400 MHz): δ (CDCl$_3$): 1.62-1.64 (2H, p, *J* = 6 Hz, -C**H$_2$**, C6); 1.75 (2H, s, N**H$_2$**); 2.615-2.70 (2H, m, -C**H$_2$**, C3); 3.058-3.81(1H, m, -C**H**, C2); 3.31-3.72 (2H, m, -C**H$_2$**, C5); 3.54-3.57 (2H m, -C**H$_2$**, C7); 7.19 (3H, t, *J* = 7.2 Hz, C8,11,14, Ar); 7.28 (6H, t, *J* = 8.0 Hz, C7,7',10,10',13,13', Ar); 7.43 (H, d, *J* = 7.6 Hz, C6,6',9,9',12,12', Ar). The protons of the CONH- and -OH were too broad to be observed. ^{13}C NMR (125 MHz): δ (CDCl$_3$): 32.44 (C6); 35.52 (C3); 37.25 (C5); 53.78 (C2); 58.79 (C7); 67.14 (C4); 126.93-144.61 (18C, Ar); 174.41 (C1). Elemental analysis: Found: C, 68.88; H, 6.37; N, 5.52; S, 7.32 (Required for C$_{25}$H$_{28}$N$_2$O$_2$S.H$_2$O C, 68.46; H, 6.89; N, 6.39; S, 7.31).   HRMS-ESI (+ve): Calculated for C$_{25}$H$_{29}$N$_2$O$_2$S (M+H) 421.1944, found 421.1949. IR: KBr disc, υ_{max} (cm^{-1}): 1669.4 (C=O stretch for amide), 3384.6 (NH stretch for primary amine).

(*R*)-2-Amino-N-(2-aminoethyl)-3-(tritylthio)propanamide (151)
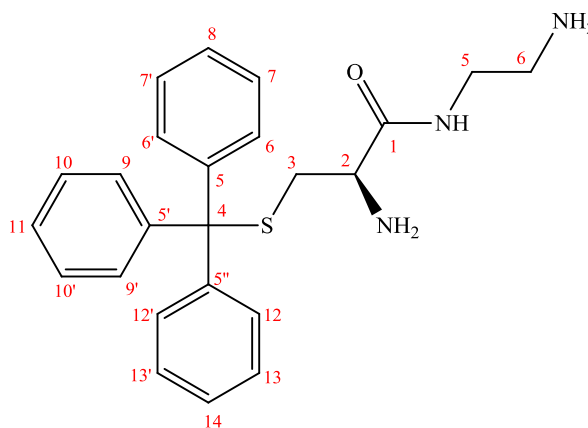
Using General Procedure G: (*R*)-Methyl 2-amino-3-(tritylthio)propanoate (**148**) (120 mg, 0.32 mmol) and ethylenediamine (1 mL) gave compound **151** (0.07 g, 54 %) as a brown gum. ^{1}H NMR (400 MHz): δ (CDCl$_3$): 1.43 (2H, -N**H$_2$**); 2.57-2.62 (1H, dd, *J* = 12.8, *J* = 8 Hz, -C**Ha**Hb, C3); 2.70-2.74 (1H, dd, *J* = 12.8, *J* = 4 Hz, –CHa**Hb,** C3); 2.768-2.796 (2H, t, *J* = 6 Hz, -C**H$_2$**, C6); 3.03-3.06 (1H, dd, *J* = 8.0, *J* = 4 Hz, -C**H** ,C2); 3.22-3.26(2H, q, *J* = 6 Hz, -C**H$_2$**, C5); 7.20 (3H, t, *J* = 7.6 Hz, C8,11,14, Ar); 7.32 (6H, t, *J* = 8.0 Hz, C7,7',10,10',13,13', Ar); 7.46 (6H, d, *J* = 8.0 Hz, C6,6',9,9',12,12', Ar). The protons of the the NH2 and CONH- were too broad to be observed. ^{13}C NMR (125 MHz): δ (CDCl$_3$): 37.69 (C3); 41.72 (C6); 42.17(C5); 54.28 (C2); 67.20 (C4); 127.01-144.7 (18C, Ar); 173.48 (C1).   Elemental analysis: Found: C, 71.68; H, 6.71; N, 9.06; S, 7.66 (Required for C$_{24}$H$_{27}$N$_3$OS C, 71.08; H, 6.71; N, 10.36; S, 7.86).   HRMS-ESI (+ve): Calculated for C$_{24}$H$_{28}$N$_3$OS (M+H) 406.1948, foun 406.1944. IR: KBr disc, υ_{max} (cm^{-1}): 1659.9 (C=O stretch for amide), 3353.7 (NH stretch for primary amine).

4.4.5 Synthesis of ester analogues

3.4.5.1 General Procedure H: Esterification *via* microwave irradiation. The L-cysteine derivative (0.36 mmol) and the required primary alcohol (1 mL) were combined in a Biotage microwave vial (0.5 – 2.0 mL) and concentrated H_2SO_4 (8%, 0.1 mL) was added. The tube was sealed and irradiated for 5 min at 100 °C. The mixture was neutralized with saturated aqueous Na_2CO_3 and extracted with ethyl acetate (3 x 10 mL). The combined organic fractions were dried over anhydrous magnesium sulphate, evaporated under reduced pressure and the residue was then purified using gravity column chromatography [ethyl acetate:*n*-hexane (50:50)] to give the esters as viscous oils. The corresponding hydrochloride salts were formed by dissolving in the oil in anhydrous diethyl ether (10 mL) and adding etheral HCl (2 eq) until the hydrochloride salt precipitated. The precipitate was filtered, washed with diethyl ether and dried in a vacuum oven (40 °C for 24 h) to give the corresponding ester derivatives.

(*R*)-Butyl 2-amino-3-(tritylthio)propanoate hydrochloride (142).
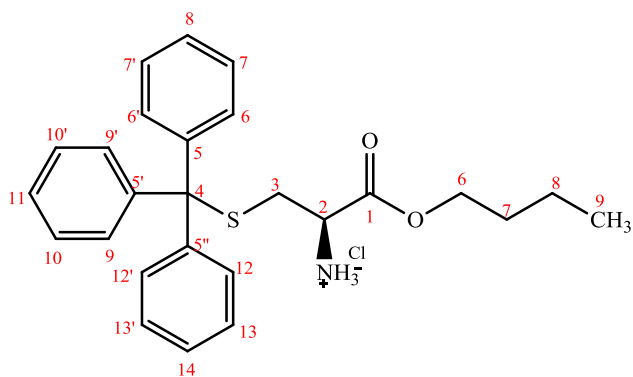
General Procedure E: Trityl alcohol (0.572 g, 2.2 mmol) and L-cysteine butyl ester (**146**) (0.426 g, 2 mmol) gave compound **142** (0.034 g, 27) as a brown powder. Mpt:

85-86 °C. ^{1}H NMR (400 MHz): δ (CDCl$_3$): 0.89 (3H, t, J = 7.2 Hz, -C**H$_3$**, C9); 1.29 (2H, sextet, J = 7.2 Hz, -C**H$_2$**, C8); 1.52 (2H, pentet, J = 6.8 Hz, -C**H$_2$**, C7); 2.45 (1H, dd, J = 12.4, J = 8 Hz, –C**Ha**Hb, C3); 2.54 (1H, dd, J = 12.4 Hz, J = 4.8 Hz - CHa**Hb**, C3); 3.18 (1H, dd, J = 8, J = 4.8 Hz, –C**H**, C2); 4.05 (2H, t, J = 6.8 Hz, -C**H$_2$**, C6); 7.19 (3H, t, J = 7.6 Hz, C8,11,14, Ar); 7.28 (6H, t, J = 8.0 Hz, C7,7',10,10',13,13', Ar); 7.42 (6H, d, J = 8.0 Hz, C6,6', 9,9',12,12', Ar). The protons of the NH$_2$ were too broad to be observed. ^{13}C NMR (125 MHz): δ (CDCl$_3$): 13.76 (C9); 19.14 (C8); 30.59 (C7); 37.16 (C3); 54.00 (C2); 65.07 (C6); 66.91 (C4); 126.84-129.67 (15C, Ar; 126.84, 128.02, 129.67); 144.66 (3C, C5, 5', 5''); 173.96 (C1). Elemental analysis: Found: C, 68.87; H, 6.55; N, 2.99; Cl 7.13; S, 6.77 (Required for: C$_{25}$H$_{29}$ClN$_2$O$_2$S C, 68.48; H, 6.63; N, 3.07; S, 7.03). HRMS-ESI (+ve): Calculated for C$_{26}$H$_{30}$NO$_2$S (M+H) 420.1992, found 420.1992. IR: KBr disc, (cm^{-1}): 1742.4 (C=O stretch for ester).

(*R*)-Butyl 2-amino-3-((1,1,2-triphenylethyl)thio) propanoate hydrochloride (143).
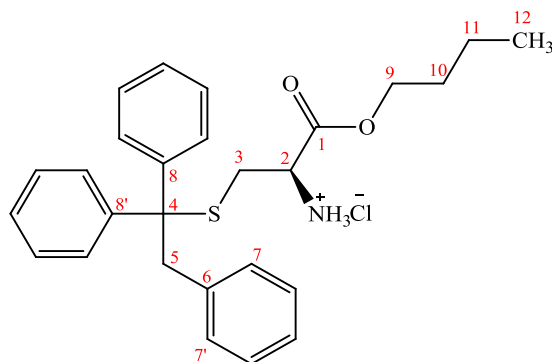
Using General Procedure H: (*R*)-2-Amino-3-((1,1,2-triphenylethyl)thio)propanoic acid (**101**) (0.1 g, 0.36 mmol) and n-butanol (1 mL) gave compound **143** (0.025 g, 15 %) as a white powder. Mpt: 72-73 °C. ^{1}H NMR (400 MHz): δ (CDCl$_3$): 0.92 (3H, t, J = 7.6 Hz, -C**H$_3$**, C12); 1.32 (2H, sextet, J = 7.6 Hz, -C**H$_2$**, C11); 1.57(2H, pentet, J = 6.4 Hz, -C**H$_2$**, C10); 2.43 (1H, dd, J = 12.4, J = 8.0 Hz, -C**Ha**Hb, C3); 2.59 (1H, dd, J = 12.4 Hz, J = 4.8 Hz, -CH**Hb**,C3); 3.13 (1H, m, -C**H**, C2); 3.62

(2H, s, -C**H₂**, C5); 4.06 (2H, t, J = 6.4 Hz, -C**H₂**, C9); 7.64 (2H, d, J = 6.4 Hz, C7,7');
7.02-7.33 (13H, m, Ar). The protons of the NH₂ were too broad to be observed. ^{13}C
NMR (125 MHz): δ (DMSO-d_6): 13.45 (C12); 18.4 (C11); 29.11 (C10); 29.81 (C3);
44.87 (C5); 51.10 (C2); 61.54 (C4); 65.50 (C9); 126.17-130.87 (15C, Ar); 136.23
(C6); 143.78 (2C, C8,8'); 167,86 (C1). Elemental analysis: Found: C, 67.95; H, 6.75;
N, 2.86; Cl, 7.12; S, 6.82 (Required for: $C_{27}H_{32}NO_2S.1/2CH_3OH$ C, 67.95; H, 7.05;
Cl, 7.29; N, 2.88; S, 6.60). HRMS-ESI (+ve): Calculated for $C_{27}H_{32}NO_2S$ (M+H)
434.2148, found 434.2141. IR: ATR, υ_{max} (cm^{-1}): 1741 (C=O stretch for ester).

(*R*)-2-Hydroxyethyl 2-amino-3-(tritylthio)propanoate (144)
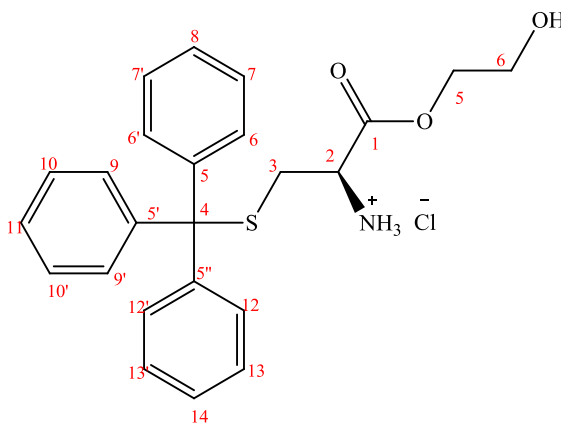
Using General Procedure H: STLC (180 mg 0.5 mmol) and ethylene glycol (1 mL)
gave compound **144** (0.045 g, 20 %) as a pale yellow powder. Mpt: 102-106 °C. ^{1}H
NMR (400 MHz): δ (CDCl₃): 1.91 (2H, s, N**H₂**); 2.28-2.62 (2H, m, -C**H₂,** C3);
3.26-3.29 (1H, t, *J* = 5.6 Hz, -C**H,** C2); 3.84-3.86 (2H, t, *J* = 4.8 Hz, -C**H₂**, C6);
4.16-4.23 (2H, m, -C**H₂,** C5); 7.23 (3H, t, *J* = 7.2 Hz, C8,11,14, Ar); 7.32 (6H, t, *J* =
8.4 Hz, C7,7',10,10',13,13', Ar); 7.46 (6H, d, *J* = 7.6 Hz, C6,6',9,9',12,12', Ar).
^{13}C NMR (125 MHz): δ (CDCl₃): 37.15 (C3); 54.06 (C6); 60.97 (C2); 66.94 (C5);
67.23(C4); 127.07-144.61 (18C, Ar); 173.9 (C1). Elemental analysis: Found: C,
64.81; H, 6.15; N, 2.81; Cl, 7.39; S, 6.98 (Required for $C_{24}H_{26}ClNO_3S$ C, 64.92; H,
5.90; N, 3.15; Cl, 7.22; S, 7.39). HRMS-ESI (+ve): Calculated for $C_{24}H_{26}NO_3S$

(M+H) 408.1628, found 408.1622. IR: KBr disc, υ_{max} (cm^{-1}): 1751.4 (C=O stretch for ester), 3378.7 (OH stretch).

(*R*)-1-(3-Hydroxypropoxy)-1-oxo-3-(tritylthio)propan-2-amine hydrochloride (145)
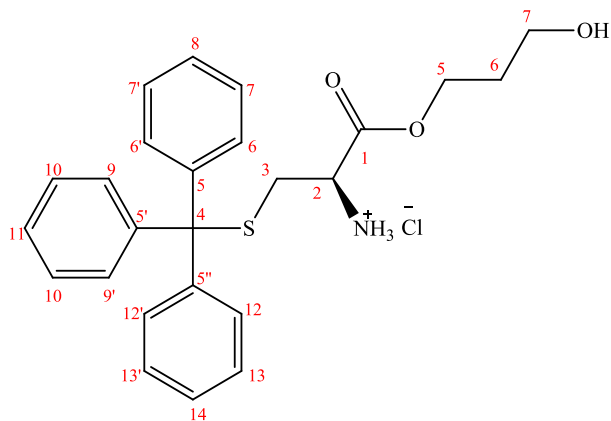
Using General Procedure H: STLC (180 mg 0.5 mmol) and propylene glycol (1 mL) gave compound **145** (0.053 g, 23 %) as a pale yellow powder. Mpt: 82-83 °C. ^{1}H NMR (400 MHz): δ (CDCl$_3$): 1.64 (2H, s, N**H$_2$**); 1.85-1.88 (2H, pentet, *J* = 6.0 Hz, -C**H$_2$**, C6); 2.47-2.52 (1H, dd, *J* = 12.4 *J* = 7.6 H -C**Ha**Hb, C3); 2.55-2.59 (1H, dd, *J* = 12.4, *J* = 4.8 Hz, -CHa**Hb**, C3); 3.18-3.21 (1H, dd, *J* = 7.6, *J* = 4.8 Hz –C**H**, C2); 3.61-3.66 (2H, t, *J* = 6Hz, -C**H$_2$**, C7); 4.20-4.24 (2H, t, *J* = 5.6 Hz, -C**H$_2$**, C5); 7.20 (3H, t, *J* = 7.2 Hz, C8,11,14, Ar); 7.30 (6H, t, *J* = 7.6 Hz, C7,7',10,10',13,13', Ar); 7.44 (6H, d, *J* = 7.2 Hz, C6,6',9,9',13,13', Ar). Proton of OH was too broad to be observed. ^{13}C NMR (125 MHz): δ (CDCl$_3$): 31.74 (C6); 37.20 (C3); 54.09 (C7); 59.22 (C2); 62.30 (C5); 67.13 (C4); 127.02-144.71 (18C, Ar); 174.27 (C1). Elemental analysis: Found: C, 58.12; H, 6.93; N, 2.59; Cl, 6.95; S, 6.58 (Required for C$_{25}$H$_{28}$ClNO$_3$S.3H$_2$O C, C, 58.64; H, 6.69; N, 2.74; Cl, 6.92; S, 6.26). HRMS-ESI (+ve): Calculated for C$_{25}$H$_{28}$NO$_3$S (M+H) 422.1784, found 422.1784. IR: KBr disc, υ_{max} (cm^{-1}): 1743.4 (C=O stretch for ester), 3379.7 (OH stretch).

4.4.5.2 Synthesis of ester via coupling with the L-cysteine ester: The requisite alcohol was coupled to the synthesised L-cysteine ester using boron trifluoroetherate using an adaptation of General Procedure E.

Synthesis of L-cysteine-n-butyl ester (146)
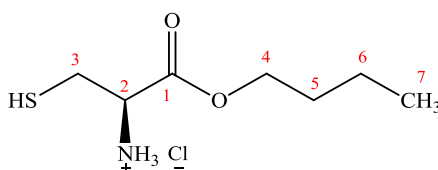
L-cysteine hydrochloride (4 g, 25 mmol) were dissolved in a solution of hydrochloric acid (3M) in 1-butanol (20 mL) and the reaction refluxed at 100 °C for 5h. The mixture was cooled and concentrated under reduced pressure. The solid residue was recrystallised from ethyl acetate to give compound **146** (2.5 g, 46 %) as white crystals. Mpt: 140-142 °C(literature: 76 °C).[167] ^{1}H NMR (400 MHz): δ (DMSO-d_6): 0.88 (3H, t, J = 7.2 Hz, -**CH$_3$**, C7); 1.37 (2H, sextet, J = 7.2 Hz, -**CH$_2$**, C6); 1.60 (2H, pentet, J = 6.8 Hz, -**CH$_2$**, C5); 2.99-3.06 (2H, dd, J = 14.8, J = 5.2 Hz, **CH$_2$**, C3); 4.16-4.23(2H, m, -**CH$_2$**, C4); 4.37 (1H, t, J = 5.2 Hz, -**CH**, C2). The protons of the NH$_2$ were too broad to be observed. ^{13}C NMR (125 MHz): δ (DMSO-d_6): 14.07 (C7); 19.07 (C6); 24.82 (C5); 39.66 (C3); 54.46 (C2); 66.13 (C4); 168.36 (C1). HRMS-ESI (+ve): Calculated for C$_7$H$_{16}$NO$_2$S (M+H) 178.0896, found 178.0900. IR: KBr disc, υ_{max} (cm^{-1}): 3430.2 (NH stretch for primary amine), 1745.9 (C=O stretch of carbonyl).

(*R*)-Butyl 2-amino-3-((diphenyl(pyridin-4-yl)methyl)thio)propanoate dihydrochloride (147).

237
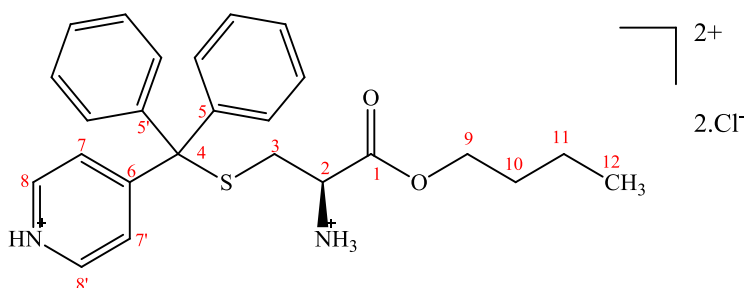
Using General Procedure E: Diphenyl(pyridin-4-yl)methanol (**83**) (0.574 g, 2.2 mmol) and L-cysteine butyl ester (**146**) (0.426 g, 2 mmol) gave compound **147** (0.144 g, 15 %) as a brown powder. Mpt: 85-86 °C. ^{1}H NMR (400 MHz): δ (CDCl$_3$): 0.82 (3H, t, *J* = 7.2 Hz, -C**H$_3$**, C12); 1.23 (2H, sextet, *J* = 7.2 Hz, -C**H$_2$**, C11); 1.47 (2H, pentet, *J* = 7.2 Hz, -C**H$_2$**, C10); 2.39 (1H, dd, *J* = 12.4, *J* = 8.0 Hz – C**Ha**Hb, C3); 2.45 (1H, dd, *J* = 12.4, *J* = 4.8 Hz, -CHa**H$_b$**, C3); 3.17 (1H, t, *J* = 4.8 Hz, -C**H**, C2); 4.03 (2H, t, *J* = 6.8 Hz, -C**H$_2$**, C9); 7.15-7.36 (12, m, Ar); 8.44 (2H, d, *J* = 4.8 Hz, C8,8'). The protons of the NH$_2$ were too broad to be observed. ^{13}C NMR (125 MHz): δ (CDCl$_3$): 13.76 (C12); 19.11 (C11); 30.54 (C10); 36.78 (C3); 53.847 (C2); 65.12 (C9); 65.88 (C4); 125.33-129.15 (12C, Ar); 143.0 (2C, C5,5'); 149.71 (2C, C8,8'); 163.62 (C6); 173.75 (C1). Elemental analysis: Found: C, 60.77; H, 5.83; N, 5.54; Cl, 13.85; S, 5.93 (Required for: C$_{25}$H$_{30}$Cl$_2$N$_2$O$_2$S C, 60.85; H, 6.13; N, 5.68; Cl, 14.37; S, 6.50). HRMS-ESI (+ve): Calculated for C$_{25}$H$_{29}$N$_2$O$_2$S (M+H) 421.1944, found 421.1944. IR: KBr disc, (cm^{-1}): 1741.9 (C=O stretch for ester), 3398.9 (NH stretch for primary amine).

4.4.6 Synthesis of cyclic amine analogues

N-BOC-pyrrolidinemethanol (152).
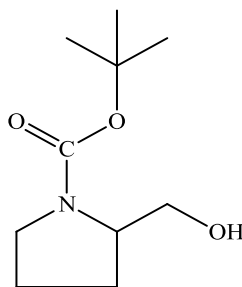
Pyrrolidine 2-methanol (0.5 g, 4.94 mmol) was dissolved in THF (7.5 mL) and added to a solution of (BOC)$_2$O (1.18 g 5.4 mmol) in aqueous 1M K$_2$CO$_3$ (12.5 mL) and the mixture stirred for 24 hours. The reaction was quenched using 5% aqueous hydrochloric acid (pH 2) and the mixture extracted with ethyl acetate (3 x 20 mL). The combined organic fractions were dried over anhydrous magnesium sulphate and

evaporated under reduced pressure. The residue was then purified by gravity column chromatography [ethyl acetate: *n*-hexane (50:50)] to give compound **152** (0.871 g, 80 %) as a colourless oil. ^{1}H NMR (400 MHz): δ (CDCl$_3$): 1.48-1.55 (11H, m); 1.78-1.81 (2H, m); 2.01-1.05 (1H); 3.30-3.46 (2H,m); 3.58-3.64 (2H,m); 3.97 (1H, s). ^{13}C NMR(400 MHz): δ (CDCl$_3$): 24.07; 28.39; 28.74; 47.57; 60.22; 67.83; 80.22; 155.84. HRMS-ESI (+ve): Calculated for C$_{10}$H$_{20}$NO$_3$ (M+H) 202.1438, found 202.1400

N-BOC-pyrrolidine-2-methylacetylthioester (154)
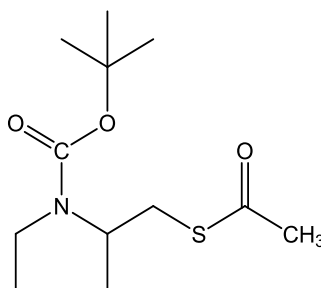
Triphenylphosphine (1.008 g, 3.85 mmol) and DIAD (777 µL, 3.85 mmol) were dissolved in dry THF (21 mL) and the mixture stirred at 0 °C until a white precipitates formed. N-BOC-pyrrolidinemethanol (**152**) (700 mg, 3.39 mmol) was dissolved in THF (7 mL) with thioacetic acid (273 µL, 3.85 mmol) and then added slowly to the solution of PPh$_3$-DIAD at 0 °C and stirred for 24 hours at room temperature. The mixture was evaporated under reduced pressure and the residue purified by gravity column chromatography [ethyl acetate:*n*-hexane (10:90)]. The oil was triturated with *n*-hexane, filtered and the *n*-hexane solution (filtrate) evaporated to give compound **154** (0.482 g, 55 %) as a yellow liquid. ^{1}H NMR (400 MHz): δ (CDCl$_3$): 1.50 (9H, s); 1.69-1.71 (2H, m); 1.71-1.79 (1H, m); 1.79-1.93 (2H, m); 2.35 (2H, s); 3.15-3.42 (4H, m); 3.89-3.95 (1H, m). HRMS-ESI (+ve): Calculated for C$_{12}$H$_{22}$NO$_3$S (M+H) 260.1315, found 260.1200.

N-BOC-pyrrolidine 2-methylthiol (156).
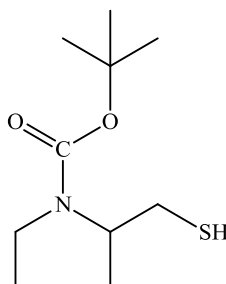
N-BOC-pyrrolidine-2-methylacetylthioester (**154**) (160 mg 0.61 mmol) was dissolved in 1M aqueous potassium carbonate solution:methanol:water (1:6:2 mL), the mixture stirred for 30 minutes and then evaporated under reduced pressure to give compound **156** (0.125 g, 94 %) as colourless liquid. ^{1}H NMR (400 MHz): δ (CDCl$_3$): 1.41-1.45 (11H); 1.78-1.99 (4H, m); 2.5-2.59 (1H,m); 3.34-3.5 (2H, m), 3.83 (1H, s). HRMS-ESI (+ve): Calculated for C$_{10}$H$_{20}$NO$_2$S (M+H) 218.1209, found 218.1100.

2-((Tritylthio)methyl)pyrrolidine (158)
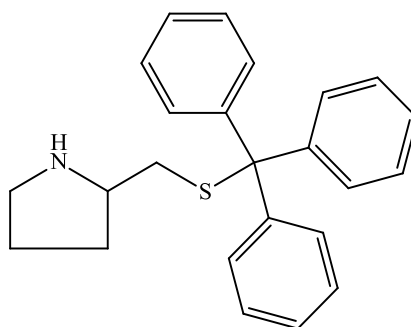
N-BOC-pyrrolidine 2-methylthiol (**156**) (136.5 mg, 0.626 mmol) and trityl alcohol (162.7 mg, 0.626 mmol) were dissolved in acetic acid (1 mL) and stirred for 1 hour. The mixture was cooled to 0 °C and boron trifluoroetherate (0.09 mL, 0.82 mmol) was added slowly under nitrogen. The mixture was stirred for a further 2 hours at

room temperature and then quenched with sodium acetate (6 mL) and water (6 mL). The mixture was extracted with ethyl acetate (3 x 20 mL) and the combined organic fractions dried (MgSO$_4$). The solvents were removed under reduced pressure and the residue purified by gravity column chromatography [methanol:chloroform (10:90)] to give the desired product **158** (0.16 g, 72 %) as a pale yellow gum. ^{1}H NMR (400 MHz): δ (CDCl$_3$): 1.22-1.32 (1H, m); 1.6-1.72 (2H, m); 1.72-1.82 (1H, m); 2.28-2.42 (2H, m); 2.8-2.88 (2H, m); 2.92-3.2 (1H, m); 7.16-7.43 (15H, ArH). The protons of the NH were too broad to be observed. ^{13}C NMR (125 MHz): δ (CDCl$_3$): 24.85, 31.02, 37.05, 46.1, 57.91, 66.79, 126.65-144.81 (18C, Ar). Elemental analysis: Found: C, 71.14; H, 6.81; N, 3.63; S, 7.32 (Required for C$_{24}$H$_{25}$NS C, 71.40; H, 6.71; N, 6.66; S, 7.52). HRMS-ESI (+ve): Calculated for C$_{24}$H$_{26}$NS (M+H) 360.1780, found 360.1168. IR: ATR, υ_{max} (cm^{-1}): 3467.2 (NH stretch for amine).

Tert-butyl 2-((tritylthio)methyl)pyrrolidine-1-carboxylate (160)
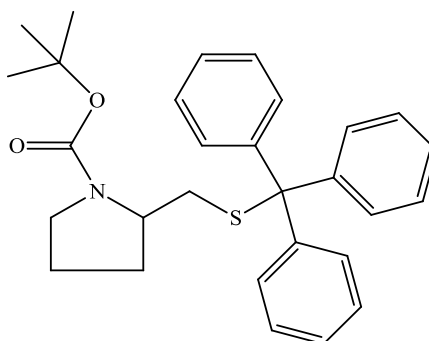
N-BOC-pyrrolidine 2-methylthiol **156** (136.5 mg, 0.626 mmol) was dissolved in anhydrous dichloromethane (5 mL), treated with trityl chloride (261.7 mg, 0.939 mmol) and triethylamine (174 µL, 1.24 mmol) and the mixture stirred for 24h at room temperature. The reaction was evaporated under reduced pressure and the residue was purified by flash column chromatography (Biotage SP4) [methanol: chlroform (10:90)] to give **160** (0.165 g, 57 %) as a white powder. Mpt: 145-146 °C. ^{1}H NMR (400 MHz): δ (CDCl$_3$): 1.30-1.42 (10H, m); 1.57-1.66 (2H, m); 1.81-1.89 (1H, m); 2.05-2.07 (1H, m); 2.45-2.47(1H, m); 3.21-3.31 (2H, m); 3.80 (1H, m);

7.17-7.42 (15H, Ar). ^{13}C NMR (125 MHz): δ (CDCl$_3$): 22.95; 28.57; 30.47; 35.58; 53.34; 55.54; 66.78; 126.70-144.92 (18C, ArH); 154.34. Elemental analysis: Found: C, 75.78; H, 7.23; N, 2.67; S, 6.37 (Required for C$_{29}$H$_{33}$NO$_2$S C, 75.78; H, 7.24; N, 3.05; S, 6.98). HRMS-ESI (+ve): Calculated for C$_{29}$H$_{34}$NO$_2$S (M+H) 460.2305, found 560.1781. IR: KBr disc, (cm^{-1}): 1676.7 (C=O stretch for ester).

N-BOC-piperidine methanol (153).
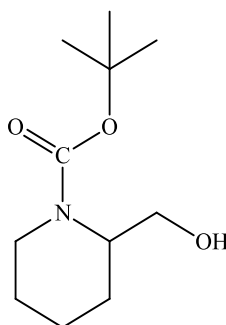
The title compound was prepared using the same method used for the preparation of **152**: Piperidinemethanol (0.5 g, 4.35 mmol) gave compound **153** (0.8 g, 86%) as colourless oil. ^{1}H NMR (400 MHz): δ (CDCl$_3$): 1.42-1.47 (11H, m); 1.59-1.69 (4H, m); 3.58-3.64(1H, pentet); 3.80-3.87 (2H, m); 3.93-3.96 (2H, m); 4.30-4.32 (1H ,m). ^{13}C NMR (125 MHz): δ (CDCl$_3$): 19.70; 25.31; 28.52, 40.02, 52.56; 61.788; 79.91; 156.23. HRMS-ESI (+ve): Calculated for C$_{11}$H$_{22}$NO$_3$ (M+H) 216.1594, found 216.1500.

N-BOC-piperidine -2-methylacetylthioester (155)
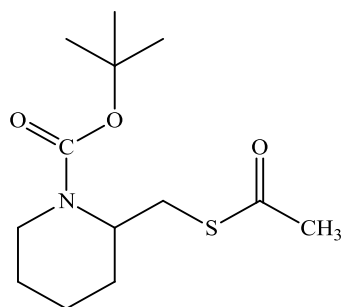
The title compound was prepared using the same method used for the preparation of **154**: N-BOC-piperidinemethanol (**153**) (728 mg, 3.39 mmol) gave compound **155** (0.486 g, 53 %) as yellow oil. ^{1}H NMR (400 MHz): δ (CDCl$_3$): 1.40-1.40 (11H, m); 1.58-1.66 (4H, m); 2.31(2H, s); 2.74-2.80 (1H, t); 3.06-3.20 (2H, m); 3.98-4.01 (1H, m); 4.35 (1H, s). ^{13}C NMR (125 MHz): δ (CDCl$_3$): 18.81, 25.22, 27.41, 28.40, 29.72, 30.50, 38.81, 49.52, 79.50, 154.91, 195.32. HRMS-ESI (+ve): Calculated for C$_{13}$H$_{23}$NNaO$_3$S (M+Na) 296.1296, found 295.9600.

N-BOC-piperidine 2-methylthiol (157).
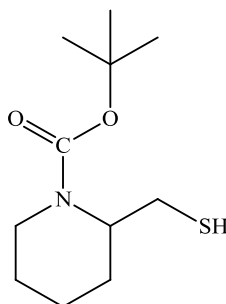
The title compound was prepared using the same method used for the preparation of **156**: N-BOC-piperidine-2-methylacetylthioester (**155**) (486 mg 1.78 mmole) gave compound **157** (0.379 g, 92 %) as colourless liquid. ^{1}H NMR (400 MHz): δ (CDCl$_3$): 1.37-1.5 (12H ,m); 1.57-1.65 (4H, m); 1.82-1.85 (1H, m); 2.71-2.94 (2H, m); 3.9-4.01 (1H, m); 4.4 (1H, s). ^{13}C NMR (125 MHz): δ (CDCl$_3$): 18.79; 22.01; 24.56;

25.25; 26.39; 29.43; 69.82; 79.61; 155.33.   HRMS-ESI (+ve): Calculated for $C_{11}H_{22}NO_2S$ (M+H) 232.1366, found 232.04.

Tert-butyl 2-(mercaptomethyl)piperidine-1-carboxylate (159)
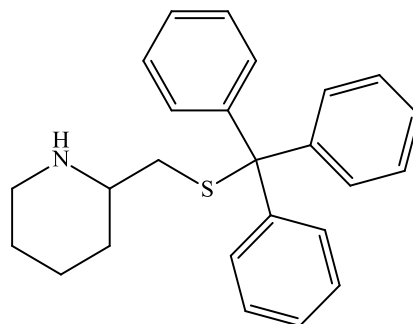
The title compound was prepared using the same method used for the preparation of **158**: N-BOC-piperidine 2-methylthiol (**157**) (190 mg, 0.823 mmol) gave compound **159** (0.14 g, 46 %) as a pale yellow gum. ^{1}H NMR (400 MHz): δ (CDCl$_3$): 0.95-1.03 (1H, m); 1.10-1.17 (1H, m); 1.25-1.32 (1H, m); 1.43-1.58 (2H, m); 1.65-168 (1H, m); 2.01-2.08 (1H, m); 2.08-2.29 (2H, dd,); 2.42-2.48 (1H, t); 2.93-2.99 (1H, m);7.19-7.44 (15H, Ar). ^{13}C NMR (125 MHz): δ (CDCl$_3$): 24.60; 26.03; 32.56; 38.84; 46.99; 55.90; 66.52; 126.70-144.93 (18C, Ar). The protons of the NH were too broad to be observed. Elemental analysis: Found: C, 78.73; H, 7.23; N, 3.47; S, 8.29 (Required for $C_{25}H_{27}NS.1/2H_2O$ C, 78.49; H, 7.38; N, 3.66; S, 8.38). HRMS-ESI (+ve): Calculated for $C_{25}H_{28}NS$ (M+H) 374.1937, found 374.1942. IR: ATR, υ_{max} (cm^{-1}): 3367.2 (NH stretch for amine).

244

Tert-butyl 2-((tritylthio)methyl)piperidine-1-carboxylate (161)
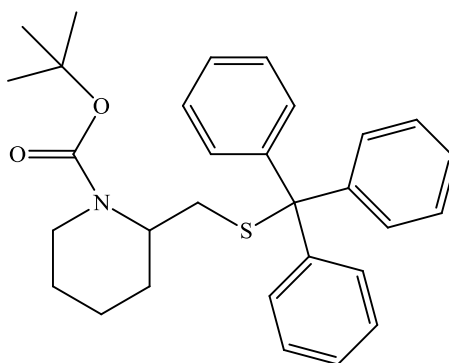
The title compound was prepared using the same method used for the preparation of **160**: N-BOC-piperidine 2-methylthiol (**157**) (188.5 mg, 0.820) gave compound **161** (0.135 g, 35 %) as a white powder. Mpt: 133-134 °C. ^{1}H NMR (400 MHz): δ (CDCl$_3$): 1.132-1.20 (1H, m); 1.27-1.34 (2H, m); 1.42-1.57 (11H, m); 1.63-1.67 (1H, m); 2.24.08-2.33 (2H, dd,); 2.40-2.44 (1H,t); 3.86-3.89 (1H, m); 4.35(1H, m); 7.19-7.46 (15H, Ar). ^{13}C NMR (125 MHz): δ (CDCl$_3$): 18.87, 25.25, 27.73, 28.54, 32.08, 66.35, 77.31, 80.02, 126.68-146.93(18C, Ar), 154.92. Elemental analysis: Found: C, 77.59; H, 7.24; N, 2.03; S, 8.29 (Required for C$_{30}$H$_{35}$NO$_2$SC, 76.06; H, 7.45; N, 2.96; S, 6.77). HRMS-ESI (+ve): Calculated for C$_{30}$H$_{35}$NNaO$_2$S (M+Na) 496.2286, found 496.1168. IR: KBr disc, (cm^{-1}): 1690.2 (C=O stretch for ester).

4.5 Biological evaluation

4.5.1 Measurement of ATPase (IC$_{50}$)

All compounds were measured once to determine their (IC$_{50}$) and separate compounds that inhibit basal Eg5 activity from those that do not. The inhibition of the basal Eg5 activity of the active compounds was then measured in triplicate at the same time.

General test procedure was as follows:[65, 70]

- All the experiments were done at 25°C.
- Inhibitors were prepared as a stock solution at 50 mM in DMSO.
- Eg5$_{1-368}$ (molecular mass 40997.64 Da) was kindly provided by Kristal Kaan in a stock solution of 10 mg/ml (243.8 µM).
- ATPase buffer coupled with pyruvate kinase/lactate dehydrogenase was added to a 96-well µclear plate.
- The inhibitor was added to the plate in 12 point concentrations of 1.5-fold serial dilution with DMSO as blank.
- Eg5$_{1-368}$ was added to plate and quickly mixed to a final concentration of 100 nM.
- ATPase rate were determined by measuring the derease of absorbance at 340 nm using a Sunrise photometer (Tecan, Maennedorf, Switzerland).
- The data were analyzed using Excel and Kaleidagraph 3.0 (Synergy Software, Reading, PA).

4.5.2 Cell proliferation assay

All compounds that inhibit Eg5 activity were tested to determine its growth inhibition (EC$_{50}$) against cell proliferation of K562. Five selected inhibitors (compounds **101**, **108**, **109**, **112** and **129**) were tested in four tumour cell lines (BxPC-3, HCT116, NCI-H1299 and K562).

General test procedure was as follows:[56]

Cells were seeded in triplicates in 96-well assay plates at 1250 cells (BxPC-3, HCT116), 2500 cells (NCI-H1299), and 5000 cells (K562) per well in 100 μL of the respective growth medium. Medium blanks and cell blanks for every cell line were also prepared.

- Next day, inhibitors were added with a starting concentration of 100 μM in a 3-fold serial dilution series.
- After 72 h of inhibitor addition, 10% Alamar Blue (Invitrogen, Paisley, UK) was added into each well.
- After 2-12 h (depending on the cell line) the absorbance was measured at 570 and 600 nm.
- All values were corrected for the absorbance of the medium blank and the corrected cell blanks were set to 100%.
- Calculations for determining the relative proliferation were performed using equations described in the manufacturer's manual.
- The EC_{50} values were determined using a sigmoidal dose-response fitting (variable slope) with GraphPad Prism 5.01 for Windows (GraphPad Software, San Diego, USA).

4.5.3 MDR Assays

The MDR ratio for five selected inhibitors (compounds **101**, **108**, **109**, **112** and **129**) was determined using a proliferation assay with human cervix carcinoma KB-V1 cells, overexpressing MDR1 at both the mRNA and protein level and its parental cell line KB-3-1.

General test procedure was as follows:[56]

- Cells were seeded in triplicates in 96-well assay plates at 2000 cells (KB-3-1 and KB-V1) per well in 100 μL of the respective growth medium.
- For KB-V1, no vinblastine was added for the duration of the assay.

- In another set of plates, 1 µM Zosuquidar trihydrochloride (Diverchim, Montataire, France) was added to suppress Pgp-overexpression.
- The setup and measurements assay were the same as the cell proliferation assay described before.
- The MDR ratio was calculated by dividing the EC_{50} value for a particular drug in the mdr1-overexpressing KB-V1 cells by the EC_{50} value obtained in the parental KB-3-1 cells.
- The decreased resistance of the overexpression of Pgp in presence of the specific Pgp inhibitor Zosuquidar confirms that the efflux by Pgp is indeed responsible for the observed drug resistance.
- Statistical significance of differences in the EC_{50} values was assessed using ANOVA with GraphPad Prism 5.03 for Windows (GraphPad Software, San Diego, CA).

4.6 Molecular modelling using the docking program GOLD 4.0

GOLD (Genetic Optimisation for Ligand Docking) is a genetic algorithm for docking ligands into protein binding sites. GOLD is supplied with the Hermes visualiser to aid the docking. The process and parameters used are detailed in the following sections.

4.6.1 Ligand and protein flexibility

GOLD generally allows partial protein flexibility. The docking process allows the optimization of hydroxyl groups during docking to allow optimal H-bonding to the ligand. The same is done with NH_3^+ groups unless they are held strongly by H-bonds of neighbouring protein residues.

Ligand rotatable bonds are treated flexibly during the docking and only the non-rotatable bonds in the ligand were held.

4.6.2 Docking setup

The docking process includes the following steps:

Preparation of protein: the pdb protein file was loaded into in the 3D Hermes viewer, all the hydrogen atoms were added and water molecules were deleted. The co crystalized STLC ligand was removed during docking.

Definition of the binding site: the centre of binding site was defined from a protein atom within the Hermes visualizer. The selected atom was the carbon of the carbonyl backbone of Ile236 (atom number 1901). The coordinates were thus defined as 6.875, -23.401, 0.662. The radius of the binding site was set as 10 Å to include all the important 20 amino acids which form the binding site.

Ligand file preparation: ligands were prepared bysubjecting them to an ionization and minimization. Each ligand was docked 10 times. Some of our ligands have chiral centres; we kept the chiral centre of the L-cysteine moiety in its R configuration while the two possible isomeric configurations of the other chiral centre were docked simultaneously.

Fitness function: Gold scoring fitness function was selected. The internal ligand offset was enabled to correct the internal energy of the torsion, vdw and internal H-bond to the best energy encountered. All the other options were kept as the default.

GA selection options: the slow speed option was used to perform 100,000 operations, and automatic search option was enabled to perform 100% efficiency searches.

Docking results: All the output files were written as sdf files. The best 10 solutions of all the ligands were saved.

Chapter 5: References

1. Abulalhasan, M.; Sutcliffe, O.; Kozielski, F.; Mackay, S., Design and synthesis of novel Eg5 inhibitors. *Journal of pharmacy and pharmacology* **2010,** *62* (10), 1367 (coference abstract).
2. Brown, T. A., *Genomes*. Garland Science: New York and London 2002.
3. Stein, G. S.; Baserga, R.; Giordano, A.; Denhardt, D. T., *Cell Cycle and Growth Control*. WILEY-LISS: 1999.
4. Turner, P.; McLennan, A.; Bates, A.; White, M., *Molecular Biology*. Third Edition ed.; Tayler & Francis Group: Leeds, 2005.
5. Albert, B., *Molecular Biology of the Cell (Book)*.
6. Wood, K. W.; Cornwell, W. D.; Jackson, J. R., Past and future of the mitotic spindle as an oncology target. *Current Opinion in Pharmacology* **2001,** *1* (4), 370-377.
7. Palmer, C. G.; Livengood, D.; Warren, A. K.; Simpson, P. J.; Johnson, I. S., The action of the vincaleukolastine on mitosis in vitro. *Experimental Cell Research* **1960,** *20*, 198-201.
8. Levan, A., The effect of cholchicine on root mitosis in allium. *Hereditas* **1938,** *24* (4), 471-486.
9. Jordan, M. A.; Wilson, L., Microtubules as a target for anticancer drugs. *Nature Reviews Cancer* **2004,** *4* (4), 253-265.
10. Schiff, P. B.; Fant, J.; Horwitz, S. B., Promotion of microtubule assembly in vitro by taxol. *Nature* **1979,** *277* (5698), 665-7.
11. Schiff, P. B.; Horwitz, S. B., Taxol stabilizes microtubules in mouse fibroblast cells. *Proceedings of the National Academy of Sciences of the United States of America* **1980,** *77* (3), 1561-5.
12. Mitchison, T.; Kirschner, M., Dynamic instability of microtubule growth. *Nature* **1984,** *312* (5991), 237-242.
13. Desai, A.; Mitchison, T. J., Microtubule polymerization dynamics. *Annual Review of* Cell *and Developmental Biology* **1997,** *13*, 83-117.
14. Chen, C.-j.; Chin, J. E.; Ueda, K.; Clark, D. P.; Pastan, I.; Gottesman, M. M.; Roninson, I. B., Internal duplication and homology with bacterial transport proteins in the mdr1 (P-glycoprotein) gene from multidrug-resistant human cells. *Cell* **1986,** *47* (3), 381-389.
15. Seelig, A., Unraveling membrane-mediated substrate-transporter interactions. *Biophysical Journal* **2006,** *90* (11), 3825-6.
16. Aller, S. G.; Yu, J.; Ward, A.; Weng, Y.; Chittaboina, S.; Zhuo, R.; Harrell, P. M.; Trinh, Y. T.; Zhang, Q.; Urbatsch, I. L.; Chang, G., Structure of P-Glycoprotein Reveals a Molecular Basis for Poly-Specific Drug Binding. *Science* **2009,** *323* (5922), 1718-1722.
17. Leonard, G. D.; Fojo, T.; Bates, S. E., The role of ABC transporters in clinical practice. *Oncologist* **2003,** *8* (5), 411-24.
18. Raviv, Y.; Pollard, H. B.; Bruggemann, E. P.; Pastan, I.; Gottesman, M. M., Photosensitized labeling of a functional multidrug transporter in living drug-resistant tumor cells. *Journal of Biological Chemistry* **1990,** *265* (7), 3975-80.
19. Brady, S. T., A novel brain ATPase with properties expected for the fast axonal transport motor. *Nature* **1985,** *317* (6032), 73-5.
20. Vale, R. D.; Reese, T. S.; Sheetz, M. P., Identification of a novel force-generating protein, kinesin, involved in microtubule-based motility. *Cell* **1985,** *42* (1), 39-50.

21.   Vallee, R. B.; Sheetz, M. P., Targeting of motor proteins. *Science* **1996,** *271* (5255), 1539-44.

22.   Hirokawa, N.; Takemura, R., Kinesin superfamily proteins and their various functions and dynamics. *Experimental Cell Research* **2004,** *301* (1), 50-9.

23.   Heck, M. M. S., Dr. Dolittle and the making of the mitotic spindle. *BioEssays* **1999,** *21* (12), 985-990.

24.   Hoyt, M. A., Cellular roles of kinesin and related proteins. *Current Opinion in Cell Biology* **1994,** *6* (1), 63-68.

25.   Miki, H.; Okada, Y.; Hirokawa, N., Analysis of the kinesin superfamily: insights into structure and function. *Trends in Cell Biology* **2005,** *15* (9), 467-476.

26.   Kashlna, A. S.; Baskin, R. J.; Cole, D. G.; Wedaman, K. P.; Saxton, W. M.; Scholey, J. M., A bipolar kinesin. *Nature* **1996,** *379* (6562), 270-272.

27.   Blangy, A.; Lane, H. A.; d'Hérin, P.; Harper, M.; Kress, M.; Niggt, E. A., Phosphorylation by p34cdc2 regulates spindle association of human Eg5, a kinesin-related motor essential for bipolar spindle formation in vivo. *Cell* **1995,** *83* (7), 1159-1169.

28.   Heck, M. M.; Pereira, A.; Pesavento, P.; Yannoni, Y.; Spradling, A. C.; Goldstein, L. S., The kinesin-like protein KLP61F is essential for mitosis in Drosophila. *Journal of Cell Biology* **1993,** *123* (3), 665-79.

29.   Castillo, A.; Morse, H. C., 3rd; Godfrey, V. L.; Naeem, R.; Justice, M. J., Overexpression of Eg5 causes genomic instability and tumor formation in mice. *Cancer Research* **2007,** *67* (21), 10138-47.

30.   Castillo, A.; Justice, M. J., The kinesin related motor protein, Eg5, is essential for maintenance of pre-implantation embryogenesis. *Biochemical and biophysical research communications* **2007,** *357* (3), 694-9.

31.   Turner, J.; Anderson, R.; Guo, J.; Beraud, C.; Fletterick, R.; Sakowicz, R., Crystal structure of the mitotic spindle kinesin Eg5 reveals a novel conformation of the neck-linker. *Journal of Biological Chemistry* **2001,** *276* (27), 25496-502.

32.   Woehlke, G.; Schliwa, M., Directional motility of kinesin motor proteins. *Biochimica et Biophysica Acta (BBA) - Molecular Cell Research* **2000,** *1496* (1), 117-127.

33.   Thormählen, M.; Marx, A.; Sack, S.; Mandelkow, E., The Coiled-Coil Helix in the Neck of Kinesin. *Journal of Structural Biology* **1998,** *122* (1-2), 30-41.

34.   Skowronek, K. J.; Kocik, E.; Kasprzak, A. A., Subunits interactions in kinesin motors. *European Journal of Cell Biology* **2007,** *86* (9), 559-568.

35.   Sawin, K. E.; LeGuellec, K.; Philippe, M.; Mitchison, T. J., Mitotic spindle organization by a plus-end-directed microtubule motor. *Nature* **1992,** *359* (6395), 540-3.

36.   Kapitein, L. C.; Peterman, E. J. G.; Kwok, B. H.; Kim, J. H.; Kapoor, T. M.; Schmidt, C. F., The bipolar mitotic kinesin Eg5 moves on both microtubules that it crosslinks. *Nature* **2005,** *435* (7038), 114-118.

37.   Sharp, D. J.; McDonald, K. L.; Brown, H. M.; Matthies, H. J.; Walczak, C.; Vale, R. D.; Mitchison, T. J.; Scholey, J. M., The Bipolar Kinesin, KLP61F, Cross-links Microtubules within Interpolar Microtubule Bundles of Drosophila Embryonic Mitotic Spindles. *Journal of Cell Biology* **1999,** *144* (1), 125-138.

38. Valentine, M.; Fordyce, P.; Block, S., Eg5 steps it up! *Cell Division* **2006,** *1* (1), 31.

39. Valentine, M. T.; Gilbert, S. P., To step or not to step? How biochemistry and mechanics influence processivity in Kinesin and Eg5. *Current Opinion in Cell Biology* **2007,** *19* (1), 75-81.

40. Crevel, I. M. T. C.; Lockhart, A.; Cross, R. A., Kinetic evidence for low chemical processivity in ncd and Eg5. *Journal of Molecular Biology* **1997,** *273* (1), 160-170.

41. Valentine, M. T.; Fordyce, P. M.; Krzysiak, T. C.; Gilbert, S. P.; Block, S. M., Individual dimers of the mitotic kinesin motor Eg5 step processively and support substantial loads in vitro. *Nature Cell Biology* **2006,** *8* (5), 470-476.

42. Rice, S.; Lin, A. W.; Safer, D.; Hart, C. L.; Naber, N.; Carragher, B. O.; Cain, S. M.; Pechatnikova, E.; Wilson-Kubalek, E. M.; Whittaker, M.; Pate, E.; Cooke, R.; Taylor, E. W.; Milligan, R. A.; Vale, R. D., A structural change in the kinesin motor protein that drives motility. *Nature* **1999,** *402* (6763), 778-784.

43. Vale, R. D.; Milligan, R. A., The Way Things Move: Looking Under the Hood of Molecular Motor Proteins. *Science* **2000,** *288* (5463), 88-95.

44. Sablin, E. P.; Kull, F. J.; Cooke, R.; Vale, R. D.; Fletterick, R. J., Crystal structure of the motor domain of the kinesin-related motor ncd. *Nature* **1996,** *380* (6574), 555-9.

45. Kull, F. J.; Sablin, E. P.; Lau, R.; Fletterick, R. J.; Vale, R. D., Crystal structure of the kinesin motor domain reveals a structural similarity to myosin. *Nature* **1996,** *380* (6574), 550-5.

46. Sack, S.; Muller, J.; Marx, A.; Thormahlen, M.; Mandelkow, E. M.; Brady, S. T.; Mandelkow, E., X-ray structure of motor and neck domains from rat brain kinesin. *Biochemistry* **1997,** *36* (51), 16155-65.

47. Gulick, A. M.; Bauer, C. B.; Thoden, J. B.; Rayment, I., X-ray Structures of the MgADP, MgATP, and MgAMPPNP Complexes of the Dictyostelium discoideum Myosin Motor Domain. *Biochemistry* **1997,** *36* (39), 11619-11628.

48. Kikkawa, M.; Sablin, E. P.; Okada, Y.; Yajima, H.; Fletterick, R. J.; Hirokawa, N., Switch-based mechanism of kinesin motors. *Nature* **2001,** *411* (6836), 439-45.

49. Mayer, T. U.; Kapoor, T. M.; Haggarty, S. J.; King, R. W.; Schreiber, S. L.; Mitchison, T. J., Small Molecule Inhibitor of Mitotic Spindle Bipolarity Identified in a Phenotype-Based Screen. *Science* **1999,** *286* (5441), 971-974.

50. DeBonis, S.; Simorre, J.-P.; Crevel, I.; Lebeau, L.; Skoufias, D. A.; Blangy, A.; Ebel, C.; Gans, P.; Cross, R.; Hackney, D. D.; Wade, R. H.; Kozielski, F., Interaction of the Mitotic Inhibitor Monastrol with Human Kinesin Eg5 *Biochemistry* **2002,** *42* (2), 338-349.

51. Maliga, Z.; Mitchison, T., Small-molecule and mutational analysis of allosteric Eg5 inhibition by monastrol. *BMC Chemical Biology* **2006,** *6* (1), 2.

52. Maliga, Z.; Kapoor, T. M.; Mitchison, T. J., Evidence that Monastrol Is an Allosteric Inhibitor of the Mitotic Kinesin Eg5. *Chemistry & Biology* **2002,** *9* (9), 989-996.

53. Cross, R. A., Molecular motors: Kinesin s dynamically dockable neck. *Current biology : CB* **2000,** *10* (3), R124-R126.

54. Cochran, J. C.; Gatial, J. E., 3rd; Kapoor, T. M.; Gilbert, S. P., Monastrol inhibition of the mitotic kinesin Eg5. *Journal of Biological Chemistry* **2005,** *280* (13), 12658-67.

55. Yan, Y.; Sardana, V.; Xu, B.; Homnick, C.; Halczenko, W.; Buser, C. A.; Schaber, M.; Hartman, G. D.; Huber, H. E.; Kuo, L. C., Inhibition of a Mitotic Motor Protein: Where, How, and Conformational Consequences. *Journal of Molecular Biology* **2004,** *335* (2), 547-554.

56. Kaan, H. Y. K.; Ulaganathan, V.; Rath, O.; Prokopcová̀, H.; Dallinger, D.; Kappe, C. O.; Kozielski, F., Structural Basis for Inhibition of Eg5 by Dihydropyrimidines: Stereoselectivity of Antimitotic Inhibitors Enastron, Dimethylenastron and Fluorastrol. *Journal of Medicinal Chemistry* **2010,** *53* (15), 5676-5683.

57. Case, R. B.; Rice, S.; Hart, C. L.; Ly, B.; Vale, R. D., Role of the kinesin neck linker and catalytic core in microtubule-based motility. *Current Biology* **2000,** *10* (3), 157-160.

58. Gartner, M.; Sunder-Plassmann, N.; Seiler, J.; Utz, M.; Vernos, I.; Surrey, T.; Giannis, A., Development and Biological Evaluation of Potent and Specific Inhibitors of Mitotic Kinesin Eg5. *ChemBioChem* **2005,** *6* (7), 1173-1177.

59. Müller, C.; Gross, D.; Sarli, V.; Gartner, M.; Giannis, A.; Bernhardt, G.; Buschauer, A., Inhibitors of kinesin Eg5: antiproliferative activity of monastrol analogues against human glioblastoma cells. *Cancer Chemotherapy and Pharmacology* **2007,** *59* (2), 157-164.

60. Klein, E.; DeBonis, S.; Thiede, B.; Skoufias, D. A.; Kozielski, F.; Lebeau, L., New chemical tools for investigating human mitotic kinesin Eg5. *Bioorganic & Medicinal Chemistry* **2007,** *15* (19), 6474-6488.

61. Svetlík, J.; Veizerová, L.; Kettmann, V., Biginelli-like reaction with dialkyl acetone-1,3-dicarboxylates: a remarkable case of steric control. *Tetrahedron Letters* **2008,** *49* (21), 3520-3523.

62. Svetlik, J.; Veizerova, L.; Mayer, T. U.; Catarinella, M., Monastrol analogs: a synthesis of pyrazolopyridine, benzopyranopyrazolopyridine, and oxygen-bridged azolopyrimidine derivatives and their biological screening. *Bioorganic & Medicinal Chemistry Letters* *20* (14), 4073-6.

63. Hotha, S.; Yarrow, J. C.; Yang, J. G.; Garrett, S.; Renduchintala, K. V.; Mayer, T. U.; Kapoor, T. M., HR22C16: A Potent Small-Molecule Probe for the Dynamics of Cell Division. *Angewandte Chemie International Edition* **2003,** *42* (21), 2379-2382.

64. Garcia-Saez, I.; DeBonis, S.; Lopez, R.; Trucco, F.; Rousseau, B.; Thuery, P.; Kozielski, F., Structure of human Eg5 in complex with a new monastrol-based inhibitor bound in the R configuration. *Journal of Biological Chemistry* **2007,** *282* (13), 9740-7.

65. DeBonis, S.; Skoufias, D. A.; Lebeau, L.; Lopez, R.; Robin, G.; Margolis, R. L.; Wade, R. H.; Kozielski, F., In vitro screening for inhibitors of the human mitotic kinesin Eg5 with antimitotic and antitumor activities. *Molecular Cancer Therapeutics* **2004,** *3* (9), 1079-90.

66. Skoufias, D. A.; DeBonis, S.; Saoudi, Y.; Lebeau, L.; Crevel, I.; Cross, R.; Wade, R. H.; Hackney, D.; Kozielski, F., S-trityl-L-cysteine is a reversible, tight binding inhibitor of the human kinesin Eg5 that specifically blocks

mitotic progression. *Journal of Biological Chemistry* **2006,** *281* (26), 17559-69.

67. Morrison, J. F., Kinetics of the reversible inhibition of enzyme-catalysed reactions by tight-binding inhibitors. *Biochimica et Biophysica Acta* **1969,** *185* (2), 269-86.

68. Kim, E. D.; Buckley, R.; Learman, S.; Richard, J.; Parke, C.; Worthylake, D. K.; Wojcik, E. J.; Walker, R. A.; Kim, S., Allosteric drug discrimination is coupled to mechanochemical changes in the kinesin-5 motor core. *Journal of Biological Chemistry* **2010,** *285* (24), 18650-61.

69. Kaan, H. Y.; Ulaganathan, V.; Hackney, D. D.; Kozielski, F., An allosteric transition trapped in an intermediate state of a new kinesin-inhibitor complex. *Biochemical Journal* **2009,** *425* (1), 55-60.

70. DeBonis, S.; Skoufias, D. A.; Indorato, R.-L.; Liger, F.; Marquet, B.; Laggner, C.; Joseph, B.; Kozielski, F., Structure-Activity Relationship of S-Trityl-l-Cysteine Analogues as Inhibitors of the Human Mitotic Kinesin Eg5. *Journal of Medicinal Chemistry* **2008,** *51* (5), 1115-1125.

71. Ogo, N.; Oishi, S.; Matsuno, K.; Sawada, J.-i.; Fujii, N.; Asai, A., Synthesis and biological evaluation of l-cysteine derivatives as mitotic kinesin Eg5 inhibitors. *Bioorganic & Medicinal Chemistry Letters* **2007,** *17* (14), 3921-3924.

72. Cox, C. D.; Breslin, M. J.; Mariano, B. J.; Coleman, P. J.; Buser, C. A.; Walsh, E. S.; Hamilton, K.; Huber, H. E.; Kohl, N. E.; Torrent, M.; Yan, Y.; Kuo, L. C.; Hartman, G. D., Kinesin spindle protein (KSP) inhibitors. Part 1: The discovery of 3,5-diaryl-4,5-dihydropyrazoles as potent and selective inhibitors of the mitotic kinesin KSP. *Bioorganic & Medicinal Chemistry Letters* **2005,** *15* (8), 2041-2045.

73. Cox, C. D.; Torrent, M.; Breslin, M. J.; Mariano, B. J.; Whitman, D. B.; Coleman, P. J.; Buser, C. A.; Walsh, E. S.; Hamilton, K.; Schaber, M. D.; Lobell, R. B.; Tao, W.; South, V. J.; Kohl, N. E.; Yan, Y.; Kuo, L. C.; Prueksaritanont, T.; Slaughter, D. E.; Li, C.; Mahan, E.; Lu, B.; Hartman, G. D., Kinesin spindle protein (KSP) inhibitors. Part 4: Structure-based design of 5-alkylamino-3,5-diaryl-4,5-dihydropyrazoles as potent, water-soluble inhibitors of the mitotic kinesin KSP. *Bioorganic & Medicinal Chemistry Letters* **2006,** *16* (12), 3175-3179.

74. Coleman, P. J.; Schreier, J. D.; Cox, C. D.; Fraley, M. E.; Garbaccio, R. M.; Buser, C. A.; Walsh, E. S.; Hamilton, K.; Lobell, R. B.; Rickert, K.; Tao, W.; Diehl, R. E.; South, V. J.; Davide, J. P.; Kohl, N. E.; Yan, Y.; Kuo, L.; Prueksaritanont, T.; Li, C.; Mahan, E. A.; Fernandez-Metzler, C.; Salata, J. J.; Hartman, G. D., Kinesin spindle protein (KSP) inhibitors. Part 6: Design and synthesis of 3,5-diaryl-4,5-dihydropyrazole amides as potent inhibitors of the mitotic kinesin KSP. *Bioorganic & Medicinal Chemistry Letters* **2007,** *17* (19), 5390-5395.

75. Fraley, M. E.; Garbaccio, R. M.; Arrington, K. L.; Hoffman, W. F.; Tasber, E. S.; Coleman, P. J.; Buser, C. A.; Walsh, E. S.; Hamilton, K.; Fernandes, C.; Schaber, M. D.; Lobell, R. B.; Tao, W.; South, V. J.; Yan, Y.; Kuo, L. C.; Prueksaritanont, T.; Shu, C.; Torrent, M.; Heimbrook, D. C.; Kohl, N. E.; Huber, H. E.; Hartman, G. D., Kinesin spindle protein (KSP) inhibitors. Part 2: The design, synthesis, and characterization of 2,4-diaryl-2,5-

dihydropyrrole inhibitors of the mitotic kinesin KSP. *Bioorganic & Medicinal Chemistry Letters* **2006,** *16* (7), 1775-1779.

76. Garbaccio, R. M.; Fraley, M. E.; Tasber, E. S.; Olson, C. M.; Hoffman, W. F.; Arrington, K. L.; Torrent, M.; Buser, C. A.; Walsh, E. S.; Hamilton, K.; Schaber, M. D.; Fernandes, C.; Lobell, R. B.; Tao, W.; South, V. J.; Yan, Y.; Kuo, L. C.; Prueksaritanont, T.; Slaughter, D. E.; Shu, C.; Heimbrook, D. C.; Kohl, N. E.; Huber, H. E.; Hartman, G. D., Kinesin spindle protein (KSP) inhibitors. Part 3: Synthesis and evaluation of phenolic 2,4-diaryl-2,5-dihydropyrroles with reduced hERG binding and employment of a phosphate prodrug strategy for aqueous solubility. *Bioorganic & Medicinal Chemistry Letters* **2006,** *16* (7), 1780-1783.

77. Cox, C. D.; Breslin, M. J.; Whitman, D. B.; Coleman, P. J.; Garbaccio, R. M.; Fraley, M. E.; Zrada, M. M.; Buser, C. A.; Walsh, E. S.; Hamilton, K.; Lobell, R. B.; Tao, W.; Abrams, M. T.; South, V. J.; Huber, H. E.; Kohl, N. E.; Hartman, G. D., Kinesin spindle protein (KSP) inhibitors. Part V: Discovery of 2-propylamino-2,4-diaryl-2,5-dihydropyrroles as potent, water-soluble KSP inhibitors, and modulation of their basicity by [β]-fluorination to overcome cellular efflux by P-glycoprotein. *Bioorganic & Medicinal Chemistry Letters* **2007,** *17* (10), 2697-2702.

78. Xiao, S.; Shi, X.-X., The first highly stereoselective approach to the mitotic kinesin Eg5 inhibitor HR22C16 and its analogues. *Tetrahedron: Asymmetry* **2010,** *21* (2), 226-231.

79. Cox, C. D.; Coleman, P. J.; Breslin, M. J.; Whitman, D. B.; Garbaccio, R. M.; Fraley, M. E.; Buser, C. A.; Walsh, E. S.; Hamilton, K.; Schaber, M. D.; Lobell, R. B.; Tao, W.; Davide, J. P.; Diehl, R. E.; Abrams, M. T.; South, V. J.; Huber, H. E.; Torrent, M.; Prueksaritanont, T.; Li, C.; Slaughter, D. E.; Mahan, E.; Fernandez-Metzler, C.; Yan, Y.; Kuo, L. C.; Kohl, N. E.; Hartman, G. D., Kinesin Spindle Protein (KSP) Inhibitors. 9. Discovery of (2S)-4-(2,5-Difluorophenyl)-N-[(3R,4S)-3-fluoro-1-methylpiperidin-4-yl]-2-(hydroxymethyl)-N-methyl-2-phenyl-2,5-dihydro-1H-pyrrole-1-carboxamide (MK-0731) for the Treatment of Taxane-Refractory Cancer. *Journal of Medicinal Chemistry* **2008,** *51* (14), 4239-4252.

80. Garbaccio, R. M.; Tasber, E. S.; Neilson, L. A.; Coleman, P. J.; Fraley, M. E.; Olson, C.; Bergman, J.; Torrent, M.; Buser, C. A.; Rickert, K.; Walsh, E. S.; Hamilton, K.; Lobell, R. B.; Tao, W.; South, V. J.; Diehl, R. E.; Davide, J. P.; Yan, Y.; Kuo, L. C.; Li, C.; Prueksaritanont, T.; Fernandez-Metzler, C.; Mahan, E. A.; Slaughter, D. E.; Salata, J. J.; Kohl, N. E.; Huber, H. E.; Hartman, G. D., Kinesin spindle protein (KSP) inhibitors. Part 7: Design and synthesis of 3,3-disubstituted dihydropyrazolobenzoxazines as potent inhibitors of the mitotic kinesin KSP. *Bioorganic & Medicinal Chemistry Letters* **2007,** *17* (20), 5671-5676.

81. Sunder-Plassmann, N.; Sarli, V.; Gartner, M.; Utz, M.; Seiler, J.; Huemmer, S.; Mayer, T. U.; Surrey, T.; Giannis, A., Synthesis and biological evaluation of new tetrahydro-[beta]-carbolines as inhibitors of the mitotic kinesin Eg5. *Bioorganic & Medicinal Chemistry* **2005,** *13* (22), 6094-6111.

82. Barsanti, P. A.; Wang, W.; Ni, Z.-J.; Duhl, D.; Brammeier, N.; Martin, E.; Bussiere, D.; Walter, A. O., The discovery of tetrahydro-[beta]-carbolines as

inhibitors of the kinesin Eg5. *Bioorganic & Medicinal Chemistry Letters* **2010,** *20* (1), 157-160.

83. Sakowicz, R.; Finer, J. T.; Beraud, C.; Crompton, A.; Lewis, E.; Fritsch, A.; Lee, Y.; Mak, J.; Moody, R.; Turincio, R.; Chabala, J. C.; Gonzales, P.; Roth, S.; Weitman, S.; Wood, K. W., Antitumor activity of a kinesin inhibitor. *Cancer Research* **2004,** *64* (9), 3276-80.
84. Cytokinetics. WO2005061460; 2005.
85. Cytokinetics. WO2005042697; 2005.
86. Cytokinetics. WO2004100873; 2004.
87. Cytokinetics. WO2004103282; 2004.
88. Cytokinetics. WO2005013888; 2005.
89. Cytokinetics. WO2007067752; 2007.
90. Chiron. WO2004111058; 2004.
91. Chiron. WO2004113335; 2004.
92. AstraZeneca. WO2006018627; 2006.
93. AstraZeneca. WO2006008523; 2006.
94. Matsuno, K.; Sawada, J.-i.; Asai, A., Therapeutic potential of mitotic kinesin inhibitors in cancer. *Expert Opinion on Therapeutic Patents* **2008,** *18*, 253-274.
95. Cytokinetics (2001). WO2001030768.
96. http://www.cytokinetics.com/ispinesib (accessed on 1/2011).
97. Tang, P. A.; Siu, L. L.; Chen, E. X.; Hotte, S. J.; Chia, S.; Schwarz, J. K.; Pond, G. R.; Johnson, C.; Colevas, A. D.; Synold, T. W.; Vasist, L. S.; Winquist, E., Phase II study of ispinesib in recurrent or metastatic squamous cell carcinoma of the head and neck. *Investigational new drugs* **2008,** *26* (3), 257-64.
98. Sarli, V.; Giannis, A., Targeting the Kinesin Spindle Protein: Basic Principles and Clinical Implications. *Clinical Cancer Research* **2008,** *14* (23), 7583-7587.
99. Chu, Q. S.; Holen, K. D.; Rowinsky, E. K.; Wilding, G.; Volkman, J. L.; Orr, J. B.; Williams, D. D.; Hodge, J. P.; Sabry, J., Phase I trial of novel kinesin spindle protein (KSP) inhibitor SB-715992 IV Q 21 days. *Journal of Clinical Oncology (Meeting Abstracts)* **2004,** *22* (14_suppl), 2078-.
100. Heath, E. I.; Alousi, A.; Eder, J. P.; Valdivieso, M.; Vasist, L. S.; Appleman, L.; Bhargava, P.; Colevas, A. D.; Lorusso, P. M.; Shapiro, G., A phase I dose escalation trial of ispinesib (SB-715992) administered days 1-3 of a 21-day cycle in patients with advanced solid tumors. *Journal of Clinical Oncology (Meeting Abstracts)* **2006,** *24* (18_suppl), 2026-.
101. Tripathy, D., Capecitabine in combination with novel targeted agents in the management of metastatic breast cancer: underlying rationale and results of clinical trials. *Oncologist* **2007,** *12* (4), 375-89.
102. Holen, K.; Belani, C.; Wilding, G.; Ramalingam, S.; Heideman, J.; Ramanathan, R.; Bowen, C.; Williams, D.; Hodge, J.; Dar, M., Phase I study to determine tolerability and pharmacokinetics (PK) of SB-743921, a novel kinesin spindle protein (KSP) inhibitor. 2006;24:2000. *American Society of Clinical Oncology* **2006**.
103. Cytokinetics/GSK (2003). WO2003088903.
104. http://clinicaltrials.gov/ct2/show/NCT00821249 (accessed on 1/2011).

105. www.merck.com (accessed on 1/2011).

106. Peters, T.; Lindenmaier, H.; Haefeli, W.; Weiss, J., Interaction of the mitotic kinesin Eg5 inhibitor monastrol with P-glycoprotein. *Naunyn-Schmiedeberg's Archives of Pharmacology* **2006,** *372* (4), 291-299.

107. Borst, P.; Evers, R.; Kool, M.; Wijnholds, J., A Family of Drug Transporters: the Multidrug Resistance-Associated Proteins. *Journal of the National Cancer Institute* **2000,** *92* (16), 1295-1302.

108. Ferte, J., Analysis of the tangled relationships between P-glycoprotein-mediated multidrug resistance and the lipid phase of the cell membrane. *European Journal of Biochemistry* **2000,** *267* (2), 277-94.

109. Johnstone, R. W.; Ruefli, A. A.; Smyth, M. J., Multiple physiological functions for multidrug transporter P-glycoprotein? *Trends in Biochemical Sciences* **2000,** *25* (1), 1-6.

110. Brier, S.; Lemaire, D.; DeBonis, S.; Forest, E.; Kozielski, F., Molecular Dissection of the Inhibitor Binding Pocket of Mitotic Kinesin Eg5 Reveals Mutants that Confer Resistance to Antimitotic Agents. *Journal of Molecular Biology* **2006,** *360* (2), 360-376.

111. Tcherniuk, S.; van Lis, R.; Kozielski, F.; Skoufias, D. A., Mutations in the human kinesin Eg5 that confer resistance to monastrol and S-trityl-l-cysteine in tumor derived cell lines. *Biochemical Pharmacology* *79* (6), 864-872.

112. Jackson, J.; Auger, K.; Gilmartin, A.; Eng, W.; Luo, L.; Concha, N.; Parrish, C.; Sutton, D.; Diamond, M.; Giardiniere, M.; Zhang, S.; Huang, P. A., Resistance Mechanism for the KSP Inhibitor *Ispinesib* Implicates Point Mutations in the Compound Binding Site. *AACR-NCI-EORTC* **2005,** *November (poster presentation).*

113. Wittayanarakul, K.; Sutcliffe, O. B.; Kaan, H.-Y. K.; Kozielski, F.; Mackay, S. P., Investigating the allosteric inhibition of human kinesin Eg5 by molecular dynamics. *Journal of Chemical Information and Modelling (Submitted)* **2010**.

114. Hatano, M.; Suzuki, S.; Ishihara, K., Highly Efficient Alkylation to Ketones and Aldimines with Grignard Reagents Catalyzed by Zinc(II) Chloride. *Journal of the American Chemical Society* **2006,** *128* (31), 9998-9999.

115. Boivin, R. P.; Luu-The, V.; Lachance, R.; Labrie, F.; Poirier, D., Structure-Activity Relationships of 17α Derivatives of Estradiol as Inhibitors of Steroid Sulfatase. *Journal of Medicinal Chemistry* **2000,** *43* (23), 4465-4478.

116. Silverman, G. S.; Rakita, P. E., *Handbook of Grignard reagents*. MARCEL DEKKER: 1996.

117. Clive, D. L. J.; Pham, M. P., Conversion of Weinreb Amides into Benzene Rings Incorporating the Amide Carbonyl Carbon. *The Journal of Organic Chemistry* **2009,** *74* (4), 1685-1690.

118. Bailey, W. F.; Punzalan, E. R., Convenient general method for the preparation of primary alkyllithiums by lithium-iodine exchange. *The Journal of Organic Chemistry* **1990,** *55* (19), 5404-5406.

119. Kazmierski, W. M.; Aquino, C.; Chauder, B. A.; Deanda, F.; Ferris, R.; Jones-Hertzog, D. K.; Kenakin, T.; Koble, C. S.; Watson, C.; Wheelan, P.; Yang, H.; Youngman, M., Discovery of Bioavailable 4,4-Disubstituted Piperidines as Potent Ligands of the Chemokine Receptor 5 and Inhibitors of

the Human Immunodeficiency Virus-1. *Journal of Medicinal Chemistry* **2008,** *51* (20), 6538-6546.

120. König, W.; Geiger, R.; Siedel, W., Neue S-Schutzgruppen für Cystein. *Chemische Berichte* **1968,** *101* (2), 681-693.

121. Kristen M. Amore, N. E. L., Microwave-Promoted Esterification Reactions: Optimization and Scale-Up. *Macromolecular Rapid Communications* **2007,** *28* (4), 473-477.

122. Maycock, C. D.; Stoodley, R. J., Studies related to thiirans. Part 1. Synthesis of chiral thiirancarboxylates. *Journal of the Chemical Society* **1979**, 1852 - 1857.

123. Laurent, S.; Botteman, F.; Vander Elst, L.; Muller, R. N., Optimising the design of paramagnetic MRI contrast agents: influence of backbone substitution on the water exchange rate of Gd-DTPA derivatives. *Magnetic Resonance Materials in Physics, Biology and Medicine* **2004,** *16* (5), 235-245.

124. Mays, J. R.; Restituyo, J. A.; Katzenberger, R. J.; Wassarman, D. A.; Rajski, S. R., Cyclic disulfides as functional mimics of the histone deacetylase inhibitor FK-228. *Tetrahedron Letters* **2007,** *48* (26), 4579-4583.

125. Panwar, P.; Chopra, M.; Kumar Sharma, R.; Chatal, J.F., Synthesis of novel bifunctional Schiff-base ligands derived from condensation of 1-(p-nitrobenzyl)ethylenediamine and 2-(p-nitrobenzyl)-3-monooxo-1,4,7-triazaheptane with salicylaldehyde. *New Journal of Chemistry* **2003,** *27* (7), 1054-1058.

126. Younghwa, N.; Harold, K., Quinone-cyclized Porfiromycins. *Heterocycles* **2001,** *55* (7), 1347-1363.

127. Petersson, M. J.; Jenkins, I. D.; Loughlin, W. A., The use of phosphonium anhydrides for the synthesis of 2-oxazolines, 2-thiazolines and 2-dihydrooxazine under mild conditions. *Organic & Biomolecular Chemistry* **2009,** *7* (4), 739-746.

128. Kapeller, D. C.; Hammerschmidt, F., Preparation and Configurational Stability of Chiral Chloro-[D1]methyllithiums of 98% Enantiomeric Excess. *Journal of the American Chemical Society* **2008,** *130* (7), 2329-2335.

129. Amato, C.; Devillers, S. b.; Calas, P.; Delhalle, J.; Mekhalif, Z., New Semifluorinated Dithiols Self-Assembled Monolayers on a Copper Platform. *Langmuir* **2008,** *24* (19), 10879-10886.

130. Llama, E. F.; del Campo, C.; Capo, M.; Anadon, M., Synthesis and antinociceptive activity of 9-phenyl-oxy or 9-acyl-oxy derivatives of xanthene, thioxanthene and acridine. *European Journal of Medicinal Chemistry* **1989,** *24* (4), 391-396.

131. Fujii, T.; Hao, W.; Yoshimura, T., New method for the preparation of dibenzo[b, f][1,4]thiazepines. *Heteroatom Chemistry* **2004,** *15* (3), 246-250.

132. McCormack, A. C.; More O'Ferrall, R. A.; O'Donoghu, A. C.; Rao, S. N., Protonated Benzofuran, Anthracene, Naphthalene, Benzene, Ethene, and Ethyne: Measurements and Estimates of pKa and pKR. *Journal of the American Chemical Society* **2002,** *124* (29), 8575-8583.

133. Shyamasundar, N.; Caluwe, P., Lithium aluminum hydride reduction of peri-alkoxy-9,10-anthraquinones. *The Journal of Organic Chemistry* **1981,** *46* (8), 1552-1557.

134. Zhu, X.-Q.; Dai, Z.; Yu, A.; Wu, S.; Cheng, J.-P., Driving Forces for the Mutual Conversions between Phenothiazines and Their Various Reaction Intermediates in Acetonitrile. *The Journal of Physical Chemistry B* **2008,** *112* (37), 11694-11707.

135. Brown, M. L.; Eidam, H. A.; Paige, M.; Jones, P. J.; Patel, M. K., Comparative molecular field analysis and synthetic validation of a hydroxyamide-propofol binding and functional block of neuronal voltage-dependent sodium channels. *Bioorganic & Medicinal Chemistry* **2009,** *17* (19), 7056-7063.

136. Choudhury-Mukherjee, I.; Schenck, H. A.; Cechova, S.; Pajewski, T. N.; Kapur, J.; Ellena, J.; Cafiso, D. S.; Brown, M. L., Design, Synthesis, and Evaluation of Analogues of 3,3,3-Trifluoro-2-Hydroxy-2-Phenyl-Propionamide as Orally Available General Anesthetics. *Journal of Medicinal Chemistry* **2003,** *46* (12), 2494-2501.

137. Hatano, M.; Suzuki, S.; Takagi, E.; Ishihara, K., Highly efficient synthesis of functionalized tertiary alcohols catalyzed by potassium alkoxide-crown ether complexes. *Tetrahedron Letters* **2009,** *50* (26), 3171-3174.

138. Sydnes, L. K.; Holmelid, B.; Kvernenes, O. H.; Valdersnes, S.; Hodne, M.; Boman**,** K., Stereospecific synthesis of allylic and homoallylic alcohols from functionalized propargylic alcohols. *ARKIVOC (Archive for Organic Chemistry)* **2008,** *xiv* (1551-7012), 242-268.

139. http://www.mathsisfun.com/geometry/dihedral-angles.html (accessed on 1/2011).

140. Shi, J.; Orth, J. D.; Mitchison, T., Cell type variation in responses to antimitotic drugs that target microtubules and kinesin-5. *Cancer Research* **2008,** *68* (9), 3269-76.

141. Nakai, R.; Iida, S.; Takahashi, T.; Tsujita, T.; Okamoto, S.; Takada, C.; Akasaka, K.; Ichikawa, S.; Ishida, H.; Kusaka, H.; Akinaga, S.; Murakata, C.; Honda, S.; Nitta, M.; Saya, H.; Yamashita, Y., K858, a novel inhibitor of mitotic kinesin Eg5 and antitumor agent, induces cell death in cancer cells. *Cancer Research* **2009,** *69* (9), 3901-9.

142. Lee, M. S.; Johansen, L.; Zhang, Y.; Wilson, A.; Keegan, M.; Avery, W.; Elliott, P.; Borisy, A. A.; Keith, C. T., The novel combination of chlorpromazine and pentamidine exerts synergistic antiproliferative effects through dual mitotic action. *Cancer Reearch* **2007,** *67* (23), 11359-67.

143. Cox, C. D.; Breslin, M. J.; Whitman, D. B.; Coleman, P. J.; Garbaccio, R. M.; Fraley, M. E.; Zrada, M. M.; Buser, C. A.; Walsh, E. S.; Hamilton, K.; Lobell, R. B.; Tao, W.; Abrams, M. T.; South, V. J.; Huber, H. E.; Kohl, N. E.; Hartman, G. D., Kinesin spindle protein (KSP) inhibitors. Part V: Discovery of 2-propylamino-2,4-diaryl-2,5-dihydropyrroles as potent, water-soluble KSP inhibitors, and modulation of their basicity by [beta]-fluorination to overcome cellular efflux by P-glycoprotein. *Bioorganic & Medicinal Chemistry Letters* **2007,** *17* (10), 2697-2702.

144. Matin, A.; Konings, W. N.; Kuenen, J. G.; Emmens, M., Active transport of amino acids by membrane vesicles of Thiobacillus neapolitanus. *Journal of General Microbiology* **1974,** *83* (2), 311-8.

145. Ghose, A. K.; Viswanadhan, V. N.; Wendoloski, J. J., Prediction of Hydrophobic (Lipophilic) Properties of Small Organic Molecules Using

Fragmental Methods: An Analysis of ALOGP and CLOGP Methods. *The Journal of Physical Chemistry A* **1998,** *102* (21), 3762-3772.

146. Farrugia, L., WinGX suite for small-molecule single-crystal crystallography. *Journal of Applied Crystallography* **1999,** *32* (4), 837-838.

147. Eastham, J. F.; Cannon, D. Y., Ortho substitution of benzyl type Grignard reagents by cyanogen and thiocyanogen. *Journal of Organic Chemistry* **1960,** *25*, 1504-6.

148. Li, S.; Zhou, Z.; Huang, Y.; Shi, L., Synthetic application of elemento-organic compounds of the 15th and 16th groups. 81. Reactions of carbonyl compounds with benzyldibutyltelluronium bromide mediated by different strong bases. *Journal of the Chemical Society, Perkin Trans. 1* **1991,** (5), 1099-100.

149. Rodgman, A.; Wright, G. F., Oxymercuration of trans-1,2-diphenyl-1-propene. *Journal of American Chemical Society* **1954,** *76*, 1382-3.

150. Villani, F. J.; King, M. S.; Papa, D., The chemistry of the benzylpyridines. III. 4-Benzylpyridyl- and 4-benzylmethylpiperidyl carbinols and esters. *Journal of Organic Chemistry* **1952,** *17*, 249-54.

151. Longfellow, C. F.; Jackson, A. O. Hydroxytriphenylvinyl halides having estrogenic activity.*U.S. Patent* 2429556, 1947.

152. Alexander, L. L.; Fuson, R. C., Reversibility of the Friedel-Crafts reaction. Hydrogenation. *Journal of American Chemical Society* **1936,** *58*, 1745-7.

153. Bielawski, B.; Chrzaszczewska, A., Separation of racemic tertiary alcohols into optical antipodes. *Lodz. Tow. Nauk., Wydz. 3, Acta Chimica.* **1966,** *11*, 105-18.

154. Stevens, C. L.; DeYoung, J. J., Epoxy ethers. VI. A triphenyl substituted epoxy ether. *Journal of American Chemical Society* **1954,** *76*, 718-20.

155. Ungnade, H. E.; Kline, E. F.; Crandall, E. W., Condensations of aromatic aldehydes and aryl carbinols with aluminum chloride and aromatic systems. *Journal of American Chemical Society* **1953,** *75*, 3333-6.

156. Coleman, M. P.; Boyd, M. K., S-Pixyl Analogues as Photocleavable Protecting Groups for Nucleosides. *J. Org. Chem.* **2002,** *67* (22), 7641-7648.

157. Cadogan, J. I. G.; Hey, D. H.; Sanderson, W. A., Organic peroxides. III. Bis(9-benzyl-9-fluorenyl) peroxide. A new source of benzyl radicals. *Journal of American Chemical Society* **1960,** 3203-10.

158. Adegoke, E. A.; Emokpae, T. A.; Ephraim-Bassey, H.; Oyelola, C. A., Synthesis of 3-benzoyl-3,4-dihydro-2H- and 3,4-dihydro-2,2-disubstituted benzopyrans via alkynyl Grignard reagents. *Journal of Heterocyclic Chemistry* **1987,** *24* (6), 1705-8.

159. Tadros, W.; Farahat, K.; Robson, J. M., Synthetic estrogens related to triphenylethylene. I. *Journal of Chemical Scoiety.* **1949**, 439-41.

160. Okuma, K.; Nojima, A.; Matsunaga, N.; Shioji, K., Reaction of Benzyne with Salicylaldehydes: General Synthesis of Xanthenes, Xanthones, and Xanthols. *Organic Letters* **2009,** *11* (1), 169-171.

161. Ohwada, T.; Shudo, K., Reaction of diphenylmethyl cations in a strong acid. Participation of carbodications with positive charge substantially delocalized over the aromatic rings. *Journal of American Chemical Society* **1988,** *110* (6), 1862-70.

162.	Tsuruta, T., Michael and some related reactions. *Bulletin of the Institute for Chemical Research, Kyoto Univ.* **1953,** *31*, 190-200.

163.	Alberola, A.; Pedrosa, R.; Perez Bragado, J. L.; Rodriguez Amo, J. F., Alkylaluminum compounds. XXVIII. The behavior of anhydrides and esters toward triphenylaluminum. *Anales de Quimica* **1982,** *78* (2), 159-65.

164.	Maltese, M., Reductive Demercuration in Deprotection of Trityl Thioethers, Trityl Amines, and Trityl Ethers. *The Journal of Organic Chemistry* **2001,** *66* (23), 7615-7625.

165.	Okarvi, S.; Torfs, P.; Adriaens, P.; Verbruggen, A., Synthesis, radiolabelling and biological evaluation of terminal oxamide derivatives of mercaptoacetyltriglycine. *Journal of Labelled Compounds and Radio pharmaceuticals* **2002,** *45* (5), 407-421.

166.	Braunova, A.; Pechar, M.; Laga, R.; Ulbrich, K., Hydrolytically and reductively degradable high-molecular-weight poly(ethylene glycol)s. *Macromolecular Chemistry and Physics* **2007,** *208* (24), 2642-2653.

167.	Voullie, M.; Laurre, M.; Maillard, G.; Muller, P.; Zaoui, R. *Cysteine derivatives* patent: **1961**, 8 pp ; Addn to Fr 1,241,102 (CA 55, 25782f)